

Identification and Molecular Characterization of Inhibitors of Necroptosis

Doctoral thesis at the Medical University of Vienna
for obtaining the academic degree

Doctor of Philosophy

Submitted by

Astrid Fauster, MSc

Supervisor:

Prof. Giulio Superti-Furga

Center for Physiology and Pharmacology, Medical University of Vienna

Währinger Straße 13A/HP, 1090 Vienna, Austria

CeMM Research Center for Molecular Medicine
of the Austrian Academy of Sciences

Lazarettgasse 14, AKH BT 25.3, 1090 Vienna, Austria

Vienna, 2/2016

Acknowledgments

I treasure my PhD years at CeMM. I wish to thank everybody contributing to making this institute a very unique place in terms of scientific opportunity and atmosphere.

First and foremost, I want to thank my supervisor **Giulio Superti-Furga** for providing me with the opportunity to perform my PhD thesis in his laboratory. His scientific wits and foresight, incessant enthusiasm, and the collegial environment he takes care to create make his lab a very special and inspiring place to work in. I am grateful for the advice, patience, and encouragement he provided, and the certainty to always be able to rely on his support.

I greatly appreciate and wish to thank **Manuele Rebsamen**, who helped and supported, and pushed, and was patient, and critical, and precise, and altogether exactly the person you would want to shape your scientific mind. To put it with his own usual understatement: I think he was ok ("this is Swiss for amazing").

Further, I want to express my gratitude to my thesis committee members **Sylvia Knapp** and **Thomas Decker** for their valuable input and feedback over the course of my PhD, as well as for backing me up at critical decision points.

I also want to thank **Kilian Huber** and **Richard Kumaran Kandasamy** for their scientific support, as well as motivating and kind words when needed.

Particular thanks go to **Johannes Bigenzahn** for scientific exchange and fruitful collaboration, his unsurpassed detailed memory, arguments, sharing ups and downs, and always being there for me.

I am grateful to **Manuela Bruckner** for her friendly spirit, endless patience, and always helping out, both with work and chocolate.

Stefania Scorzoni, thank you for pinkifying my life in- and outside the lab. (Gloves!)

Thanks to **Anna Skucha**, **Anna Moskovskich**, **Branka Radic-Sarikas** and **Roberto Giambruno** for sharing science - and for being friends.

Big thanks to **Gregory Vladimer**, **Berend Snijder**, and **Leonhard Heinz** for readily providing help, feedback, support, proofreading, a tea mug, and squash drill.

Thanks also to all other **GSF lab members**. You are a very special crowd of clever, amiable and creative people, and it made me very happy to work with you.

I cannot thank my **friends** enough for fun times, travels, evenings out, listening, caring, and sharing with me. So many happy, warm, memorable moments! I am very lucky to have you.

Most importantly, I wish to thank **Helga & Rupert Fauster** for their love and support. I cannot imagine finer or more wonderful parents than you are.

*“50 Years ago we suggested that cell death was ‘programmed’
or written into the developmental pattern of cells.*

*Since that time we have come to understand
the phenomenon of apoptosis [. . .]*

*We have also recognized alternative patterns
in which cells die [. . .]*

*Because of all the new possibilities and new discoveries,
the future in this field looks to be even more exciting
than the last 50 years.*

It remains a joy to feel that one is a scientist.”

(Lockshin, 2015)

Richard A. Lockshin is a cellular biologist and one of the pioneers in the field of apoptosis. His work on the role of cell death during insect development formed the basis of a landmark paper, published in 1964 together with Carroll M. Williams, in which they first coined the term ‘programmed cell death’ (Lockshin & Williams, 1964).

Declaration

The work performed by the author of this thesis was carried out in the laboratory of Prof. Giulio Superti-Furga at CeMM Research Center for Molecular Medicine of the Austrian Academy of Sciences. This cumulative thesis describes already published results and the author of the thesis is first author on both manuscripts included. The individual contributions of all authors are listed in detail in the prologue and interlude preceding the manuscripts. All other parts of this thesis were written by the author herself.

Chapter 2.1 has been published in Cell Death & Disease: Fauster, A.*, Rebsamen, M.*, Huber, K.V., Bigenzahn, J.W., Stukalov, A., Lardeau, C.H., Scorzoni, S., Bruckner, M., Gridling, M., Parapatics, K., et al. (2015). A cellular screen identifies ponatinib and pazopanib as inhibitors of necroptosis. Cell Death Dis 6, e1767. (doi: 10.1038/cddis.2015.130)

Chapter 2.2 has been published in Molecular & Cellular Proteomics: Bigenzahn, J.W.*, Fauster, A.*, Rebsamen, M., Kandasamy, R.K., Scorzoni, S., Vladimer, G.I., Mueller, A.C., Gstaiger, M., Zuber, J., Bennett, K.L., et al. (2015). An inducible retroviral expression system for tandem affinity purification mass-spectrometry-based proteomics identifies as an MLKL HSP90 client. Molecular & Cellular Proteomics. Proteomics (pii: mcp.O115.055350 [Epub ahead of print])

*: *equal contribution*

The publications in chapter 2.2 and 2.4 are reprinted with permissions from the Nature Publishing Group under the terms of a Creative Commons Attribution 4.0 International License and the American Society for Biochemistry and Molecular Biology, respectively.

Table of Contents

Acknowledgements	2
Declaration	4
List of Figures and Tables	7
Abbreviations	8
Abstract	11
Zusammenfassung	13
1. Introduction	15
1.1 Cell Death	15
1.1.1 Development of the Programmed Cell Death Concept	16
1.1.2 Evolution of the Concept of Programmed Necrosis	17
1.2 Types of Programmed Necrotic Cell Death	18
1.2.1 Ferroptosis	18
1.2.2 Mitochondrial Permeability Transition (MPT)-Dependent Necrosis	19
1.2.3 Parthanatos	19
1.2.4 Pyroptosis	20
1.2.5 NETosis/ETosis	20
1.2.6 Interconnectivity of Cell Death Pathways	20
1.3 Necroptosis	21
1.3.1 Triggers of Necroptosis	21
1.3.2 Key Players of the Necroptosis Signaling Pathway	22
1.4 Molecular Mechanisms and Regulation of TNF-Induced Necroptosis	24
1.4.1 Complex I Formation and NF- κ B Activation	24
1.4.2 Formation of the Apoptosis-Promoting Complex II	26
1.4.3 RHIM Domain-Mediated Necrosome Formation	27
1.4.4 Necroptosis Execution by MLKL	28
1.4.5 Necroptosis-Independent Functions of RIPK1 and RIPK3	30
1.5 Necroptosis in Health and Disease	30
1.5.1 Physiological Relevance of Necroptotic Cell Death	32
1.5.2 Contribution of Necroptosis to Pathophysiological Processes	32
1.6 Experimental Systems and Tools to Study Necroptosis	33
1.6.1 Distinguishing Features of Necroptotic Cell Death	33
1.6.2 Cellular Models of Necroptosis	34
1.6.3 Tool Compounds to Block Necroptosis	34
1.6.4 Mouse Models to Study Necroptosis	36
1.7 Experimental Approaches for Identification of Necroptosis Inhibitors and Target Deconvolution	37
1.8 Experimental Approaches for Identification of Novel Targets in Necroptosis Signaling	40
1.9 Aims of This Thesis	43

2. Results	44
2.1 Prologue	44
2.2 A Cellular Screen Identifies Ponatinib and Pazopanib as Inhibitors of Necroptosis	45
2.3 Interlude	65
2.4 An Inducible Retroviral Expression System for Tandem Affinity Purification Mass-Spectrometry-Based Proteomics Identifies MLKL as an HSP90 Client	66
3. Discussion	105
3.1 Regulated Necrotic Cell Death as a Therapeutic Target	105
3.2 Targeting Necroptosis	106
3.3 The FDA-Approved Drugs Ponatinib and Pazopanib Inhibit Necroptosis	110
3.4 An Inducible Expression System for TAP-MS Approaches Enables Identification of MLKL as an HSP90 Client	112
3.5 Towards Necroptosis Inhibitors for Clinical Use	114
3.6 Conclusion and Future Prospects	117
References	119
Curriculum Vitae	136

List of Figures and Tables

Figure 1: Morphological Aspects of Apoptosis and Necrosis

Figure 2: Triggers of Necroptosis

Figure 3: Domain Organization of the RIP Kinase Family

Figure 4: Signaling Events Downstream of TNFR1 Activation

Figure 5: Crystal Structure of Full-Length Mouse MLKL

Figure 6: Chemical Structures of Necroptosis Inhibitors

Table 1: Necroptosis-Related Diseases

Abbreviations

4HB	four-helix bundle
AIFM1	apoptosis inducing factor, mitochondria associated 1
AML	acute myeloid leukemia
AP	affinity purification
AP-1	activator protein-1
APAF1	apoptotic peptidase activating factor 1
ATP	adenosine triphosphate
BCL2	B-cell CLL/lymphoma 2
BH3	Bcl-2 homology 3
BRAF	B-Raf proto-oncogene, serine/threonine kinase
CARD	caspase activation and recruitment domain
CASP8	caspase 8
CDC37	cell division cycle 37
CEBPA	CCAAT/enhancer binding protein alpha
CETSA	cellular thermal shift assay
c-FLIP	cellular FLICE-like inhibitory protein, also known as CFLAR (CASP8 and FADD like apoptosis regulator)
c-FLIP _L	long form of c-FLIP
ciAP	cellular inhibitor of apoptosis protein, also known as BIRC (baculoviral IAP repeat containing)
CRISPR/Cas9	clustered regularly interspaced short palindromic repeats/CRISPR associated protein 9
CYLD	cylindromatosis (turban tumor syndrome)
CYPD	cyclophilin D, also known as PPID (peptidylprolyl isomerase D)
DAI	DNA-dependent activator of interferon regulator factors, also known as ZBP1 (Z-DNA binding protein 1)
DAMP	danger-associated molecular pattern
DD	death domain
FADD	Fas associated via death domain
FAS	Fas cell surface death receptor
FASLG	Fas ligand
FDA	Food and Drug Administration
FGFR	fibroblast growth factor receptor
GPX4	glutathione peroxidase 4
GSDMD	gasdermin D
GSH	glutathione
GWAS	genome-wide association study
HOIL-1	heme-oxidized IRP2 ubiquitin ligase 1, also known as RBCK1 (RanBP-type and C3HC4-type zinc finger containing 1)
HOIP	HOIL-1-interacting protein, also known as RNF31 (ring finger protein 31)
HSP90	heat shock protein 90
IAP	inhibitor of apoptosis protein
IDO1	indoleamine 2,3-dioxygenase 1
IFN	interferon

IKK	inhibitor of nuclear factor kappa-B kinase
IL	interleukin
I κ B α	NF-kappa-B inhibitor alpha, also known as NFKBIA (nuclear factor of kappa light polypeptide gene enhancer in B-cells inhibitor, alpha)
IR	ischemia-reperfusion
LC	liquid chromatography
LUBAC	linear ubiquitin chain assembly complex
MAPK	mitogen-activated protein kinase
MLKL	mixed lineage kinase domain-like
MPT	mitochondrial permeability transition
mRNA	messenger RNA
MS	mass spectrometry
Nec-1	Necrostatin-1
Nec-1s	7-Cl-O-Nec-1
NEMO	NF-kappa-B essential modulator, also known as IKBKG (inhibitor of kappa light polypeptide gene enhancer in B-cells, kinase gamma)
NETs	neutrophil extracellular traps
NF- κ B	nuclear factor kappa-B
NLS	nuclear localization signal
NOD	nucleotide-binding oligomerization domain
NRAS	neuroblastoma RAS viral (v-ras) oncogene homolog
NSA	necrosulfonamide
PARP	poly(ADP-ribose) polymerase
PDGFR	platelet derived growth factor receptor
PGAM5	PGAM family member 5, serine/threonine protein phosphatase, mitochondrial
Ph+ ALL	Philadelphia chromosome-positive acute lymphoblastic leukemia
PIP	phosphatidylinositol phosphate
PIP4K2C	phosphatidylinositol-5-phosphate 4-kinase, type II, gamma
PKR	protein kinase R, also known as EIF2AK2 (eukaryotic translation initiation factor 2 alpha kinase 2)
PPM1B	protein phosphatase, Mg ²⁺ /Mn ²⁺ dependent 1B
pRSHIC	retroviral expression of SH-tagged proteins for interaction proteomics and color-tracing
RCC	renal cell carcinoma
RHIM	receptor interacting protein homotypic interaction motif
RIPK	receptor interacting serine/threonine kinase
RNAi	RNA interference
ROS	reactive oxygen species
SAR	structure-activity relationship
SH	streptavidin-hemagglutinin
SNP	single-nucleotide polymorphism
SMAC	second mitochondria-derived activator of caspase, also known as DIABLO (diablo, IAP-binding mitochondrial protein)
SHARPIN	SHANK associated RH domain interactor
shRNA	small hairpin RNA
siRNA	small interfering RNA
SIRS	systemic inflammatory response syndrome

TAB	TGF-beta activated kinase 1/MAP3K7 binding protein
TACE	TNF-alpha-converting enzyme, also known as ADAM17 (ADAM metallopeptidase domain 17)
TAK1	transforming growth factor-beta-activated kinase 1, also known as MAP3K7 (mitogen-activated protein kinase kinase kinase 7)
TAOK3	TAO kinase 3
TAP	tandem affinity purification
TCR	T cell receptor
TLR	Toll-like receptor
TNF	tumor necrosis factor
TNFR1	tumor necrosis factor receptor 1, also known as TNFRSF1A (tumor necrosis factor receptor superfamily member 1A)
TP53	tumor protein p53
TRADD	TNFRSF1A-associated via death domain
TRAF2	TNF receptor associated factor 2
TRAIL	TNF-related apoptosis-inducing ligand, also known as TNFSF10 (tumor necrosis factor superfamily member 10)
TRIF	TIR domain-containing adapter inducing interferon-beta, also known as TICAM1 (toll like receptor adaptor molecule 1)
TRPM7	transient receptor potential cation channel, subfamily M, member 7
VEGFR	vascular endothelial growth factor receptor, also known as FLT (fms related tyrosine kinase)
Z-VAD-fmk	Z-Val-Ala-Asp fluoromethyl ketone

Abstract

The balance between cell proliferation and cell death is crucial for the homeostasis of multicellular organisms. Cells that have become obsolete, damaged or infected can be eliminated by genetically encoded death programs. Multiple regulated cell death pathways exist, and disease pathologies and tissue damage ensue when these processes are disturbed. Necroptosis is a pro-inflammatory form of programmed necrotic cell death that has been shown to be involved in the pathophysiology of several human diseases, including myocardial infarction, stroke, and atherosclerosis. Necroptotic cell death depends on receptor interacting serine/threonine kinase (RIPK)3 and its substrate mixed-lineage kinase domain-like (MLKL). RIPK3 activation is mediated by the upstream adaptor proteins RIPK1, TIR domain-containing adapter inducing interferon-beta (TRIF) or DNA-dependent activator of interferon regulator factors (DAI) upon death receptor or Toll-like receptor (TLR) stimulation, bacterial or viral infection, and in the context of sterile inflammation. Necroptotic cell death has a beneficial role in innate immune responses against intracellular pathogens. In contrast, it exacerbates sterile-injury induced inflammation. Limiting pathological necrosis by interfering with programmed necrotic cell death thus represents a promising therapeutic strategy. However, no necroptosis inhibitors are currently available for clinical use. For this reason, I aimed at identifying pharmacological agents that block necroptotic cell death.

In the course of this thesis, I performed a phenotypic screen for necroptosis inhibitors on a representative panel of drugs with Food and Drug Administration (FDA)-approval, implying established pharmacokinetic and safety profiles. I identified the kinase inhibitors ponatinib and pazopanib, both used as anti-cancer therapeutics, to potently and specifically block necroptotic cell death. In order to unravel the precise molecular mode of action effectuating necroptosis inhibition, I chose to apply an unbiased chemical proteomics-based target deconvolution approach to ponatinib. This study provides the first comprehensive description of the cellular target spectrum of this clinically used drug, notably revealing key members of the necroptosis signaling pathway. By a series of complementary, biochemical assays, I showed that pazopanib preferentially targets RIPK1, whereas ponatinib directly binds and blocks both RIPK1 and RIPK3. This work thus establishes ponatinib as the first dual RIPK1/RIPK3 inhibitor.

As detailed understanding of the protein network underlying necroptosis signaling is expected to reveal novel entry points for targeted modulation and therapeutic intervention, I furthermore aimed at providing the basis for mass spectrometry (MS)-based mapping of the necroptosis pathway. To this end, an inducible, retroviral expression system enabling tandem affinity purification (TAP)-based interaction studies in the respective physiologically relevant cellular setting was established and characterized. I demonstrated the feasibility of studying

cell death-inducing proteins using this vector system by a constitutively active mutant form of MLKL, leading to the identification of MLKL as a novel heat shock protein 90 (HSP90) client protein.

Collectively, the work I present here has identified necroptosis inhibitors among compounds currently undergoing clinical development and already approved drugs, as well as unraveled their molecular mode of action. These findings thus provide a consolidated basis for medicinal chemistry approaches aimed at the development of anti-necroptosis agents for future clinical application in necroptosis-associated human diseases.

Zusammenfassung

Das Gleichgewicht zwischen Zellproliferation und Zelltod ist von entscheidender Bedeutung für die Homöostase multizellulärer Organismen. Die Beseitigung obsolet gewordener, geschädigter oder infizierter Zellen kann durch genetisch kodierte Zelltodprogramme bewerkstelligt werden. Es gibt mehrere regulierte Zelltod-Signalwege, und deren Störung kann zur Entstehung von Krankheitspathologie und Gewebeschäden führen. Nekroptose ist eine entzündungsfördernde, programmierte Form nekrotischen Zelltods und trägt zur Pathophysiologie verschiedener menschlicher Erkrankungen, unter anderem Herzinfarkt, Schlaganfall und Arteriosklerose, bei. Nekroptotischer Zelltod kann durch Ligandenbindung an Toll-like- oder Todesrezeptoren, bakterielle und virale Infektionen, sowie im Rahmen steriler Entzündungen ausgelöst werden. Die Signaltransduktion erfolgt über die Proteine RIPK3 und MLKL, wobei die Kinase RIPK3 durch eines der vorgeschalteten Adapterproteine RIPK1, TRIF oder DAI aktiviert wird. Während Nekroptose im Rahmen der angeborenen Immunantwort gegen intrazelluläre Erreger einen vorteilhaften Effekt hat, verstärkt sie die schädlichen Auswirkungen steriler Entzündungen. Die Eingrenzung pathologischer Nekrose durch pharmakologische Nekroptose-Inhibition stellt somit eine vielversprechende Behandlungsstrategie dar, jedoch sind gegenwärtig keine Nekroptose-Inhibitoren für den klinischen Gebrauch verfügbar. Ich setzte mir daher zum Ziel, pharmakologische Wirkstoffe zu identifizieren, welche den nekroptotischen Zelltod blockieren.

Im Zuge meiner Doktorarbeit habe ich eine repräsentative Auswahl zugelassener, und damit bezüglich Pharmakokinetik und Sicherheit erprobter, Arzneimittel auf Nekroptose-Inhibition getestet. Ich zeige, dass die beiden in der Krebstherapie eingesetzten Kinase-Inhibitoren Ponatinib und Pazopanib den nekroptotischen Zelltod spezifisch und mit hoher Wirksamkeit blockieren. Um den zugrundeliegenden molekularen Mechanismus aufzuklären, identifizierte ich die zellulären Angriffspunkte von Ponatinib mittels chemischer Proteomik und liefere damit die erste umfassende Aufstellung der molekularen Wirkorte dieses Medikaments. Bemerkenswerterweise finden sich die wichtigsten Proteine des Nekroptose-Signaltransduktionswegs unter den Wirkstoffzielen. Mittels verschiedenerer biochemischer Tests bestätigte ich, dass Ponatinib sowohl RIPK1 als auch RIPK3 bindet und hemmt, während Pazopanib bevorzugt RIPK1 zum Angriffspunkt hat. Ponatinib ist somit der erste beschriebene duale RIPK1/RIPK3 Inhibitor.

Da die detaillierte Beschreibung des Nekroptose-assoziierten Protein-Netzwerks die Identifizierung zusätzlicher Angriffspunkte für die gezielte Modulation und therapeutische Intervention erwarten lässt, setzte ich mir des Weiteren zum Ziel, die Voraussetzungen für die Massenspektrometrie-basierte Kartierung des Nekroptose-Signaltransduktionswegs zu schaffen. Zu diesem Zweck wurde ein induzierbares, retrovirales Expressionssystem,

welches sich für Protein-Interaktionsstudien auf Basis von Affinitätsreinigung im Zweischnitt-Verfahren eignet und im jeweils physiologisch relevanten zellulären Zusammenhang angewendet werden kann, etabliert. Das System eignet sich weiter für die Analyse von Proteinen deren Expression zytotoxische Effekte hervorruft, wie ich anhand einer konstitutiv aktiven Form von MLKL demonstriere. Im Rahmen dieser Experimente entdeckte und charakterisierte ich die Bedeutung des molekularen Chaperon HSP90 für die Stabilität und Funktionalität von MLKL.

Zusammengenommen identifiziere ich in der vorliegenden Arbeit neue Nekroptose-Inhibitoren unter bereits zugelassenen sowie derzeit in klinischer Testung befindlichen Medikamenten und beschreibe den jeweils zugrundeliegenden molekularen Wirkmechanismus. Diese Ergebnisse schaffen somit eine konsolidierte chemische Basis für die Entwicklung klinisch relevanter Inhibitoren des nekroptotischen Zelltods.

1. Introduction

1.1. Cell Death

Cell death is crucially involved in ontogeny, tissue homeostasis, and pathologies (Pasparakis & Vandenabeele, 2015). The end-stage of cell death is defined by irreversible plasma membrane permeabilization or complete breakdown of cells into discrete fragments commonly referred to as apoptotic bodies (Galluzzi et al, 2014a). Cells may either undergo passive death upon irreparable physical damage, or actively decide to auto-eliminate through tightly controlled self-destruction mechanisms. Accordingly, cell death instances are divided into the two wide, mutually exclusive categories 'accidental' and 'regulated' (Galluzzi et al, 2014b). Accidental cell death refers to cellular demise occurring in an uncontrollable manner in response to extreme physicochemical or mechanical insults (Galluzzi et al, 2014a). While occurring *in vivo* as a consequence of burns or traumatic injuries, accidental cell death cannot be prevented or modulated by therapeutic intervention, as the immediate structural disassembly caused by exposure to severe physical, chemical or mechanical stimuli is insensitive to pharmacological or genetic intervention. Conversely, regulated cell death involves a genetically encoded molecular machinery and its course can thus be modified by targeted biochemical or genetic interference (Galluzzi et al, 2014a). Regulated cell death occurs as part of physiologic programs or can be activated as a consequence of microenvironmental perturbations, once the adaptive responses attempting to restore cellular homeostasis have failed. Accordingly, regulated cell death elicited in context of pathophysiological conditions, such as stress, injury or infection, often occurs in a relatively delayed manner, and is linked to tissue damage and disease pathogenesis (Linkermann et al, 2014c). The term programmed cell death is used to describe completely physiologic instances of regulated cell death occurring as part of a developmental program, maintenance of tissue homeostasis or immune responses (Galluzzi et al, 2014a). Programmed cell death is, for example, required to shape hands and feet during embryonic development by eliminating the intradigital tissue (Jacobson et al, 1997). Similarly, it serves to dispose of cells that are abnormal, nonfunctional, misplaced or potentially dangerous to the organism. Programmed cell death thus eliminates cells having experienced irreparable DNA damage, developing T and B lymphocytes that fail to express potentially useful antigen-specific receptors or produce self-reactive receptors, as well as lymphocytes activated by an infection in order to terminate the immune response and avoid autoimmune responses (Fuchs & Steller, 2011). Lastly, the tightly controlled balance between programmed cell death and cell proliferation determines the turnover kinetics of various cell populations in adult tissues and is therefore required to ensure and regulate the proper maintenance of normal tissue morphology and function in multi-cellular organisms (Pasparakis & Vandenabeele, 2015).

1.1.1. Development of the Programmed Cell Death Concept

The first descriptions of physiological cell death date back to the mid-nineteenth century (Lockshin & Zakeri, 2001). In 1842, soon after establishment of the cell theory by Schleiden and Schwann, and backed by technical advances in the field of microscopy, Carl Vogt reported cell death to occur in the metamorphic midwife toad (Vogt, 1842). Subsequent studies extended the discovery of naturally occurring cell death to non-metamorphic development and turnover of cell populations in adulthood (Clarke & Clarke, 1996). The term 'programmed cell death' was first used in 1964 by Lockshin and Williams (Lockshin & Williams, 1964), introducing the concept that cells follow a sequence of controlled events towards self-destruction. In 1972, Kerr et al. (Kerr et al, 1972) coined the term 'apoptosis', a Greek word meaning 'falling off', to describe a morphological distinct form of cellular demise. Apoptotic cell death is characterized by cell shrinkage, chromatin condensation, nuclear fragmentation, membrane blebbing, and shedding of apoptotic bodies followed by their engulfment by neighboring cells (Figure 1a) (Majno & Joris, 1995). Soon thereafter, Schweichel and Merker (Schweichel & Merker, 1973) reported the existence of three distinct cell death morphologies based on studying the response of rat embryos to toxin exposure. In an early attempt to classify cell death, they proposed to distinguish type I cell death (apoptosis), type II cell death (autophagy), involving extensive vacuolization of the cytoplasm, and type III cell death (necrosis), featuring neither apoptotic nor autophagic characteristics. This initial negative morphologic definition of necrosis has been reconsidered more recently, as necrotic cells can similarly exhibit a panel of common features (Figure 1b) (Kroemer et al, 2008; Krysko et al, 2008). Similarly, usage of the term 'autophagic cell death' based on

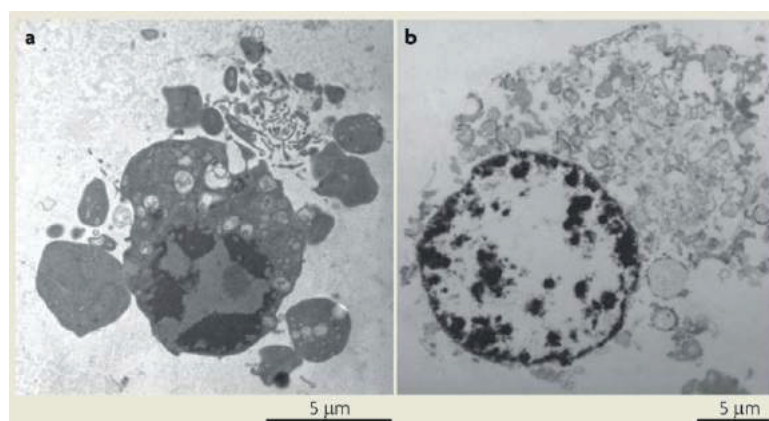


Figure 1: Morphological Aspects of Apoptosis and Necrosis. (a) Apoptosis is marked by cell shrinkage, chromatin condensation, nuclear fragmentation, membrane blebbing, formation of apoptotic bodies, and rapid phagocytosis by neighboring cells. **(b)** Necrotic cells exhibit an increase in cell volume, organelle swelling, loss of plasma membrane integrity, cellular collapse, and release of cellular contents. (Reprinted by permission from Macmillan Publishers Ltd: *Nature Reviews Molecular Cell Biology* 11, Vandenabeele P, Galluzzi L, Vanden Berghe T, Kroemer G, *Molecular mechanisms of necroptosis: an ordered cellular explosion*, 700-714, © 2010)

morphological consideration has later been questioned (Kroemer & Levine, 2008). In few cases, the active contribution of the autophagy machinery to physiological cell death could be demonstrated. However, as the autophagy pathway is activated by cellular stress, various forms of cell death can be accompanied by autophagic features (Denton et al, 2011). The first genes dedicated to the control of programmed cell death were identified through genetic studies on nematode development (Ellis & Horvitz, 1986). The *Caenorhabditis elegans* genes *ced-3* and *ced-4*, homologues of human caspases, were found to be required for somatic cell death. This discovery established the first molecular basis for the notion that genetically determined pathways steer programmed cell death. Caspases constitute a family of cysteine-dependent aspartate-directed proteases which can be activated by apoptotic stimuli to proteolytically degrade cytoplasmic and nuclear target proteins (Shalini et al, 2014). Their pivotal function for apoptosis execution has made caspase activation the hallmark of apoptotic processes. The insight that certain instances of cell death, instead of occurring merely incidentally, are a genetically controlled process of substantial medical relevance, spurred interest in the subject. The increased attention and research efforts entailed a deeper understanding of the pathway, key players, and biochemical mechanisms governing apoptosis. Milestone discoveries as, for instance, identification of B-cell CLL/lymphoma 2 (*BCL2*) as an anti-apoptosis gene (Vaux et al, 1988), the pro-apoptotic roles of tumor protein p53 (TP53) (Lowe et al, 1993; Yonish-Rouach et al, 1991) and recognition of Fas cell surface death receptor (FAS) as a death-transducing receptor (Trauth et al, 1989; Yonehara et al, 1989), linked the concept of apoptosis to the fields of cancer and immunology. For a long time, apoptosis remained the only recognized form of regulated cell death. More recently, in light of the accumulating evidence that necrotic cell death can similarly be executed by genetically encoded, tightly regulated signal transduction pathways, the concept of programmed necrosis has been established (Berghe et al, 2014).

1.1.2. Evolution of the Concept of Programmed Necrosis

The notion of necrosis constituting a purely accidental cell death modality was first challenged by the discovery that, depending on the cell type, cell death induced by tumor necrosis factor (TNF) can be accompanied by either apoptotic or necrotic morphology (Laster et al, 1988). Caspase inhibition had been deemed to routinely protect cells from apoptosis, yet it was reported to dramatically increase the sensitivity of the murine fibrosarcoma cell line L929 to undergo TNF-induced necrotic cell death (Vercammen et al, 1998). Correspondingly, cell death induced by Fas associated via death domain (FADD) multimerization in a caspase 8 (CASP8)-deficient Jurkat cell line was shown to exhibit necrotic features (Kawahara et al, 1998). In 2000, Holler et al. (Holler et al, 2000) found this caspase-independent cell death pathway triggered by Fas ligand (FASLG), TNF-related apoptosis-inducing ligand (TRAIL) or TNF to rely on the enzymatic activity of RIPK1. Besides the discovery of RIPK1 as a distinct

molecular component required for this form of non-apoptotic cell death, the notion of some forms of necrosis being regulated was further strengthened by the subsequent description of a Poly(ADP-ribose) polymerase (PARP)-mediated necrotic cell death pathway induced by DNA damage (Zong, 2004). The term programmed necrosis (Chan et al, 2003) is since used to describe a genetically controlled cell death process that is morphologically characterized by cytoplasmic granulation, organelle swelling, and an increase in cell volume, eventually resulting in plasma membrane rupture and cellular leakage (Figure 1b) (Vandenabeele et al, 2010). In 2005, Degterev et al. (Degterev et al, 2005) discovered Necrostatin-1 (Nec-1), a small-molecule inhibitor of programmed necrosis triggered by ligation of death receptors in absence of caspase activity, and introduced the term 'necroptosis' for this non-apoptotic cell death pathway. RIPK1 was identified as the primary cellular target mediating the anti-necroptotic effect of Nec-1 (Degterev et al, 2008). Soon thereafter, the obligate requirement of the RIPK1-related kinase RIPK3 for necroptosis signaling was uncovered (Cho et al, 2009; He et al, 2009; Zhang et al, 2009). More recently, the function of the pseudokinase MLKL as downstream mediator of necroptotic cell death was identified (Sun et al, 2012; Zhao et al, 2012). The discovery of necroptosis and the growing understanding of its molecular mechanisms has sparked considerable interest in programmed necrotic cell death, leading to the successive discovery of multiple different modes of regulated necrosis (Berghe et al, 2014).

1.2. Types of Programmed Necrotic Cell Death

Several other cell death processes share the morphological hallmarks of necroptosis, but occur independently of RIPK1 and RIPK3 or upon their inhibition (Berghe et al, 2014). The progressing characterization of these various modes of programmed necrotic cell death has prompted a switch in the classification from morphological criteria to quantitative biochemical methods (Galluzzi et al, 2011). Besides necroptosis, which will be described in detail in the following chapters, several subroutines of programmed necrosis are now being distinguished from each other by a particular aspect of the cell death process:

1.2.1. Ferroptosis

The term ferroptosis refers to a recently discovered iron-dependent pathway of regulated necrosis under the control of glutathione peroxidase 4 (GPX4) (Dixon et al, 2012; Yang et al, 2014). This enzyme catalyzes the reduction of lipid peroxides using glutathione (GSH) as reductant, and thus protects cells from oxidative damage (Brigelius-Flohé & Maiorino, 2013). Ferroptotic cell death was first described in a chemical screen for compounds exhibiting selective lethality in RAS-transformed tumor cells (Dixon et al, 2012). In detail, the small molecule erastin was found to induce ferroptosis via inhibition of the plasma membrane

cystine/glutamate antiporter system x_c^- , which supplies the cell with the cystine required for GSH synthesis. Whereas erastin-elicited ferroptosis is insensitive to inhibitors of apoptosis, necroptosis or autophagy, a synthetic small molecule with antioxidant properties termed ferrostatin-1 specifically blocks ferroptotic cell death (Dixon et al, 2012). Ferroptosis can moreover be inhibited by iron chelators such as desferrioxamine, though the precise role of iron in this cell death process is yet incompletely understood. It is presumed that iron-dependent production of reactive oxygen species (ROS) and loss-of-function of GPX4 caused by GSH depletion result in accumulation of lipid peroxides and cell death (Dixon & Stockwell, 2014). Besides constituting an interesting anticancer mechanism, ferroptosis has so far been implicated in renal and hepatic ischemia-reperfusion (IR) injury, and neurological disorders (Friedmann Angeli et al, 2014; Linkermann et al, 2014b; Seiler et al, 2008).

1.2.2. Mitochondrial Permeability Transition (MPT)-Dependent Necrosis

MPT denotes an abrupt increase in the permeability of the inner mitochondrial membrane to small solutes caused by opening of the MPT pore in response to ROS overproduction or cytosolic Ca^{2+} overload (Elrod & Molkentin, 2013). Pore opening is controlled by the mitochondrial matrix protein cyclophilin D (CYPD), the sole genetically confirmed constituent of the MPT pore (Baines et al, 2005; Javadov & Kuznetsov, 2013; Nakagawa et al, 2005; Schinzel et al, 2005). Accordingly, MPT-dependent regulated necrosis can be blocked pharmacologically using the CYPD inhibitors sangliferin A (Clarke et al, 2002) or cyclosporin A (Halestrap & Davidson, 1990). *In vivo*, CYPD-mediated regulated necrosis has been reported in context of IR injury-linked pathologies. More specifically, CYPD deficiency has been demonstrated to exert protective effects in mice subjected to ischemic injury of the heart (Baines et al, 2005; Nakagawa et al, 2005), brain (Schinzel et al, 2005) and kidneys (Devalaraja-Narashimha et al, 2009; Linkermann et al, 2013a).

1.2.3. Parthanatos

The main molecular feature of parthanatos is the hyperactivation of PARP1 (Andrabi et al, 2008). Consequently, this form of regulated necrosis can be blocked pharmacologically by PARP1 inhibition. PARPs are a family of enzymes that transfer ADP-ribose groups from NAD^+ to various target proteins (Gibson & Kraus, 2012). PARP1 is activated by DNA damage and plays a critical role in the repair of DNA breaks. However, persistent DNA damage causes PARP1 overactivation. The resulting massive PARylation of proteins leads to NAD^+ depletion and release of apoptosis inducing factor, mitochondria associated 1 (AIFM1) from the mitochondria, which translocates into the nucleus and induces chromatin degradation (Galluzzi et al, 2014b; Wang et al, 2011; Yu et al, 2002). Parthanatos has been mostly studied in context of neuropathologies such as Parkinson's disease, but is also implicated in cellular injury following IR and retinal degeneration (Galluzzi et al, 2014b; Lee et al, 2013).

1.2.4. Pyroptosis

Pyroptosis occurs after canonical and non-canonical inflammasome stimulation and has been shown to depend on activation of caspase-1, as well as murine caspase-11 (Berghe et al, 2014; Bergsbaken et al, 2009). The rapid osmotic cell lysis has been proposed to be caused by caspase-dependent formation of plasma membrane pores, disrupting cellular ionic gradients (Fink & Cookson, 2006). Two recent studies identified gasdermin D (GSDMD) as a target of caspase-1 and caspase-11, with an essential role in pyroptosis execution (Kayagaki et al, 2015; Shi et al, 2015). Active caspase-1 moreover mediates the maturation and release of the pyrogenic cytokines interleukin (IL)-1 β and IL-18, which renders pyroptotic cell death highly immunogenic (Bergsbaken et al, 2009). Pyroptosis is considered part of the innate immune response, acting as an antimicrobial defense mechanism during inflammation. Indeed, the term pyroptosis has initially been introduced to describe the distinct form of death that macrophages undergo upon infection with *Salmonella enterica* serovar Typhimurium (Brennan & Cookson, 2000), and the *in vivo* relevance of pyroptotic cell death has since been demonstrated in various models of bacterial and viral infection (Doitsh et al, 2013; Henry & Monack, 2007; Sansonetti et al, 2000).

1.2.5. NETosis/ETosis

NETosis is a form of neutrophil-specific regulated cell death characterized by chromatin condensation and the release of neutrophil extracellular traps (NETs) (Brinkmann et al, 2004). This cell death modality critically relies on ROS produced by members of the NADPH oxidase family and can thus be blocked pharmacologically by inhibitors targeting these enzymes (Remijnsen et al, 2010). NETs, which consist of DNA, chromatin and histones, allow neutrophils to immobilize and kill infectious agents and thus represent a defense mechanism against microorganisms (Remijnsen et al, 2011). The more general term ETosis has been introduced after this cell death modality had been reported to also occur in eosinophils, mast cells and macrophages (Wartha & Henriques-Normark, 2008).

1.2.6. Interconnectivity of Cell Death Pathways

Apoptosis is tightly interconnected with some of the signaling pathways leading to regulated necrosis (Linkermann & Green, 2014). For one part, this functional interplay depends on the fact that both forms of cellular demise share a number of common signal transducers. Secondly, extensive crosstalk between these pathways has been shown to occur in form of negative feedback circuitries, whereby one cell death pathway actively inhibits the other (Long & Ryan, 2012). The various subroutines of regulated necrosis are likewise interrelated (Galluzzi et al, 2014b). Despite being triggered by distinct upstream activators, the different pathways partially rely on the same signaling mediators. Furthermore, the different signaling cascades employ common biochemical mechanisms to execute cell death, primarily

involving the dysregulation of redox metabolism and bioenergetics, which results in osmotic swelling, energetic catastrophe, and, ultimately, loss of membrane integrity (Berghe et al, 2014).

1.3. Necroptosis

Necroptosis is the so far best-characterized form of regulated necrosis. Necroptotic cell death can be induced in response to pathogen infection as well as sterile cell injury (Chan et al, 2015). The key effector molecules are the signal transmitters RIPK1 and RIPK3, and the pseudokinase MLKL, which effectuates plasma membrane destabilization (Silke et al, 2015).

1.3.1. Triggers of Necroptosis

Necroptosis can be triggered by several receptors that are implicated in the detection of cellular stress, injury and infection (Figure 2) (Tait et al, 2014). TNF was the first stimulus found to induce regulated necrosis (Laster et al, 1988) and the necroptosis signaling pathway initiated by tumor necrosis factor receptor 1 (TNFR1) ligation has been particularly well

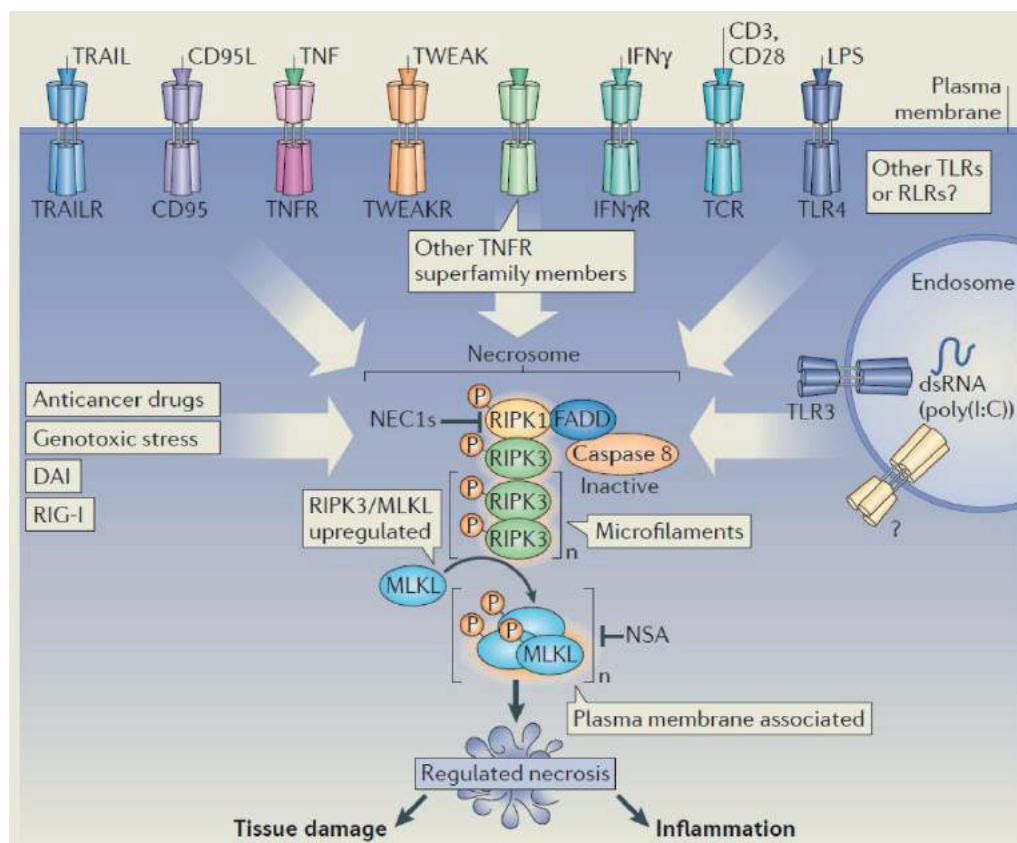


Figure 2: Triggers of Necroptosis. Necroptotic cell death can be initiated by ligation of TNFR1 and other death receptors in the TNF superfamily, IFNs, TLR and TCR signaling, viral infection or DNA damage. (Reprinted by permission from Macmillan Publishers Ltd: *Nature Reviews Molecular Cell Biology* 15, Berghe TV, Linkermann A, Jouan-Lanhouet S, Walczak H, Vandenabeele P, *Regulated necrosis: the expanding network of non-apoptotic cell death pathways*, 135-147, © 2014)

studied. Other death receptor ligands in the TNF superfamily, including FASLG and TRAIL, have similarly been shown capable of triggering necroptosis (Holler et al, 2000). Necroptosis can moreover be induced by ligation of TLR3 and TLR4, which employ the receptor interacting homotypic interaction motif (RHIM) domain-containing adaptor protein TRIF to activate RIPK3 (He et al, 2011; Kaiser et al, 2013). Likewise, the RHIM domain-containing protein DAI can activate RIPK3 in context of viral infection (Upton et al, 2012). More recently, both type I and type II interferons (IFNs) were shown to induce necroptosis depending on protein kinase R (PKR) in apoptosis-deficient cells (Thapa et al, 2013). Furthermore, activation of FADD- or CASP8-deficient T cells by T cell receptor (TCR) stimulation leads to RIPK1/RIPK3-mediated necroptosis (Ch'en et al, 2008). Upon genotoxic stress, RIPK3 can get activated in a RIPK1-dependent manner through assembly of a multi-protein complex termed ripoptosome (Feoktistova et al, 2011; Tenev et al, 2011).

1.3.2. Key Players of the Necroptosis Signaling Pathway

RIPK1 and RIPK3 are part of the seven member-containing RIP kinase family (Zhang et al, 2010). All RIPK family members share a homologous kinase domain, but harbor different functional domains (Figure 3) (Zhang et al, 2010). Whereas the functions of RIPK4-7 are yet poorly understood, RIPK1-3 have been assigned important roles in inflammation and cell death (Humphries et al, 2014). The C-terminal caspase activation and recruitment domain (CARD)-containing RIPK2 is an important mediator of nucleotide-binding oligomerization

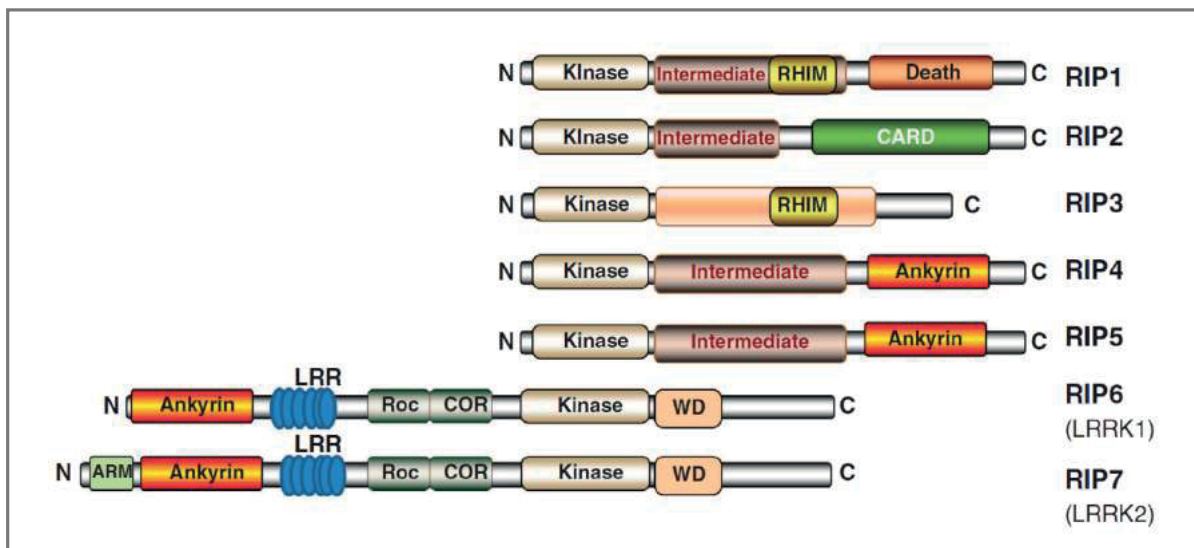


Figure 3: Domain Organization of the RIP Kinase Family. RIP kinases are a family of serine/threonine kinases. All seven members share the homologous kinase domain, but harbor different functional domains including RHIM, CARD, DD (Death), ankyrin repeat (Ankyrin), leucin-rich repeat (LRR), armadillo repeat (ARM), Ras in complex proteins/domain C-terminal of Roc (Roc/COR), and WD40 repeat (WD). (Reprinted by permission from Macmillan Publishers Ltd: *Cell Death and Differentiation* 22, Humphries F, Yang S, Wang B, Moynagh PN, RIP kinases: key decision makers in cell death and innate immunity, 225-236, © 2014)

domain (NOD) signaling (Nembrini et al, 2009; Park et al, 2007) and mucosal immunity (Balamayooran et al, 2011; Shimada et al, 2009). RIPK1 harbors a death domain (DD), allowing direct interaction with the intracellular DD of death receptors or other DD-containing proteins such as TNFRSF1A-associated via death domain (TRADD) (Chaudhary et al, 1997; Hsu et al, 1996a; Varfolomeev et al, 1996). Notably, RIPK1 and RIPK3 are the only RIPK family members possessing a RHIM domain (Humphries et al, 2014). The family designation 'receptor-interacting protein' stems from the first description of RIPK1 as a FAS-binding protein (Stanger et al, 1995). RIPK1 represents a critical regulatory node in the control of multiple cellular pathways mediating cell survival, inflammation and cell death (Ofengeim & Yuan, 2013). Most attention has been directed to its role as a molecular decision point between pro-inflammatory and cell death signaling after TNFR1 stimulation (Humphries et al, 2014). Given its relevance as a central hub at the crossroads of multiple signaling pathways decisive for cellular fate, RIPK1 underlies tight and complex regulation. Regulatory events described to impact on RIPK1 function include phosphorylation, ubiquitination, deubiquitination, as well as interaction with multiple ubiquitin receptors (Ofengeim & Yuan, 2013). RIPK3 was first identified based on its homology and binding to RIPK1 (Sun et al, 1999; Yu et al, 1999). Accordingly, early studies focused on its impact on the nuclear factor kappa-B (NF- κ B) pathway, demonstrating that RIPK3 overexpression is able to modulate NF- κ B signaling and induce apoptosis (Pazdernik et al, 1999). However, both NF- κ B activation and apoptosis signaling proceed normally in *Ripk3*^{-/-} cells (Newton et al, 2004), undermining the notion of a major role for RIPK3 in these pathways (Moriwaki & Chan, 2013). First cues for a role of RIPK3 in necroptosis arose from the observation that overexpression of a non-cleavable RIPK3 mutant triggered caspase-independent cell death (Feng et al, 2007). Soon thereafter, three parallel studies reported RIPK3 and its kinase activity to be involved in TNF-induced necroptosis downstream of RIPK1 (Cho et al, 2009; He et al, 2009; Zhang et al, 2009). Whereas RIPK1 is required to convey the activating signal to RIPK3 solely in context of death receptor-induced necroptosis, RIPK3 is now considered the convergence point of necroptosis execution, as it integrates activatory signals from various upstream inducers and RIPK3-mediated phosphorylation of MLKL is essential for necroptosis to occur (Lu et al, 2014). The second reported substrate of RIPK3 is the PGAM family member 5, serine/threonine protein phosphatase, mitochondrial (PGAM5) (Wang et al, 2012). However, as TNF-induced necroptosis was not impaired by neither small hairpin RNA (shRNA)-mediated knockdown of *Pgam5* (Murphy et al, 2013; Remijnsen et al, 2014), nor by widespread depletion of mitochondria (Tait et al, 2013), PGAM5 may not constitute a crucial component of the necroptosis machinery (Chan et al, 2015). The membrane rupture-inducing protein MLKL is the most terminal-known necroptosis effector to date and no other function has so far been ascribed to this protein (Czabotar & Murphy, 2015). MLKL was determined to

be the obligate downstream executor of necroptosis by a high throughput chemical screen for necroptosis inhibitors, which identified MLKL as target of the tool compound necrosulfonamide (NSA) (Sun et al, 2012), as well as by an shRNA screen for necroptosis effectors (Zhao et al, 2012). MLKL has been designated a pseudokinase, as two of the three key catalytic motifs for phosphoryl transfer activity are absent, rendering the protein enzymatically inactive (Manning et al, 2002; Murphy & Silke, 2014). Despite lacking catalytic activity, MLKL can bind adenosine triphosphate (ATP), which is however not required for necroptosis execution (Murphy et al, 2013).

1.4. Molecular Mechanisms and Regulation of TNF-Induced Necroptosis

TNFR1 is the prototypic DD-containing member of the TNF receptor family and mediates diverse signaling events after TNF binding (Christofferson et al, 2014). TNF is a pleiotropic, pro-inflammatory cytokine which plays an important role in innate immune responses and the regulation of immune cells. It is mainly derived from activated macrophages, but can also be released from other cell types (Wajant et al, 2003). Initially produced as type II transmembrane protein (Kriegler et al, 1988; Tang et al, 1996), the soluble, homotrimeric cytokine is released by TNF- α -converting enzyme (TACE)-mediated proteolytic cleavage (Black et al, 1997). Depending on the cell type, cellular activation state and microenvironment, the intricate signaling network operating downstream of TNFR1 can result in NF- κ B activation and survival, apoptosis or necroptosis in response to TNF (Figure 4) (Vandenabeele et al, 2010). The decision which signaling route will be taken critically relies on the composition of the signal transduction complexes that are formed upon ligand-receptor binding.

1.4.1. Complex I Formation and NF- κ B Activation

TNF binding to the preassembled TNFR1 trimer (Chan et al, 2000) triggers assembly of the short-lived, membrane-proximal, supramolecular complex I, which is composed of TRADD, TNF receptor associated factor 2 (TRAF2), RIPK1, cellular inhibitor of apoptosis (cIAP)1, cIAP2, and the linear ubiquitin chain assembly complex (LUBAC) (Micheau & Tschopp, 2003; Rieser et al, 2013). Signals emanating from complex I lead to NF- κ B-dependent induction of a number of pro-inflammatory and survival genes, including transcriptional targets required to counteract the cytotoxic effects of TNF (Chan et al, 2015). Complex I thus constitutes a critical checkpoint in the cellular decision between death and survival. In detail, TNFR1 ligation leads to DD-mediated recruitment of TRADD (Hsu et al, 1995) and RIPK1 (Hsu et al, 1996a). TRADD subsequently recruits TRAF2 (Hsu et al, 1996b), and thereby the ubiquitin ligases cIAP1 and cIAP2 (Rothe et al, 1995; Shu et al, 1996). Activated by proximity-induced dimerization, cIAP1 and cIAP2 decorate RIPK1 with K63 and K11 polyubiquitin chains

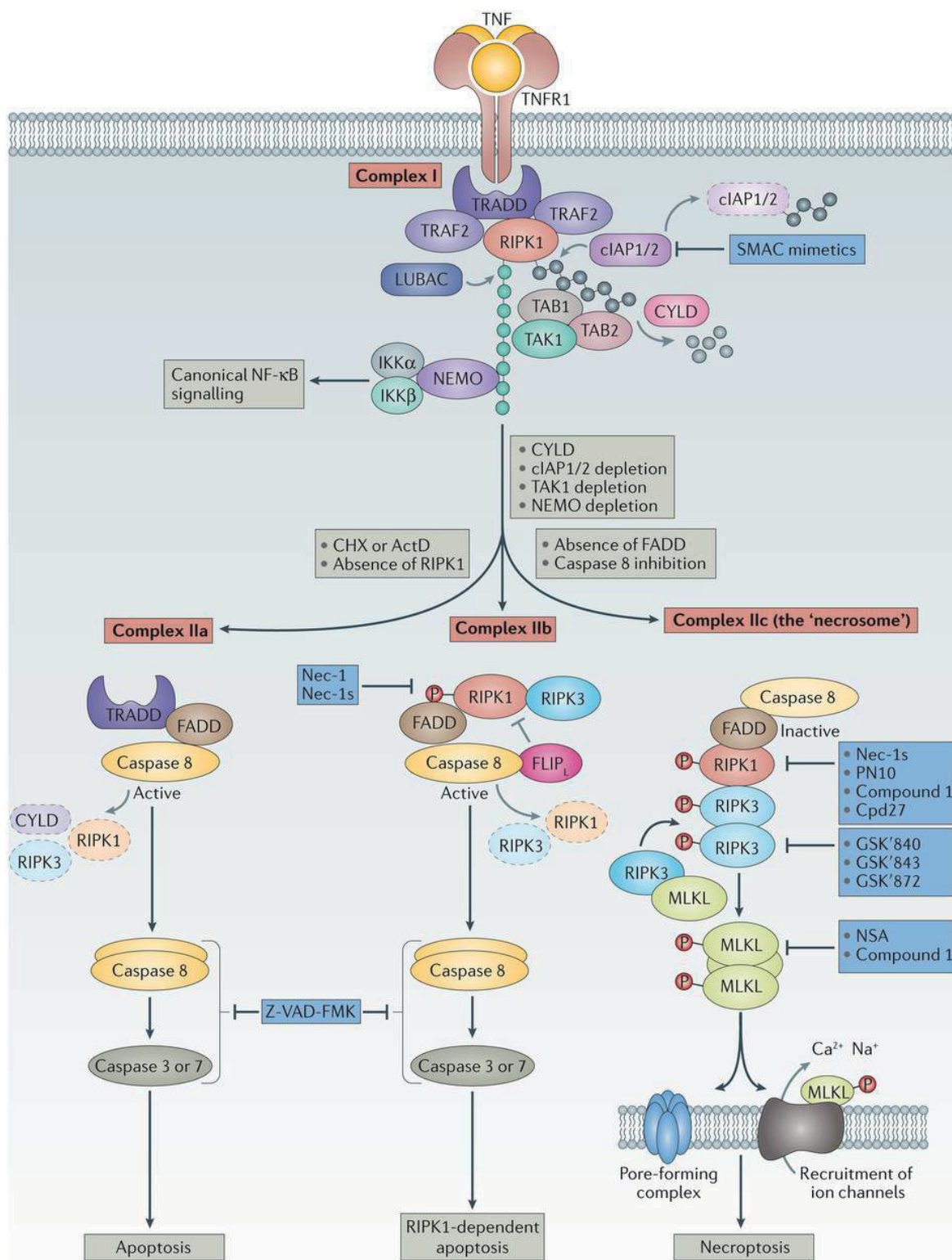


Figure 4: Signaling Events Downstream of TNFR1 Activation. TNF binding to TNFR1 triggers assembly of complex I, initiating NF-κB-dependent pro-survival signaling. Translational inhibition by cycloheximide (CHX) or actinomycin D (ActD) as well as RIPK1 deubiquitination by CYLD or loss of cIAP1/2 lead to induction of apoptosis via complex IIa or IIb. In conditions impeding full caspase activation, RIPK1 and RIPK3 form the necrosome, entailing MLKL activation and necroptotic cell death. (Reprinted by permission from Macmillan Publishers Ltd: *Nature Reviews Drug Discovery*, advance online publication, 18 January 2016, doi:10.1038/nrd.2015.6, Conrad M, Angeli JPF, Vandenabeele P, Stockwell BR, *Regulated necrosis: disease relevance and therapeutic opportunities*)

(Dynek et al, 2010; Varfolomeev et al, 2008). Ubiquitination of RIPK1 facilitates recruitment of the E3 ligase complex LUBAC, which consists of SHANK associated RH domain interactor (SHARPIN), heme-oxidized IRP2 ubiquitin ligase 1 (HOIL-1) and HOIL-1-interacting protein (HOIP), and catalyzes linear ubiquitination (Haas et al, 2009; Rieser et al, 2013). The ubiquitin network created within complex I is essential for recruitment of downstream components of the NF- κ B and mitogen-activated protein kinase (MAPK) signaling pathways (de Almagro & Vucic, 2015). The ubiquitin chains serve as landing platform for the inhibitor of nuclear factor kappa-B kinase (IKK) complex, consisting of IKK1, IKK2 and NF-kappa-B essential modulator (NEMO), as well as for transforming growth factor-beta-activated kinase 1 (TAK1) and its ubiquitin binding partners TGF-beta activated kinase 1/MAP3K7 binding protein (TAB)1 and TAB2 (Christofferson et al, 2014; O'Donnell & Ting, 2012). TAK1 activates the IKK complex, which in turn phosphorylates NF-kappa-B inhibitor alpha (I κ B α). I κ B α inhibits NF- κ B proteins by masking their nuclear localization signals (NLSs) and thus sequestering them in an inactive state in the cytoplasm. Phosphorylation marks I κ B α for ubiquitination and subsequent proteosomal degradation, allowing the thus liberated NF- κ B to translocate to the nucleus and activate transcription (O'Donnell & Ting, 2012). TNFR1 moreover induces activation of the MAPK pathway and the transcription factor activator protein-1 (AP-1) (Silke et al, 2015). Transcriptional targets of TNFR1 actively counteracting cell death signaling include cIAP1 and cIAP2, as well as the long form of cellular FLICE-like inhibitor protein (c-FLIP_L), inhibiting CASP8 (Chu et al, 1997; Kreuz et al, 2001; Wang et al, 1998). Dimerization of CASP8 and c-FLIP_L prevents apoptosis due to inhibition of full CASP8 activation (Pop et al, 2011). Yet, the heterodimer retains caspase activity towards RIPK1, RIPK3 and cylindromatosis (turban tumor syndrome) (CYLD), and thus simultaneously blocks necroptosis (O'Donnell et al, 2011; Oberst et al, 2011). The deubiquitinating enzyme CYLD and the ubiquitin-editing enzyme A20 are further transcriptional targets of NF- κ B (Humphries et al, 2014). A20 negatively regulates NF- κ B signaling and apoptosis by first removing the activating K63-linked polyubiquitin chains from RIPK1 to then promote K48-linked ubiquitination, targeting the protein for proteosomal degradation (Wertz et al, 2004). A recent study furthermore demonstrated a function for A20 in preventing overt necroptosis by inhibiting RIPK3 polyubiquitination (Onizawa et al, 2015). RIPK1 deubiquitination by CYLD similarly blunts NF- κ B signaling, but instead triggers cell death (Moquin et al, 2013). CYLD thus acts as a key switch in regulating the activation of apoptosis and necroptosis over cell survival signaling.

1.4.2. Formation of the Apoptosis-Promoting Complex II

Upon deubiquitination RIPK1 leaves complex I and translocates to the cytosol to associate with FADD, TRADD and pro-caspase-8, forming the apoptosis-inducing signaling platform complex II (Micheau & Tschopp, 2003; Wang et al, 2008). Assembly of complex II can

similarly be triggered by use of inhibitor of apoptosis protein (IAP) antagonists or loss of the cIAP proteins, which are responsible for ubiquitinating and thus stabilizing complex I (Wang et al, 2008). Within complex IIa, pro-caspase-8 gets processed into its active form, resulting in apoptotic cell death (Micheau & Tschopp, 2003). Active CASP8 moreover suppresses necroptosis by cleaving and thus inactivating RIPK1 (Lin et al, 1999), RIPK3 (Feng et al, 2007), and CYLD (O'Donnell et al, 2011). Complex II can also be formed independently of death receptor signaling upon genotoxic stress or in response to pattern recognition receptor activation through interaction between TRIF and RIPK1 (Feoktistova et al, 2011; Tenev et al, 2011). This complex IIb, also termed ripoptosome, contains CASP8, FADD, c-FLIP_L and RIPK1. Assembly of the ripoptosome requires RIPK1 kinase activity and can lead to CASP8-mediated apoptosis or RIPK3-dependent necroptosis, depending on the regulation of caspase activity by the cellular FLICE-like inhibitory protein (c-FLIP) isoforms (Feoktistova et al, 2011; Tenev et al, 2011). In conditions blocking caspase activity or impeding their full activation, stabilization of RIPK1 and RIPK3 prompts conversion into complex IIc, termed necrosome (Cho et al, 2009).

1.4.3. RHIM Domain-Mediated Necrosome Formation

Within the necrosome, RIPK1 and RIPK3 engage in a series of auto- and cross-phosphorylation events, which are essential for necroptosis induction (Cho et al, 2009). Thus, whereas the initial cellular decision between survival and apoptosis relies on the ubiquitination status of RIPK1, necroptosis signaling depends on its kinase activity. Yet, direct phosphorylation of RIPK3 by RIPK1 has not been demonstrated. Recent evidence rather supports a function for RIPK1 in initiating the nucleation event required for RIPK3 oligomerization and auto-phosphorylation (Chan et al, 2015). It has been shown that inducible dimerization of RIPK3 as well as expression of a phosphomimetic RIPK3 mutant can trigger MLKL-dependent necroptosis in absence of RIPK1 (Cook et al, 2014; McQuade et al, 2013; Orozco et al, 2014; Wu et al, 2014). Accordingly, it has been suggested that RHIM domain-driven interaction between the two kinases leads to RIPK3 auto-activation (Li et al, 2012; Silke et al, 2015). The RHIM domain is a conserved signaling motif defined by a tetrapeptide core flanked by hydrophobic residues, predominantly adopting β -sheet folding (Chan et al, 2015). Four RHIM-domain containing proteins have been identified in humans: RIPK1, RIPK3, DAI, and TRIF. These signaling proteins share roles in innate immunity, cell death, or both, as a common denominator (Kaiser & Offermann, 2005; Ofengeim & Yuan, 2013; Rebsamen et al, 2009). Moreover, all RHIM domain-containing adaptors have a strong tendency to form amyloid fibrils *in vitro* either by themselves or in complex with a second RHIM-domain containing protein (Li et al, 2012). Interestingly, viral RHIM-domain containing inhibitors that bind and block RIPK3 have been described (Rebsamen et al, 2009; Upton et al, 2012). These viral proteins function to prevent virus-induced necroptosis and thus allow the

virus to establish productive infection, as execution of necroptotic cell death critically relies on formation of the unique RHIM domain-dependent amyloid scaffold in the necrosome for RIPK3 activation and induction of downstream signaling. Active RIPK3 binds and phosphorylates MLKL, unleashing its activity as necroptosis executor (Sun et al, 2012; Zhao et al, 2012). RIPK3-MLKL binding requires RIPK3 itself to be phosphorylated on S227 in human, or T231 and S232 in mouse cells. Upon interaction, RIPK3 phosphorylates human MLKL on T357 and S358, and mouse MLKL on S345, S347 and T349, respectively (Murphy et al, 2013; Sun et al, 2012). Phosphorylation of S345 in the activation loop of the pseudokinase domain of murine MLKL, corresponding to S358 in the human protein, represents the essential step for execution of necroptotic cell death (Murphy et al, 2013; Tanzer et al, 2015).

1.4.4. Necroptosis Execution by MLKL

MLKL mediates necroptosis execution through its N-terminal four-helix bundle (4HB) (Chen et al, 2013; Dondelinger et al, 2014; Hildebrand et al, 2014). Activation of MLKL likely occurs through a molecular switch mechanism. Phosphorylation of the pseudokinase domain induces a conformational change by which the 4HB domain is released (Hildebrand et al, 2014; Murphy et al, 2013). The phospho-mimetic S345D MLKL mutant protein is constitutively active and triggers cell death upon expression (Murphy et al, 2013). This stimulus-independent necroptosis proceeds even in absence of RIPK3, corroborating that MLKL phosphorylation is the crucial role played by RIPK3 in necroptosis signaling. The structures of mouse (Figure 5a) (Murphy et al, 2013) and human (Murphy et al, 2014) MLKL have recently been solved, helping to further unveil the molecular mechanism of MLKL activation. The integrity of the pseudoactive site of MLKL seems to be intrinsically intertwined with the activation of the necroptosis executory function of the protein (Murphy & Silke, 2014). The residues K219 and Q343 located within the pseudoactive site of murine MLKL have been reported to interact (Figure 5b) (Murphy et al, 2013). Similar to S345D, also K219M or Q343A mutations cause cell death. Mutation of these residues presumably emulates activatory conformational changes in the MLKL protein, similar to those triggered by RIPK3-mediated phosphorylation of the activation loop (Murphy et al, 2013; Murphy & Silke, 2014). Moreover, it was shown that expression of the executioner 4HB domain by itself is sufficient for initiation of necroptosis (Chen et al, 2013; Dondelinger et al, 2014; Hildebrand et al, 2014), providing further evidence that conformational release of this region is sufficient to induce cell killing (Czabotar & Murphy, 2015). Interestingly, a recent study identified additional phosphorylation events on MLKL, potentially contributing to fine-tuning of its activation potential (Tanzer et al, 2015). Phosphorylation of one of these sites, S228, may be involved in relieving a suppressive interaction between RIPK3 and MLKL, suggestive of a so far unappreciated role of RIPK3 in constraining MLKL activation. Downstream execution of

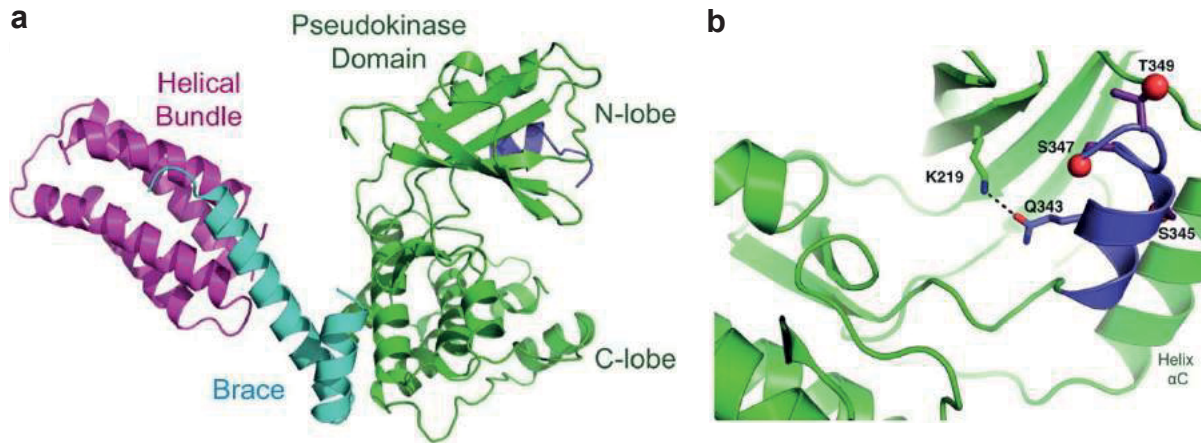


Figure 5: Crystal Structure of Full-Length Mouse MLKL. (a) MLKL contains an N-terminal 4HB (Helical Bundle) domain (magenta) connected via a two-helix brace (cyan) to the C-terminal pseudokinase domain (green). The N-lobe of the pseudokinase domain contains the activation loop helix (violet). (b) Close-up view of the MLKL pseudoactive site with K219:Q343 interaction and phosphorylation sites S345, S347, and T349 highlighted. (Reprinted and adapted with permission from Elsevier: *Immunity* 39, Murphy James M, Czabotar Peter E, Hildebrand Joanne M, Lucet Isabelle S, Zhang J-G, Alvarez-Diaz S, Lewis R, Lalaoui N, Metcalf D, Webb Andrew I, et al., *The Pseudokinase MLKL Mediates Necroptosis via a Molecular Switch Mechanism*, 443-453, © 2013)

necroptosis critically relies on 4HB domain-mediated MLKL homooligomerization and membrane translocation. Whereas formation of high molecular weight oligomers is clearly required for necroptotic cell death (Dondelinger et al, 2014), there are conflicting reports on whether MLKL forms trimers (Cai et al, 2013), tetramers (Chen et al, 2013) or hexamers (Wang et al, 2014a). Yet another study proposed formation of MLKL homotrimers in the cytoplasm, which incorporate into high molecular weight membrane-localized complexes upon cell death signaling (Hildebrand et al, 2014). Similarly, the exact molecular mechanism by which the 4HB domain induces membrane rupture is still a matter of debate. The MLKL oligomers have been proposed to disrupt osmotic homeostasis via altering ion flux through either acting on the membrane themselves or targeting membrane proteins (Cai et al, 2013; Chen et al, 2013; Dondelinger et al, 2014; Wang et al, 2014a). In detail, one study reported increased Ca^{2+} influx through transient receptor potential cation channel, subfamily M, member 7 (TRPM7) as an executioner mechanism of MLKL (Cai et al, 2013). Another study found MLKL-mediated regulation of Na^{2+} channels to be causative for ion influx, increased osmotic pressure and membrane rupture (Chen et al, 2013). Subsequent reports revealed that the 4HB domain of MLKL is capable of binding to phosphatidylinositol phosphates (PIPs) (Dondelinger et al, 2014; Wang et al, 2014a) as well as cardiolipin (Wang et al, 2014a). It was suggested that, through interaction with these negatively charged lipids, the MLKL oligomers become incorporated into both plasma and intracellular membranes, and thus directly disrupt membrane integrity by pore formation (Wang et al, 2014a). Indeed, inhibition

of PI(5)P and PI(4,5)P₂ formation specifically blocked TNF-induced necroptosis, but not apoptosis (Dondelinger et al, 2014). Additionally, the 4HB-containing N-terminal region of MLKL was found sufficient to mediate leakage of PIP-containing liposomes, further corroborating the notion of MLKL assembling into a pore that facilitates osmosis-mediated membrane rupture (Dondelinger et al, 2014; Wang et al, 2014a). The conflicting earlier reports on the requirement of Ca²⁺ (Cai et al, 2013) or Na²⁺ (Chen et al, 2013) influx for necroptosis would be reconciled by a model in which MLKL directly disrupts the membrane, as both phenomena could be a result of pore formation. However, another study challenged the idea of the 4HB domain engaging phospholipid membranes by simple positive-negative charge pairing (Hildebrand et al, 2014). The polarity of charged residues in the 4HB domain is poorly conserved between orthologs from different species, whereas their presence in specific positions is preserved. Alanine scanning mutagenesis led to the identification of two clusters on opposing faces of the 4HB domain that are required for cell killing (Hildebrand et al, 2014). Whereas the integrity of one cluster was crucial for membrane localization, mutations in the other cluster allowed membrane translocation of MLKL, but prevented cell killing. These results indicate that membrane localization of MLKL is necessary, but not sufficient to induce necroptotic cell death, suggesting that additional, yet unidentified mechanisms are required for the 4HB domain to execute cell death (Hildebrand et al, 2014).

1.4.5. Necroptosis-Independent Functions of RIPK1 and RIPK3

Besides necroptosis, RIPK1 kinase function is required for ripoptosome-mediated apoptosis induction (Feoktistova et al, 2011; Tenev et al, 2011; Wang et al, 2008). Moreover, RIPK1 has been reported to activate JNK- and AP-1-mediated TNF transcription in a kinase-dependent manner under certain conditions (Christofferson et al, 2012; McNamara et al, 2013). DAI-mediated RIPK1/RIPK3 complex formation can likewise induce NF-κB-dependent cytokine expression (Kaiser et al, 2008; Rebsamen et al, 2009). Independently from cell death signaling, RIPK3 has been shown to directly contribute to inflammatory cytokine activation in the context of TLR stimulation or virus infection. More precisely, RIPK3 has been implicated in activation of the NLRP3 inflammasome and IL-1β release in cIAP-depleted macrophages, CASP8-deficient dendritic cells and RNA-virus infected cells (Kang et al, 2013; Vince et al, 2012; Wang et al, 2014b).

1.5. Necroptosis in Health and Disease

Necroptosis has been shown to contribute to pathology connected with sterile-injury induced inflammation as well as different diseases associated with chronic inflammation (Table 1) (Chan et al, 2015). The detrimental role of necroptosis in different human disease conditions raises the question why this cell death module has been evolutionarily preserved. The

Table 1: Necroptosis-Related Diseases

Cause of Cell Injury	Disease / Pathogen	(References)
Viral infection	Vaccinia virus	(Cho et al, 2009)
	Murine cytomegalovirus	(Upton et al, 2010; Upton et al, 2012)
	Herpes simplex virus	(Guo et al, 2015; Huang et al, 2015)
	Human immunodeficiency virus type-1	(Pan et al, 2014)
Bacterial infection	<i>Staphylococcus aureus</i>	(Kitur et al, 2015)
	<i>Salmonella enterica</i> serovar Typhimurium	(Robinson et al, 2012)
Sterile injury-induced inflammation	Retinal degeneration	(Kataoka et al, 2015; Murakami et al, 2013; Murakami et al, 2012)
	Ethanol-induced liver injury	(Roychowdhury et al, 2013)
	Non-alcoholic steatohepatitis	(Gautheron et al, 2014)
	Multiple sclerosis	(Ofengeim et al, 2015)
	Atherosclerosis	(Lin et al, 2013)
	Ischemia-reperfusion kidney injury	(Linkermann et al, 2013a)
	Myocardial infarction	(Oerlemans et al, 2012)
	Ischemia-reperfusion-induced brain injury	(Degterev et al, 2005; Northington et al, 2010)
	Gaucher's disease	(Vitner et al, 2014)
Pancreatitis	(He et al, 2009; Wu et al, 2013a)	

probably best evidenced role for necroptosis *in vivo* to date is the regulation of viral infection (Cho et al, 2009; Upton et al, 2010). In this context, necroptosis serves a beneficial role by limiting virus replication and promoting innate immune responses against infected cells by causing danger-associated molecular pattern (DAMP) release, and thus furthering immune cell activation (Chan et al, 2015). Many viruses encode apoptosis inhibitors, which led to the hypothesis that the necroptotic pathway evolved as a backup mechanism to trigger cell death in suchlike infected cells (Mocarski et al, 2015; Mocarski et al, 2012). Intriguingly, virus-encoded RHIM domain-containing inhibitors of RIPK1-RIPK3 signaling have likewise been identified (Guo et al, 2015; Huang et al, 2015; Upton et al, 2010). The existence of such inhibitors is suggestive of a common immune evasion strategy, and corroborates the notion of necroptotic cell death as the outcome of a co-evolutionary process with certain virus species that target vertebrates. According to this concept, the pathological role of necroptosis in sterile injury-induced inflammation may represent the flipside of this evolutionary rivalry with the viruses (Chan et al, 2015).

1.5.1. Physiological Relevance of Necroptotic Cell Death

In line with the notion that necroptosis serves to eliminate unwanted cells in situations where the preferred apoptosis pathway is blocked (Vandenabeele et al, 2010), interdigital cells or thymocytes from mice lacking apoptotic peptidase activating factor 1 (*Apaf1*) die by necroptosis with identical timing and to the same extent at which these cells undergo apoptosis in wild-type mice (Chautan et al, 1999). Under physiological conditions, CASP8 and FADD act as gatekeepers preventing necroptotic cell death. Indeed, genetic studies in mice have revealed that necroptosis is actively suppressed in many cell types both during development and in adult tissues. Deficiency in *Fadd* or *Casp8* leads to embryonic lethality (Varfolomeev et al, 1998; Yeh et al, 1998; Zhang et al, 1998) due to necroptosis-mediated loss of the endothelial cells responsible for vasculature formation in the developing yolk sac. This CASP8-dependent prenatal death can be rescued by co-deletion of *Ripk3* (Kaiser et al, 2011; Oberst et al, 2011). Likewise, loss of *Ripk1* permits embryogenesis to proceed normally in *Fadd*^{-/-} mice (Zhang et al, 2011). Disabling the ability of CASP8 to inhibit RIPK3 in an organ-specific manner in adult mice has been shown to induce RIPK3-dependent inflammation and cell death in the intestine and skin (Bonnet et al, 2011; Weinlich et al, 2013; Welz et al, 2011). Similarly, antigen-driven clonal expansion of T lymphocytes in context of compromised function of FADD or CASP8 results in RIPK3-dependent necroptosis (Ch'en et al, 2011; Lu et al, 2011). Various pathogens can induce activation of RIPK3 (Kitur et al, 2015; Pan et al, 2014; Robinson et al, 2012), and necroptosis has been demonstrated to play a crucial role in limiting infection with vaccinia virus (Cho et al, 2009), murine cytomegalovirus (Upton et al, 2010; Upton et al, 2012), and herpes simplex virus (Guo et al, 2015; Huang et al, 2015). A recent study moreover showed that necroptosis efficiently induces dendritic cell-mediated cross-priming of CD8⁺ T cells via RIPK1-dependent NF- κ B activation within dying cells (Yatim et al, 2015).

1.5.2. Contribution of Necroptosis to Pathophysiological Processes

Based on evidence derived from mouse models of human diseases, RIPK1, RIPK3 and MLKL have been assigned roles as mediators of tissue damage (Silke et al, 2015). However, due to the multifarious roles of these proteins in the regulation of cell survival, inflammation and cell death, delineating their precise contribution to these disease processes has proven challenging. Pathologies which have been linked to necroptosis include retinal degeneration and retinitis pigmentosa (Kataoka et al, 2015; Murakami et al, 2013; Murakami et al, 2012; Sato et al, 2013), ethanol-induced liver injury (Roychowdhury et al, 2013), non-alcoholic steatohepatitis (Gautheron et al, 2014), multiple sclerosis (Ofengeim et al, 2015) and atherosclerosis (Lin et al, 2013). Necroptosis has moreover been shown to contribute to IR-induced tissue injury in the kidney (Linkermann et al, 2013a), brain (Degterev et al, 2005;

Northington et al, 2010), and myocardial infarction (Oerlemans et al, 2012). Detrimental roles for necroptotic cell death have furthermore been identified in Gaucher's disease (Vitner et al, 2014), cerulein-induced pancreatitis (He et al, 2009; Wu et al, 2013a) as well as in cecal ligation puncture sepsis, TNF-induced systemic inflammatory response syndrome (SIRS) and TNF-induced hyper-acute shock (Duprez et al, 2011; Linkermann et al, 2012; Newton et al, 2014; Polykratis et al, 2014). RIPK3 deficiency leads to prolonged kidney and heart allograft survival, suggesting a role for necroptosis-induced inflammation in transplant rejection (Lau et al, 2013; Pavlosky et al, 2014). In addition to its implication in the aforementioned pathologies, necroptotic cell death has been suggested to contribute to the amplification and chronification of inflammation (Pasparakis & Vandenabeele, 2015). Many of the cytokines produced during immune responses, as for instance TNF family members or IFNs, can potently induce cell death. The loss of membrane integrity in cells dying by necroptosis leads to the release of DAMPs, which in turn further fuel inflammation (Kaczmarek et al, 2013; Linkermann et al, 2014c).

1.6. Experimental Systems and Tools to Study Necroptosis

A number of cell types can undergo necroptotic cell death upon stimulation *in vitro*. These cell lines and primary cells have been crucial in gaining insight into the molecular details of the necroptosis pathway. Likewise, genetic studies in mice have furthered understanding of the various functions carried out by the proteins involved in necroptotic signaling in disease models as well as during development. However, detection of necroptotic cell death *in vivo* has been hampered by a lack of definite molecular markers robustly distinguishing necroptosis from other forms of cellular demise. In contrast to the well-established methods to routinely identify apoptotic cells in primary tissue, comparable reagents for detection of necroptosis are only now becoming available.

1.6.1. Distinguishing Features of Necroptotic Cell Death

Necrotic morphology and absence of caspase-3 activation discern necrosis from apoptosis, yet they do not allow discriminating different forms of programmed necrotic cell death (Pasparakis & Vandenabeele, 2015). Other classical apoptosis markers, such as phosphatidylserine exposure and DNA breaks, may also be found in necrotic cells (Günther et al, 2011; Sawai & Domae, 2011). The RIPK1-inhibitor Nec-1, which had been widely used to define necroptosis, was found to have an off-target effect on the immunomodulatory enzyme indoleamine 2,3-dioxygenase 1 (IDO1) (Takahashi et al, 2012). Usage of Nec-1 as a criterion for necroptosis is further undermined by the emerging evidence for RIPK1 kinase-dependent functions beyond necroptotic cell death (Pasparakis & Vandenabeele, 2015). Necroptosis can however be molecularly defined by dependence on RIPK3 and MLKL, as

their absence prevents necroptotic cell death. Moreover, phosphorylation of human MLKL on residues T357 and S358 represents a specific biochemical mark for necroptosis (Sun et al, 2012). A recently developed antibody recognizing phosphorylated MLKL thus constitutes the first specific tool for identification of necroptotic cells and their detection in primary human tissues (Wang et al, 2014a).

1.6.2. Cellular Models of Necroptosis

The death receptor ligands TNF, FASLG and TRAIL are commonly employed to induce necroptosis in cellular model systems. Triggering necroptosis signaling *in vitro* usually requires inhibition of apoptosis, which can be achieved by caspase inhibitors such as Z-Val-Ala-Asp fluoromethyl ketone (Z-VAD-fmk), or the absence of upstream apoptosis adaptors by genetic knockout or small interfering RNA (siRNA)-mediated knockdown of *FADD* or *CASP8* (Degterev et al, 2014). One of the most frequently used model systems for studying necroptosis are FADD-deficient Jurkat cells. This cell line was created in a forward genetic approach using chemical mutagenesis to identify genes that are essential for FAS-induced apoptosis (Juo et al, 1999). Whilst being resistant to FASLG-induced cell death, these cells readily undergo necroptosis upon TNF stimulation (Lawrence & Chow, 2005). Other frequently used cell types are the human colorectal adenocarcinoma cell line HT-29 and the myeloid lymphoma cell line U937. Murine cell lines commonly used to study necroptotic cell death are L929 and NIH3T3-N, as well as mouse embryonic fibroblasts. In L929 cells, necroptosis can be induced by singular treatment with either TNF (Vercaemmen et al, 1997) or Z-VAD-fmk, which triggers autocrine TNF production (Wu et al, 2010). However, depending on the cell type, the presence of further sensitizing agents besides caspase inhibitors may be needed to counteract NF- κ B-dependent pro-survival signaling. To this end, the protein synthesis inhibitor cycloheximide or cIAP1/2 inhibition by second mitochondria-derived activator of caspase (SMAC) mimetics such as Birinapant (Krepler et al, 2013) or BV6 (Varfolomeev et al, 2007) can be used. Notably, several commonly used epithelial cancer cell lines, including HeLa and HEK293 cells, are resistant to necroptosis. This lack of sensitivity could partially be explained by absence of RIPK3 expression (He et al, 2009). Whereas RIPK3 is expressed in multiple adult tissues, it is often silenced in cancer cell lines, suggestive of an advantageous effect of RIPK3 elimination (Morgan & Kim, 2015).

1.6.3. Tool Compounds to Block Necroptosis

A number of compounds targeting RIPK1, RIPK3 or MLKL have been developed in the past years (Figure 6). These small molecule inhibitors have proven useful tools in exploring the activation of the necroptosis pathway both *in vitro* and *in vivo*. Nec-1 is the most commonly employed RIPK1 inhibitor so far (Degterev et al, 2005). However, its use is restricted by non-specific activity as well as limited metabolic stability, which results in a short *in vivo* half-life

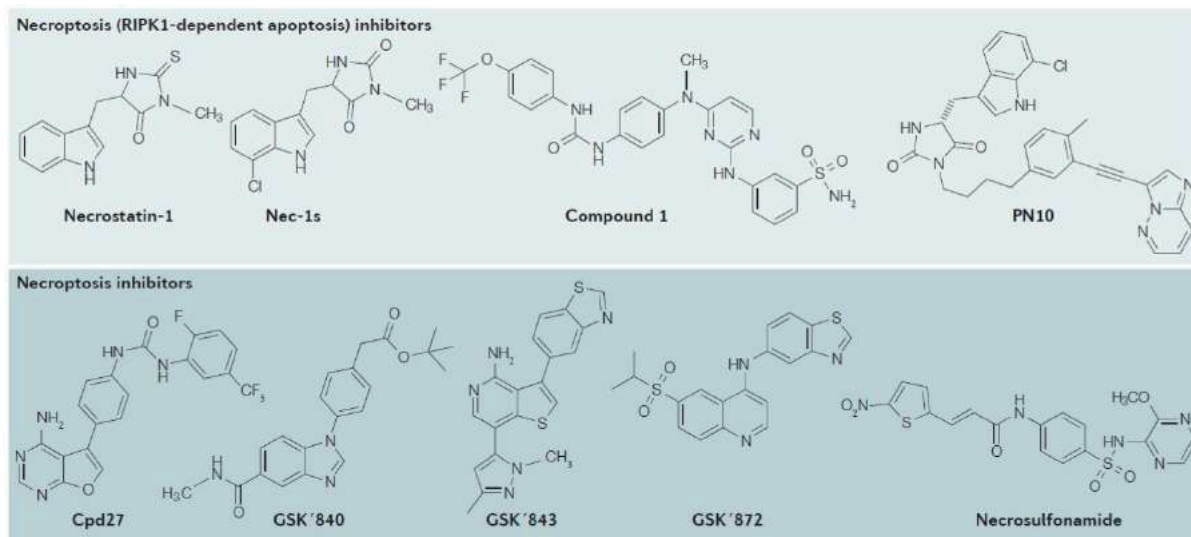


Figure 6: Chemical Structures of Necroptosis Inhibitors. The selected small molecules inhibit necroptotic cell death by targeting either RIPK1 (Necrostatin-1, Nec-1s, PN10, Cpd27), RIPK3 (GSK'840, GSK'843, GSK'872) or MLKL (Compound 1, Necrosulfonamide). (Adapted and reprinted by permission from Macmillan Publishers Ltd: *Nature Reviews Drug Discovery*, advance online publication, 18 January 2016, doi:10.1038/nrd.2015.6, Conrad M, Angeli JPF, Vandenabeele P, Stockwell BR, *Regulated necrosis: disease relevance and therapeutic opportunities*)

(Takahashi et al, 2012; Teng et al, 2005). The optimized RIPK1 inhibitor 7-Cl-O-Nec-1 (Nec-1s) is structurally related to Nec-1, but displays improved potency, specificity and pharmacokinetic properties (Degterev et al, 2005; Degterev et al, 2012). Efforts to identify next generation RIPK1 inhibitors have led to the development of Cpd27 (Harris et al, 2013), as well as GSK'963, which targets RIPK1 with high potency and selectivity, but is structurally distinct from necrostatins (Berger et al, 2015). Inhibitors described for RIPK3 include GSK'843 and GSK'872, targeting both murine and human RIPK3, as well as the human-selective small molecule GSK'840 (Kaiser et al, 2013; Mandal et al, 2014). Whereas all three compounds efficiently block necroptosis, high concentrations of GSK'843 and GSK'872 trigger rapid apoptosis in the absence of caspase inhibition (Mandal et al, 2014). Interestingly, the B-Raf proto-oncogene, serine/threonine kinase (BRAF) inhibitor dabrafenib was found to have an off-target effect on RIPK3, with possible implications for its use in melanoma therapy (Geserick et al, 2015; Li et al, 2014). The pseudokinase MLKL can be targeted using NSA, which forms a covalent bond with Cys86 of human MLKL, but fails to inhibit the mouse protein lacking the orthologous Cys residue (Sun et al, 2012). The small molecule termed compound 1 binds the mouse MLKL pseudokinase domain and blocks oligomerization and membrane translocation (Hildebrand et al, 2014). The inhibitor Nec-7 has been shown to block necroptosis, though its specific target has remained elusive so far (Zheng et al, 2008). Finally, HSP90 inhibition can be used as an unselective tool to inhibit

necroptotic cell death by causing degradation of the proteins involved in the necroptosis signaling pathway (Cho et al, 2009; Holler et al, 2000; Lewis et al, 2000; Li et al, 2015).

1.6.4. Mouse Models to Study Necroptosis

Genetic studies and extensive crosses using *Ripk1*^{-/-}, *Ripk3*^{-/-}, and *Mlkl*^{-/-} mice have led to a greater understanding of the function of these three proteins in embryonic development and beyond (Silke et al, 2015). *Ripk1*-deficient mice die soon after birth and this early lethality has long remained a conundrum (Kelliher et al, 1998). The perinatal death is associated with aberrant CASP8-dependent apoptosis in the gut and systemic inflammation, largely driven by necroptosis. The lethality of *Ripk1*-deficient mice can thus be genetically rescued by concomitant deletion of *Ripk3* and *Fadd* or *Casp8* (Dillon et al, 2014; Kaiser et al, 2014; Rickard et al, 2014). Whereas necroptosis signaling relies on the catalytic activity of RIPK1, its kinase function is dispensable for NF-κB activation (Cho et al, 2009). Yet, loss of the kinase-independent scaffolding function of RIPK1 was found responsible for the early lethality of knockout animals, as mutant mice expressing catalytically inactive D138N or K45A versions of RIPK1 are viable (Kaiser et al, 2014; Newton et al, 2014). Importantly, these mutant mice are resistant to necroptosis, in turn corroborating the requirement of RIPK1 kinase function for this process. In contrast to *Ripk1* knockout mice, *Ripk3*^{-/-} mice are viable (Newton et al, 2004) and could be employed to confirm the crucial role of RIPK3 in necroptosis signaling *in vivo* (Cho et al, 2009; He et al, 2011). Interestingly, whereas mice expressing catalytically inactive K51A RIPK3 behave like *Ripk3* knockout mice (Mandal et al, 2014), mice expressing D161N mutant RIPK3 die during mid-gestation due to RIPK1- and CASP8-dependent apoptosis (Newton et al, 2014). Selective small molecule RIPK3 inhibitors can confer this apoptosis-activating property also to wild-type as well as mutant K51A RIPK3 (Mandal et al, 2014). The CASP8 activation triggered by RIPK3 inhibitors or the D161N mutation may thus be due to a conformational change in RIPK3, which increases its propensity to engage RIPK1, whilst being defective for necroptosis signaling (Newton, 2015; Oberst, 2015). *Mlkl* knockout mice are viable and fertile (Murphy et al, 2013; Wu et al, 2013a). Whereas MLKL-deficient cells can undergo apoptosis, they are resistant to necroptotic cell death, substantiating the role of MLKL as necroptosis downstream effector (Wu et al, 2013a). Genetic ablation of *Ripk3* or *Mlkl*, as well as catalytic inhibition of RIPK1 by Nec-1, have been shown to ameliorate disease outcome in various mouse models of human diseases (Khan et al, 2014; Newton, 2015; Zhou & Yuan, 2014) and the potential implication for necroptosis in the pathophysiology of several human inflammatory diseases has been revealed by this means. However, due to its known off-target effects (Takahashi et al, 2012) the results obtained with Nec-1 may require reevaluation using the optimized analogue Nec-1s (Degterev et al, 2008; Teng et al, 2005). Furthermore, given the emerging evidence that RIPK3 is capable of triggering inflammation in a cell death-independent manner (Kang et al,

2013; Vince et al, 2012; Wang et al, 2014b), it will be important to distinguish which RIPK3 signaling axis contributes to the respective disease phenotypes. Insight into the necroptosis-independent functions of RIPK3 may be gained by comparison of *Ripk3*^{-/-} and *Mlkl*^{-/-} mice. Yet, it remains to be clarified if also MLKL has additional functions beyond necroptosis execution.

1.7. Experimental Approaches for Identification of Necroptosis Inhibitors and Target Deconvolution

Common avenues for drug discovery can be separated into target-based versus systems-based approaches (Eder et al, 2014). Target-based approaches are hypothesis-driven and aim to modulate a biological system by pharmacological interference with a specific target or component. In contrast, systems-based or reverse pharmacology approaches rely on hypothesis-agnostic assays. In such phenotypic screening approaches, large numbers of compounds are assayed for a desirable effect in the physiological context of cells or whole organisms without prior understanding of their mode of action or specific targets (Lee & Bogoy, 2013; Moffat et al, 2014). On the basis of this unbiased, function-first strategy, efforts to identify the respective drug target are undertaken only afterwards. Such an approach can reveal the implication of proteins or pathways which have not yet been associated with a particular biological output. Molecules identified by phenotype-based screening may have a higher likelihood of showing clinical efficacy than those derived from target-based approaches. Even well-validated drugs developed in a target-based fashion often fail later during development as, in the face of the complexity of intra- and intercellular signaling or resistance mechanisms, inhibition of a single target may prove insufficient (Moffat et al, 2014). Clinical inefficacy may similarly originate in toxicity issues or the insufficiency of the drug to, despite robust target binding, block the disease-relevant activity or interaction (Eder et al, 2014). These drawbacks associated with target-based approaches are avoided in phenotype-based screening, as the desired phenotype and potential side effects are directly assessed in the context of a complex biological system. Phenotypic screening approaches typically monitor cellular processes such as signaling and transcription, cell growth and death, or classic phenotypic traits such as morphology, motility or differentiation (Moffat et al, 2014). Accordingly, the types of readouts applied range from determining gene expression, cytotoxicity or cell cycle phase, to measuring biochemical events such as protein expression, localization, degradation or post-translation modifications. Besides the selectivity of the readout, assembling the chemical library to be queried according to the scope and setup of the respective assay is of vital importance. Target-based assays commonly employ focused libraries, tailored to impact on a certain target or target family. In contrast, compound libraries for phenotypic screening should be assembled with the aim of achieving maximum biological

and chemical diversity (Petroni et al, 2013; Wassermann et al, 2014). Furthermore, to show activity in phenotypic screening approaches, the small molecules need to penetrate the cells. The chemical libraries should thus be tailored to contain compounds meeting the required physicochemical properties regarding solubility and cellular permeability (Wassermann et al, 2014). Commonly used screening concentrations range around 10 μ M or higher, though may further manifestation of the polypharmacology properties of the queried compounds. Accordingly, the interpretation of screening results may be curbed by the necessity to delineate which target is responsible for mediating the desired phenotypic effect (Wassermann et al, 2014). Increased robustness and potency of the resulting data can be achieved by screening either more than a single compound concentration or generally in a titration-based manner (Inglese et al, 2006; Zhang et al, 2013). A broad classification separates compounds into tools, probes, and drugs. Whereas tool compounds can be widely used to study general biological mechanisms, they may not be selective (Wassermann et al, 2014). In contrast, probes are designed to interrogate a particular target or pathway, though may not be as widely applicable. Lastly, drugs are small molecules whose beneficial effects are exploited pharmaceutically to prevent, diagnose, treat, or cure disease. These small molecules have undergone extensive optimization of their physicochemical properties to meet the stringent requirements for drug approval regarding toxicity, bioavailability and metabolic stability. Indeed, only ~1200 new drugs have gained approval by the FDA over the last 60 years (Munos, 2009). Whereas a number of tool compounds inhibiting different necroptosis signaling pathway members have been described to date, transition of a promising molecule into an approved drug may prove time-consuming and costly, or fail altogether due to safety issues (Hay et al, 2014). Drug repurposing can enhance efficiency of drug development tracks by circumventing omission caused by toxicity not predicted by preclinical studies (Ashburn & Thor, 2004; Strittmatter, 2014). Accordingly, assaying compounds that have originally been developed for another indication, and are thus established as safe and tolerable for humans, may help to overcome the initial bottleneck in the drug development process (Ashburn & Thor, 2004). Such compounds may then be assigned new purposes in other disease states, as either their particular target may play a role in another clinical condition, or they may act through previously unrecognized targets in different diseases. To identify the targets of a given compound whose molecular mechanism of action is unknown, a wide panel of experimental strategies can be applied. Based on the assumption that physical interaction is a prerequisite for functional effects, most of these methods exploit the affinity between the small molecule and its putative target (Terstappen et al, 2007). The recently developed thermal-stability profiling method monitors drug target engagement by combining cellular thermal shift assays (CETSA) (Molina et al, 2013) with quantitative mass spectrometry (Huber et al, 2015; Savitski et al, 2014). These assays take

advantage of changes in the thermal stability of proteins mediated by ligand binding, and thus allow assessing the effect of the unmodified chemical agent on the thermal profile of the entire proteome in living cells. Affinity chromatography-based techniques require immobilization of the small molecule by attachment to a solid support, termed matrix. This method is applicable to any small molecule which can be derivatized to introduce the functional group required for immobilization without disrupting the biological activity of the compound (Terstappen et al, 2007). After incubation of the small molecule-matrix with protein extract, unbound proteins are removed by a series of washing steps. The subsequently eluted, specifically bound proteins can be identified by immunodetection or MS. In order to distinguish proteins veritably binding to the small molecule from contaminants interacting non-specifically with the matrix, several experimental refinement strategies have been developed. In the comparison variant, the identical experimental workflow is performed using a non-bioactive structural analogue of the small molecule, and the results then compared to those with the active ligand. The so-termed competition strategy uses an excess of free ligand, leading to elution of the target protein. Finally, in serial affinity chromatography protocols, the protein eluate is incubated with fresh matrix after the initial incubation step. While most of the specific proteins are bound by the first matrix, non-specifically binding proteins are equally distributed between the two matrices (Yamamoto et al, 2006). Yet, none of these methods can distinguish specific drug targets from proteins which strongly interact with and thus piggyback on the aforementioned. Accordingly, these approaches require subsequent validation experiments to confirm direct binding between the query compound and the target proteins identified. On the upside, affinity chromatography-based methods allow testing the compound interaction with target proteins in their native state, including post-translational modifications (Rix & Superti-Furga, 2009). They may however perform poor in cases where the small molecule fails to engage lowly expressed target proteins with sufficiently high binding affinity. Expression-cloning-based strategies for target deconvolution circumvent problems related to poor target protein expression by artificially increasing it (Terstappen et al, 2007). In yeast or mammalian three-hybrid systems (Caligiuri et al, 2006; Licitra & Liu, 1996) a cDNA vector collection is used for expression of potentially interacting proteins fused to a transcriptional activator domain. Binding of a target protein to the ligand molecule is subsequently monitored via proximity-induced reporter gene expression. Further expression-based target deconvolution methods include phage display (Sche et al, 1999) and messenger RNA (mRNA) display (McPherson et al, 2002), both involving iterative amplification steps aiding the identification of targets with low binding affinity or expression level (Terstappen et al, 2007). Lastly, protein microarrays feature a library of purified proteins immobilized on a microscope slide, which is probed with a labeled derivative of the query ligand for target detection (MacBeath & Schreiber, 2000). However,

strategies relying on recombinant protein expression come at the expense of potentially changed properties of the proteins compared to their native counterparts, as well as potential loss of post-translational modifications and native protein complexes, all of which may affect ligand binding.

1.8. Experimental Approaches for Identification of Novel Targets in Necroptosis Signaling

Target discovery aims at finding proteins whose modulation halts disease progression or leads to disease reversal. Integration of both genomic and proteomic information aids in gaining molecular understanding of the mechanisms governing disease phenotypes (Lindsay, 2003). Employing such an integrated approach for comprehensive functional mapping of a disease pathway can thus create the premise for finding and prioritizing novel targets. Commonly used techniques for target discovery include genomics, proteomics, genetic association as well as forward and reverse genetics. A genomics strategy aims at finding novel disease-associated targets owing to their differential expression patterns in diseased tissue. However, the results of such studies are often confounded by a large number of false positive and negative hits (Lindsay, 2003). Yet, comparing the expression patterns of necroptosis-resistant NIH3T3-A cells to NIH3T3-N, a necroptosis-proficient clone of the same cell line, was one of the strategies leading to identification of the role of RIPK3 in necroptotic cell death (Zhang et al, 2009). Genetic association describes the co-occurrence of a certain genotype with a specific phenotypic trait, and can thus be used to identify disease-associated genes or gene variants. Rare genetic disorders, as for example cystic fibrosis (Ratjen & Döring, 2003) or Huntington's disease (Young, 2003), are caused by a single mutated gene. Here, identification of the respective mutations greatly aided deciphering the underlying disease mechanism and was a prerequisite for therapeutic targeting. However, in contrast to single-gene disorders, most common diseases are complex and likely influenced by multiple genes (Tabor et al, 2002). The relation between major diseases and common genetic variants, usually single-nucleotide polymorphisms (SNPs), are the focus of genome-wide association studies (GWASs) (Manolio, 2010). A variant is referred to as disease-associated if it is found more frequently in diseased people as opposed to the healthy control cohort. However, while GWASs link a variant to a disorder, they do not allow inferring whether the gene is causal for disease occurrence (Manolio, 2010). In contrast, forward or reverse genetics approaches establish a more direct connection between a particular gene and the phenotype or trait in question. Forward genetics aims at finding the genetic basis responsible for a specific phenotype. Such an approach involves generation of a large number of random mutants by radiation, chemicals or insertional mutagenesis (Carette et al, 2009; Lindsay, 2003). Individual mutants exhibiting the phenotype of interest are subsequently isolated and

the respective affected gene is mapped. The recently introduced near-haploid KBM7 cell line has empowered forward genetic screening approaches in human cells, leading to groundbreaking discoveries as for instance the host factors required for Ebola virus entry (Carette et al, 2009; Carette et al, 2011). Conversely, reverse genetics studies the phenotypic effect of modifying or disrupting a gene of interest. Reverse genetics approaches classically relied on introduction of directed deletions or point mutations, gene silencing or non-targeted disruption by chemical or insertional mutagenesis (Hardy et al, 2010). The advent of sophisticated genomic tools such as siRNA, shRNA and, more recently, clustered regularly interspaced short palindromic repeats/CRISPR associated protein 9 (CRISPR/Cas9) technology in combination with high-throughput functional genomics has significantly advanced the scope and power of genetic screening (Shalem et al, 2015). Both genome-wide as well as kinase/phosphatase-targeted RNA interference (RNAi) approaches have been successfully applied to study necroptosis, aiding identification of the pathway members RIPK3 and MLKL (Cho et al, 2009; He et al, 2009; Hitomi et al, 2008; Zhao et al, 2012). However, changes in the amount of mRNA do not always directly translate into altered protein levels. Hence, proteomic strategies may offer a more direct assessment of differential expression than genomics. Yet, data derived from whole proteome approaches tend to be biased towards highly expressed proteins, while membrane proteins may be underrepresented (Hopf et al, 2007). On the plus side, proteomic strategies offer the possibility to examine post-translational modifications, as for example phosphorylation. Quantitative phosphoproteomics constitutes a powerful tool to dissect cellular signaling pathways and has been utilized to detect RIPK3-dependent phosphorylation events upon necroptosis induction (Zhong et al, 2014). Functional proteomics uses affinity-based techniques to determine protein-protein interactions and to systematically analyze the composition of protein complexes (Graves & Haystead, 2002). The necroptosis executioner MLKL (Sun et al, 2012) as well as protein phosphatase, Mg²⁺/Mn²⁺ dependent 1B (PPM1B) (Chen et al, 2015) were identified as interactors of RIPK3 using such an affinity purification (AP)-based MS approach. Affinity-based proteomics moreover allows the comprehensive mapping of the protein interaction network encompassing a specific cellular signaling pathway. By systematically affinity-tagging known and candidate pathway components, this concept can be used to deconstruct signaling cascades and identify novel players associated with a specific cellular process, as has been exemplified for the TNF/NF- κ B signal transduction pathway (Bouwmeester et al, 2004). Obtaining such a global interaction chart of a disease-relevant pathway, as for instance necroptosis, may empower identification and selection of novel potential therapeutic targets. AP-based liquid chromatography (LC)-coupled MS generally involves fusion of the protein of interest to a generic tag (Köcher & Superti-Furga, 2007). Expression of these fusion proteins in the appropriate cellular and

functional context allows assembly of bait-containing protein complexes. The tag is subsequently used as an affinity handle to purify the bait protein together with its interaction partners by immobilization on a suitable chromatography resin (Gavin & Hopf, 2006). The purified protein complexes are then subjected to MS analysis to identify the respective components. Due to the fact that a single purification step is often insufficient to remove nonspecifically co-purifying proteins, different composite tags allowing a second separation step have been introduced (Li, 2011). This TAP technique has been shown to dramatically reduce background level (Gingras et al, 2007) and has thus become the MS-based proteomics method of choice to study protein interaction. Critical factors for obtaining high confidence interaction data are the cellular context chosen for expression of the bait protein as well as the positioning of the affinity tag. The nature and location of the tag should be selected mindfully in order to avoid interference with protein function (Köcher & Superti-Furga, 2007). To ensure that all relevant interacting proteins are actively expressed, the interaction mapping should be performed in a relevant biological cell system, proficient for the respective pathway in question. Potential toxicity issues caused by exogenous expression of certain proteins can be overcome by employing inducible systems, permitting to steer timing and extent of transcriptional activation.

1.9. Aims of This Thesis

Necroptosis is involved in the pathophysiology of several human disorders, including many inflammatory disease states as well as IR-induced injuries. On this account, targeting necroptosis to limit pathological necrosis and to combat inflammation represents an attractive, new therapeutic option. However, no inhibitors of necroptosis are available for clinical application to date.

In this study, we thus aimed to (1) identify cytoprotective pharmacological agents blocking necroptosis. To this end, we applied a phenotypic screening approach using a representative panel of FDA-approved drugs. Given their established safety profile and favorable pharmacological properties, identification of necroptosis inhibitors among already approved drugs creates a consolidated chemical basis for the development of drug-like inhibitors for necroptosis-related clinical application. To (2) unravel the precise molecular mode of action of the identified inhibitors, we used both an unbiased chemical proteomics approach, as well as a series of more targeted, biochemical assays for target deconvolution.

Detailed understanding of the molecular mechanisms involved in the regulation of necroptosis is expected to open further avenues for therapeutic intervention and targeted modulation. To pave the way for studying the protein network underlying necroptotic cell death, we set out to (3) establish an inducible retroviral expression system meeting the requirements for MS-based mapping of the necroptosis pathway in the relevant physiological setting. We (4) demonstrated applicability of this novel expression system by delineating the network properties of a cancer-associated gene variant, as well as by charting the interactome of the cell death-inducing MLKL S358D mutant.

2. Results

2.1. Prologue

A Cellular Screen Identifies Ponatinib and Pazopanib as Inhibitors of Necroptosis

Fauster, A.*, Rebsamen, M.*, Huber, K. V., Bigenzahn, J. W., Stukalov, A., Lardeau, C. H., Scorzoni, S., Bruckner, M., Gridling, M., Parapatics, K., Colinge, J., Bennett, K. L., Kubicek, S., Krautwald, S., Linkermann, A., and Superti-Furga, G. (2015) *Cell Death Dis* 6, e1767

*: *equal contribution*

In this study we performed a phenotypic screen in FADD-deficient Jurkat cells undergoing TNF-induced necroptotic cell death in order to identify clinically relevant necroptosis inhibitors. In recognition of their established pharmacokinetics and safety profiles, we chose to screen a representative panel of already approved drugs. The publication reports the identification and characterization of the two anti-cancer agents ponatinib and pazopanib as efficient inhibitors of necroptosis along with elucidation of the respective underlying molecular mode of action (Fauster et al, 2015).

The author of this thesis designed research, performed the chemical screen, analyzed and interpreted data, performed the vast majority of validation experiments and wrote the manuscript. M. Rebsamen designed research, contributed to validation experiments, interpreted data and wrote the manuscript. K. V. M. Huber and M. Gridling performed chemical proteomics experiments. J. W. Bigenzahn, S. Scorzoni, and M. Bruckner helped with validation experiments. K. Parapatics and K. L. Bennett carried out mass spectrometric analyses. A. Stukalov and J. Colinge performed statistical analysis. C.-H. Lardeau and S. Kubicek assisted with the chemical screen and data analysis. S. Krautwald and A. Linkermann interpreted data and gave experimental advice. G. Superti-Furga designed research, interpreted data and contributed to writing of the manuscript.

A cellular screen identifies ponatinib and pazopanib as inhibitors of necroptosis

A Fauster^{1,3}, M Rebsamen^{1,3}, KVM Huber¹, JW Bigenzahn¹, A Stukalov^{1,4}, C-H Lardeau¹, S Scorzoni¹, M Bruckner¹, M Gridling¹, K Parapatics¹, J Colinge¹, KL Bennett¹, S Kubicek¹, S Krautwald², A Linkermann² and G Superti-Furga^{*1}

Necroptosis is a form of regulated necrotic cell death mediated by receptor-interacting serine/threonine-protein kinase 1 (RIPK1) and RIPK3. Necroptotic cell death contributes to the pathophysiology of several disorders involving tissue damage, including myocardial infarction, stroke and ischemia-reperfusion injury. However, no inhibitors of necroptosis are currently in clinical use. Here we performed a phenotypic screen for small-molecule inhibitors of tumor necrosis factor- α (TNF- α)-induced necroptosis in Fas-associated protein with death domain (FADD)-deficient Jurkat cells using a representative panel of Food and Drug Administration (FDA)-approved drugs. We identified two anti-cancer agents, ponatinib and pazopanib, as submicromolar inhibitors of necroptosis. Both compounds inhibited necroptotic cell death induced by various cell death receptor ligands in human cells, while not protecting from apoptosis. Ponatinib and pazopanib abrogated phosphorylation of mixed lineage kinase domain-like protein (MLKL) upon TNF- α -induced necroptosis, indicating that both agents target a component upstream of MLKL. An unbiased chemical proteomic approach determined the cellular target spectrum of ponatinib, revealing key members of the necroptosis signaling pathway. We validated RIPK1, RIPK3 and transforming growth factor- β -activated kinase 1 (TAK1) as novel, direct targets of ponatinib by using competitive binding, cellular thermal shift and recombinant kinase assays. Ponatinib inhibited both RIPK1 and RIPK3, while pazopanib preferentially targeted RIPK1. The identification of the FDA-approved drugs ponatinib and pazopanib as cellular inhibitors of necroptosis highlights them as potentially interesting for the treatment of pathologies caused or aggravated by necroptotic cell death.

Cell Death and Disease (2015) 6, e1767; doi:10.1038/cddis.2015.130; published online 21 May 2015

Programmed cell death has a crucial role in a variety of biological processes ranging from normal tissue development to diverse pathological conditions.^{1,2} Necroptosis is a form of regulated cell death that has been shown to occur during pathogen infection or sterile injury-induced inflammation in conditions where apoptosis signaling is compromised.^{3–6} Given that many viruses have developed strategies to circumvent apoptotic cell death, necroptosis constitutes an important, pro-inflammatory back-up mechanism that limits viral spread *in vivo*.^{7–9} In contrast, in the context of sterile inflammation, necroptotic cell death contributes to disease pathology, outlining potential benefits of therapeutic intervention.¹⁰ Necroptosis can be initiated by death receptors of the tumor necrosis factor (TNF) superfamily,¹¹ Toll-like receptor 3 (TLR3),¹² TLR4,¹³ DNA-dependent activator of IFN-regulatory factors¹⁴ or interferon receptors.¹⁵ Downstream signaling is subsequently conveyed via RIPK1¹⁶ or TIR-domain-containing adapter-inducing interferon- β ,^{8,17} and

converges on RIPK3-mediated^{13,18–20} activation of MLKL.²¹ Phosphorylated MLKL triggers membrane rupture,^{22–26} releasing pro-inflammatory cellular contents to the extracellular space.²⁷ Studies using the RIPK1 inhibitor necrostatin-1 (Nec-1)²⁸ or RIPK3-deficient mice have established a role for necroptosis in the pathophysiology of pancreatitis,¹⁹ arteriosclerosis,²⁹ retinal cell death,³⁰ ischemic organ damage and ischemia-reperfusion injury in both the kidney³¹ and the heart.³² Moreover, allografts from RIPK3-deficient mice are better protected from rejection, suggesting necroptosis inhibition as a therapeutic option to improve transplant outcome.³³ Besides Nec-1, several tool compounds inhibiting different pathway members have been described,^{12,16,21,34,35} however, no inhibitors of necroptosis are available for clinical use so far.^{2,10} In this study we screened a library of FDA approved drugs for the precise purpose of identifying already existing and generally safe chemical agents that could be used as necroptosis inhibitors. We identified the two

¹CeMM Research Center for Molecular Medicine of the Austrian Academy of Sciences, Vienna, Austria and ²Division of Nephrology and Hypertension, Christian-Albrechts-University, Kiel 24105 Germany

*Corresponding author: G Superti-Furga, CeMM Research Center for Molecular Medicine of the Austrian Academy of Sciences, Lazarettgasse 14, AKH BT25.3, Vienna 1090 Austria. Tel: +43 664 4042300; Fax: +43 140160970000; Email: gsuperti@cemmm.oeaw.ac.at

³These authors contributed equally to this work.

⁴Current address: Innate Immunity Laboratory, Max-Planck Institute of Biochemistry, Martinsried/Munich, Germany.

Abbreviations: CETSA, cellular thermal shift assay; EC₅₀, half maximal effective concentration; FADD, Fas-associated protein with death domain; FasL, Fas ligand; FDA, Food and Drug Administration; IC₅₀, half maximal inhibitory concentration; LCMS-MS, liquid chromatography tandem mass spectrometry; MBP, myelin basic protein; MLKL, mixed lineage kinase domain-like protein; Nec-1, necrostatin-1; NSA, necrosulfonamide; PDGFR β , platelet-derived growth factor receptor β ; RIPK, receptor-interacting serine/threonine-protein kinase; TAB1, TGF- β -activated kinase 1 and MAP3K7-binding protein 1; TAK1, transforming growth factor- β -activated kinase 1; TLR, Toll-like receptor; TNF- α , tumor necrosis factor- α ; TRAIL, TNF-related apoptosis-inducing ligand; VEGFR, vascular endothelial growth factor receptor

Received 16.2.15; revised 31.3.15; accepted 06.4.15; Edited by M Agostini

structurally distinct kinase inhibitors pazopanib and ponatinib as potent blockers of necroptosis targeting the key enzymes RIPK1/3.

Results

A drug screen in FADD-deficient Jurkat cells identifies ponatinib and pazopanib as necroptosis inhibitors. To identify novel necroptosis inhibitors for potential clinical use, we screened a panel of 268 FDA-approved drugs with diverse mechanisms of action for their ability to block TNF- α -induced necroptosis in FADD deficient human Jurkat T-cells^{36,37} (Figure 1a). We confirmed the validity of our experimental setup using the RIPK1 inhibitor Nec-1^{28,37} (Supplementary Figure 1a). To selectively identify inhibitors effective at low concentrations, the compounds were assayed at 0.5 and 1.5 μ M. Among the drugs investigated, the protein kinase inhibitors ponatinib and pazopanib robustly rescued cell viability at both concentrations (Figure 1b). Ponatinib (AP24534) is an oral multi-targeted tyrosine kinase inhibitor developed for treatment of chronic myeloid leukemia and Philadelphia chromosome-positive acute lymphoblastic leukemia.^{38,39} This BCR-ABL inhibitor is used as second-line treatment for patients who have acquired resistance to standard therapy. Pazopanib is an oral receptor tyrosine

kinase inhibitor approved for treatment of patients with advanced renal cell carcinoma and soft tissue sarcoma^{40,41} targeting vascular endothelial growth factor receptor (VEGFR)-1, -2, -3, platelet-derived growth factor receptor β (PDGFR β) and c-Kit.⁴² We confirmed the screening results (Supplementary Figures 1b–e) and performed dose–response curves to quantitatively assess the inhibitory potency of the two drugs. Pazopanib and ponatinib blocked necroptosis with comparable or higher efficiency than Nec-1 (data not shown) and its improved analog Nec-1s.⁴³ The half maximal effective concentration (EC₅₀) for inhibiting necroptosis in this setting was measured to be 89 nM for ponatinib, 254 nM for pazopanib and 238 nM for Nec-1s (Figure 1c). Drug toxicity was assessed by determining the half maximal inhibitory concentration (IC₅₀) (Figure 1d and Supplementary Figure 1f), which was 1.6 μ M for ponatinib and 6.6 μ M for pazopanib, highlighting the window of opportunity for necroptosis inhibition.

Ponatinib and pazopanib specifically block necroptotic but not apoptotic cell death triggered by various death receptor ligands in human cells. Ponatinib is one of the five BCR-ABL inhibitors currently approved for clinical use, the others being imatinib, nilotinib, dasatinib and bosutinib.⁴⁴ The target spectra of the latter four have been analyzed previously and show extensive overlap.^{45,46} To investigate

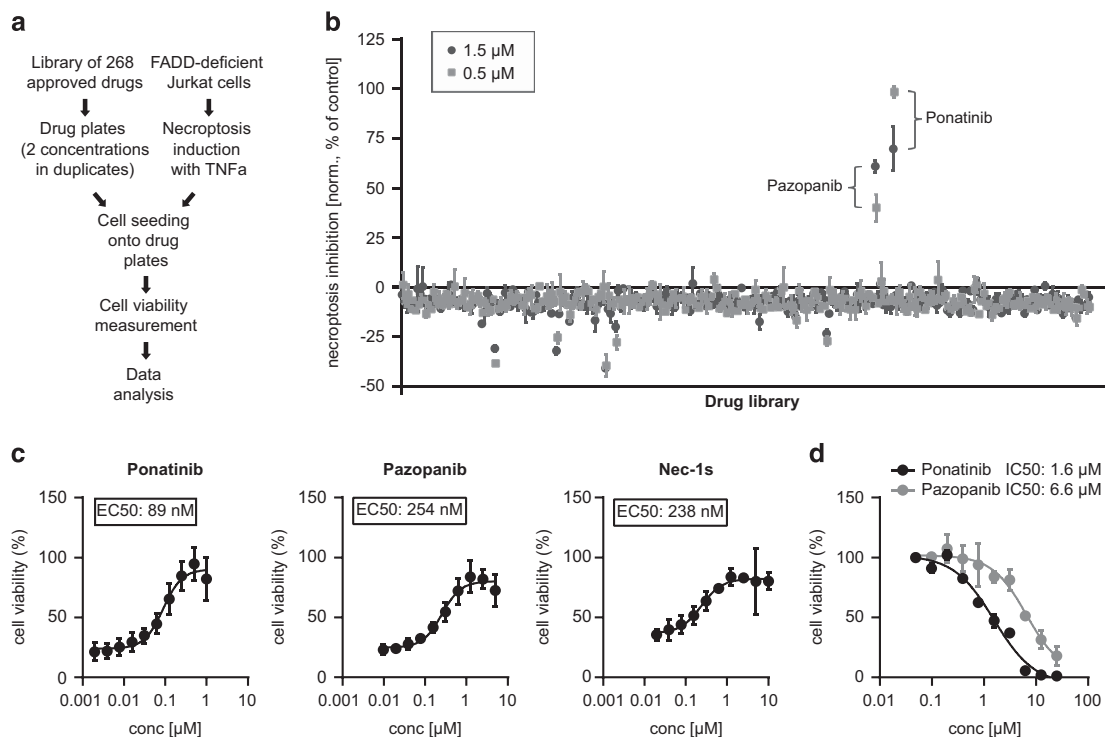


Figure 1 A cell-based drug screen identifies ponatinib and pazopanib as necroptosis inhibitors. (a) Schematic overview of the drug screen workflow. (b) Normalized necroptosis inhibition values depicted as percentage of control (DMSO = 0, Nec-1 [10 μ M] = 100) for drugs tested on FADD-deficient Jurkat cells treated overnight with 10 ng/ml TNF- α . Values represent mean value \pm S.D. for 268 drugs assayed at 1.5 (dark gray) or 0.5 μ M (light gray) in duplicates, respectively. (c) FADD-deficient Jurkat cells were treated overnight with 10 ng/ml TNF- α and ponatinib or pazopanib as indicated. Data were normalized to untreated control cells and represent mean value \pm S.D. of four independent experiments performed in triplicates. (d) FADD-deficient Jurkat cells were treated for 24 h with ponatinib or pazopanib as indicated. Data represent mean value \pm S.D. of two independent experiments performed in triplicates and normalized to untreated control. Cell viability was assessed using a luminescence-based readout for ATP (CellTiter Glo) throughout

whether the effect of ponatinib was caused by a target shared with the other BCR-ABL inhibitors, we assayed their potential to block necroptosis and their toxicity (Figure 2a). In contrast to the protection conferred by ponatinib treatment, none of the other drugs prevented necroptotic cell death. Dasatinib showed a modest effect but only at drug concentrations high enough to induce toxicity. These results suggest that ponatinib mediates its protective effect through one or multiple targets, which are not shared by the other BCR-ABL inhibitors. Similarly, necroptosis inhibition by pazopanib did not appear to be mediated through its main targets, as vandetanib, another VEGFR inhibitor,⁴⁷ did not confer protection (Figure 2b). To examine the inhibitory effect of the two drugs in an additional cellular model of programmed necrosis, we treated human adenocarcinoma HT-29 cells with TNF- α in presence of the Smac mimetic birinapant,⁴⁸ and the pan-caspase inhibitor z-VAD-FMK. Ponatinib and pazopanib rescued TNF- α /Smac mimetic/z-VAD-FMK (TSZ)-induced necroptotic cell death, whereas neither of the other four BCR-ABL inhibitors nor vandetanib did (Figure 2c and Supplementary Figure 2a). Ponatinib blocked necroptosis more efficiently in HT-29 cells (EC_{50} : 50 nM; Figure 2d) and was less toxic (IC_{50} : 8.9 μ M; Figure 2e) than in FADD-deficient Jurkat cells. Pazopanib blocked necroptosis less potently in HT-29 cells (EC_{50} : 873 nM; Figure 2d) while also showing reduced toxicity (IC_{50} > 10 μ M; Figure 2e). The inhibitory effect of the two drugs in HT-29 cells was not confined to TNF-driven necroptosis as cell death induced by TNF-related apoptosis-inducing ligand (TRAIL) and Fas ligand (FasL) was similarly blocked by ponatinib and pazopanib (Figures 2f and g and Supplementary Figure 2b). In contrast, none of the drugs inhibited apoptotic cell death triggered by FasL (Figure 2h and Supplementary Figure 2c). Similar to the inhibitory effect observed in human cells, both ponatinib and pazopanib were also capable of blocking necroptotic cell death with comparable potency in murine 3T3-SA cells (Supplementary Figures 3a and b). In L929 cells, ponatinib conferred protection as well, yet the effect was partial and confined to a small dosage window around 100 nM, above which the combined treatment of ponatinib, TNF- α and z-VAD-FMK induced toxicity (Supplementary Figures 3c and d). Altogether these data demonstrate that ponatinib and pazopanib are potent inhibitors of necroptosis.

Chemical proteomics identifies necroptosis pathway members as targets of ponatinib.

To characterize the molecular mode of action by which the two drugs mediate necroptosis inhibition, we used a chemical proteomic strategy to identify the cellular targets of ponatinib,⁴⁹ as pazopanib has been described to bind RIPK1.⁵⁰ We designed an analog of ponatinib (c-ponatinib) that contained an *N*-aminopropyl linker (Figure 3a), providing the basis for coupling the compound to a bead matrix and thereby allowing subsequent affinity purification of drug-binding proteins. We confirmed that the modification did not interfere with the necroptosis inhibitory capacity of ponatinib. Indeed, c-Ponatinib blocked necroptosis with only a minor reduction in potency (Figure 3b). For drug pull-down experiments, we treated FADD-deficient Jurkat cells for two hours with TNF- α to

induce necroptotic signaling complex formation followed by cell lysis. The lysates were incubated with the c-ponatinib drug matrix in presence or absence of an excess of competing free ponatinib.⁵¹ Analysis of the competed samples enabled discrimination of *bona fide* drug binders from contaminant proteins interacting with the bead matrix. Liquid chromatography tandem mass spectrometry (LCMS-MS) followed by bioinformatic analysis revealed a total of 38 kinases and 22 non-kinase proteins (Figure 3c and Supplementary Table 1) specific for ponatinib. The comparison with previously determined target profiles of other BCR-ABL inhibitors^{45,46} revealed a large overlap in the target spectra. Twenty-three of the 38 identified kinases have been observed to interact with at least one of the other BCR-ABL inhibitors. Of note, among the proteins unique to the target spectrum of ponatinib, we found all the key components of the necroptosis machinery: RIPK1, RIPK3 and MLKL. In addition, we identified TAK1, TGF-beta-activated kinase 1 and MAP3K7-binding protein 1 (TAB1) and TAB2, key components of the TNF-signaling pathway, which have recently been proposed to also exert a regulatory function in necroptotic cell death.^{52,53} The specificity of these necroptosis-relevant proteins for ponatinib was in accordance with the absence of necroptosis inhibition observed with the other clinical BCR-ABL inhibitors (Figure 2a). The chemical proteomic approach provided a target profile of ponatinib that comprised all crucial components of the necroptosis signaling pathway, perfectly in line with the inhibitory effect observed.

Ponatinib blocks necroptosis by inhibiting RIPK1 and RIPK3 activity.

Given that RIPK1, RIPK3 and MLKL interact upon necroptosis induction,^{21,54} we set out to assess which of them constitutes a direct target of ponatinib. To test the inhibitory effect of ponatinib on the pseudokinase MLKL, we generated HT-29 cells expressing a constitutively active MLKL S358D mutant upon doxycycline treatment (Supplementary Figure 4a). Induction of MLKL S358D expression led to cell death, which could be blocked by the MLKL inhibitor necrosulfonamide (NSA) (Figures 4a and b).²¹ In contrast, ponatinib did not prevent cell death driven by MLKL S358D expression, strongly suggesting that this protein is not a direct drug target. Next, we assessed the effect of ponatinib on RIPK1 and RIPK3 by monitoring their phosphorylation status upon necroptosis induction (Figure 4c). Time-dependent phosphorylation of RIPK1, RIPK3 and MLKL in TSZ-treated HT-29 cells was blocked by ponatinib. Indeed, competitive binding assays demonstrated that ponatinib could directly bind RIPK1 *in vitro* with high affinity (K_d : 37 nM) (Figure 4d). The impact of ponatinib and other BCR-ABL inhibitors on the catalytic activity of recombinant RIPK1 and RIPK3 was assessed in kinase assays (Figure 4e and Supplementary Figure 4b). Ponatinib strongly blocked phosphorylation of the generic substrate myelin basic protein (MBP), indicating inhibitory activity on both kinases. In agreement with the protective effect seen in FADD-deficient Jurkat cells at high drug concentration (Figure 2a), dasatinib also interfered with RIPK3 activity at the concentration tested (10 μ M) (Figure 4e). Ponatinib blocked recombinant RIPK3 with an IC_{50} of 0.64 μ M in this kinase assay (Figure 4f). We further monitored RIPK3

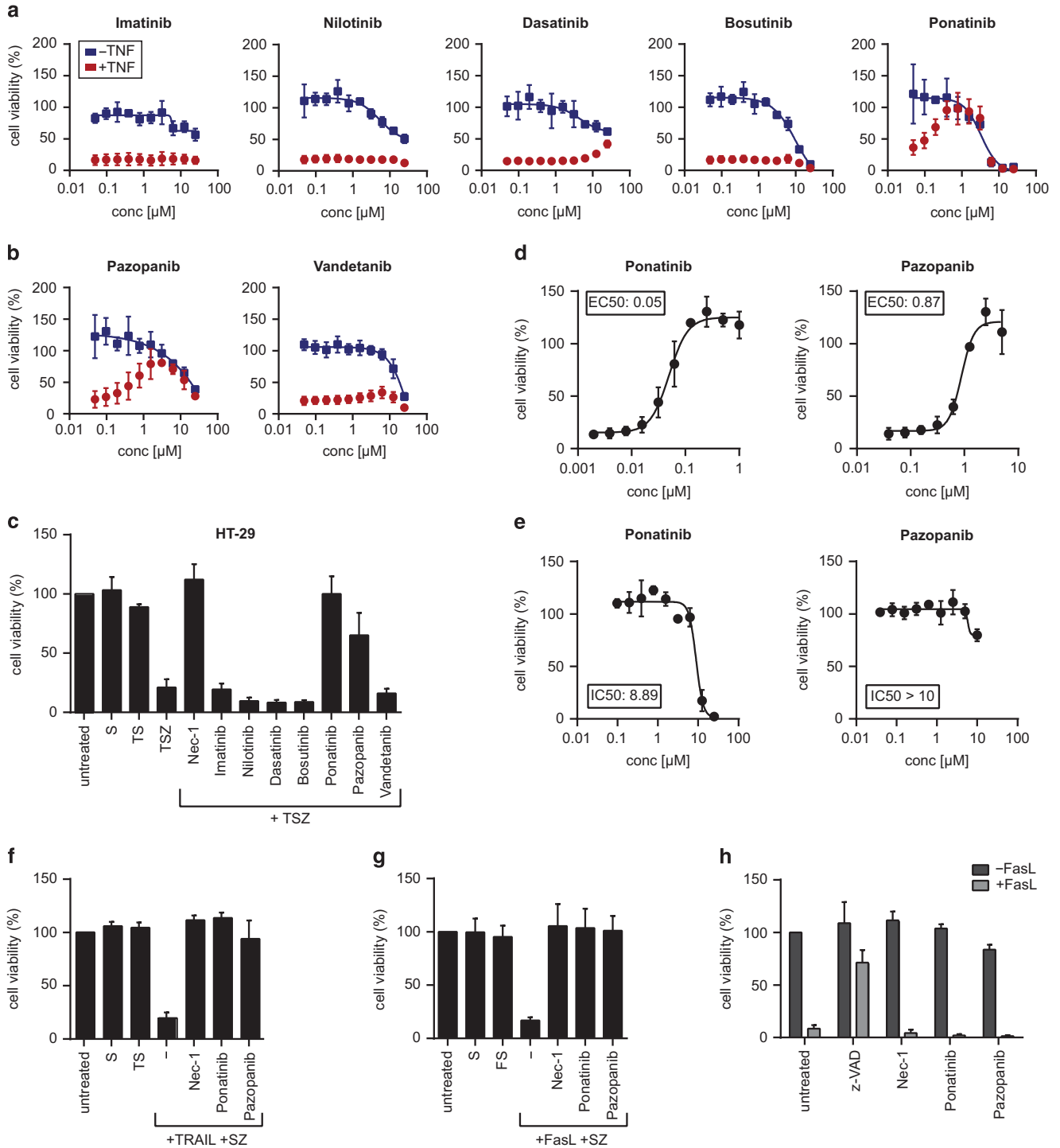


Figure 2 Ponatinib and pazopanib efficiently and specifically block necroptosis. (a and b) Cell viability was determined in FADD-deficient Jurkat cells treated overnight with (red circles) or without (blue rectangles) 10 ng/ml TNF- α and drugs as indicated. (c) Cell viability was assessed in HT-29 cells treated overnight with 20 ng/ml TNF- α (T), 500 nM Smac mimetic (S), 20 μM caspase inhibitor z-VAD (Z) and the compounds indicated (Nec-1, 10 μM ; all others, 1 μM). (d) HT-29 cells were treated with TSZ and ponatinib or pazopanib as indicated. (e) HT-29 cells were treated with ponatinib or pazopanib at concentrations indicated for 24 h. (f) Cell viability was assessed in HT-29 cells treated overnight with 200 ng/ml TRAIL or (g) 200 ng/ml human FasL together with 500 nM Smac mimetic (S), 20 μM z-VAD (Z) and either 10 μM Nec-1, 0.5 μM ponatinib or 5 μM pazopanib. Data represent mean value \pm S.D. of two independent experiments performed in triplicates and normalized to untreated control. (h) Cell viability was determined in Jurkat E6.1 cells treated with 100 ng/ml human FasL and 10 μM z-VAD, 10 μM Nec-1, 0.5 μM ponatinib or 5 μM pazopanib for 24 h. Data represent mean value \pm S.D. of two independent experiments performed in triplicates and normalized to untreated control. Cell viability was assessed using a luminescence-based readout for ATP (CellTiter Glo) throughout

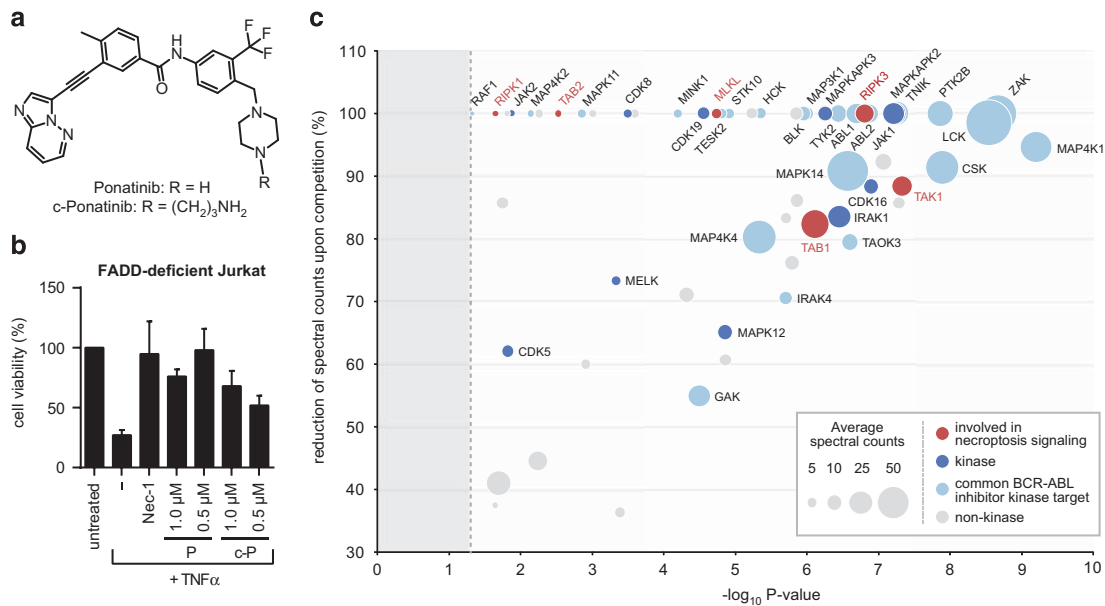


Figure 3 Chemical proteomics identifies necroptosis pathway members as targets of ponatinib. (a) Structure of ponatinib and the analog c-ponatinib used for affinity purification. (b) Cell viability was determined in FADD-deficient Jurkat cells treated overnight with 10 ng/ml TNF- α , 10 μ M Nec-1 and ponatinib (P) or c-ponatinib (c-P) as indicated. Cell viability was assessed using a luminescence-based readout for ATP (CellTiter Glo). Data represent mean value \pm S.D. of two independent experiments performed in triplicates and normalized to untreated control. (c) Proteins identified in mass-spectrometry-based affinity purification experiment with c-ponatinib. The x-axis of the bubble plot represents the statistical significance (P -value) of protein enrichment over the competition assay with free ponatinib estimated using the modified Decontaminator method (see Materials and Methods), and the y-axis the reduction in spectral counts (%) upon competition. Bubble size is proportional to the average spectral counts in non-competed condition. Dashed line indicates the P -value threshold (0.05)

autophosphorylation (Supplementary Figure 4c), which was efficiently blocked by ponatinib, whereas the RIPK1 inhibitor Nec-1s showed no effect. Considering the different IC₅₀ values observed for cellular viability and these *in vitro* kinase assays, we set out to verify whether endogenous RIPK3 is targeted by ponatinib in cells at the concentration (0.5 μ M) used throughout this study. To this end, we performed cellular thermal shift assays (CETSA), monitoring protein stabilization induced by drug binding.^{51,55} Indeed, ponatinib treatment led to a shift in the RIPK3 thermostability curve, indicative of target engagement (Figures 4g and h). Moreover, in contrast to Nec-1, ponatinib was capable of preventing phosphorylation of MLKL induced by RIPK3 or MLKL overexpression (Figure 4i and Supplementary Figure 4d). In line with these results, ponatinib efficiently blocked binding of RIPK3 to MLKL (Figure 4j). These data demonstrate the ability of ponatinib to directly target RIPK1 and RIPK3, the two key mediators of necroptosis signaling. Besides pazopanib directly binding ($K_d = 260$ nM)⁵⁰ and inhibiting RIPK1 kinase activity (Supplementary Figure 4b), it did not block MLKL S358D-driven necroptosis (Supplementary Figure 5a) and only moderately affected RIPK3 activity in recombinant kinase assays (Supplementary Figure 5b). Similar to Nec-1, pazopanib blocked TSZ-induced phosphorylation of MLKL, while it had only a minor effect when MLKL phosphorylation was triggered by RIPK3 or MLKL overexpression (Figure 4i and Supplementary Figure 4d). Furthermore, pazopanib did not interfere with the binding of RIPK3 to MLKL (Figure 4j). Taken together these data point to RIPK1 as the main mediator of necroptosis inhibition by pazopanib.

Discussion

In this study we performed a cellular screen with FDA-approved drugs to identify necroptosis inhibitors. While tool compounds blocking necrotic cell death by targeting RIPK1,^{28,35} RIPK3¹² and MLKL^{21,34} have been developed, no necroptosis inhibitors are in clinical use to date. Dabrafenib has been recently proposed as a possible candidate.⁵⁶ Our screen identified two kinase inhibitors, ponatinib and pazopanib, blocking necroptosis in human cells at submicromolar EC₅₀ concentrations. Both drugs inhibited necroptotic signaling triggered by various cell death receptors, whereas they did not interfere with apoptosis. Regarding the mode of action underlying the necroptosis inhibition by pazopanib, our results suggested that the effect is not mediated through its established targets. Indeed, vandetanib, which has a largely overlapping target spectrum, comprising VEGFR-2, KIT and PDGFR, did not protect from necroptotic cell death.^{42,47} Altogether the data point to RIPK1 as the main functional target mediating the protective effect of pazopanib. Pazopanib is used for treatment of advanced renal cell carcinoma⁴⁰ and advanced soft tissue sarcoma⁴¹ at a daily dose of 800 mg, resulting in plasma concentrations between 20 and 40 μ M.^{57,58} In our cellular systems, pazopanib conferred full necroptosis protection at 1–5 μ M concentration, suggesting a large therapeutic window for potential clinical application. Ponatinib was developed to treat patients having acquired the BCR-ABL T315I mutation, which confers resistance to all other clinically approved ABL1 tyrosine kinase inhibitors.³⁸ In our experimental settings, ponatinib was more potent in inhibiting necroptosis than the widely used RIPK1 inhibitor Nec-1s. To understand the molecular basis for the inhibitory action of

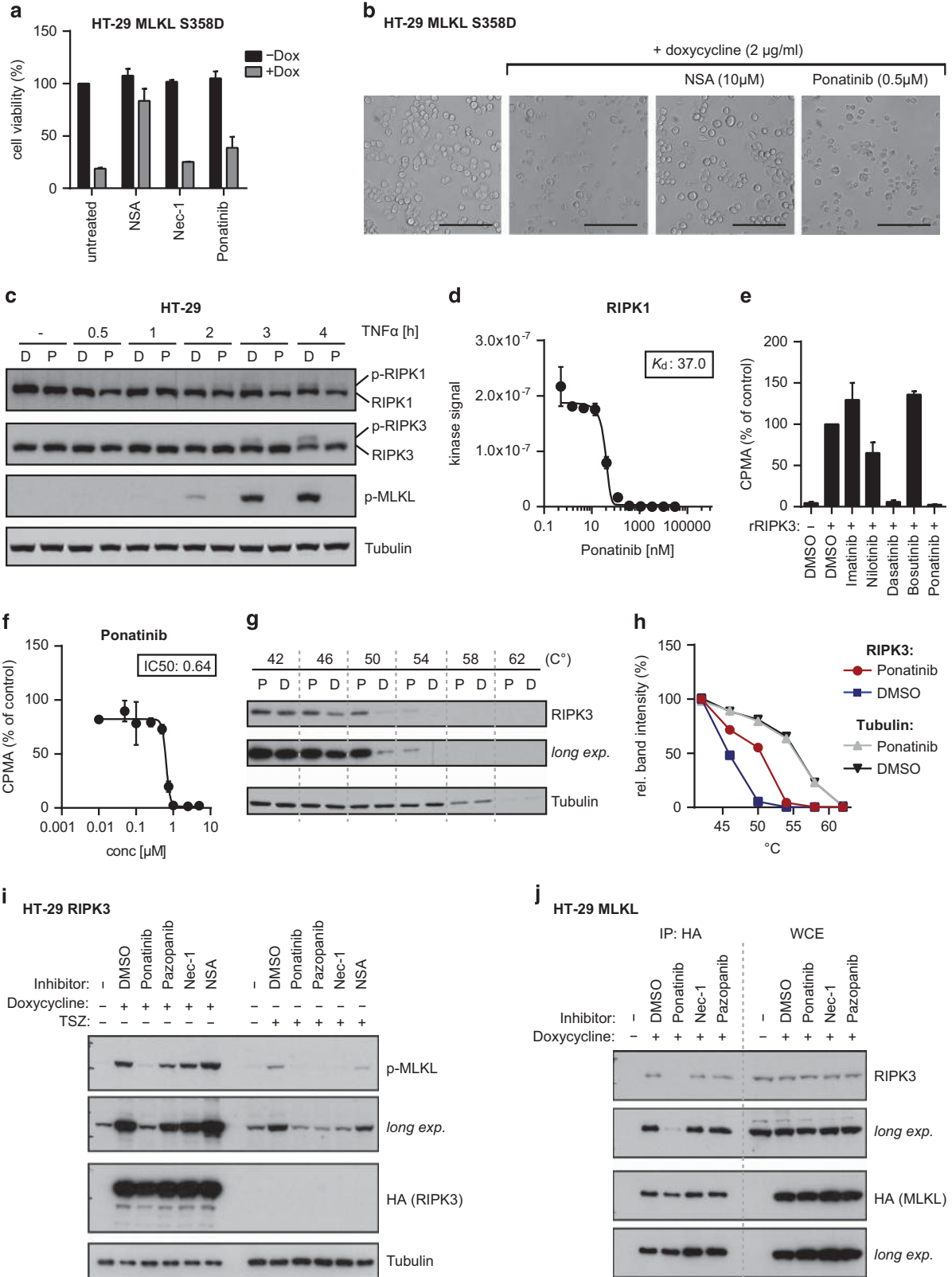


Figure 4 RIPK1 and RIPK3 are targets of ponatinib. (a) Cell viability was determined in HT-29 cells with doxycycline-inducible MLKL S358D expression treated overnight with 2 $\mu\text{g/ml}$ doxycycline and 10 μM NSA, 10 μM Nec-1 or 0.5 μM ponatinib. Cell viability was assessed using a luminescence-based readout for ATP (CellTiter Glo). Data represent mean value \pm S.D. of three independent experiments performed in triplicates and normalized to untreated control. (b) Microscopy (brightfield, $\times 10$) of HT-29 MLKL S358D cells induced with 2 $\mu\text{g/ml}$ doxycycline overnight and treated with the compounds as indicated. Scale bar, 100 μm . (c) HT-29 cells were treated with 500 nM Smac mimetic, 20 μM z-VAD, 0.5 μM ponatinib (P) or DMSO (D) for a total of 4.5 h in the presence of TNF- α (10 ng/ml) for the time indicated. Cells were lysed and immunoblotted with the indicated antibodies. Data shown are representative of two independent experiments. (d) Direct binding assay for ponatinib and RIPK1. Data represent mean value \pm S.D. of two independent experiments. (e) *In vitro* kinase assay using recombinant RIPK3. Phosphorylation of MBP was monitored in presence of 10 μM of the kinase inhibitors stated or (f) ponatinib as indicated. Data represent mean value \pm S.D. of two independent experiments normalized to DMSO control. (g) CETSA performed in FADD-deficient Jurkat cells treated with 500 nM ponatinib (P) or DMSO (D) control. Cells were lysed by three freeze–thaw cycles and immunoblotted with the antibodies indicated. Data shown are representative of two independent experiments. (h) Quantification of band intensity (ImageJ) of RIPK3 and Tubulin immunoblots shown in g. (i) HT-29 cells with doxycycline-inducible expression of HA-tagged RIPK3 were treated with 0.5 μM ponatinib, 5 μM pazopanib, 10 μM Nec-1 or 10 μM NSA and stimulated overnight with 1 $\mu\text{g/ml}$ doxycycline or for 2 h with 10 ng/ml TNF- α , 500 nM Smac mimetic and 20 μM z-VAD. Cells were lysed and immunoblotted with the indicated antibodies. Data shown are representative of two independent experiments. (j) HT-29 cells with doxycycline-inducible expression of HA-tagged MLKL were treated overnight with 1 $\mu\text{g/ml}$ doxycycline in presence of 0.5 μM ponatinib, 5 μM pazopanib, 10 μM Nec-1 or 10 μM NSA. Cell lysates were subjected to immunoprecipitation and immunoprecipitates (IP) and whole cell extracts (WCE) were analyzed by immunoblotting with the indicated antibodies. Data shown are representative of two independent experiments

ponatinib, we investigated its target profile by performing drug affinity purifications. Interestingly, in contrast to other clinical BCR-ABL inhibitors,^{45,46} ponatinib targets the key components of the necroptosis signaling pathway: RIPK1, RIPK3 and MLKL, as well as TAK1, TAB1 and TAB2. Our data support that ponatinib directly binds and inhibits both RIPK1 and RIPK3. Despite the relatively high IC_{50} value observed in *in vitro* RIPK3 kinase assays, effective target engagement and inhibition at the concentration used in cellular assays were demonstrated by thermal protein stabilization as well as loss of MLKL binding and phosphorylation. Thus ponatinib is, to our knowledge, the first necroptosis inhibitor capable of concurrently targeting both RIPK1 and RIPK3. The relative contribution of single kinase inhibition to the cellular protection cannot be readily assessed. However, this property of ponatinib could be advantageous in protecting cells from a broader range of stimuli, including those acting independently of RIPK1 or RIPK1 kinase activity.^{12,59} In addition, ponatinib bound TAK1 with high affinity ($K_d = 0.6$ nM) (Supplementary Figure 6a). Besides its well established function in NF- κB activation and prevention of cell death, TAK1 has recently been proposed to have a role in RIPK1/RIPK3-dependent necroptosis by taking part in a positive feed forward loop.^{52,53} A specific TAK1 inhibitor was not able to confer protection to necroptosis in our system, indicating that necroptosis inhibition by ponatinib could not be mediated solely by targeting TAK1 (Supplementary Figures 6b and c). In terms of drug concentration, the effective dose needed for necroptosis inhibition lies within plasma levels (120–140 nM) obtainable in patients treated with the recommended oral dose of 45 mg ponatinib given once daily.³⁹ While blocking RIPK3 protects cells from a broader range of necroptosis-inducing stimuli than RIPK1 inhibition, recent studies have raised concern about the therapeutic potential of targeting RIPK3 kinase activity.^{60,61} Selective small-molecule RIPK3 inhibitors, as well as a kinase-dead RIPK3 D161N mutant protein, have been shown to promote caspase-8-dependent apoptosis.^{60,61} While the RIPK3 D161N mutation is embryonically lethal,⁶¹ kinase-dead *Rip3*^{K51A/K51A} mice develop normally.⁶⁰ This indicates that RIPK3 kinase activity *per se* is not required for viability and suggests that additional conformational changes are required to trigger apoptosis.⁶⁰ Thus, development of therapeutically valuable RIPK3 inhibitors can be envisaged. Ponatinib and pazopanib have been developed and approved as anti-cancer treatment, and their safety profiles have been

evaluated in this context, with both drugs reported to cause severe side effects.^{62,63} In this regard, chemical proteomic profiling of ponatinib identified several novel targets in addition to RIPK1 and RIPK3. The definition of the cellular target spectrum might be useful in gaining a better understanding of the molecular mechanisms underlying the adverse effects reported in leukemia patients undergoing long-term drug treatment.^{62,64} Necroptosis inhibitors hold most promise for treatment of clinical conditions in which necroptotic cell death can be anticipated as, for example, in ischemia-reperfusion damage following transplantation or vessel occlusion.⁶⁵ These situations would require only single or short-term inhibitor treatment. Therefore potential side effects triggered by ponatinib or pazopanib in such acute settings might differ from those described for long-term anti-cancer treatment and would require cautious evaluation. The identification of two FDA-approved drugs as new inhibitors of necroptosis, together with elucidation of their mechanism of action, warrants a series of careful studies in animal models covering a large variety of necroptosis-associated pathologies. These studies will clarify the potential for necroptosis-related clinical application of these drugs which, given their potency in cellular assays and favorable pharmacological properties, could otherwise serve as basis for optimization in the development of drug-like necroptosis inhibitors.

Materials and Methods

Cell culture and reagents. HEK293T, 3T3-SA and L929 were obtained from ATCC (Manassas, VA, USA) and ECACC (Salisbury, UK). Jurkat E6.1 were kindly provided by W Ellmeier (Vienna), FADD-deficient Jurkat I2.1 and HT-29 by P Schneider (Lausanne). Cells were cultured in DMEM (Sigma-Aldrich, St. Louis, MO, USA), MEM (Gibco, Grand Island, NY, USA) or RPMI medium (Sigma-Aldrich) supplemented with 10% (v/v) FBS (Gibco) and antibiotics (100 U/ml penicillin and 100 mg/ml streptomycin) (Sigma-Aldrich). The reagents used were as follows: recombinant human TNF- α (300-01A, Peprotech, Rocky Hill, NJ, USA), recombinant murine TNF- α (315-01A, Peprotech), necrostatin-1 (N9037, Sigma-Aldrich), RIPK1 Inhibitor II 7-Cl-O-Nec-1 (Nec-1s) (504297, Merck Millipore, Billerica, MA, USA), ponatinib (S1490, Selleck Chemicals, Houston, TX, USA), pazopanib (P-6706, LC Laboratories, Woburn, MA, USA), imatinib (I-5577, LC Laboratories), nilotinib (S1033, Selleck Chemicals), dasatinib (S1021, Selleck Chemicals), vandetanib (S1046, Selleck Chemicals), SMAC mimetic Birinapant (S7015, Selleck Chemicals), z-VAD-FMK (AG-CP3-0002, Adipogen, San Diego, CA, USA), FasLigand (ALX-522-020-C005, Enzo, Farmingdale, NY, USA), recombinant human TRAIL (310-04, Peprotech), BMS-345541 (B9935, Sigma-Aldrich), c-ponatinib (WuXi AppTec, Shanghai, China), doxycycline (D9891, Sigma-Aldrich), NSA (480073, Merck Millipore), TAK1 inhibitor NP-009245 (AnalytiCon Discovery GmbH, Potsdam, Germany), propidium iodide (P4170, Sigma-Aldrich), recombinant

RIPK3 (R09-10G, Signalchem, Richmond, BC, Canada), recombinant RIPK1 (R07-10G, Signalchem), [γ -³²P]ATP (SRP-30, Hartmann Analytic GmbH, Braunschweig, Germany) and MBP (ab792, Abcam, Cambridge, UK). Bosutinib was a kind gift from Oridis Biomed (Graz, Austria).

Antibodies. Antibodies used were p-IkBa (Ser32/36) (9246S, Cell Signaling, Danvers, MA, USA), actin (AA01-A, Cytoskeleton, Denver, CO, USA), IkBa (SC-371, Santa Cruz, Dallas, TX, USA), tubulin (ab7291 Abcam), phospho-MLKL (Ser385) (ab187091, Abcam), RIPK1 (610458, BD Biosciences, Franklin Lakes, NJ, USA), RIPK3 (12107, Cell Signaling), HA (SC-805, Santa Cruz) and HA-7 (H6533, Sigma-Aldrich). The secondary antibodies used were goat anti-mouse HRP (115-035-003, Jackson ImmunoResearch, West Grove, PA, USA), goat anti-rabbit HRP (111-035-003, Jackson ImmunoResearch), Alexa Fluor 680 goat anti-mouse (A-21057, Molecular probes, Grand Island, NY, USA) and IRDye 800 donkey anti-rabbit (611-732-127, Rockland, Limerick, PA, USA).

Plasmids. RIPK3⁶⁶ and MLKL (PCR-amplified from KBM7 cDNA) were subcloned into vector pDONR221 using Gateway technology (Invitrogen, Grand Island, NY, USA). MLKL S358D mutant was generated with the QuikChange Lightning Site-Directed Mutagenesis Kit (Agilent Technologies, Santa Clara, CA, USA) using primers MLKL_S358D_fw (3'-GGAA AACACAGACTGACATGAG TTTGGGAAGT-5') and MLKL_S358D_rv (3'-AGTTCCCA AACTCATGTCAGTCT GTGTTTTCC-5'). Following sequence verification, cDNAs were transferred into the Gateway-compatible expression vectors TSHgwICPB or TgwSHICPB with N-(RIPK3) or C-terminal (MLKL, MLKL S358D) Strep-HA tag, respectively.

Generation of HT-29 cell lines with inducible overexpression. HT-29 cells were retrovirally transduced with MSCV-RIEP vector (pMSCV-rTA3-IRES-EcoR-PGK-PuroR)⁶⁷ to generate ecotropic receptor and rTA3 co-expressing cell lines. In brief, HEK293T cells were transiently transfected with pGAG-POL, pVSV-G, pADVANTAGE and MSCV-RIEP. After 24 h the medium was replaced with fresh medium. Forty-eight hours later the virus-containing supernatant was harvested, filtered (0.45 μ m), supplemented with 8 μ g/ml protamine sulfate (Sigma-Aldrich) and added to 40–60% confluent HT-29 cells. Twenty-four hours after infection, the medium was replaced with fresh medium. Another 24 h later, the medium was supplemented with 2 μ g/ml puromycin (Sigma-Aldrich) to select for infected cells. rTA3-expressing HT-29 cells were similarly transduced with retrovirus produced in HEK293T cells using the respective target gene-encoding inducible expression vector and pGAG-POL, pADVANTAGE and pEcoEnv. Blasticidin (25 μ g/ml; Invivogen, San Diego, CA, USA) was used for selection of infected cells. Target gene expression was induced by adding 1–2 μ g/ml doxycycline.

Immunoblotting. Whole cell extracts were prepared using Nonidet-40 lysis buffer (1% NP-40, 50 mM HEPES pH 7.4, 250 mM NaCl, 5 mM EDTA, one tablet of EDTA-free protease inhibitor (Roche Diagnostics, Indianapolis, IN, USA) per 50 ml, 10 mM NaF and 1 mM Na₃VO₄) for 10 min on ice. Lysates were cleared by centrifugation in a microcentrifuge (13 000 r.p.m., 10 min, 4 °C). Proteins were quantified with BCA (Pierce, Grand Island, NY, USA). Cell lysates were resolved by SDS-PAGE and transferred to nitrocellulose membranes Protran BA 85 (GE Healthcare, Little Chalfont, UK). The membranes were immunoblotted with the indicated antibodies. The bound antibodies were visualized with horseradish peroxidase-conjugated antibodies against rabbit or mouse IgG using the ECL Western blotting system (GE Healthcare) or Odyssey Infrared Imager (LI-COR, Lincoln, NE, USA).

Immunoprecipitation. Immunoprecipitations were performed as previously described.⁶⁸ In brief, the lysates were precleared (30 min, 4 °C) on Sepharose6 beads (Sigma-Aldrich) and subsequently incubated (3 h, 4 °C) with monoclonal anti-HA agarose antibody (Sigma-Aldrich). Beads were recovered by centrifugation and washed three times with lysis buffer before analysis by SDS-PAGE and immunoblotting.

Viability assays. Cells were seeded in 12-, 24- or 96-well plates at proper cell density. For necroptosis or apoptosis assays, cells were incubated with the indicated compound combinations at concentrations stated for 14–24 h. Smac mimetic and z-VAD-FMK were added 30–60 min before treatment with TNF- α , FasL or TRAIL. Cell viability was determined using CellTiter Glo Luminescent Cell Viability Assay (Promega, Fitchburg, WI, USA) according to the manufacturer's instructions. Luminescence was recorded with a SpectraMax M5Multimode plate reader

(Molecular Devices, Sunnyvale, CA, USA). For flow cytometry-based determination of viability, cells were harvested, collected by centrifugation, washed once and resuspended in staining buffer (1 \times PBS, 10% FBS). Cells were incubated with 0.5 μ g/ml PI for 10 min at room temperature (RT) in the dark. Flow cytometric analyses were performed on an LSR Fortessa (BD Biosciences) and analyzed with FlowJo software version 7.6.3 (Tree Star Inc, Ashland, OR, USA). Cell size was evaluated by forward scatter. PI-negative normal-sized cells were considered living and data were normalized to values of untreated controls. For detection of apoptosis, cells were resuspended in Annexin V Binding Buffer (BioLegend, San Diego, CA, USA) and stained with 0.5 μ g/ml PI and Alexa Fluor 647 Annexin V (BioLegend) according to manufacturer's instructions.

Drug screen. The drug screen was performed in 384-well plates at a final compound concentration of 1.5 μ M and 0.5 μ M measured in duplicates. The compounds were transferred into drug plates by acoustic droplet ejection using an Echo 520 liquid handler (LABCYTE, Sunnyvale, CA, USA). Necroptosis was induced in FADD-deficient Jurkat cells by addition of 10 ng/ml TNF- α immediately before seeding onto drug plates at a density of 1 \times 10⁴ cells/well. After 16 h incubation, cell viability was determined using CellTiter Glo Luminescent Cell Viability Assay according to manufacturer's instructions. Data analysis was performed by calculating a percentage of control to normalize for variability across different plates. The signal for the negative control DMSO wells was set to 0%, whereas the wells containing the positive control Nec-1 were put to 100% for each plate individually. Screen hits were defined as compounds (i) whose normalized signal was at least 3 S.D. away from the DMSO control, and (ii) that gave >20% rescue compared with the DMSO controls.

Chemical proteomics. Drug-affinity matrices were prepared as described previously.⁵¹ In brief, 25 nmol of c-ponatinib were immobilized on 50 μ l NHS-activated Sepharose 4 Fast Flow beads (GE Healthcare Bio-Sciences AB, Uppsala, Sweden). 10 mg whole cell lysate was used as protein input per replicate. Affinity chromatography and elution were performed in duplicate. After elution, the enriched proteins were reduced with dithiothreitol (DTT) and cysteine residues were alkylated by incubation with iodoacetamide. The samples were digested with modified porcine trypsin (Promega). Five percent of the digested eluates were purified and concentrated by C18 reversed-phase material. Subsequently, samples were analyzed in duplicates by gel-free one-dimensional LCMS.

MS data analysis. Precursor and MS/MS peaks were extracted from the RAW files and saved in the MGF format using msconvert tool (ProteoWizard Library v2.1.2708, www.proteowizard.sourceforge.net) for subsequent protein identification. An initial database search was performed with broader mass tolerance and conservative score threshold to re-calibrate the mass lists for optimal final protein identification. For the initial protein database search, Mascot (www.matrixscience.com, v2.3.0.2) was used. Error tolerances on the precursor and fragment ions were \pm 10 p.p.m. and \pm 0.6 Da, respectively, and the database search limited to fully-tryptic peptides with maximum one missed cleavage, carbamidomethyl cysteine and methionine oxidation set as fixed and variable modifications, respectively. The Mascot peptide ion score threshold was set to 30, and at least three peptide identifications per protein were required. Searches were performed against the human UniProtKB/SwissProt database (www.uniprot.org release 2013.01) including all protein isoforms. The initial peptide identifications were used to deduce independent linear transformations for precursor and fragment masses that would minimize the mean square deviation of measured masses from theoretical. Re-calibrated mass list files were searched against the same human protein database by a combination of Mascot and Phenyx (GeneBio SA, Geneva, Switzerland; version 2.5.14) search engines using narrower mass tolerances (\pm 4 p.p.m. and \pm 0.3 Da). One missed tryptic cleavage site was allowed. Carbamidomethyl cysteine was set as a fixed modification and oxidized methionine was set as a variable modification. To validate the proteins, Mascot and Phenyx output files were processed by internally developed parsers. Proteins with \geq 2 unique peptides above a score T1, or with a single peptide above a score T2 were selected as unambiguous identifications. Additional peptides for these validated proteins with score > T3 were also accepted. For Mascot searches, the following thresholds were used: T1 = 14, T2 = 40 and T3 = 10; Phenyx thresholds were set to 4.2, 4.75 and 3.5, respectively (P -value < 10⁻³). The validated proteins retrieved by the two algorithms were merged, any spectral conflicts discarded and grouped according to shared peptides. A false discovery rate of < 1% for protein identifications and < 0.1% for peptides (including the ones exported with lower scores) was

determined by applying the same procedure against a database of reversed protein sequences. The statistical significance of protein enrichment in c-ponatinib assay versus free ponatinib competition assay was calculated using the modification of the Decontaminator method.⁶⁹ In addition to Mascot protein scores that were proposed as an estimate of protein abundance by the original algorithm, the modified version also included Phenix protein scores and spectral counts. The algorithm first estimated three measure-specific *P*-values for each putative interaction, and, in contrast to,⁶⁹ *P*-value calculation utilized the quantiles of the measurements rather than the original data. The Fisher's method was used to combine the three resulting *P*-values into a single *P*-value for drug-protein interaction specificity. We have also correlated interaction *P*-values with the magnitude of competition effect represented by the fold reduction of spectral counts on free compound competition. Fold reduction was computed as the ratio of median spectral counts observed in experiments with and without competition. In each condition, four spectral counts were available for the median (two biological replicates and two technical for each).

Competition binding assays. Competition binding assays were performed by DiscoverRx (Fremont, CA, USA) according to the following protocol: kinase-tagged T7 phage strains were prepared in an *Escherichia coli* host derived from the BL21 strain. *E. coli* were grown to log phase and infected with T7 phage and incubated with shaking at 32 °C until lysis. The lysates were centrifuged and filtered to remove cell debris. The remaining kinases were produced in HEK293 cells and subsequently tagged with DNA for qPCR detection. Streptavidin-coated magnetic beads were treated with biotinylated small-molecule ligands for 30 min at RT to generate affinity resins for kinase assays. The liganded beads were blocked with excess biotin and washed with blocking buffer (SeaBlock (Pierce), 1% BSA, 0.05% Tween-20 and 1 mM DTT) to remove unbound ligand and to reduce nonspecific binding. Binding reactions were assembled by combining kinases, liganded affinity beads and test compounds in 1x binding buffer (20% SeaBlock, 0.17x PBS, 0.05% Tween-20 and 6 mM DTT). All reactions were performed in polystyrene 96-well plates in a final volume of 0.135 ml. The assay plates were incubated at RT with shaking for 1 h and the affinity beads were washed with wash buffer (1x PBS and 0.05% Tween-20). The beads were then resuspended in elution buffer (1x PBS, 0.05% Tween-20 and 0.5 μM nonbiotinylated affinity ligand) and incubated at RT with shaking for 30 min. The kinase concentration in the eluates was measured by qPCR. For kinase-binding constant determination, an 11-point 3-fold serial dilution of each test compound was prepared in 100% DMSO at 100x final test concentration and subsequently diluted to 1x in the assay (final DMSO concentration = 1%). Most *K_d*s were determined using a compound top concentration = 30 000 nM. If the initial *K_d* determined was < 0.5 nM (the lowest concentration tested), the measurement was repeated with a serial dilution starting at a lower top concentration. A *K_d* value reported as 40 000 nM indicates that the *K_d* was determined to be > 30 000 nM. Binding constants (*K_d*) were calculated with a standard dose-response curve using the Hill equation:

$$\text{Response} = \text{background} + \frac{(\text{signal} - \text{background})}{1 + (K_d / \text{Hill Slope} / \text{Dose})^{\text{Hill Slope}}}$$

The Hill Slope was set to -1. Curves were fitted using a non-linear least square fit with the Levenberg-Marquardt algorithm.

Recombinant kinase assays. Recombinant RIPK1 or RIPK3 protein was incubated with the substrate MBP in kinase assay buffer (40 mM Tris-HCl pH 7.5, 10 mM MgCl₂ and 1 mM DTT) in presence of 50 μM ATP, 5 μCi [³²P]ATP and the indicated inhibitors in a total volume of 20 μl. Reactions were incubated at RT for 20 min before termination by addition of 12.5 μl guanidinium chloride (7.5 μM). The terminated reactions were spotted onto a SAM2 Biotin Capture membrane (Promega) and further processed according to the manufacturer's instructions. Kinase activity was measured in a Tri-Carb 2810TR liquid scintillation analyzer (Perkin Elmer, Waltham, MA, USA). Data were normalized to a DMSO-treated control sample. For autoradiography, the reactions were stopped by addition of 5 μl 4x Laemmli buffer and incubated for 5 min at 95 °C. Samples were resolved by SDS-PAGE followed by gel drying for 2 h at 80 °C in a Model 583 Gel Dryer (Bio-Rad, Hercules, CA, USA). Visualization was performed using a BAS-IP MS 2025 imaging plate (Fuji Photo Film Co., Ltd., Tokyo, Japan) and a Typhoon TRIO Variable Mode Imager (GE Healthcare).

Cellular thermal shift assay (CETSA). Drug target engagement in cells, causing stabilization of the respective protein, was analyzed essentially as described previously.⁵⁵ Briefly, FADD-deficient Jurkat cells were seeded into 12-well

plates at a density of 1x10⁶ cells/ml and treated for 3 h with cell media containing 0.5 μM ponatinib or 0.05% DMSO. After treatment, cells were collected by centrifugation and resuspended in 1x PBS. The cell suspension was aliquoted into PCR tubes and heated for 3 min at 42, 46, 50, 54, 58 or 62 °C. Subsequently, cells were lysed by three consecutive freeze-thaw cycles using liquid nitrogen. The soluble fraction was separated from precipitated proteins by centrifugation at 13000 r.p.m. and 4 °C for 20 min. The supernatant, containing the soluble proteins, was transferred to a fresh tube and analyzed by immunoblotting.

Microscopy. Microscopy images were taken at 10x with a Leica DFC310 FX on a Leica DM IL LED (Leica Microsystems, Wetzlar, Germany).

Conflict of Interest

The authors declare no conflict of interest.

Acknowledgements. We thank all members of the Superti-Furga laboratory for discussions and invaluable feedback, the Bennett laboratory for the proteomic analyses and the Kubicek group for help with the chemical screen. We are grateful to Alex Bullock for scientific discussion. We further thank Gregory Vladimer and Berend Snijder for critically reading the manuscript. This work was supported by the Austrian Academy of Sciences, ERC grant to GS-F (i-FIVE 250179), EMBO long-term and Marie Curie fellowships to MR (ALTF 1346-2011, IEF 301663), Austrian Science Fund grant for JWB (FWF SFB F47), EU grant to KVMH and MG (FP7 ASSET 259348), the Medical Faculty of Kiel University for SK and Fresenius Medical Care, Germany for SK and AL.

1. Fuchs Y, Steller H. Programmed cell death in animal development and disease. *Cell* 2011; **147**: 742–758.
2. Pasparakis M, Vandenabeele P. Necroptosis and its role in inflammation. *Nature* 2015; **517**: 311–320.
3. Linkermann A, Green DR. Necroptosis. *N Engl J Med* 2014; **370**: 455–465.
4. Chan FK-M, Luz NF, Moriwaki K. Programmed Necrosis in the Cross Talk of Cell Death and Inflammation. *Annu Rev Immunol* 2014; **33**: 141210135520002.
5. Christofferson DE, Li Y, Yuan J. Control of Life-or-Death Decisions by RIP1 Kinase. *Annu Rev Physiol* 2014; **76**: 129–150.
6. Nikolettoupolou V, Markaki M, Palikaras K, Tavernarakis N. Crosstalk between apoptosis, necrosis and autophagy. *Biochim Biophys Acta* 2013; **1833**: 3448–3459.
7. Upton JW, Kaiser WJ, Mocarski ES. Virus Inhibition of RIP3-dependent necrosis. *Cell Host Microbe* 2010; **7**: 302–313.
8. Mocarski ES, Upton JW, Kaiser WJ. Viral infection and the evolution of caspase 8-regulated apoptotic and necrotic death pathways. *Nat Rev Immunol* 2011; **12**: 79–88.
9. Humphries F, Yang S, Wang B, Moynagh PN. RIP kinases: key decision makers in cell death and innate immunity. *Cell Death Differ* 2014; **22**: 225–236.
10. Linkermann A, Stockwell BR, Krautwald S, Anders H-J. Regulated cell death and inflammation: an auto-amplification loop causes organ failure. *Nat Rev Immunol* 2014; **14**: 759–767.
11. Holler N, Zaru R, Micheau O, Thome M, Attinger A, Valitutti S et al. Fas triggers an alternative, caspase-8-independent cell death pathway using the kinase RIP as effector molecule. *Nat Immunol* 2000; **1**: 489–495.
12. Kaiser WJ, Sridharan H, Huang C, Mandal P, Upton JW, Gough PJ et al. Toll-like Receptor 3-mediated Necrosis via TRIF, RIP3, and MLKL. *J Biol Chem* 2013; **288**: 31268–31279.
13. Zhang DW, Shao J, Lin J, Zhang N, Lu BJ, Lin SC et al. RIP3, an energy metabolism regulator that switches TNF-induced cell death from apoptosis to necrosis. *Science* 2009; **325**: 332–336.
14. Upton Jason W, Kaiser William J, Mocarski Edward S. DAI/ZBP1/DLM-1 complexes with RIP3 to mediate virus-induced programmed necrosis that is targeted by murine cytomegalovirus vIRA. *Cell Host Microbe* 2012; **11**: 290–297.
15. Thapa RJ, Nogusa S, Chen P, Maki JL, Lerro A, Andrade M et al. Interferon-induced RIP1/RIP3-mediated necrosis requires PKR and is licensed by FADD and caspases. *Proc Natl Acad Sci USA* 2013; **110**: E3109–E3118.
16. Degterev A, Hitomi J, Germscheid M, Ch'en IL, Korkina O, Teng X et al. Identification of RIP1 kinase as a specific cellular target of necrostatins. *Nat Chem Biol* 2008; **4**: 313–321.
17. He S, Liang Y, Shao F, Wang X. Toll-like receptors activate programmed necrosis in macrophages through a receptor-interacting kinase-3-mediated pathway. *Proc Natl Acad Sci USA* 2011; **108**: 20054–20059.
18. Cho Y, Challa S, Moquin D, Genga R, Ray TD, Guildford M et al. Phosphorylation-driven assembly of the RIP1-RIP3 complex regulates programmed necrosis and virus-induced inflammation. *Cell* 2009; **137**: 1112–1123.
19. He S, Wang L, Miao L, Wang T, Du F, Zhao L et al. Receptor interacting protein kinase-3 determines cellular necrotic response to TNF-α. *Cell* 2009; **137**: 1100–1111.

20. Galluzzi L, Vanden Berghe T, Vanlangenakker N, Buettner S, Eisenberg T, Vandenabeele P *et al*. Programmed necrosis from molecules to health and disease. *Int Rev Cell Mol Biol* 2011; **289**: 1–35.
21. Sun L, Wang H, Wang Z, He S, Chen S, Liao D *et al*. Mixed lineage kinase domain-like protein mediates necrosis signaling downstream of RIP3 kinase. *Cell* 2012; **148**: 213–227.
22. Wang H, Sun L, Su L, Rizo J, Liu L, Wang L-F *et al*. Mixed lineage kinase domain-like protein MLKL causes necrotic membrane disruption upon phosphorylation by RIP3. *Mol Cell* 2014; **54**: 133–146.
23. Dondelinger Y, Declercq W, Montessuit S, Roelandt R, Goncalves A, Bruggeman I *et al*. MLKL compromises plasma membrane integrity by binding to phosphatidylinositol phosphates. *Cell Rep* 2014; **7**: 971–981.
24. Su L, Quade B, Wang H, Sun L, Wang X, Rizo J. A plug release mechanism for membrane permeation by MLKL. *Structure* 2014; **22**: 1489–1500.
25. Cai Z, Jitkaew S, Zhao J, Chiang H-C, Choksi S, Liu J *et al*. Plasma membrane translocation of trimerized MLKL protein is required for TNF-induced necroptosis. *Nat Cell Biol* 2013; **16**: 55–65.
26. Chen X, Li W, Ren J, Huang D, He W-t, Song Y *et al*. Translocation of mixed lineage kinase domain-like protein to plasma membrane leads to necrotic cell death. *Cell Res* 2013; **24**: 105–121.
27. Kaczmarek A, Vandenabeele P, Krysko Dmitri V. Necroptosis: the release of damage-associated molecular patterns and its physiological relevance. *Immunity* 2013; **38**: 209–223.
28. Degterev A, Huang Z, Boyce M, Li Y, Jagtap P, Mizushima N *et al*. Chemical inhibitor of nonapoptotic cell death with therapeutic potential for ischemic brain injury. *Nat Chem Biol* 2005; **1**: 112–119.
29. Lin J, Li H, Yang M, Ren J, Huang Z, Han F *et al*. A role of RIP3-mediated macrophage necrosis in atherosclerosis development. *Cell Rep* 2013; **3**: 200–210.
30. Murakami Y, Matsumoto H, Roh M, Giani A, Kataoka K, Morizane Y *et al*. Programmed necrosis, not apoptosis, is a key mediator of cell loss and DAMP-mediated inflammation in dsRNA-induced retinal degeneration. *Cell Death Differ* 2013; **21**: 270–277.
31. Linkermann A, Brasen JH, Darding M, Jin MK, Sanz AB, Heller JO *et al*. Two independent pathways of regulated necrosis mediate ischemia-reperfusion injury. *Proc Natl Acad Sci USA* 2013; **110**: 12024–12029.
32. Oerlemans MIFJ Liu J, Arslan F, Ouden K, Middelaar BJ, Doevendans PA *et al*. Inhibition of RIP1-dependent necrosis prevents adverse cardiac remodeling after myocardial ischemia-reperfusion *in vivo*. *Basic Res Cardiol* 2012; **107**: 270.
33. Lau A, Wang S, Jiang J, Haig A, Pavlosky A, Linkermann A *et al*. RIPK3-mediated necroptosis promotes donor kidney inflammatory injury and reduces allograft survival. *Am J Transplant* 2013; **13**: 2805–2818.
34. Hildebrand JM, Tanzer MC, Lucet IS, Young SN, Spall SK, Sharma P *et al*. Activation of the pseudokinase MLKL unleashes the four-helix bundle domain to induce membrane localization and necroptotic cell death. *Proc Natl Acad Sci USA* 2014; **111**: 15072–15077.
35. Harris PA, Bandyopadhyay D, Berger SB, Campobasso N, Capriotti CA, Cox JA *et al*. Discovery of small molecule RIP1 kinase inhibitors for the treatment of pathologies associated with necroptosis. *ACS Med Chem Lett* 2013; **4**: 1238–1243.
36. Joo P, Woo MS, Kuo CJ, Signorelli P, Biemann HP, Hannun YA *et al*. FADD is required for multiple signaling events downstream of the receptor Fas. *Cell Growth Differ* 1999; **10**: 797–804.
37. Lawrence CP, Chow SC. FADD deficiency sensitises Jurkat T cells to TNF- α -dependent necrosis during activation-induced cell death. *FEBS Lett* 2005; **579**: 6465–6472.
38. O'Hare T, Shakespeare WC, Zhu X, Eide CA, Rivera VM, Wang F *et al*. AP24534, a Pan-BCR-ABL inhibitor for chronic myeloid leukemia, potently inhibits the T315I mutant and overcomes mutation-based resistance. *Cancer Cell* 2009; **16**: 401–412.
39. Cortes JE, Kantarjian H, Shah NP, Bixby D, Mauro MJ, Flinn I *et al*. Ponatinib in refractory Philadelphia chromosome-positive leukemias. *N Engl J Med* 2012; **367**: 2075–2088.
40. Ward JE, Stadler WM. Pazopanib in renal cell carcinoma. *Clin Cancer Res* 2010; **16**: 5923–5927.
41. van der Graaf WT, Blay JY, Chawla SP, Kim DW, Bui-Nguyen B, Casali PG *et al*. Pazopanib for metastatic soft-tissue sarcoma (PALETTE): a randomised, double-blind, placebo-controlled phase 3 trial. *Lancet* 2012; **379**: 1879–1886.
42. Harris PA, Bolor A, Cheung M, Kumar R, Crosby RM, Davis-Ward RG *et al*. Discovery of 5-[[4-[(2,3-dimethyl-2H-indazol-6-yl)methylamino]-2-pyrimidinyl]amino]-2-methyl-benzene-sulfonamide (Pazopanib), a novel and potent vascular endothelial growth factor receptor inhibitor. *J Med Chem* 2008; **51**: 4632–4640.
43. Teng X, Degterev A, Jagtap P, Xing X, Choi S, Denu R *et al*. Structure-activity relationship study of novel necroptosis inhibitors. *Bioorg Med Chem Lett* 2005; **15**: 5039–5044.
44. O'Hare T, Zabriskie MS, Eiring AM, Deininger MW. Pushing the limits of targeted therapy in chronic myeloid leukaemia. *Nat Rev Cancer* 2012; **12**: 513–526.
45. Hantschel O, Rix U, Superti-Furga G. Target spectrum of the BCR-ABL inhibitors imatinib, nilotinib and dasatinib. *Leuk Lymphoma* 2008; **49**: 615–619.
46. Rensing Rix LL, Rix U, Colinge J, Hantschel O, Bennett KL, Stranzl T *et al*. Global target profile of the kinase inhibitor bosutinib in primary chronic myeloid leukemia cells. *Leukemia* 2008; **23**: 477–485.
47. Wedge SR, Ogilvie DJ, Dukes M, Kendrew J, Chester R, Jackson JA *et al*. ZD6474 inhibits vascular endothelial growth factor signaling, angiogenesis, and tumor growth following oral administration. *Cancer Res* 2002; **62**: 4645–4655.
48. Vince JE, WW-L Wong, Khan N, Feltham R, Chau D, Ahmed AU *et al*. IAP antagonists target cIAP1 to induce TNF α -dependent apoptosis. *Cell* 2007; **131**: 682–693.
49. Rix U, Superti-Furga G. Target profiling of small molecules by chemical proteomics. *Nat Chem Biol* 2009; **5**: 616–624.
50. Davis MI, Hunt JP, Herrgard S, Ciceri P, Wodicka LM, Pallares G *et al*. Comprehensive analysis of kinase inhibitor selectivity. *Nat Biotechnol* 2011; **29**: 1046–1051.
51. Huber KVM, Salah E, Radic B, Gridling M, Elkins JM, Stukalov A *et al*. Stereospecific targeting of MTH1 by (S)-crizotinib as an anticancer strategy. *Nature* 2014; **508**: 222–227.
52. Morioka S, Broglie P, Omori E, Ikeda Y, Takaesu G, Matsumoto K *et al*. TAK1 kinase switches cell fate from apoptosis to necrosis following TNF stimulation. *J Cell Biol* 2014; **204**: 607–623.
53. Mihaly SR, Ninomiya-Tsuji J, Morioka S. TAK1 control of cell death. *Cell Death Differ* 2014; **21**: 1667–1676.
54. Li J, McQuade T, Siemer Ansgar B, Napetschnig J, Moriwaki K, Hsiao Y-S *et al*. The RIP1/RIP3 necrosome forms a functional amyloid signaling complex required for programmed necrosis. *Cell* 2012; **150**: 339–350.
55. Molina DM, Jafari R, Ignatshchenko M, Seki T, Larsson EA, Dan C *et al*. Monitoring drug target engagement in cells and tissues using the cellular thermal shift assay. *Science* 2013; **341**: 84–87.
56. Li JX, Feng JM, Wang Y, Li XH, Chen XX, Su Y *et al*. The B-RafV600E inhibitor dabrafenib selectively inhibits RIP3 and alleviates acetaminophen-induced liver injury. *Cell Death Dis* 2014; **5**: e1278.
57. Hurwitz HI, Dowlati A, Saini S, Savage S, Suttle AB, Gibson DM *et al*. Phase I trial of pazopanib in patients with advanced cancer. *Clin Cancer Res* 2009; **15**: 4220–4227.
58. Hutson TE, Davis ID, Machiels JPH, De Souza PL, Rottey S, Bi Hong *et al*. Efficacy and safety of pazopanib in patients with metastatic renal cell carcinoma. *J Clin Oncol* 2009; **28**: 475–480.
59. Kaiser WJ, Daley-Bauer LP, Thapa RJ, Mandal P, Berger SB, Huang C *et al*. RIP1 suppresses innate immune necrotic as well as apoptotic cell death during mammalian parturition. *Proc Natl Acad Sci USA* 2014; **111**: 7753–7758.
60. Mandal P, Berger Scott B, Pillay S, Moriwaki K, Huang C, Guo H *et al*. RIP3 induces apoptosis independent of pro-necrotic kinase activity. *Mol Cell* 2014; **56**: 481–495.
61. Newton K, Dugger DL, Wickliffe KE, Kapoor N, de Almagro MC, Vucic D *et al*. Activity of protein kinase RIPK3 determines whether cells die by necroptosis or apoptosis. *Science* 2014; **343**: 1357–1360.
62. Cortes JE, Kim DW, Pinilla-Ibarz J, le Coutre P, Paquette R, Chuah C *et al*. A phase 2 trial of ponatinib in Philadelphia chromosome-positive leukemias. *N Engl J Med* 2013; **369**: 1783–1796.
63. Sternberg CN, Davis ID, Mardiak J, Szczylik C, Lee E, Wagstaff J *et al*. Pazopanib in locally advanced or metastatic renal cell carcinoma: results of a randomized phase III trial. *J Clin Oncol* 2010; **28**: 1061–1068.
64. Hantschel O, Rix U, Schmidt U, Burckstummer T, Kneidinger M, Schutze G *et al*. The Btk tyrosine kinase is a major target of the Bcr-Abl inhibitor dasatinib. *Proc Natl Acad Sci USA* 2007; **104**: 13283–13288.
65. Linkermann A, Hackl MJ, Kunzendorf U, Walczak H, Krautwald S, Jevnikar AM. Necroptosis in immunity and ischemia-reperfusion injury. *Am J Transplant* 2013; **13**: 2797–2804.
66. Rebsamen M, Heinz LX, Meylan E, Michallet M-C, Schroder K, Hofmann K *et al*. DAI/ZBP1 recruits RIP1 and RIP3 through RIP homotypic interaction motifs to activate NF- κ B. *EMBO Rep* 2009; **10**: 916–922.
67. Zuber J, Rappaport AR, Luo W, Wang E, Chen C, Vaseva AV *et al*. An integrated approach to dissecting oncogene addiction implicates a Myb-coordinated self-renewal program as essential for leukemia maintenance. *Genes Dev* 2011; **25**: 1628–1640.
68. Rebsamen M, Pochini L, Stasyk T, de Araujo ME, Galluccio M, Kandasamy RK *et al*. SLC38A9 is a component of the lysosomal amino acid sensing machinery that controls mTORC1. *Nature* 2015; **519**: 477–81.
69. Lavallee-Adam M, Cloutier P, Coulombe B, Blanchette M. Modeling contaminants in AP-MS/MS experiments. *J Proteome Res* 2011; **10**: 886–895.



Cell Death and Disease is an open-access journal published by Nature Publishing Group. This work is licensed under a Creative Commons Attribution 4.0 International License. The images or other third party material in this article are included in the article's Creative Commons license, unless indicated otherwise in the credit line; if the material is not included under the Creative Commons license, users will need to obtain permission from the license holder to reproduce the material. To view a copy of this license, visit <http://creativecommons.org/licenses/by/4.0/>

Supplementary Information accompanies this paper on Cell Death and Disease website (<http://www.nature.com/cddis>)

Supplementary Figure Legends

Supplementary Figure 1

(a) Cell viability was determined in FADD-deficient Jurkat cells treated overnight with 10 ng/ml TNF α and 10 μ M Nec-1. Representative microscopy (brightfield, 10x) for each condition is shown. Scale bar, 50 μ m. (b) Cell viability was assessed in FADD-deficient Jurkat cells treated overnight with 10 ng/ml TNF α and 10 μ M Nec-1 or ponatinib and pazopanib as indicated. Data represent mean value \pm s.d. of two independent experiments performed in triplicates and normalized to untreated control. Cell viability was assessed using a luminescence-based readout for ATP (CellTiter Glo). (c) Microscopy (brightfield, 10x) of FADD-deficient Jurkat treated overnight with 10 ng/ml TNF α and ponatinib or pazopanib as indicated. Scale bar, 50 μ m. (d) FADD-deficient Jurkat cells were treated for 6 h with 10 ng/ml TNF α and 10 μ M Nec-1, 0.5 μ M ponatinib or 1 μ M pazopanib. Representative flow cytometry blots and gating strategy to determine the percentage of viable cells by size and propidium iodide (PI) exclusion is shown. (e) FADD-deficient Jurkat cells were treated for 2-6 h with 10 ng/ml TNF α and 10 μ M Nec-1, 0.5 μ M ponatinib or 1 μ M pazopanib. The percentage of living cells was determined by PI exclusion and flow cytometry. Data represent mean value \pm s.d. of two replicates. (f) FADD-deficient Jurkat cells were treated for 24 h with Nec-1 or Nec-1s as indicated. Data represent mean value \pm s.d. of two independent experiments performed in triplicates and normalized to untreated control. Cell viability was assessed using a luminescence-based readout for ATP (CellTiter Glo).

Supplementary Figure 2

(a) Cell viability was determined in HT-29 cells treated overnight with 20 ng/ml TNF α (T), 500 nM Smac mimetic (S), 20 μ M caspase inhibitor z-VAD (Z) and the indicated compounds (Nec-1, 10 μ M; all others, 1 μ M). Percentage of living cells was determined by size and PI exclusion using flow cytometry. Data were normalized to untreated control and represent mean value \pm s.d. of two independent experiments. (b) Cell viability was assessed in HT-29 cells treated overnight with 100 ng/ml TRAIL or 100 ng/ml human FasL together with 500 nM Smac mimetic (S), 20 μ M z-VAD (Z), and either 10 μ M Nec-1, 1 μ M ponatinib or 1 μ M pazopanib. Percentage of living cells was

determined by size and PI exclusion using flow cytometry. Data were normalized to untreated control and represent mean value \pm s.d. of two independent experiments. (c) Annexin V-positivity (AV) was measured in Jurkat E6.1 cells treated with 100 ng/ml human FasL and 10 μ M z-VAD, 10 μ M Nec-1, 0.5 μ M ponatinib or 5 μ M pazopanib for 13 h. Percentage of cells positive for AV and PI was determined using flow cytometry. Data represent mean value \pm s.d. of two independent experiments.

Supplementary Figure 3

(a) Cell viability was measured in 3T3-SA cells treated overnight with 1 ng/ml murine TNF α (T), 1 μ M z-VAD (Z), 10 μ M Nec-1s or ponatinib and pazopanib at the indicated concentrations. (b) 3T3-SA cells were treated for 24 h with ponatinib or pazopanib as indicated. (c) Cell viability was measured in L929 cells treated overnight with 50 ng/ml murine TNF α (T), 10 μ M z-VAD (Z), 10 μ M Nec-1 or ponatinib and pazopanib at the indicated concentrations. (d) L929 cells were treated for 24 h with ponatinib or pazopanib as indicated. All data shown represent mean value \pm s.d. of at least two independent experiments performed in triplicates and normalized to untreated control. Cell viability was assessed using a luminescence-based readout for ATP (CellTiter Glo) throughout.

Supplementary Figure 4

(a) HT-29 cells with inducible expression of HA-tagged MLKL S358D were induced (+) or not (-) with 2 μ g/ml doxycycline (Dox) for 8 h. Cells were lysed and immunoblotted as indicated. (b) *In vitro* kinase assay using recombinant RIPK1. Phosphorylation of MBP was monitored in presence of 10 μ M of the indicated kinase inhibitors. Data represent mean value \pm s.d. of two independent experiments and are normalized to DMSO control. (c) Autoradiograph of *in vitro* kinase assay using recombinant RIPK3. Phosphorylation of MBP and RIPK3 autophosphorylation were assessed in the presence of 10 μ M ponatinib or Nec-1s. (d) HT-29 cells with doxycycline-inducible expression of HA-tagged wildtype MLKL were treated overnight with 1 μ g/ml doxycycline and 0.5 μ M ponatinib, 5 μ M pazopanib, 10 μ M Nec-1 or 10 μ M NSA. Cells were lysed and immunoblotted with the indicated antibodies. Data shown are representative of two independent experiments.

Supplementary Figure 5

(a) Cell viability was determined in HT-29 MLKL S358D cells treated overnight with 2 μ g/ml

doxycycline (Dox) and 5 μ M pazopanib. Cell viability was assessed using a luminescence-based readout for ATP (CellTiter Glo). Data represent mean value \pm s.d. of two independent experiments performed in triplicates and normalized to untreated control. **(b)** *In vitro* kinase assay using recombinant RIPK3. Phosphorylation of myelin basic protein (MBP) was monitored in presence of 10 μ M of the kinase inhibitors indicated. Data represent mean value \pm s.d. of two independent experiments normalized to DMSO control.

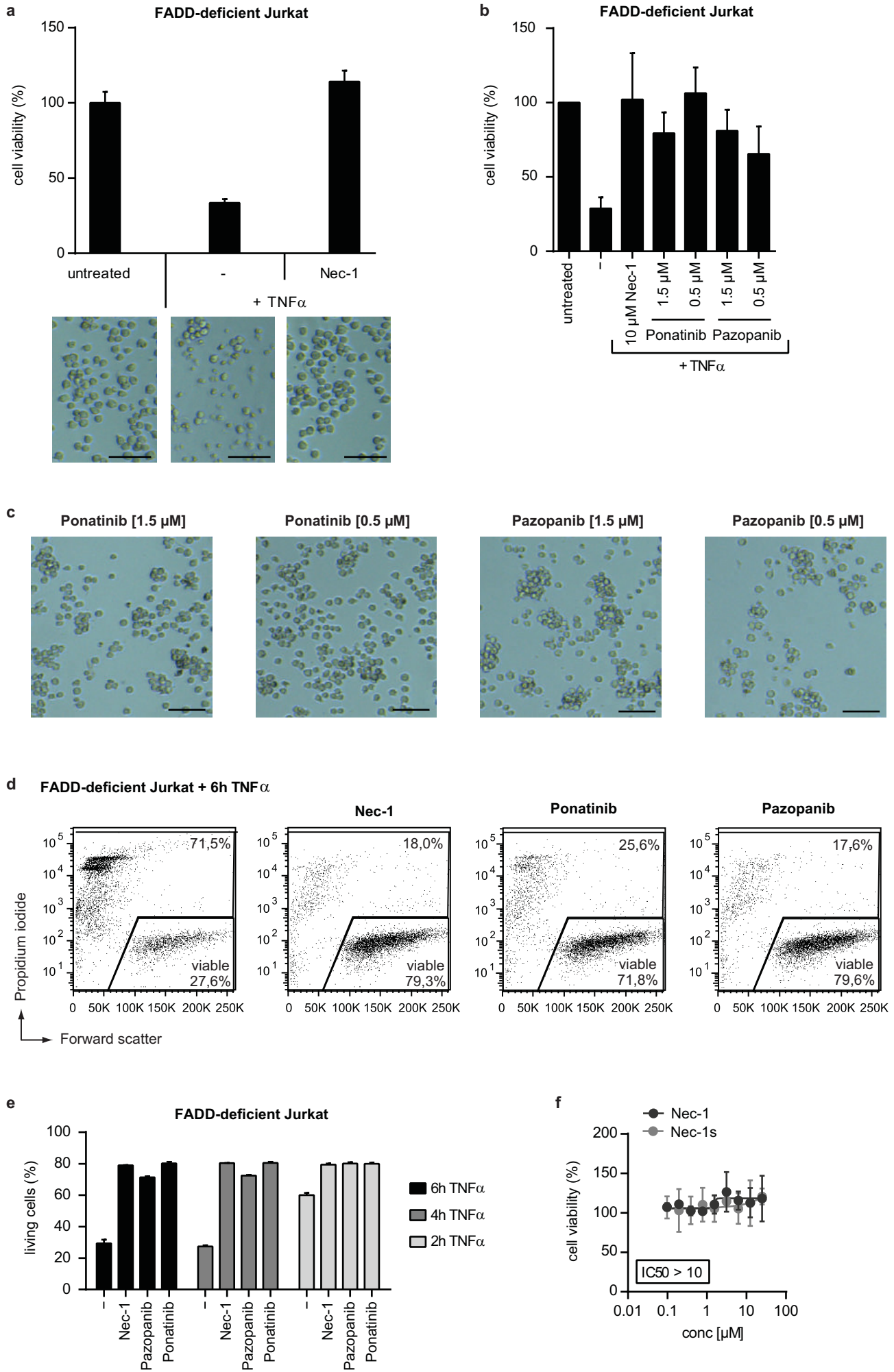
Supplementary Figure 6

(a) Direct binding assay results for ponatinib and TAK1. Data represent mean value \pm s.d. of two independent experiments. **(b)** Cell viability was assessed in FADD-deficient Jurkat cells treated overnight with 10 ng/ml TNF α and 10 μ M Nec-1 or TAK1 inhibitor (TAK1i; NP-009245) as indicated. Data were normalized to untreated control cells and represent mean value \pm s.d. of two independent experiments performed in triplicates. Cell viability was assessed using a luminescence-based readout for ATP (CellTiter Glo). **(c)** Jurkat E6.1 cells were stimulated for the time indicated with 10 ng/ml TNF α and 10 μ M TAK1i (NP-009245) or the IKK inhibitor BMS-345541. Cells were then lysed and subjected to immunoblotting with the antibodies stated. Data shown is representative of two independent experiments.

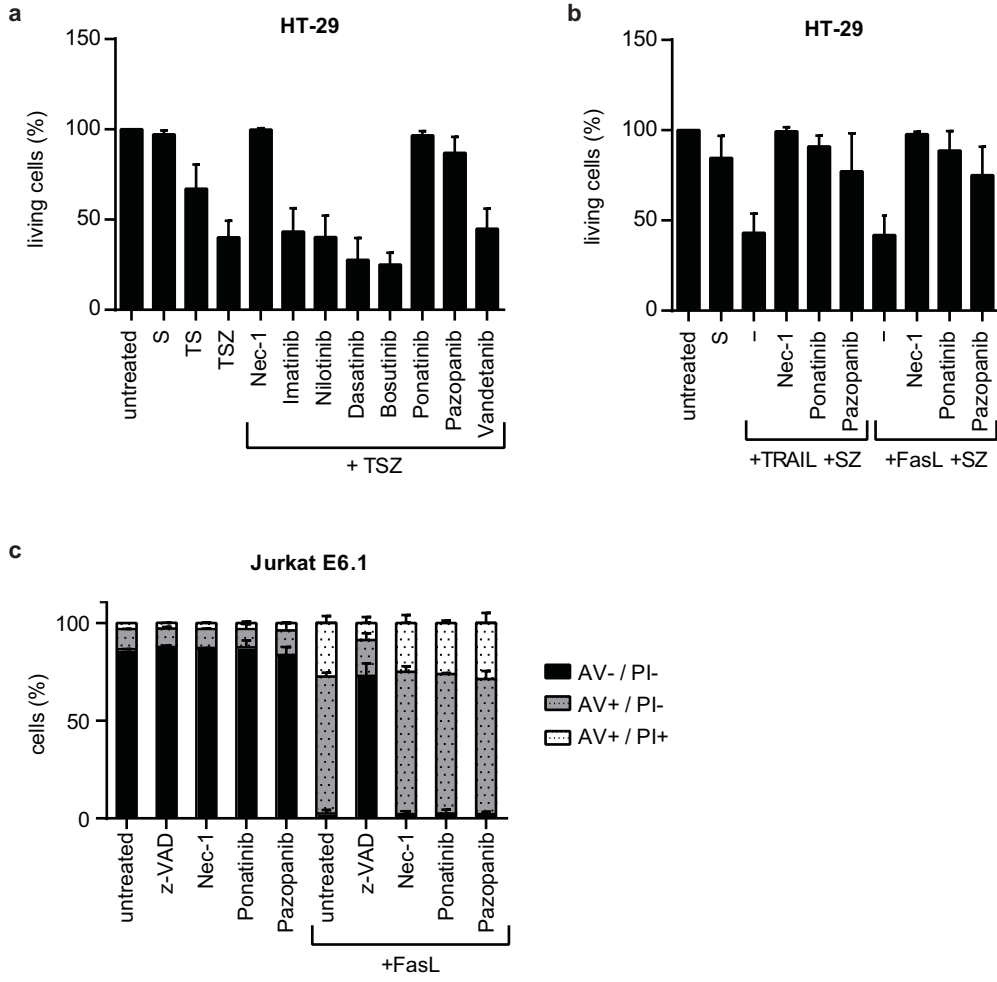
Supplementary Table 1

Average (Av.) and total spectral counts (SC) for proteins identified by LCMS/MS analysis in c-ponatinib pulldowns performed with or without competing (comp.) free ponatinib. P-values were estimated using the modified Decontaminator method (see Materials and Methods) and the significance threshold was set to 0.05.

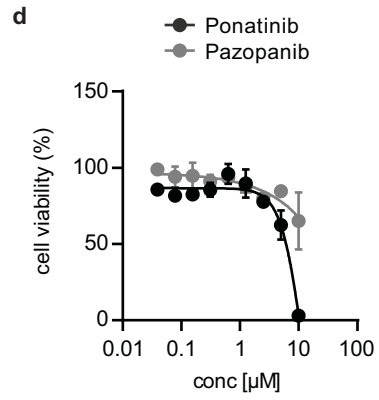
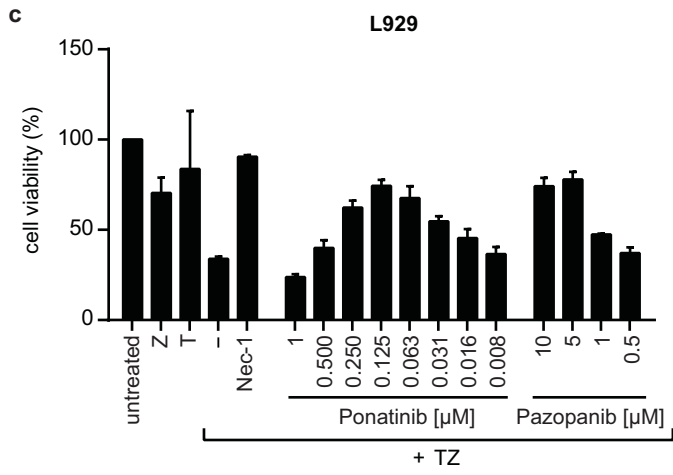
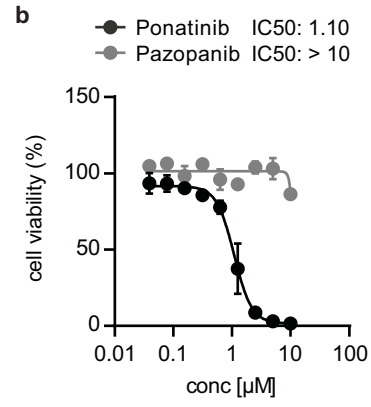
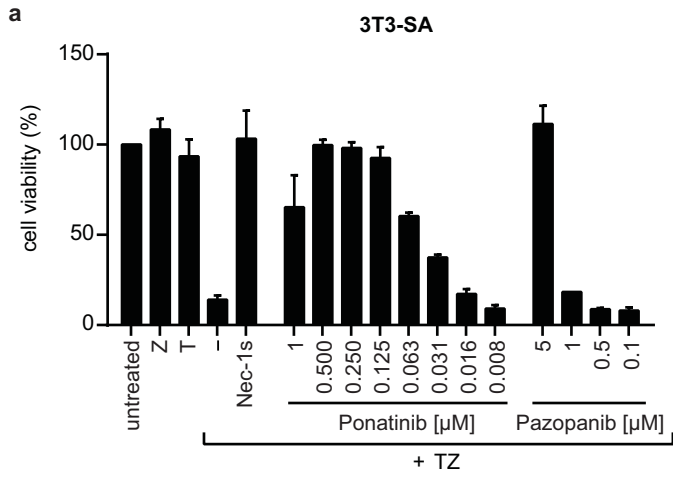
Supplementary Figure 1



Supplementary Figure 2

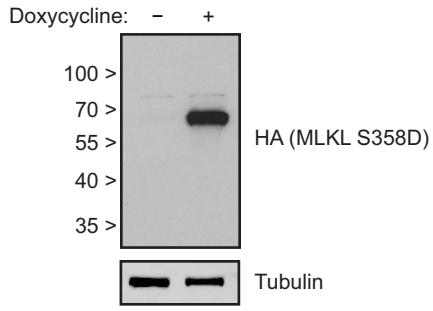


Supplementary Figure 3

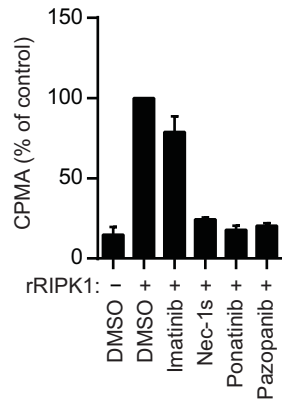


Supplementary Figure 4

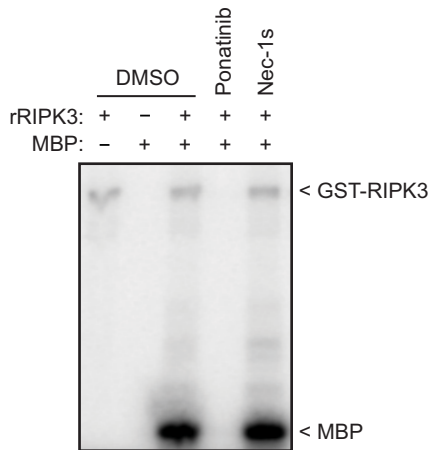
a HT-29 MLKL S358D



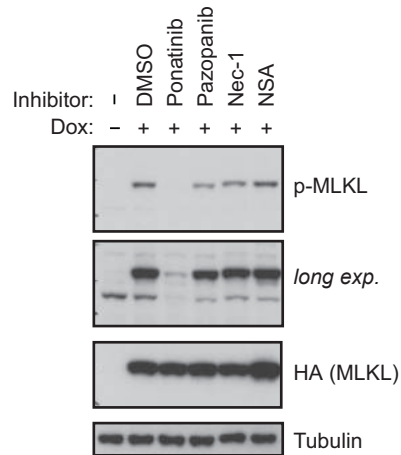
b RIPK1



c RIPK3

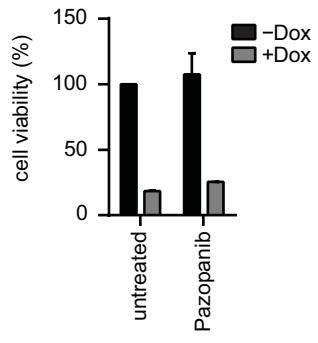


d HT-29 MLKL

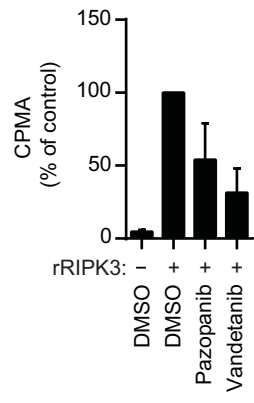


Supplementary Figure 5

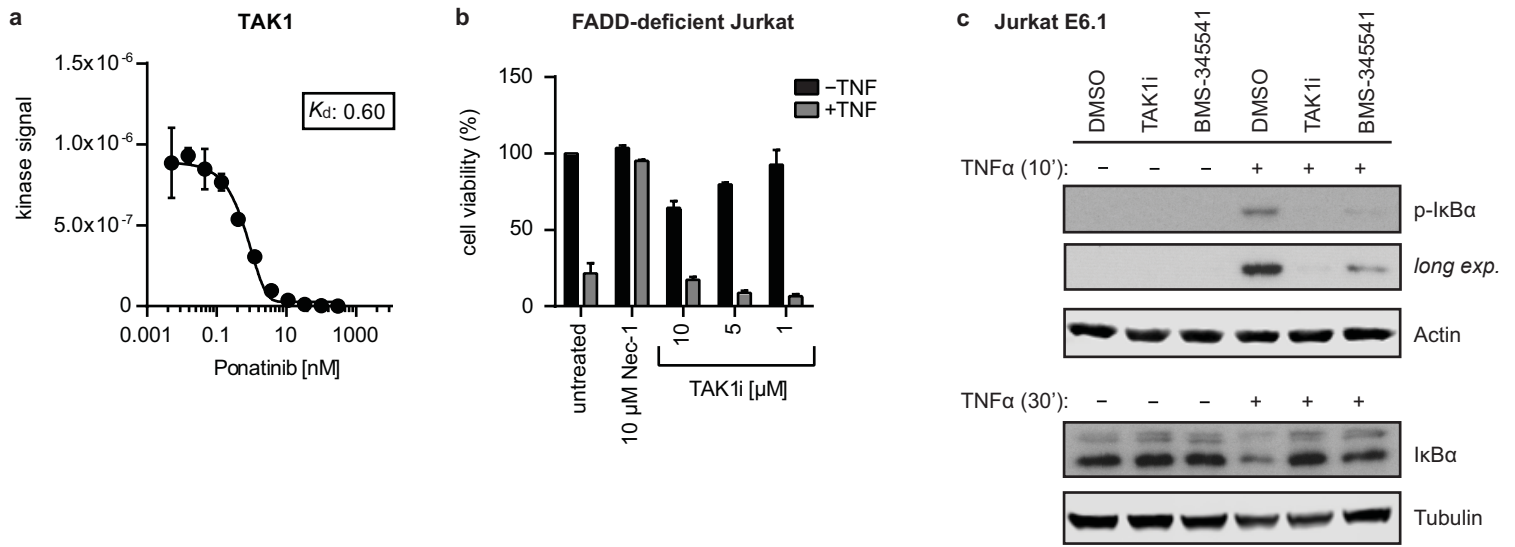
a HT-29 MLKL S358D



b RIPK3



Supplementary Figure 6



Supplementary Table 1: Average (Av.) and total spectral counts (SC) for proteins identified by LC-MS/MS analysis in c-ponatinib pulldowns performed without or with competing (comp.) free ponatinib. Kinases are highlighted in **bold** and kinase targets shared by other BCR-ABL inhibitors (45, 46) are marked with *. Proteins involved in necroptosis signaling are highlighted in **red**.

Protein label	Full protein name	Av. SC	Total SC	Av. SC comp.	Total SC comp.	p-value	
MAP4K1	Mitogen-activated protein kinase kinase kinase kinase 1	46.75	187	2.5	10	6.34E-10	*
ZAK	Mitogen-activated protein kinase kinase kinase MLT	65.25	261	0	0	2.12E-09	*
LCK	Tyrosine-protein kinase Lck	98.5	394	0.75	3	2.91E-09	*
CSK	Tyrosine-protein kinase CSK	52.25	209	4.5	18	1.28E-08	*
PTK2B	Protein-tyrosine kinase 2-beta	32.5	130	0	0	1.37E-08	*
MAP3K7	Mitogen-activated protein kinase kinase kinase 7	19.5	78	2.25	9	4.72E-08	
YWHAB	14-3-3 protein beta/alpha	7	28	1	4	5.18E-08	
TNIK	TRAF2 and NCK-interacting protein kinase	26.75	107	0	0	5.6E-08	*
JAK1	Tyrosine-protein kinase JAK1	21.5	86	0	0	5.81E-08	
MAPKAPK2	MAP kinase-activated protein kinase 2	23.5	94	0	0	6.16E-08	
YWHAE	14-3-3 protein epsilon	13	52	1	4	8.52E-08	
CDK16	Cyclin-dependent kinase 16	10.75	43	1.25	5	1.28E-07	
ABL2	Abelson tyrosine-protein kinase 2	17.25	69	0	0	1.37E-07	*
RIPK3	Receptor-interacting serine/threonine-protein kinase 3	17	68	0	0	1.56E-07	
UNC119	Protein unc-119 homolog A	20.5	82	0	0	2.01E-07	
ABL1	Abl1 human spliceform 1a (myristoylated)	13.75	55	0	0	2.23E-07	*
TAOK3	Serine/threonine-protein kinase TAO3	13	52	2	8	2.52E-07	*
MAPK14	Mitogen-activated protein kinase 14	79.25	317	7.25	29	2.7E-07	*
IRAK1	Interleukin-1 receptor-associated kinase 1	24.25	97	4	16	3.54E-07	
TYK2	Non-receptor tyrosine-protein kinase TYK2	14	56	0	0	3.65E-07	*
MAPKAPK3	MAP kinase-activated protein kinase 3	10.5	42	0	0	5.53E-07	
TAB1	TGF-beta-activated kinase 1 and MAP3K7-binding protein 1	38.25	153	6.75	27	7.74E-07	
MAP3K1	Mitogen-activated protein kinase kinase kinase 1	9	36	0	0	1.01E-06	*
BLK	Tyrosine-protein kinase Blk	9.5	38	0	0	1.12E-06	*
YWHAQ	14-3-3 protein theta	9	36	1.25	5	1.38E-06	
PLEKHF2	Pleckstrin homology domain-containing family F member 2	8.25	33	0	0	1.41E-06	
YWHAZ	14-3-3 protein zeta/delta	10.5	42	2.5	10	1.61E-06	
YWHAH	14-3-3 protein eta	6	24	0.25	1	1.98E-06	
IRAK4	Interleukin-1 receptor-associated kinase 4	8.5	34	2.5	10	1.99E-06	*
HCK	Tyrosine-protein kinase HCK	6	24	0	0	4.48E-06	*
MAP4K4	Mitogen-activated protein kinase kinase kinase kinase 4	54.5	218	10.75	43	4.64E-06	*
UNC119B	Protein unc-119 homolog B	6	24	0	0	5.89E-06	
STK10	Serine/threonine-protein kinase 10	5.5	22	0	0	1.23E-05	*
HSPA5	78 kDa glucose-regulated protein	7	28	2.75	11	1.38E-05	
MAPK12	Mitogen-activated protein kinase 12	10.75	43	3.75	15	1.4E-05	
TESK2	Dual specificity testis-specific protein kinase 2	5	20	0	0	1.57E-05	*
MLKL	Mixed lineage kinase domain-like protein	5	20	0	0	1.82E-05	
CDK19	Cyclin-dependent kinase 19	7.5	30	0	0	2.77E-05	
GAK	Cyclin-G-associated kinase	22.75	91	10.25	41	3.19E-05	*
YWHAG	14-3-3 protein gamma	11.25	45	3.25	13	4.76E-05	
MINK1	Misshapen-like kinase 1	4	16	0	0	6.42E-05	*
CCT4	T-complex protein 1 subunit delta	3.5	14	0	0	2.55E-04	
CDK8	Cyclin-dependent kinase 8	3.75	15	0	0	3.19E-04	
HSPA4	Heat shock 70 kDa protein 4	5.5	22	1.75	7	4.09E-04	
MELK	Maternal embryonic leucine zipper kinase	5	20	1	4	4.66E-04	
HSPA9	Stress-70 protein, mitochondrial	3.25	13	0	0	9.74E-04	
TCP1	T-complex protein 1 subunit alpha	5	20	1.5	6	1.23E-03	
MAPK11	Mitogen-activated protein kinase 11	3	12	0	0	1.40E-03	*
TAB2	TGF-beta-activated kinase 1 and MAP3K7-binding protein 2	2.5	10	0	0	2.99E-03	
CCT2	T-complex protein 1 subunit beta	3.5	14	0	0	5.50E-03	
TUBA1B	Tubulin alpha-1B chain	18.5	74	10.25	41	5.73E-03	
MAP4K2	Mitogen-activated protein kinase kinase kinase kinase 2	2.5	10	0	0	7.21E-03	
JAK2	Tyrosine-protein kinase JAK2	2.25	9	0	0	1.35E-02	
CDK5	Cyclin-dependent kinase 5	7.25	29	2.75	11	1.52E-02	
PAG1	Phosphoprotein associated with glycosphingolipid-enriched microdomains 1	2	8	0	0	1.54E-02	
TPM4	Tropomyosin alpha-4 chain	3.5	14	0.25	1	1.80E-02	
HSPA8	Heat shock cognate 71 kDa protein	29.25	117	17.25	69	2.04E-02	
RIPK1	Receptor-interacting serine/threonine-protein kinase 1	1.5	6	0	0	2.25E-02	
NAP1L1	Nucleosome assembly protein 1-like 1	2	8	1.25	5	2.29E-02	
RAF1	RAF proto-oncogene serine/threonine-protein kinase	1.25	5	0	0	4.76E-02	

2.3. Interlude

An Inducible Retroviral Expression System for Tandem Affinity Purification Mass-Spectrometry-Based Proteomics Identifies MLKL as an HSP90 Client

Bigenzahn, J. W.*, Fauster, A.*, Rebsamen, M., Kandasamy R. K., Scorzoni, S., Vladimer G. I., Müller A. C., Gstaiger M., Zuber J., Bennett, K. L., and Superti-Furga, G. (2015) *Molecular & Cellular Proteomics*, *in press*

*: *equal contribution*

Here, we established a novel inducible expression system suitable for expression of streptavidin-hemagglutinin (SH)-tagged bait proteins in a wide range of cell lines. Besides constituting a useful tool for various phenotypic analyses, the vector system is suitable for SH-based interaction proteomics approaches, thus paving the way for mapping of the necroptosis pathway. This study describes the assembly of the novel vectors along with the characterization of their expression properties. The applicability of the expression system is exemplified by analysis of the oncogenic neuroblastoma RAS viral (v-ras) oncogene homolog (NRAS) G12D mutant protein, as well as the cell death-inducing MLKL mutant S358D. Based on the interaction proteomics data, we identify and functionally validate MLKL as a novel HSP90 client protein (Bigenzahn et al, 2015).

The author of this thesis designed research, took part in cloning of the expression vectors, conducted experiments in HT-29 cells to characterize the vector system properties, carried out phenotypic and mass-spectrometric analysis of the MLKL S358D mutant as well as the majority of the ensuing validation experiments, analyzed and interpreted data, and wrote the manuscript. J. W. Bigenzahn designed research, carried out cloning of the expression vectors, conducted experiments in K-562 and KCL-22 cells to characterize the vector system properties, performed phenotypic characterization and mass spectrometric analysis of NRAS G12D in Ba/F3 cells, analyzed and interpreted data, and wrote the manuscript. M. Rebsamen interpreted data and gave experimental advice. R. K. Kandasamy helped with analysis of the mass spectrometry data. S. Scorzoni and G. I. Vladimer assisted with validation experiments. A. C. Müller carried out mass spectrometric analyses. M. Gstaiger and J. Zuber contributed new reagents or analytical tools. K. L. Bennett designed research and oversaw mass spectrometric analyses. G. Superti-Furga designed research, analyzed and interpreted data, and contributed to writing of the manuscript.

An inducible retroviral expression system for tandem affinity purification mass-spectrometry-based proteomics identifies MLKL as an HSP90 client

Running title: pRSHIC enables identification of MLKL as HSP90 client

Johannes W. Bigenzahn^{1,5}, Astrid Fauster^{1,5}, Manuele Rebsamen¹, Richard K. Kandasamy¹, Stefania Scorzoni¹, Gregory I. Vladimer¹, André C. Müller¹, Matthias Gstaiger², Johannes Zuber³, Keiryn L. Bennett¹, and Giulio Superti-Furga^{1,4,*}

¹CeMM Research Center for Molecular Medicine of the Austrian Academy of Sciences, Vienna, Austria

²Department of Biology, Institute of Molecular Systems Biology, ETH Zürich, Zürich, Switzerland

³Research Institute of Molecular Pathology (IMP), Vienna Biocenter (VBC), 1030 Vienna, Austria

⁴Center for Physiology and Pharmacology, Medical University of Vienna, Vienna, Austria

⁵These authors contributed equally to this work.

Keywords: protein-protein interaction, interaction proteomics, tandem affinity purification-mass spectrometry, streptavidin-hemagglutinin-tag, oncogene, NRAS, necroptosis, MLKL, HSP90

*** Corresponding author:**

Giulio Superti-Furga

CeMM Research Center for Molecular Medicine of the Austrian Academy of Sciences

Lazarettgasse 14, AKH BT25.3

1090 Vienna, Austria

Email: gsuperti@cemm.oeaw.ac.at

Telephone: +43 1 40160 70 001

Fax: +43 1 40160 970 000

ABSTRACT

Tandem affinity purification-mass spectrometry (TAP-MS) is a popular strategy for the identification of protein-protein interactions, characterization of protein complexes, and entire networks. Its employment in cellular settings best fitting the relevant physiology is limited by convenient expression vector systems. We developed an easy-to-handle, inducible, dually selectable retroviral expression vector allowing dose-and time dependent control of bait proteins bearing the efficient streptavidin-hemagglutinin (SH)-tag at their N- or C-termini. Concomitant expression of a reporter fluorophore allows to monitor bait-expressing cells by flow cytometry or microscopy, and enables high-throughput phenotypic assays. We used the system to successfully characterize the interactome of the neuroblastoma RAS viral oncogene homolog (NRAS) G12D mutant and exploited the advantage of reporter fluorophore expression by tracking cytokine-independent cell growth using flow cytometry. Moreover, we tested the feasibility of studying cytotoxicity-mediating proteins with the vector system on the cell death-inducing mixed lineage kinase domain-like protein (MLKL) S358D mutant. Interaction proteomics analysis of MLKL S358D identified heat shock protein 90 (HSP90) as a high-confidence interacting protein. Further phenotypic characterization established MLKL as a novel HSP90 client. In summary, this novel inducible-expression system enables SH-tag-based interaction studies in the cell line proficient for the respective phenotypic or signaling context and constitutes a valuable tool for experimental approaches requiring inducible or traceable protein expression.

INTRODUCTION

Protein-protein interactions are the basis of most cellular processes and characterizing the complexes associated with a given protein greatly increases understanding of the biological function (1). Tandem affinity purification (TAP) (2, 3) coupled to mass spectrometry (MS) constitutes a powerful technique for identifying high-confidence interaction partners of tagged bait proteins (4-6). The reduction of non-specific background binding due to dual-affinity purification has made TAP-MS the method of choice for protein interaction mapping (7-9) and more than 30 different tandem tags have been established so far by alternative combination of affinity handles (10, 11). Specifically, the purification procedure for the recently developed SH-tag (12) shows particularly high bait protein recovery (10). In combination with the flippase-flippase recognition target (Flp-*FRT*) recombination system, SH-based TAP-MS has been successfully applied to the in-depth analysis of human signaling networks (12-15) and virus-host interactions (16). A detailed interlaboratory comparative analysis of highly standardized procedure using HEK293 cells revealed a reproducibility within an individual laboratory of 98% and a reproducibility between two laboratories of more than 80%, suggesting robustness of the method using workhorse cell-lines (15).

Charting the interactome of a specific protein in the relevant physiological setting, in context of its functional signaling pathway, requires performing interaction proteomics in different cellular backgrounds. Highly efficient gene delivery to a variety of cell lines, including cell types that are difficult to transfect, can be achieved by viral vector-mediated gene transfer (17). Temporal and reversible control of bait protein expression can be achieved by using inducible expression systems, further enabling the analysis of proteins with toxic ectopic expression. Tetracycline (Tet)-On systems (18) have proven to be valuable tools for inducible expression of cDNAs or short hairpin RNAs (shRNAs) in cell lines and animals models (19, 20).

To date, TAP-MS experiments are based on Flp-In technology or viral-based transgene delivery of bait proteins fused to different affinity tags with a diverse range of expression and bait recovery efficiency (10, 11, 21). Whilst the SH-tag has comparably high bait recovery (10) and strong inter-laboratory reproducibility (15), its application has so far been restricted to the limited number of Flp-In system-competent cell lines. To overcome this limitation and widen the reach of SH-based TAP-

MS studies we established and characterized pRSHIC (retroviral expression of SH-tagged proteins for interaction proteomics and color-tracing). This novel retroviral, doxycycline-inducible Tet-On vector system is suitable for expression of SH-tagged target proteins in a wide range of cell systems. In addition to enlarging the existing toolbox for TAP-MS-based interaction proteomics, the features and versatility of pRSHIC make it a valuable tool for a broad set of phenotypic analyses. To illustrate the features of pRSHIC, we charted the interactome of the oncogenic NRAS G12D mutant protein (22, 23), as delineating the network properties of such cancer-associated gene variants is crucial to understand their impact on the disease (24). Furthermore, we demonstrated the applicability of pRSHIC to study cytotoxicity-inducing proteins using the MLKL mutant S358D (25). MLKL is the key molecule required for executing necroptosis, a form of programmed necrotic cell death (26-28). Our study identified MLKL to associate with HSP90 and functionally validated MLKL as a novel client protein of HSP90.

RESULTS AND DISCUSSION

Generation of a retroviral expression system for inducible, dose-dependent and reversible expression of SH-tagged bait proteins.

We assembled an inducible expression system in a self-inactivating retroviral vector containing a tetracycline response element tight (TRE_{tight}) promoter (29). For expression of N- or C-terminally TAP-tagged cDNAs we inserted a gateway-cloning cassette preceded or followed by two streptavidin and one hemagglutinin epitope(s) (12) (Figure 1a). The recombination efficiency of the gateway system allows high-throughput cloning and thus the vector is suitable for use with gateway-compatible cDNA- and ORF-libraries. Furthermore, we linked a fluorescent mCherry marker to the cDNA expression cassette via an internal ribosome entry site (IRES) sequence to enable tracing of bait protein-expressing cell populations by flow cytometry or microscopy. The doxycycline-controlled reverse tet transactivator protein 3 (rtTA3) (30) in combination with different TRE promoters has proven to be effective in inducing transgene expression in a broad range of cell lines and tissues *in vivo* (31). To generate Tet-On proficient cell lines the respective target cells are first stably transduced with rtTA3 or a combination of rtTA3- and the ecotropic receptor (RIEP), the latter also providing enhanced biosafety (32). Cell lines with inducible bait protein expression are then established by retroviral transduction of rtTA3 transgene-harboring target cells with the respective pRSHIC constructs (Figure 1b). Transduced cells are selected using blasticidin, and transgene expression in the target cell lines can be assessed by flow cytometry or immunoblotting prior to TAP-MS and follow-up experiments.

To characterize the properties of this novel expression system, we transduced human leukemia K-562 RIEP, KCL-22 RIEP and colorectal adenocarcinoma HT-29 RIEP cells with a vector construct encoding SH-tagged green fluorescent protein (GFP). Following selection using blasticidin, the cells were cultured in the presence of doxycycline for 24 hours to induce GFP expression. In all three cell lines >85% of the cell population efficiently induced gene expression as determined by the detection of the mCherry reporter using flow cytometry (Figures 2a-c). Target protein expression was confirmed by immunoblotting for SH-tagged GFP (Figures 2d-f). Additionally, we observed strong correlation between GFP and mCherry fluorescence (Figure 2g and Supplementary Figures 1a-c), indicating that

flow cytometry-based detection of the mCherry marker provides a reliable surrogate measure for efficient induction of transgene expression. The TREtight promoter exhibits low basal expression while promoting high-level transcription upon induction. Depending on the promoter used, the efficiency of inducible expression by Tet-regulated systems and the basal expression levels can vary between different cell types (31). For bait proteins with elevated basal expression levels in the context of the TREtight promoter, we additionally created a set of vectors harboring a TRE3G promoter (Supplementary Figure 2a), which provides strongly reduced basal expression compared to earlier versions of the TRE promoter (33) (Supplementary Figure 2b). As demonstrated in K-562 RIEP GFP cells, expression of bait proteins can be modulated by the addition of increasing concentrations of doxycycline (Figure 2h). Furthermore, we monitored induction kinetics indicating that GFP was induced within hours after doxycycline addition and continued to accumulate over 24 hours (Figure 2i). Removal of doxycycline led to a decline in GFP levels, illustrating the reversibility of bait expression (Figure 2i). Altogether, these data establish pRSHIC as a versatile inducible vector system that enables scaling and reversible expression of SH-tagged bait proteins in multiple mammalian cell types.

Phenotypic characterization and interaction-proteomic analysis of NRAS G12D in the murine pro B cell line Ba/F3

Cancer genome sequencing projects continue to reveal novel gene mutations and fusions (23). Understanding the molecular function of these genetic alterations requires characterization of their phenotypic impact on transformation and specific influence on protein-protein interactions (34, 35). We therefore chose to exemplify utility of pRSHIC through phenotypic analysis of the oncogenic G12D mutant of NRAS, a member of the rat sarcoma (RAS) family (H-, K-, and NRAS) of guanosine triphosphate (GTP)-binding proteins and frequently mutated in hematological malignancies (22). We demonstrated the growth-promoting effects and delineated the interactome of NRAS G12D in the murine bone marrow-derived pro-B cell line Ba/F3. This cell line requires interleukin (IL)-3 for survival and proliferation, and thus constitutes a convenient tool for studying oncogene-induced growth factor independence (36). We generated Tet-On competent Ba/F3 cells inducibly expressing N-terminal SH-tagged NRAS G12D or a GFP control (Supplementary Figures 3a and b). To examine NRAS G12D-mediated growth factor independence, we performed flow cytometry-based

proliferation-competition assays. While both cell populations showed equal growth in the presence of IL-3, NRAS G12D-expressing cells rapidly out-competed GFP-expressing control cells upon IL-3 withdrawal (Figure 3a). Cytokine removal led to loss of signal transducer and activator of transcription 5 (STAT5) phosphorylation in both cell lines, however, NRAS G12D cells maintained elevated mitogen-activated protein kinase kinase (MEK) 1/2 phosphorylation and hence activation of the mitogen-activated protein kinase (MAPK) pathway (Figure 3b). Consequently, NRAS G12D-expressing cells showed marked sensitivity to the MEK 1/2 inhibitors trametinib (GSK1120212) (Figure 3c) and selumetinib (AZD6244) (Figure 3d) in the absence of IL-3, as increasing drug concentrations reduced MAPK pathway activation and ribosomal protein S6 kinase 1 (S6K1) phosphorylation (Supplementary Figure 3c). In order to map the interactome of NRAS G12D, we induced bait protein expression for 24 hours with doxycycline in the presence of IL-3 and performed TAP coupled to one-dimensional gel-free liquid chromatography tandem mass spectrometry (TAP-LC-MS/MS). SAINT analysis using GFP purifications as a control for non-specific protein interactions identified Ras and Rab interactor 1 (RIN1) amongst the high-confidence interacting proteins of NRAS G12D (Figure 3e and Supplementary Table 1). Indeed, RIN1 has been described as associating with HRAS, and to preferentially bind active, GTP-loaded RAS (37). RIN1 competes with the RAF proto-oncogene serine/threonine-protein kinase (RAF1) for RAS binding (38). Furthermore, we identified phosphatidylinositol-4,5-bisphosphate 3-kinase catalytic subunit gamma isoform (p110 γ ; PK3CG) of the phosphoinositide-3-kinase (PI3K) complex as a significant interactor. Binding of active RAS isoforms to p110 γ leads to activation of the PI3K-pathway (39, 40), and the interaction with p110 α (PK3CA) is important for mutant RAS-induced cancer formation and maintenance *in vivo* (41, 42). In summary, by recapitulating the interaction partners and phenotypic features of the oncogenic NRAS G12D protein, we showed that pRSHIC is an efficient tool to functionally annotate and mechanistically characterize proteins bearing cancer-relevant mutations.

Phenotypic analysis of a cell death-inducing MLKL S358D mutant protein

The possibility of tightly controlling the timing and extent of protein expression is necessary when investigating proteins that trigger cell death. The pseudokinase MLKL plays a key role in the

execution of necroptosis, a form of non-apoptotic programmed cell death relying on the receptor-interacting serine/threonine kinase 1 (RIPK1) and RIPK3 that in recent years has been the subject of very intense research efforts (26-28). Upon activation by RIPK3-mediated phosphorylation, MLKL triggers destabilization and rupture of membranes, resulting in rapid cell death (43-47). We expressed and analyzed a constitutively active MLKL mutant, known to trigger necroptosis (25, 46). We chose to study the RIPK3-phosphorylation mimicking MLKL S358D mutant (48) in the human colorectal adenocarcinoma cell line HT-29, proficient to undergo necroptosis. We observed robust expression of the MLKL S358D mutant in HT-29 RIEP cells within six hours of doxycycline addition (Figure 4a and Supplementary Figure 4a). As we have shown previously (48), exogenous expression of constitutively active mutant versions of MLKL induces toxicity in these cells. Indeed, MLKL S358D triggered cell death within 12 hours after induction as demonstrated by cell viability measurement (Figure 4b) and microscopy (Supplementary Figure 4b). The MLKL inhibitor necrosulfonamide (NSA) (46) inhibited MLKL S358D-induced cell death (48) in a dose-dependent manner (Figure 4c). Conversely, the RIPK1 inhibitor Necrostatin-1 (Nec-1) (49) that blocks necroptosis signaling upstream of MLKL, did not confer protection. These data demonstrate that pRSHIC enables expression and, consequently, phenotypic analysis of proteins that promote cell death.

TAP-LC-MSMS analysis identifies MLKL S358D as an HSP90 client protein.

To identify novel protein interaction partners of MLKL S358D, the cells were induced for seven hours with doxycycline before harvest and TAP-LC-MSMS analysis. The known interactor RIPK3 (47) was significantly enriched in MLKL S358D pulldowns (Figure 4d). Furthermore, HSP72 (Heat shock-related 70 kDa protein 2), HSP90A/B and the kinase-adaptor co-chaperone cell division cycle 37 (CDC37) (50) were identified as high-confidence interactors based on SAINT analysis (51). These heat shock proteins act as molecular chaperones, assisting other proteins to attain and maintain proper folding (52). The comparably high CRAPome frequencies (53) assigned to HSP90 and HSP72 likely reflect the large number of client proteins they functionally interact with. Chemical inhibition of HSP90 function leads to client protein destabilization and degradation. Importantly, the HSP90 inhibitor geldanamycin (54) has been shown to block necroptotic cell death (55). This inhibitory effect

has been attributed to the destabilizing effect on the two main kinases involved in necroptosis signaling, RIPK1 and RIPK3. Both have been demonstrated to depend on HSP90 (56-58). Our TAP-MS analysis would however suggest that the interaction of MLKL with HSP90 may also contribute to this inhibitory effect (Figure 4d). In order to investigate the functional relevance of HSP90 for MLKL S358D, we induced expression in HT-29 RIEP MLKL S358D cells by doxycycline addition for 3 hours in the presence of geldanamycin, Nec-1 or NSA. Geldanamycin led to a strong decrease in MLKL S358D protein levels, whereas the other inhibitors had no effect (Figure 5a). To exclude the possibility that geldanamycin interfered with the inducible expression system *per se*, we verified that the mCherry reporter was equally expressed in both control and geldanamycin-treated samples by flow cytometry (Supplementary Figure 4c). The rapid degradation of MLKL S358D upon HSP90 inhibition suggested that this protein constitutes a novel HSP90/CDC37 client. Indeed, the closely related mixed lineage kinase 3 (MLK3) has previously been shown to be stabilized by association with HSP90, and the co-chaperone CDC37 (59). The geldanamycin-induced loss of MLKL S358D protein could be prevented by simultaneous treatment with the proteasome inhibitor MG132 (Figure 5b), whereas blocking lysosomal protein degradation using chloroquine had no effect. This data suggested that MLKL S358D was subjected to proteasomal degradation in the absence of HSP90-mediated stabilization, similar to previously described HSP90 client proteins (57). Neither Nec-1 nor ponatinib, recently described to inhibit both RIPK1 and RIPK3 (48, 60) blocked MLKL S358D-induced cell death, indicating that it proceeded independently of these kinases. Yet, the HSP90 inhibitor geldanamycin efficiently blocked MLKL S358D-dependent necroptotic cell death in HT-29 cells (Figure 5c), further corroborating the requirement of HSP90 for MLKL S358D.

Finally, we investigated the requirement of HSP90 function for the MLKL wild-type protein. Similar to the S358D mutant, geldanamycin induced destabilization of the wild-type MLKL protein and this degradation could be blocked by concomitant MG132 treatment (Figure 5d). To confirm the interaction between HSP90 and wild-type MLKL as well as the MLKL S358D mutant, we performed co-immunoprecipitation experiments. MLKL co-purified HSP90, similar to the previously described HSP90 client protein RIPK3 (58) (Figure 5e). As demonstrated by the identification and

characterization of MLKL as a novel HSP90 client, pRSHIC is an efficient tool to perform phenotypic and TAP-MS analysis of toxicity-promoting proteins.

CONCLUSIONS

We have established a retroviral-based expression system that expands the repertoire of cell lines amenable to SH-based TAP-MS experiments and thus enables interaction proteomic experiments in the physiologically relevant cellular background. The IRES-linked fluorescent reporter protein allows quick evaluation of bait protein induction by flow cytometry, fluorescence-activated cell sorting (FACS) of specific cell populations and live tracing of bait-expressing cells to assess phenotypic changes (i.e. morphology, surface marker expression, drug resistance). Intracellular localization of the bait proteins can be assessed by probing for the N- or C-terminally fused SH-tag. Moreover, the inducibility of bait expression allows proteins that promote cell death to be studied and opens the opportunity to perform targeted chemical screens in the cell system of choice.

Here, we demonstrated efficiency and applicability of pRSHIC for TAP-MS-based interaction proteomics studies on the oncogenic NRAS G12D mutant protein (22) in murine Ba/F3 cells. Furthermore, we performed interaction proteomics and detailed phenotypic analysis of the cell death-inducing MLKL S358D mutant protein (25) in HT-29 cells, leading to the identification of MLKL as a novel HSP90 client protein.

AUTHOR INFORMATION

Corresponding Author

*, CeMM Research Center for Molecular Medicine of the Austrian Academy of Sciences, Lazarettgasse 14, AKH BT25.3, 1090 Vienna, Austria, email: gsuperti@cemm.oeaw.ac.at, Telephone: +43 1 40160 70 001

Author contributions

J.W.B., A.F., K.L.B. and G.S-F. designed research; J.W.B., A.F., S.S., G.I.V., and A.C.M. performed research; J.Z. and M.G. contributed new reagents or analytical tools, J.W.B., A.F., M.R., R.K.K., G.S-F. analyzed and interpreted the data; J.W.B., A.F., and G.S-F. wrote the paper.

Conflict of interest

The authors declare no competing financial interest.

ACKNOWLEDGMENT

We are grateful to all members of the Superti-Furga laboratory for discussions and feedback and also to the Bennett laboratory for the proteomic analyses. We thank Alexey Stukalov and Peter Májek for help with data conversion. We further thank Katrin Hörmann, Branka Radic Sarikas and Leonhard Heinz for critically reading the manuscript. This work was supported by the Austrian Academy of Sciences, ERC grant to G.S.-F. (i-FIVE 250179), EMBO long-term fellowship to M.R. (ALTF 1346-2011), R.K.K. (ALTF 314-2012) and G.I.V. (ALTF 1543-2012), Marie Curie fellowship to M.R. (IEF 301663), and Austrian Science Fund grant to J.Z. (FWF SFB F4710) and J.W.B. (FWF SFB F4711).

ABBREVIATIONS

CDC37, cell division cycle 37; Flp, Flippase; Flp-*FRT*, flippase-flippase recognition target; GFP, green fluorescent protein; GTP, guanosine triphosphate; HSP90, heat shock protein 90; IL3, interleukin-3; IRES, internal ribosome entry site; MAPK, mitogen-activated protein kinase; MEK, mitogen-activated protein kinase kinase; MLK3, mixed lineage kinase 3; MLKL, mixed lineage kinase domain-like protein; Nec-1, Necrostatin-1; NRAS, neuroblastoma RAS viral oncogene homolog; NSA, necrosulfonamide; PK3CG, phosphatidylinositol-4,5-bisphosphate 3-kinase catalytic subunit gamma isoform; RAF1, RAF proto-oncogene serine/threonine-protein kinase; RAS, rat sarcoma; RIN1, Ras and Rab interactor 1; RIPK, receptor-interacting serine/threonine-protein kinase; rtTA3, reverse tet transactivator protein 3; RIEP, rtTA3-IRES-ecotropic receptor-PGK-PuroR; S6K1, ribosomal protein S6 kinase; shRNA, short hairpin RNA; SH, streptavidin-hemagglutinin-tag; TAP, tandem affinity purification; STAT5, signal transducer and activator of transcription 5; TET, tetracycline; TRE, tetracycline-responsive element; pRSHIC, retroviral expression of SH-tagged proteins for interaction proteomics and color-tracing

MATERIALS AND METHODS

Cell lines and reagents

HEK293T were obtained from ATCC (Manassas, VA, USA), K-562 and KCL-22 from DSMZ (Braunschweig, Germany). HT-29 were kindly provided by P. Schneider (Lausanne). Cells were cultured in DMEM (Sigma-Aldrich, St. Louis, MO, USA) or RPMI medium (Sigma-Aldrich) supplemented with 10% (v/v) FBS (Gibco, Grand Island, NY, USA) and antibiotics (100 U/mL penicillin and 100 mg/mL streptomycin) (Sigma-Aldrich). Ba/F3 were obtained from DMSZ and grown in RPMI supplemented with 10% (v/v) FBS (Gibco) and 1-3 ng/mL recombinant murine IL-3 (213-13, PeproTech, Rocky Hill, NJ, USA). The reagents used were as follows: doxycycline (D9891, Sigma-Aldrich), necrostatin-1 (N9037, Sigma-Aldrich), necrosulfonamide (480073, Merck Millipore, Billerica, MA, USA), geldanamycin (G-1047, AG Scientific, San Diego, CA, USA), MG132 (C2211, Sigma Aldrich), chloroquine (C6628, Sigma Aldrich), selumetinib (S1008, Selleck Chemicals, Houston, TX, USA), trametinib (S2673, Selleck Chemicals) and ponatinib (S1490, Selleck Chemicals).

Antibodies

Antibodies used were HA (SC-805, Santa Cruz, Dallas, TX, USA), HA-7-HRP (H6533, Sigma-Aldrich), MEK1/2 (#9126, Cell Signaling, Danvers, MA, USA), phospho-MEK1/2 (#2338, Cell Signaling), ERK1/2 (M5670, Sigma-Aldrich), phospho- ERK1/2 (#4370, Cell Signaling), STAT5 (610191, BD Biosciences, Franklin Lakes, NJ, USA), phospho-STAT5A/B (05-886R, Merck Millipore), phospho-p70 S6 kinase (#9234, Cell Signaling), p70 S6 kinase (SC-230, Santa Cruz), RIPK3 (12107, Cell Signaling), HSP90 (610418, BD Transduction Laboratories), actin (AAN01-A, Cytoskeleton, Denver, CO, USA), and tubulin (ab7291, Abcam, Cambridge, UK). The secondary antibodies used were goat anti-mouse HRP (115-035-003, Jackson ImmunoResearch, West Grove, PA, USA), goat anti-rabbit HRP (111-035-003, Jackson ImmunoResearch), and Alexa Fluor 680 goat anti-mouse (A-21057, Molecular probes, Grand Island, NY, USA).

Plasmids and cloning

Inducible retroviral expression vectors are derived from the pQCXIX self-inactivating retroviral vector backbone (pSIN, Clontech). pRSHIC vectors were assembled using standard cloning techniques and final expression constructs contain the following elements: pSIN-TREtight or TRE3G-HA-StrepII-Gateway cassette-IRES-mCherry-PGK-BlastR for N-terminal StrepHA tagging and pSIN-TREtight or TRE3G-Gateway cassette-StrepII-HA-IRES-mCherry-PGK-BlastR for C-terminal StrepHA tagging. Detailed cloning strategies, primers and vector information are available upon request. NRAS coding sequence was PCR-amplified from K562 cDNA and cloned into the Gateway-compatible pDONR221 entry vector using BP recombination (Invitrogen, Grand Island, NY, USA). The G12D mutant version of NRAS was generated by site-directed mutagenesis using the QuikChange Lightning Site-Directed Mutagenesis Kit (Agilent Technologies, Santa Clara, CA, USA) using the following primers 5'-GTGGTGGTTGGAGCAGATGGTGTGGGAAAAGC-3' and 5'-GCTTTTCCCAACACCATCTGCTCCAACCACCAC-3'. Cloning of RIPK3, MLKL and MLKL S358D has been described elsewhere (48). Following sequence verification, the cDNAs were transferred by LR recombination (Invitrogen) into pRSHIC vectors. All vectors are available upon request.

Generation of inducible cell lines

Human cell lines were retrovirally transduced using vector pMSCV-rtTA3-IRES-EcoR-PGK-PuroR (pMSCV-RIEP) (29) and murine cell lines were transduced with pMSCV-rtTA3-PGK-PuroR (pMSCV-RP) (29) to generate rtTA3 and ecotropic receptor-coexpressing (RIEP) or rtTA3-expressing (rtTA3) Tet-on competent cell lines, respectively. Briefly, HEK293T cells were transiently transfected with pGAG-POL, pVSV-G, pADVANTAGE and pMSCV-RIEP or pMSCV-RP. The medium was exchanged 24 h later and replaced with the medium for the respective target cell line. After 48 h the virus-containing supernatant was harvested, filtered (0.45 μ m), supplemented with 8 μ g/mL protamine sulfate (Sigma-Aldrich) and added to 40-60% confluent target cell lines. Suspension cells were subjected to spinfection (2000 *rpm*, 45 min, room temperature). 24 h after infection the medium was exchanged and replaced with fresh medium. Another 24 h later, the medium was supplemented with 1-2 μ g/mL puromycin (Sigma-Aldrich) to select for infected cells. Following puromycin selection,

RIEP- or rtTA3-expressing cell lines were similarly transduced with retrovirus produced in HEK293T cells using the respective target gene-encoding pRSHIC vector, and pGAG-POL, pADVANTAGE and pEcoEnv. Infected cells were selected by addition of 15-25 $\mu\text{g}/\text{mL}$ blasticidin (InvivoGen). Target gene expression was induced by addition of 1-2 $\mu\text{g}/\text{mL}$ doxycycline.

Immunoblotting

Cells were lysed using Nonidet-40 lysis buffer (50 mM HEPES pH 7.4, 250 mM NaCl, 5 mM EDTA, 1% NP-40, 10 mM NaF, 1 mM Na_3VO_4 , one tablet of EDTA-free protease inhibitor (Roche) per 50 ml) or IP lysis buffer (50mM Tris-HCl pH 7.5, 150mM NaCl, 5mM EDTA, 1% NP-40, 50 mM NaF, 1 mM Na_3VO_4 , 1 mM PMSF, 5 $\mu\text{g}/\text{mL}$ TPCK and protease inhibitor cocktail) for 10 min on ice. Lysates were cleared by centrifugation (13000 *rpm*, 10 min, 4°C). The proteins were quantified with BCA (Pierce, Grand Island, NY, USA) or Bradford assay using γ -globin as a standard (Bio-Rad, Hercules, CA, USA). Cell lysates were resolved by SDS-PAGE and transferred to nitrocellulose membranes Protran BA 85 (GE Healthcare, Little Chalfont, UK). The membranes were immunoblotted with the indicated antibodies. Bound antibodies were visualized with horseradish peroxidase-conjugated secondary antibodies using the ECL Western blotting system (Thermo Scientific, Waltham, MA, USA) or Odyssey Infrared Imager (LI-COR, Lincoln, NE, USA).

Immunoprecipitation

Cells were washed in PBS and lysed in ice-cold HENG buffer (50 mM HEPES-KOH [pH 7.9], 150 mM NaCl, 20 mM Na_2MoO_4 , 2 mM EDTA, 5% glycerol, 0.5% Triton X-100, one tablet of EDTA-free protease inhibitor (Roche, Indianapolis, IN, USA) per 50 ml, 20 mM NaF and 0.4 mM Na_3VO_4) for 10 min on ice. Lysates were cleared by centrifugation (13000 *rpm*, 10 min, 4°C), quantified with BCA (Pierce), and precleared (30 min, 4°C) on Sepharose6 beads (Sigma-Aldrich). Subsequently, lysates were incubated (3h, 4°C) with monoclonal anti-HA agarose antibody (Sigma-Aldrich). Beads were recovered by centrifugation and washed three times with lysis buffer before analysis by SDS-PAGE and immunoblotting.

Affinity purifications and sample preparation for liquid chromatography mass spectrometry

Tandem affinity purifications were performed as previously described (15, 61). Affinity purifications were performed as biological replicates and cell lines expressing SH-tagged GFP were used as negative controls. In brief, cell lines were incubated with 1-2 $\mu\text{g/mL}$ doxycycline for 7-24 h to induce expression of SH-tagged bait proteins. Whole cell extracts were prepared in 50 mM HEPES pH 8.0, 150 mM NaCl, 5 mM EDTA, 0.5% NP-40, 50 mM NaF, 1 mM Na_3VO_4 , 1 mM PMSF and protease inhibitor cocktail. Cell lysates were cleared by centrifugation (13000 *rpm*, 20 min, 4°C). Proteins were quantitated by Bradford assay using γ -globin as standard (Bio-Rad). 50 mg total lysate was incubated with StrepTactin sepharose beads (IBA, Göttingen, Germany). Tagged proteins were eluted with D-biotin (Alfa-Aesar, Ward Hill, MA, USA) followed by a second purification step using HA-agarose beads (Sigma-Aldrich). Protein complexes were eluted with 100 mM formic acid and immediately neutralized with triethylammonium bicarbonate buffer (Sigma-Aldrich). Samples were digested with trypsin (Promega, Fitchburg, WI, USA) and the resultant peptides desalted and concentrated with customised reversed-phase tips (62). The volume of the eluted samples was reduced to $\sim 2 \mu\text{L}$ in a vacuum centrifuge and reconstituted with 5% formic acid.

Reversed-Phase Liquid Chromatography Mass Spectrometry

Mass spectrometry was performed on a hybrid linear trap quadrupole (LTQ) Orbitrap Velos mass spectrometer (ThermoFisher Scientific, Waltham, MA) using the Xcalibur version 2.1.0 coupled to an Agilent 1200 HPLC nanoflow system (dual pump system with one pre-column and one analytical column) (Agilent Biotechnologies, Palo Alto, CA) via a nanoelectrospray ion source using liquid junction (Proxeon, Odense, Denmark). Solvents for LCMS separation of the digested samples were as follows: solvent A consisted of 0.4% formic acid in water and solvent B consisted of 0.4% formic acid in 70% methanol and 20% isopropanol. From a thermostatic microautosampler, 8 μL of the tryptic peptide mixture were automatically loaded onto a trap column (Zorbax 300SB-C18 5 μm , 5 \times 0.3 mm, Agilent Biotechnologies) with a binary pump at a flow rate of 45 $\mu\text{L}/\text{min}$. 0.1% TFA was used for loading and washing the precolumn. After washing, the peptides were eluted by back-flushing onto a 16 cm fused silica analytical column with an inner diameter of 50 μm packed with C18 reversed phase

material (ReproSil-Pur 120 C18-AQ, 3 μm , Dr. Maisch, Ammerbuch-Entringen, Germany). The peptides were eluted from the analytical column with a 27 min gradient ranging from 3 to 30% solvent B, followed by a 25 min gradient from 30 to 70% solvent B and, finally, a 7 min gradient from 70 to 100% solvent B at a constant flow rate of 100 nL/min. The analyses were performed in a data-dependent acquisition mode using a top 15 collision-induced dissociation (CID) method. Dynamic exclusion for selected ions was 60 s. A single lock mass at m/z 445.120024 was employed (63). The maximal ion accumulation time for MS in the orbitrap and MS² in the linear trap was 500 and 50 ms, respectively. Automatic gain control (AGC) was used to prevent overfilling of the ion traps. For MS and MS², AGC was set to 10⁶ and 5,000 ions, respectively. Peptides were detected in MS mode at a resolution of 60,000 (at m/z 400). The threshold for switching from MS to MS² was 2,000 counts. All samples were analysed as technical, back-to-back replicates.

Data Analysis

The acquired raw MS data files were processed with msconvert (ProteoWizard Library v2.1.2708) and converted into Mascot generic format (mgf) files. The resultant peak lists were searched against either the human or mouse SwissProt database v2014.03_20140331 (40,055 and 24,830 sequences, respectively, including isoforms obtained from varsplic.pl (64) and appended with known contaminants) with the search engines Mascot (v2.3.02, MatrixScience, London, U.K.) and Phenyx (v2.5.14, GeneBio, Geneva, Switzerland) (65). Submission to the search engines was via a Perl script that performs an initial search with relatively broad mass tolerances (Mascot only) on both the precursor and fragment ions (± 10 ppm and ± 0.6 Da, respectively). High-confidence peptide identifications were used to recalibrate all precursor and fragment ion masses prior to a second search with narrower mass tolerances (± 4 ppm and ± 0.3 Da, respectively). One missed tryptic cleavage site was allowed. Carbamidomethyl cysteine and oxidised methionine were set as fixed and variable modifications, respectively. To validate the proteins, Mascot and Phenyx output files were processed by internally-developed parsers. Proteins with ≤ 2 unique peptides above a score T1 or with a single peptide above a score T2 were selected as unambiguous identifications. Additional peptides for these validated proteins with score $> T3$ were also accepted. For Mascot and Phenyx, T1, T2, and T3 peptide

scores were equal to 16, 40, 10 and 5.5, 9.5, 3.5, respectively (P value $<10^{-3}$). The validated proteins retrieved by the two algorithms were merged, any spectral conflicts discarded and grouped according to shared peptides. By applying the same procedure against a reversed database, a false-positive detection rate (FDR) of <1 and $<0.1\%$ (including the peptides exported with lower scores) was determined for proteins and peptides, respectively. The significance of the interactions from AP-MS experiments was assessed using the SAINT software (51) and the CRAPome database. GFP pulldowns were used as the negative control (53). Commonly-known contaminants including trypsin and keratin were removed. Visualization of interaction data was performed using R statistical environment (66). All prey proteins with a SAINT score of >0.95 were identified as high-confidence interactors. Supplementary Tables S1 and S2 give the TAP-LC-MSMS analysis results for NRAS G12D and MLKL S358D, respectively. The mass spectrometry proteomics data have been deposited to the ProteomeXchange Consortium (67) via the PRIDE partner repository with the dataset identifier PXD002855.

Cell viability assays

Cells were seeded in 96-well plates at the appropriate cell density. For drug sensitivity experiments, cells were incubated with increasing drug concentrations for 72 h. For cell death assays, cells were incubated with the indicated compounds as stated or overnight (14 h). Cell viability was determined using CellTiter Glo Luminescent Cell Viability Assay (Promega, Fitchburg, WI, USA) according to the instructions provided by the manufacturer. Luminescence was recorded with a SpectraMax M5Multimode plate reader (Molecular Devices, Sunnyvale, CA, USA). Data were normalized to values of untreated controls.

Flow cytometry

Samples were analyzed on an LSR Fortessa (BD Biosciences) and data analysis was performed using FlowJo software version 7.6.3 (Tree Star Inc., Ashland, OR, USA).

Proliferation competition assay

To analyze the influence of inducible SH-tagged bait protein expression on cell proliferation and survival, pRSHIC-NRAS G12D (mCherry+) and pRSHIC-GFP (mCherry+/GFP+) transduced Ba/F3 rtTA3 cells were induced with 1 $\mu\text{g}/\text{mL}$ doxycycline. After 24 hours cells were mixed in a 1:1 ratio and cultured in the presence of doxycycline with or without IL-3. The percentage of mCherry+ and mCherry+/GFP+ populations was monitored daily by flow cytometry, gating only viable cells (FSC/SCC).

Microscopy

Microscopy images were taken at 10 \times with a Leica DFC310 FX on a Leica DM IL LED microscope (Leica Microsystems, Wetzlar, Germany) or at 20 \times on an Operetta automated confocal microscope (PerkinElmer, Waltham, MA, USA), and analyzed with ImageJ 1.44p (NIH, open source). The fluorophores used contained no overlapping spectrums and channels were imaged sequentially.

Experimental Design and Statistical Rational

Tandem affinity purifications were performed as biological replicates ($n = 2$) and analyzed by LC-MSMS as technical duplicates. Cell viability assay data were normalized to untreated control and are shown as mean value \pm s.d. of at least two independent experiments ($n \geq 2$) performed in triplicates. Flow cytometry-based proliferation competition assay data are shown as mean value \pm s.d. of at least two independent experiments ($n \geq 2$). Flow cytometry and immunoblot results shown are representative of at least two independent experiments ($n \geq 2$).

FIGURE LEGENDS

Figure 1 Main features of pRSHIC and workflow for generation of inducible cell lines. (A)

Schematic illustration of inducible TREtight-driven expression vectors with Gateway-cloning cassette fused to N- (upper) or C-terminal (lower) SH-tag. (B) Workflow for generation of inducible cell lines amenable to TAP-MS and follow-up experiments.

Figure 2 pRSHIC allows inducible, dose-dependent and reversible expression of SH-

tagged bait proteins. (A-F) Flow cytometry and immunoblot analysis of K-562 RIEP (A, D), HT-29 RIEP (B, E) and KCL-22 RIEP (C, F) GFP cells, untreated or treated with 1-2 $\mu\text{g}/\text{mL}$ doxycycline for 24 h. Immunoblots were probed with the indicated antibodies. Wild-type cells act as a baseline control. (G) Microscopy (20 \times ; brightfield, fluorescence) of HT-29 RIEP GFP cells induced or not for 24 h with 2 $\mu\text{g}/\text{mL}$ doxycycline (scale bar: 100 μm). (H) K-562 RIEP GFP cells were treated with increasing concentrations of doxycycline for 24 h. Cells were lysed and immunoblotted as indicated. (I) K-562 RIEP GFP cells were induced with 1 $\mu\text{g}/\text{mL}$ and doxycycline subsequently withdrawn for the indicated time span. Cells were lysed and immunoblotted with the indicated antibodies. Results are representative of two independent experiments (n = 2).

Figure 3 Phenotypic characterization and interaction-proteomic analysis of NRAS G12D

in Ba/F3 cells. (A) Flow cytometry-based proliferation competition assay for Ba/F3 rTA3 cells expressing NRAS G12D (mCherry+) or GFP (mCherry+/GFP+). After 24 h doxycycline induction cells were mixed at a 1:1 ratio and grown in the presence of 1 $\mu\text{g}/\text{mL}$ doxycycline with or without IL-3. The distribution of cell populations was monitored at the indicated time points using flow cytometry. Data represent mean value \pm s.d. of at least two independent experiments. (B) Ba/F3 rTA3 GFP and NRAS G12D cells were induced with 1 $\mu\text{g}/\text{mL}$ doxycycline in the presence of IL-3 for 48 h. Cells were then washed once, cultured in the presence of 1 $\mu\text{g}/\text{mL}$ doxycycline with or without IL-3 for 12h, lysed and immunoblotted with the indicated antibodies. (C-D) Cell viability of Ba/F3 rTA3 NRAS G12D-expressing cells in the presence or absence of IL-3 upon treatment with trametinib (C) or selumetinib (D) as indicated. Data represent mean value \pm s.d. of at least two independent experiments

performed in triplicates and normalized to untreated control. (E) Scatter plot summarizing the SAINT-based significance and CRAPome frequency analysis of NRAS G12D TAP-LC-MSMS experiments. Ba/F3 rtTA3 NRAS cells were grown in presence of IL-3 and induced for 24 h with 1 μ g/mL doxycycline. Data shown are based on two independent experiments (n=2), each analyzed as technical duplicates and using Ba/F3 rtTA3 GFP-expressing cells as negative control.

Figure 4 Phenotypic and TAP-LC-MSMS analysis of the cell death-inducing MLKL S358D mutant. (A) HT-29 RIEP MLKL S358D cells were treated with 2 μ g/mL doxycycline for the indicated time. Cells were lysed and immunoblotted with the indicated antibodies. (B) Cell viability of HT-29 RIEP MLKL S358D cells induced with 2 μ g/mL doxycycline for the indicated time. Data represent mean value \pm s.d. of two independent experiments performed as triplicates and normalized to the untreated control. (C) Cell viability was examined in HT-29 RIEP MLKL S358D cells untreated or treated overnight with 2 μ g/mL doxycycline and the compounds Nec-1 (10 μ M) or NSA, as indicated. Data represents the mean value \pm s.d. of two independent experiments performed as triplicates and normalized to the untreated control. (D) Scatter plot summarizing the SAINT-based significance and CRAPome frequency analysis of MLKL S358D TAP-LC-MSMS experiments. HT-29 RIEP MLKL S358D cells were induced for 7 h with 2 μ g/mL doxycycline. Data shown are based on two independent experiments (n=2), each analyzed as technical duplicates with HT-29 RIEP GFP-expressing cells used as the negative control.

Figure 5 MLKL is a novel HSP90 client protein. (A) HT-29 RIEP MLKL S358D cells were treated with 2 μ g/mL doxycycline and NSA (10 μ M), Nec-1 (10 μ M) or geldanamycin (GA, 1 μ M) for 3 h. Cells were lysed and immunoblotted with the indicated antibodies. Asterisk (*) denotes non-specific band. Data shown are representative of three independent experiments. (B) HT-29 RIEP MLKL S358D cells were pretreated for 1 h with 10 μ M MG132 or 10 μ M chloroquine (CQ) before induction with 2 μ g/mL doxycycline and the addition of 1 μ M GA or DMSO. After 3 h of incubation, cells were harvested, lysed and immunoblotted with the indicated antibodies. Data shown are representative of two independent experiments. (C) Cell viability was assessed in HT-29 RIEP

MLKL S358D cells induced with 2 $\mu\text{g}/\text{mL}$ doxycycline and treated with 10 μM NSA or GA as indicated for 14 h. Data represent mean value \pm s.d. of three independent experiments performed as triplicates and normalized to the untreated control. **(D)** HT-29 RIEP MLKL cells were pretreated for 1 h with 10 μM MG132 before induction with 2 $\mu\text{g}/\text{mL}$ doxycycline and addition of 1 μM GA or DMSO. After 3 h of incubation, cells were harvested, lysed and immunoblotted with the indicated antibodies. Data shown are representative of two independent experiments. **(E)** Expression of the indicated bait proteins was induced in HT-29 cells with 2 $\mu\text{g}/\text{mL}$ doxycycline for 6 h. Cell lysates were immunoprecipitated and whole cell extracts (WCE) and immunoprecipitates (IP) were analyzed by immunoblotting with the indicated antibodies. Asterisks (**) denote SH-tagged RIPK3. Data shown are representative of two independent experiments.

REFERENCES

1. Gavin, A. C., and Superti-Furga, G. (2003) Protein complexes and proteome organization from yeast to man. *Curr Opin Chem Biol* 7, 21-27
2. Rigaut, G., Shevchenko, A., Rutz, B., Wilm, M., Mann, M., and Seraphin, B. (1999) A generic protein purification method for protein complex characterization and proteome exploration. *Nat Biotechnol* 17, 1030-1032
3. Puig, O., Caspary, F., Rigaut, G., Rutz, B., Bouveret, E., Bragado-Nilsson, E., Wilm, M., and Séraphin, B. (2001) The Tandem Affinity Purification (TAP) Method: A General Procedure of Protein Complex Purification. *Methods* 24, 218-229
4. Dunham, W. H., Mullin, M., and Gingras, A.-C. (2012) Affinity-purification coupled to mass spectrometry: Basic principles and strategies. *Proteomics* 12, 1576-1590
5. Gingras, A.-C., Gstaiger, M., Raught, B., and Aebersold, R. (2007) Analysis of protein complexes using mass spectrometry. *Nature Reviews Molecular Cell Biology* 8, 645-654
6. Köcher, T., and Superti-Furga, G. (2007) Mass spectrometry-based functional proteomics: from molecular machines to protein networks. *Nature Methods* 4, 807-815
7. Bouwmeester, T., Bauch, A., Ruffner, H., Angrand, P.-O., Bergamini, G., Croughton, K., Cruciat, C., Eberhard, D., Gagneur, J., Ghidelli, S., Hopf, C., Huhse, B., Mangano, R., Michon, A.-M., Schirle, M., Schlegl, J., Schwab, M., Stein, M. A., Bauer, A., Casari, G., Drewes, G., Gavin, A.-C., Jackson, D. B., Joberty, G., Neubauer, G., Rick, J., Kuster, B., and Superti-Furga, G. (2004) A physical and functional map of the human TNF- α /NF- κ B signal transduction pathway. *Nature Cell Biology* 6, 97-105
8. Gavin, A.-C., Aloy, P., Grandi, P., Krause, R., Boesche, M., Marzioch, M., Rau, C., Jensen, L. J., Bastuck, S., Dümpelfeld, B., Edelmann, A., Heurtier, M.-A., Hoffman, V., Hoefert, C., Klein, K., Hudak, M., Michon, A.-M., Schelder, M., Schirle, M., Remor, M., Rudi, T., Hooper, S., Bauer, A., Bouwmeester, T., Casari, G., Drewes, G., Neubauer, G., Rick, J. M., Kuster, B., Bork, P., Russell, R. B., and Superti-Furga, G. (2006) Proteome survey reveals modularity of the yeast cell machinery. *Nature* 440, 631-636
9. Kwon, Y., Vinayagam, A., Sun, X., Dephoure, N., Gygi, S. P., Hong, P., and Perrimon, N. (2013) The Hippo Signaling Pathway Interactome. *Science* 342, 737-740
10. Li, Y. (2011) The tandem affinity purification technology: an overview. *Biotechnology Letters* 33, 1487-1499
11. Ma, H., McLean, J. R., Chao, L. F., Mana-Capelli, S., Paramasivam, M., Hagstrom, K. A., Gould, K. L., and McCollum, D. (2012) A highly efficient multifunctional tandem affinity purification approach applicable to diverse organisms. *Mol Cell Proteomics* 11, 501-511
12. Glatter, T., Wepf, A., Aebersold, R., and Gstaiger, M. (2009) An integrated workflow for charting the human interaction proteome: insights into the PP2A system. *Molecular Systems Biology* 5
13. Giambruno, R., Grebien, F., Stukalov, A., Knoll, C., Planyavsky, M., Rudashevskaya, E. L., Colinge, J., Superti-Furga, G., and Bennett, K. L. (2013) Affinity Purification Strategies for Proteomic Analysis of Transcription Factor Complexes. *Journal of Proteome Research* 12, 4018-4027
14. Hauri, S., Wepf, A., van Drogen, A., Varjosalo, M., Tapon, N., Aebersold, R., and Gstaiger, M. (2013) Interaction proteome of human Hippo signaling: modular control of the co-activator YAP1. *Molecular Systems Biology* 9, n/a-n/a
15. Varjosalo, M., Sacco, R., Stukalov, A., van Drogen, A., Planyavsky, M., Hauri, S., Aebersold, R., Bennett, K. L., Colinge, J., Gstaiger, M., and Superti-Furga, G. (2013) Interlaboratory reproducibility of large-scale human protein-complex analysis by standardized AP-MS. *Nature Methods* 10, 307-314
16. Pichlmair, A., Kandasamy, K., Alvisi, G., Mulhern, O., Sacco, R., Habjan, M., Binder, M., Stefanovic, A., Eberle, C.-A., Goncalves, A., Bürckstümmer, T., Müller, A. C., Fauster, A., Holze, C., Lindsten, K., Goodbourn, S., Kochs, G., Weber, F., Bartenschlager, R., Bowie, A. G., Bennett, K. L., Colinge, J., and Superti-Furga, G. (2012) Viral immune modulators perturb the human molecular network by common and unique strategies. *Nature* 487, 486-490

17. Yu, S. F., von Ruden, T., Kantoff, P. W., Garber, C., Seiberg, M., Ruther, U., Anderson, W. F., Wagner, E. F., and Gilboa, E. (1986) Self-inactivating retroviral vectors designed for transfer of whole genes into mammalian cells. *Proc Natl Acad Sci U S A* 83, 3194-3198
18. Gossen, M., Freundlieb, S., Bender, G., Muller, G., Hillen, W., and Bujard, H. (1995) Transcriptional activation by tetracyclines in mammalian cells. *Science* 268, 1766-1769
19. Meerbrey, K. L., Hu, G., Kessler, J. D., Roarty, K., Li, M. Z., Fang, J. E., Herschkowitz, J. I., Burrows, A. E., Ciccia, A., Sun, T., Schmitt, E. M., Bernardi, R. J., Fu, X., Bland, C. S., Cooper, T. A., Schiff, R., Rosen, J. M., Westbrook, T. F., and Elledge, S. J. (2011) The pINDUCER lentiviral toolkit for inducible RNA interference in vitro and in vivo. *Proceedings of the National Academy of Sciences* 108, 3665-3670
20. Premrsirut, Prem K., Dow, Lukas E., Kim, Sang Y., Camiolo, M., Malone, Colin D., Miething, C., Scuoppo, C., Zuber, J., Dickins, Ross A., Kogan, Scott C., Shroyer, Kenneth R., Sordella, R., Hannon, Gregory J., and Lowe, Scott W. (2011) A Rapid and Scalable System for Studying Gene Function in Mice Using Conditional RNA Interference. *Cell* 145, 145-158
21. Mak, A. B., Ni, Z., Hewel, J. A., Chen, G. I., Zhong, G., Karamboulas, K., Blakely, K., Smiley, S., Marcon, E., Roudeva, D., Li, J., Olsen, J. B., Wan, C., Punna, T., Isserlin, R., Chetyrkin, S., Gingras, A. C., Emili, A., Greenblatt, J., and Moffat, J. (2010) A lentiviral functional proteomics approach identifies chromatin remodeling complexes important for the induction of pluripotency. *Mol Cell Proteomics* 9, 811-823
22. Cox, A. D., Fesik, S. W., Kimmelman, A. C., Luo, J., and Der, C. J. (2014) Drugging the undruggable RAS: Mission Possible? *Nature Reviews Drug Discovery* 13, 828-851
23. Garraway, Levi A., and Lander, Eric S. (2013) Lessons from the Cancer Genome. *Cell* 153, 17-37
24. Gavin, A.-C., and Hopf, C. (2006) Protein co-membership and biochemical affinity purifications. *Drug Discovery Today: Technologies* 3, 325-330
25. Murphy, James M., Czabotar, Peter E., Hildebrand, Joanne M., Lucet, Isabelle S., Zhang, J.-G., Alvarez-Diaz, S., Lewis, R., Lalaoui, N., Metcalf, D., Webb, Andrew I., Young, Samuel N., Varghese, Leila N., Tannahill, Gillian M., Hatchell, Esme C., Majewski, Ian J., Okamoto, T., Dobson, Renwick C. J., Hilton, Douglas J., Babon, Jeffrey J., Nicola, Nicos A., Strasser, A., Silke, J., and Alexander, Warren S. (2013) The Pseudokinase MLKL Mediates Necroptosis via a Molecular Switch Mechanism. *Immunity* 39, 443-453
26. Chan, F. K.-M., Luz, N. F., and Moriwaki, K. (2014) Programmed Necrosis in the Cross Talk of Cell Death and Inflammation. *Annual Review of Immunology* 33, 141210135520002
27. Linkermann, A., and Green, D. R. (2014) Necroptosis. *New England Journal of Medicine* 370, 455-465
28. Pasparakis, M., and Vandenabeele, P. (2015) Necroptosis and its role in inflammation. *Nature* 517, 311-320
29. Zuber, J., Rappaport, A. R., Luo, W., Wang, E., Chen, C., Vaseva, A. V., Shi, J., Weissmueller, S., Fellman, C., Taylor, M. J., Weissenboeck, M., Graeber, T. G., Kogan, S. C., Vakoc, C. R., and Lowe, S. W. (2011) An integrated approach to dissecting oncogene addiction implicates a Myb-coordinated self-renewal program as essential for leukemia maintenance. *Genes & Development* 25, 1628-1640
30. Das, A. T., Zhou, X., Vink, M., Klaver, B., Verhoef, K., Marzio, G., and Berkhout, B. (2004) Viral Evolution as a Tool to Improve the Tetracycline-regulated Gene Expression System. *Journal of Biological Chemistry* 279, 18776-18782
31. Takiguchi, M., Dow, L. E., Prier, J. E., Carmichael, C. L., Kile, B. T., Turner, S. J., Lowe, S. W., Huang, D. C., and Dickins, R. A. (2013) Variability of inducible expression across the hematopoietic system of tetracycline transactivator transgenic mice. *PLoS ONE* 8, e54009
32. Schambach, A., Galla, M., Modlich, U., Will, E., Chandra, S., Reeves, L., Colbert, M., Williams, D. A., von Kalle, C., and Baum, C. (2006) Lentiviral vectors pseudotyped with murine ecotropic envelope: Increased biosafety and convenience in preclinical research. *Experimental Hematology* 34, 588-592

33. Loew, R., Heinz, N., Hampf, M., Bujard, H., and Gossen, M. (2010) Improved Tet-responsive promoters with minimized background expression. *BMC Biotechnology* 10, 81
34. Lambert, J.-P., Ivosev, G., Couzens, A. L., Larsen, B., Taipale, M., Lin, Z.-Y., Zhong, Q., Lindquist, S., Vidal, M., Aebersold, R., Pawson, T., Bonner, R., Tate, S., and Gingras, A.-C. (2013) Mapping differential interactomes by affinity purification coupled with data-independent mass spectrometry acquisition. *Nature Methods* 10, 1239-1245
35. Sahni, N., Yi, S., Taipale, M., Fuxman Bass, Juan I., Coulombe-Huntington, J., Yang, F., Peng, J., Weile, J., Karras, Georgios I., Wang, Y., Kovács, István A., Kamburov, A., Krykbaeva, I., Lam, Mandy H., Tucker, G., Khurana, V., Sharma, A., Liu, Y.-Y., Yachie, N., Zhong, Q., Shen, Y., Palagi, A., San-Miguel, A., Fan, C., Balcha, D., Dricot, A., Jordan, Daniel M., Walsh, Jennifer M., Shah, Akash A., Yang, X., Stoyanova, Ani K., Leighton, A., Calderwood, Michael A., Jacob, Y., Cusick, Michael E., Salehi-Ashtiani, K., Whitesell, Luke J., Sunyaev, S., Berger, B., Barabási, A.-L., Charloteaux, B., Hill, David E., Hao, T., Roth, Frederick P., Xia, Y., Walhout, Albertha J. M., Lindquist, S., and Vidal, M. (2015) Widespread Macromolecular Interaction Perturbations in Human Genetic Disorders. *Cell* 161, 647-660
36. Palacios, R., and Steinmetz, M. (1985) II-3-dependent mouse clones that express B-220 surface antigen, contain Ig genes in germ-line configuration, and generate B lymphocytes in vivo. *Cell* 41, 727-734
37. Han, L., and Colicelli, J. (1995) A human protein selected for interference with Ras function interacts directly with Ras and competes with Raf1. *Mol Cell Biol* 15, 1318-1323
38. Wang, Y., Waldron, R. T., Dhaka, A., Patel, A., Riley, M. M., Rozengurt, E., and Colicelli, J. (2002) The RAS Effector RIN1 Directly Competes with RAF and Is Regulated by 14-3-3 Proteins. *Molecular and Cellular Biology* 22, 916-926
39. Pacold, M. E., Suire, S., Perisic, O., Lara-Gonzalez, S., Davis, C. T., Walker, E. H., Hawkins, P. T., Stephens, L., Eccleston, J. F., and Williams, R. L. (2000) Crystal structure and functional analysis of Ras binding to its effector phosphoinositide 3-kinase gamma. *Cell* 103, 931-943
40. Rodriguez-Viciano, P., Warne, P. H., Dhand, R., Vanhaesebroeck, B., Gout, I., Fry, M. J., Waterfield, M. D., and Downward, J. (1994) Phosphatidylinositol-3-OH kinase as a direct target of Ras. *Nature* 370, 527-532
41. Castellano, E., Sheridan, C., Thin, May Z., Nye, E., Spencer-Dene, B., Diefenbacher, Markus E., Moore, C., Kumar, Madhu S., Murillo, Miguel M., Grönroos, E., Lassailly, F., Stamp, G., and Downward, J. (2013) Requirement for Interaction of PI3-Kinase p110 α with RAS in Lung Tumor Maintenance. *Cancer Cell* 24, 617-630
42. Gupta, S., Ramjaun, A. R., Haiko, P., Wang, Y., Warne, P. H., Nicke, B., Nye, E., Stamp, G., Alitalo, K., and Downward, J. (2007) Binding of Ras to Phosphoinositide 3-Kinase p110 α Is Required for Ras- Driven Tumorigenesis in Mice. *Cell* 129, 957-968
43. Cai, Z., Jitkaew, S., Zhao, J., Chiang, H.-C., Choksi, S., Liu, J., Ward, Y., Wu, L.-g., and Liu, Z.-G. (2013) Plasma membrane translocation of trimerized MLKL protein is required for TNF-induced necroptosis. *Nature Cell Biology* 16, 55-65
44. Chen, X., Li, W., Ren, J., Huang, D., He, W.-t., Song, Y., Yang, C., Li, W., Zheng, X., Chen, P., and Han, J. (2013) Translocation of mixed lineage kinase domain-like protein to plasma membrane leads to necrotic cell death. *Cell Research* 24, 105-121
45. Dondelinger, Y., Declercq, W., Montessuit, S., Roelandt, R., Goncalves, A., Bruggeman, I., Hulpiau, P., Weber, K., Sehon, Clark A., Marquis, Robert W., Bertin, J., Gough, Peter J., Savvides, S., Martinou, J.-C., Bertrand, Mathieu J. M., and Vandenamee, P. (2014) MLKL Compromises Plasma Membrane Integrity by Binding to Phosphatidylinositol Phosphates. *Cell Reports* 7, 971-981
46. Sun, L., Wang, H., Wang, Z., He, S., Chen, S., Liao, D., Wang, L., Yan, J., Liu, W., Lei, X., and Wang, X. (2012) Mixed Lineage Kinase Domain-like Protein Mediates Necrosis Signaling Downstream of RIP3 Kinase. *Cell* 148, 213-227
47. Wang, H., Sun, L., Su, L., Rizo, J., Liu, L., Wang, L.-F., Wang, F.-S., and Wang, X. (2014) Mixed Lineage Kinase Domain-like Protein MLKL Causes Necrotic Membrane Disruption upon Phosphorylation by RIP3. *Molecular Cell* 54, 133-146

48. Fauster, A., Rebsamen, M., Huber, K. V., Bigenzahn, J. W., Stukalov, A., Lardeau, C. H., Scorzoni, S., Bruckner, M., Gridling, M., Parapatics, K., Colinge, J., Bennett, K. L., Kubicek, S., Krautwald, S., Linkermann, A., and Superti-Furga, G. (2015) A cellular screen identifies ponatinib and pazopanib as inhibitors of necroptosis. *Cell Death Dis* 6, e1767
49. Degtarev, A., Huang, Z., Boyce, M., Li, Y., Jagtap, P., Mizushima, N., Cuny, G. D., Mitchison, T. J., Moskowitz, M. A., and Yuan, J. (2005) Chemical inhibitor of nonapoptotic cell death with therapeutic potential for ischemic brain injury. *Nature Chemical Biology* 1, 112-119
50. Siligardi, G., Panaretou, B., Meyer, P., Singh, S., Woolfson, D. N., Piper, P. W., Pearl, L. H., and Prodromou, C. (2002) Regulation of Hsp90 ATPase Activity by the Co-chaperone Cdc37p/p50cdc37. *Journal of Biological Chemistry* 277, 20151-20159
51. Choi, H., Larsen, B., Lin, Z.-Y., Breitkreutz, A., Mellacheruvu, D., Fermin, D., Qin, Z. S., Tyers, M., Gingras, A.-C., and Nesvizhskii, A. I. (2010) SAINT: probabilistic scoring of affinity purification–mass spectrometry data. *Nature Methods* 8, 70-73
52. Taipale, M., Jarosz, D. F., and Lindquist, S. (2010) HSP90 at the hub of protein homeostasis: emerging mechanistic insights. *Nature Reviews Molecular Cell Biology* 11, 515-528
53. Mellacheruvu, D., Wright, Z., Couzens, A. L., Lambert, J.-P., St-Denis, N. A., Li, T., Miteva, Y. V., Hauri, S., Sardi, M. E., Low, T. Y., Halim, V. A., Bagshaw, R. D., Hubner, N. C., al-Hakim, A., Bouchard, A., Faubert, D., Fermin, D., Dunham, W. H., Goudreault, M., Lin, Z.-Y., Badillo, B. G., Pawson, T., Durocher, D., Coulombe, B., Aebersold, R., Superti-Furga, G., Colinge, J., Heck, A. J. R., Choi, H., Gstaiger, M., Mohammed, S., Cristea, I. M., Bennett, K. L., Washburn, M. P., Raught, B., Ewing, R. M., Gingras, A.-C., and Nesvizhskii, A. I. (2013) The CRAPome: a contaminant repository for affinity purification–mass spectrometry data. *Nature Methods* 10, 730-736
54. Whitesell, L., Mimnaugh, E. G., De Costa, B., Myers, C. E., and Neckers, L. M. (1994) Inhibition of heat shock protein HSP90-pp60v-src heteroprotein complex formation by benzoquinone ansamycins: essential role for stress proteins in oncogenic transformation. *Proc Natl Acad Sci U S A* 91, 8324-8328
55. Holler, N., Zaru, R., Micheau, O., Thome, M., Attinger, A., Valitutti, S., Bodmer, J. L., Schneider, P., Seed, B., and Tschopp, J. (2000) Fas triggers an alternative, caspase-8-independent cell death pathway using the kinase RIP as effector molecule. *Nat Immunol* 1, 489-495
56. Cho, Y., Challa, S., Moquin, D., Genga, R., Ray, T. D., Guildford, M., and Chan, F. K.-M. (2009) Phosphorylation-Driven Assembly of the RIP1-RIP3 Complex Regulates Programmed Necrosis and Virus-Induced Inflammation. *Cell* 137, 1112-1123
57. Lewis, J., Devin, A., Miller, A., Lin, Y., Rodriguez, Y., Neckers, L., and Liu, Z. G. (2000) Disruption of hsp90 function results in degradation of the death domain kinase, receptor-interacting protein (RIP), and blockage of tumor necrosis factor-induced nuclear factor-kappaB activation. *J Biol Chem* 275, 10519-10526
58. Li, D., Xu, T., Cao, Y., Wang, H., Li, L., Chen, S., Wang, X., and Shen, Z. (2015) A cytosolic heat shock protein 90 and cochaperone CDC37 complex is required for RIP3 activation during necroptosis. *Proceedings of the National Academy of Sciences* 112, 5017-5022
59. Zhang, H., Wu, W., Du, Y., Santos, S. J., Conrad, S. E., Watson, J. T., Grammatikakis, N., and Gallo, K. A. (2004) Hsp90/p50cdc37 Is Required for Mixed-lineage Kinase (MLK) 3 Signaling. *Journal of Biological Chemistry* 279, 19457-19463
60. Najjar, M., Suebsuwong, C., Ray, Soumya S., Thapa, Roshan J., Maki, Jenny L., Nogusa, S., Shah, S., Saleh, D., Gough, Peter J., Bertin, J., Yuan, J., Balachandran, S., Cuny, Gregory D., and Degtarev, A. (2015) Structure Guided Design of Potent and Selective Ponatinib-Based Hybrid Inhibitors for RIPK1. *Cell Reports* 10, 1850-1860
61. Rudashevskaya, E. L., Sacco, R., Kratochwill, K., Huber, M. L., Gstaiger, M., Superti-Furga, G., and Bennett, K. L. (2013) A method to resolve the composition of heterogeneous affinity-purified protein complexes assembled around a common protein by chemical cross-linking, gel electrophoresis and mass spectrometry. *Nat Protoc* 8, 75-97

62. Rappsilber, J., Ishihama, Y., and Mann, M. (2003) Stop and go extraction tips for matrix-assisted laser desorption/ionization, nanoelectrospray, and LC/MS sample pretreatment in proteomics. *Anal Chem* 75, 663-670
63. Olsen, J. V., de Godoy, L. M., Li, G., Macek, B., Mortensen, P., Pesch, R., Makarov, A., Lange, O., Horning, S., and Mann, M. (2005) Parts per million mass accuracy on an Orbitrap mass spectrometer via lock mass injection into a C-trap. *Mol Cell Proteomics* 4, 2010-2021
64. Kersey, P., Hermjakob, H., and Apweiler, R. (2000) VARSPLIC: alternatively-spliced protein sequences derived from SWISS-PROT and TrEMBL. *Bioinformatics* 16, 1048-1049
65. Colinge, J., Masselot, A., Giron, M., Dessingy, T., and Magnin, J. (2003) OLAV: towards high-throughput tandem mass spectrometry data identification. *Proteomics* 3, 1454-1463
66. R Core Team (2014) R: A language and environment for statistical computing. R Foundation for Statistical Computing, Vienna, Austria
67. Vizcaino, J. A., Deutsch, E. W., Wang, R., Csordas, A., Reisinger, F., Rios, D., Dienes, J. A., Sun, Z., Farrah, T., Bandeira, N., Binz, P. A., Xenarios, I., Eisenacher, M., Mayer, G., Gatto, L., Campos, A., Chalkley, R. J., Kraus, H. J., Albar, J. P., Martinez-Bartolome, S., Apweiler, R., Omenn, G. S., Martens, L., Jones, A. R., and Hermjakob, H. (2014) ProteomeXchange provides globally coordinated proteomics data submission and dissemination. *Nat Biotechnol* 32, 223-226

Figure 1: Main features of pRSHIC and workflow for generation of inducible cell lines.

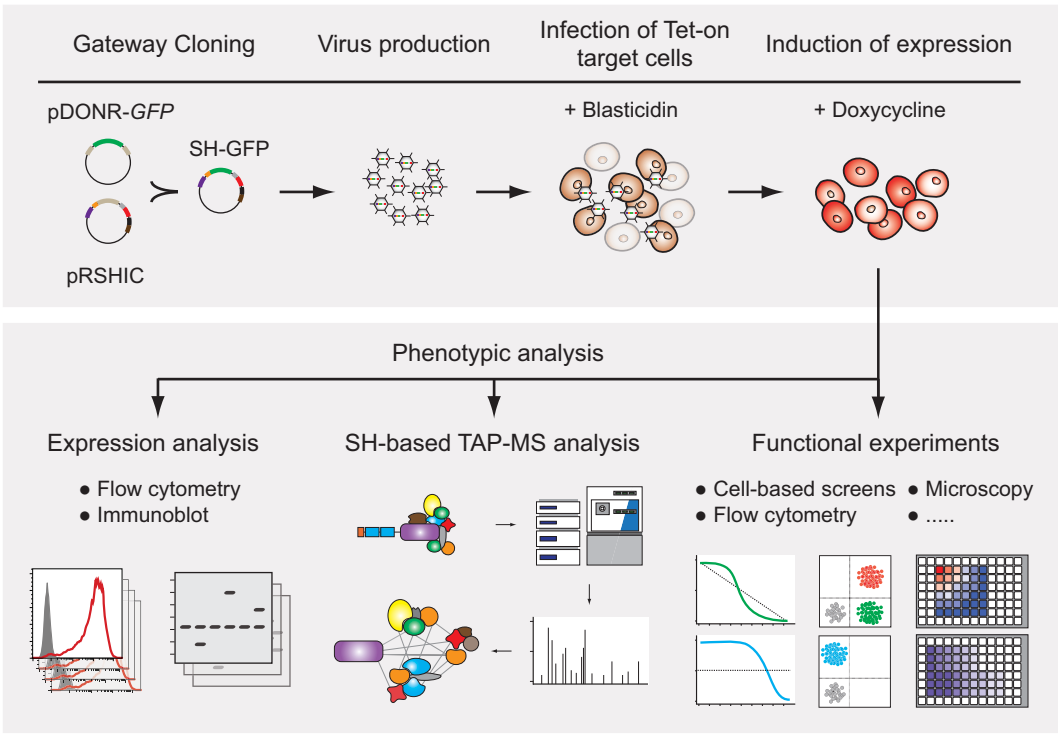
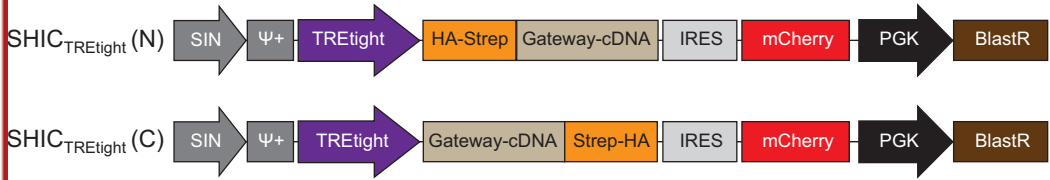


Figure 2: pRSHIC allows inducible, dose-dependent and reversible expression of SH-tagged bait proteins

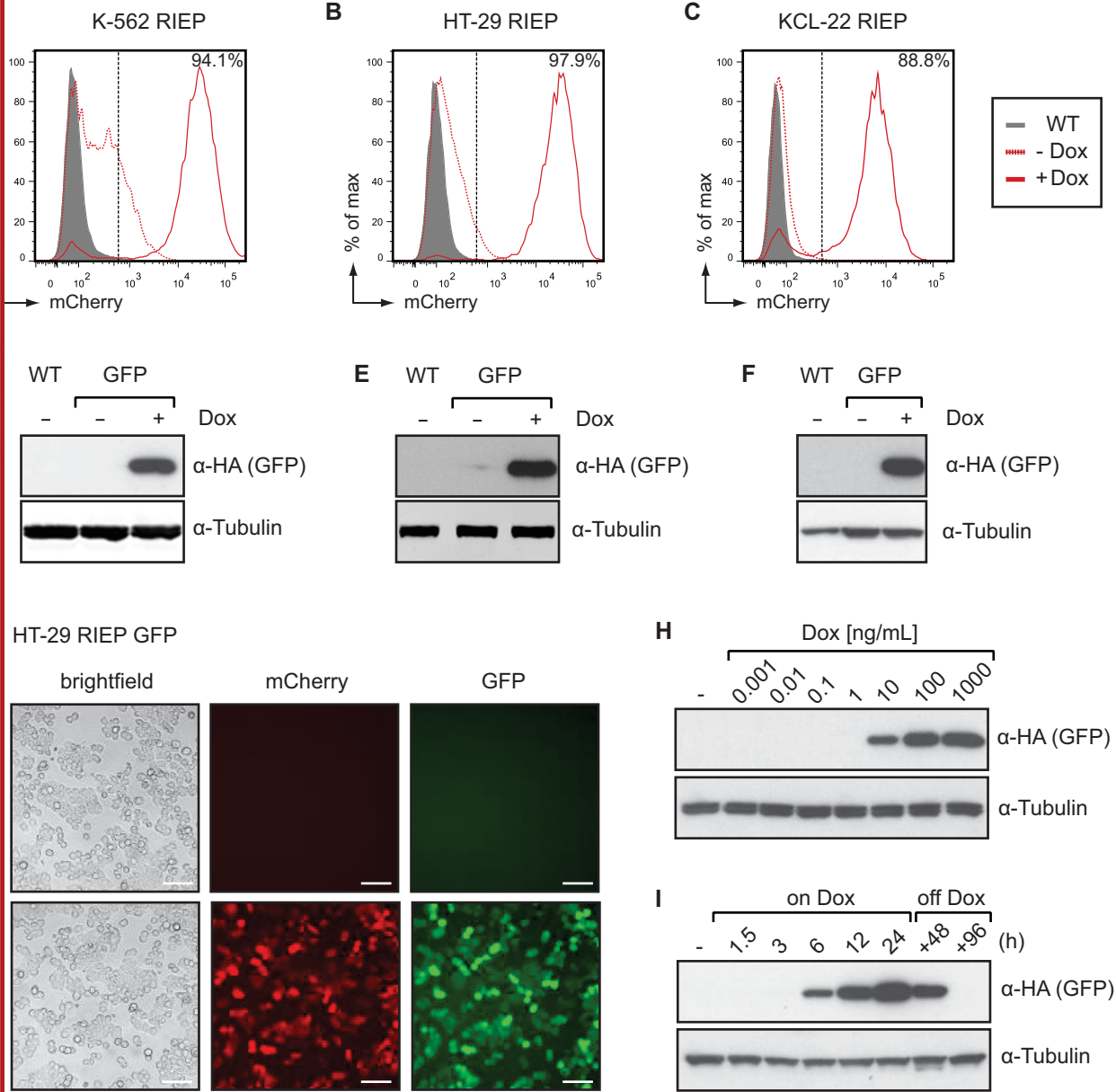
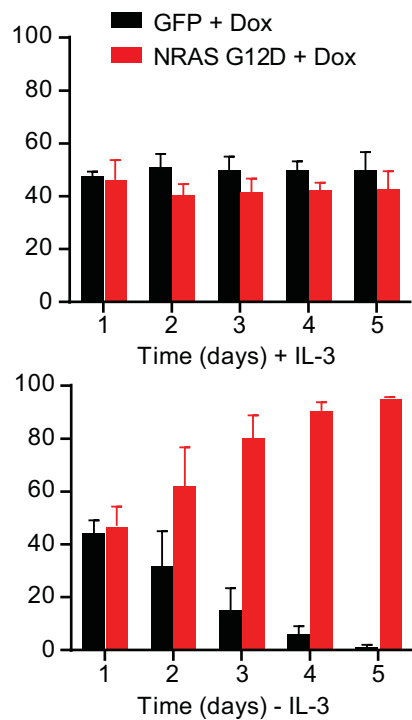
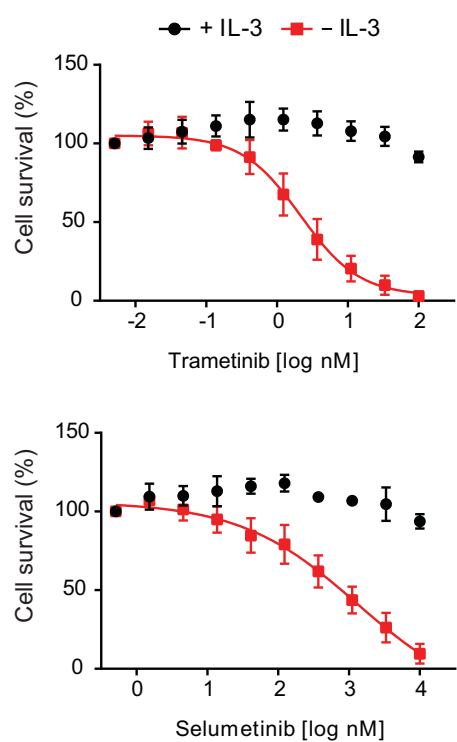
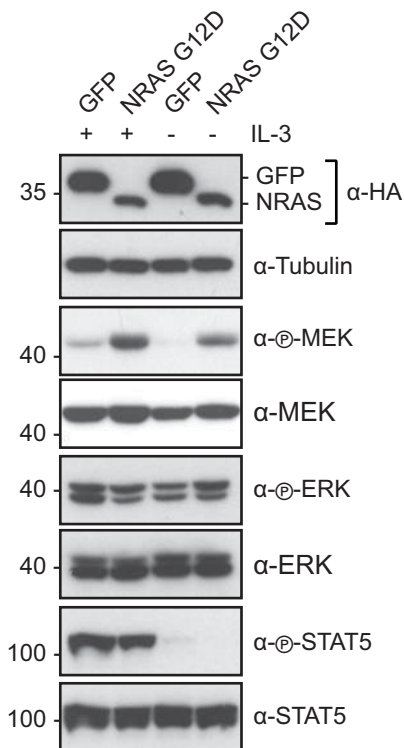


Figure 3: Phenotypic characterization and interaction-proteomic analysis of NRAS G12D in Ba/F3 cells



B



E

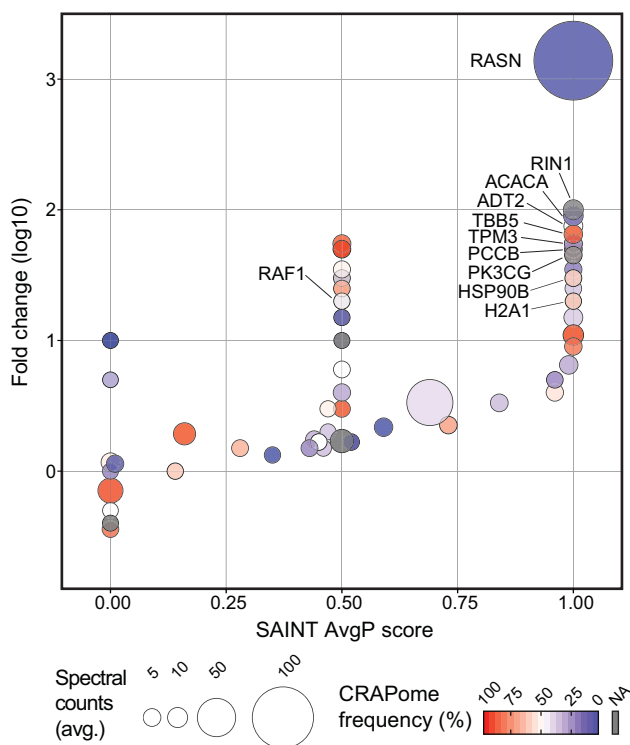


Figure 4: Phenotypic and TAP-LC-MSMS analysis of the cell death-inducing MLKL S358D mutant

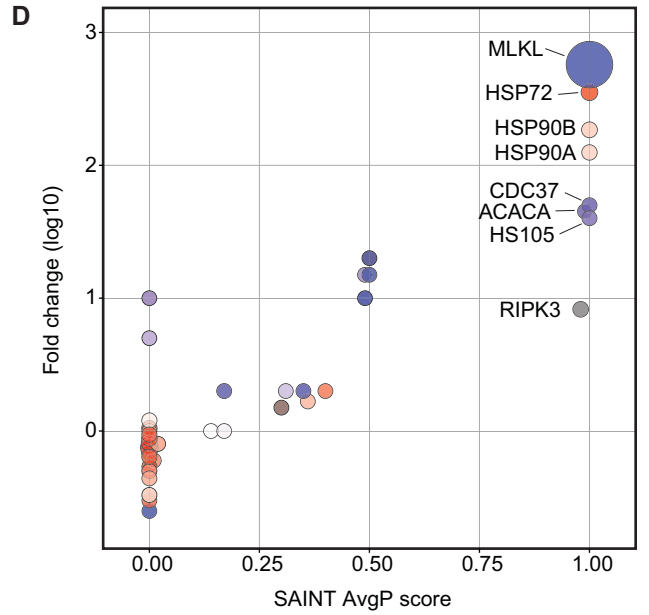
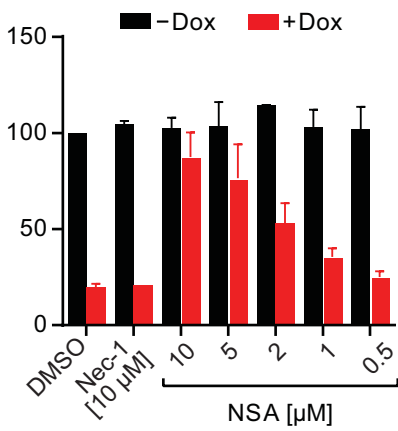
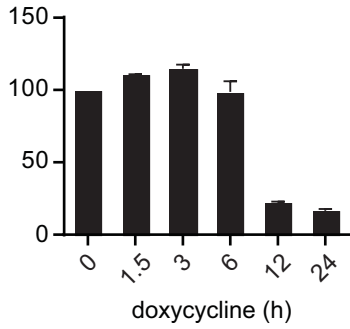
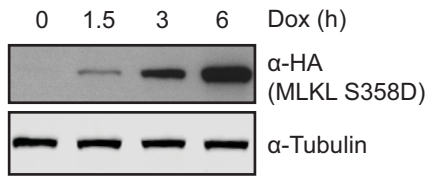
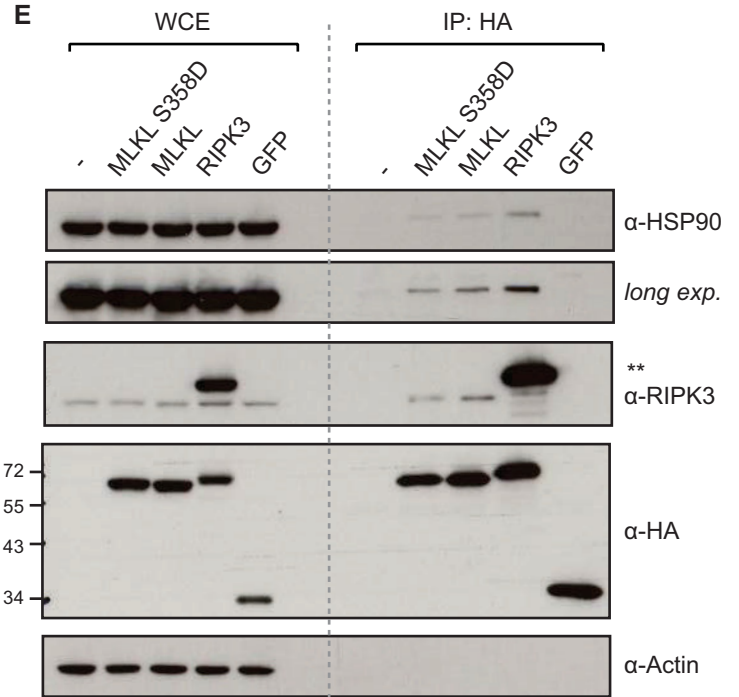
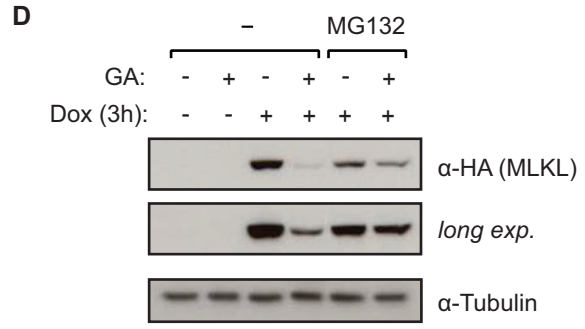
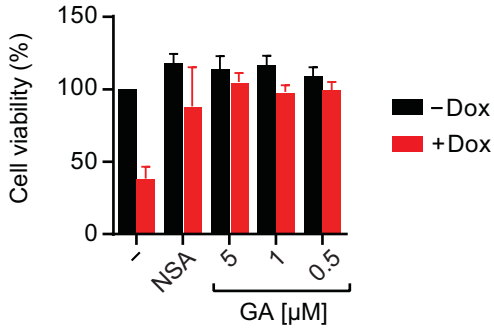
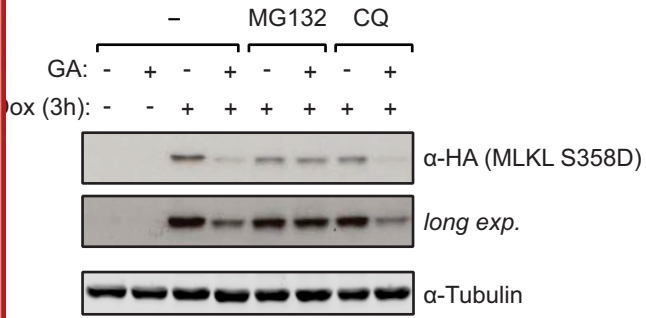
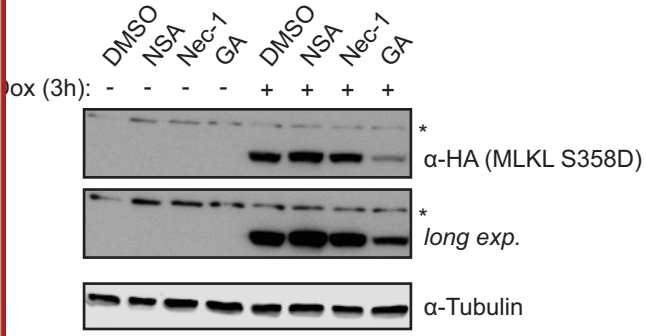


Figure 5: MLKL is a novel HSP90 client protein



Supplementary Figures for “An inducible retroviral expression system for tandem affinity purification mass-spectrometry-based proteomics identifies MLKL as an HSP90 client”

Johannes W. Bigenzahn^{1,5}, Astrid Fauster^{1,5}, Manuele Rebsamen¹, Richard K. Kandasamy¹, Stefania Scorzoni¹, Gregory I. Vladimer¹, André C. Müller¹, Matthias Gstaiger², Johannes Zuber³, Keiryn L. Bennett¹, and Giulio Superti-Furga^{1,4,*}

¹CeMM Research Center for Molecular Medicine of the Austrian Academy of Sciences, Vienna, Austria

²Department of Biology, Institute of Molecular Systems Biology, ETH Zürich, Zürich, Switzerland

³Research Institute of Molecular Pathology (IMP), Vienna Biocenter (VBC), 1030 Vienna, Austria

⁴Center for Physiology and Pharmacology, Medical University of Vienna, Vienna, Austria

⁵These authors contributed equally to this work.

Corresponding author:

Giulio Superti-Furga

CeMM Research Center for Molecular Medicine of the Austrian Academy of Sciences

Lazarettgasse 14, AKH BT25.3

1090 Vienna, Austria

Email: gsuperti@cemm.oeaw.ac.at

Telephone: +43 1 40160 70 001

Supporting Information

Supplementary Figure 1

(A-C) FACS analysis of K-562 RIEP (A), HT-29 RIEP (B) and KCL-22 RIEP (C) GFP cells untreated or treated for 24 h with 2 $\mu\text{g}/\text{mL}$ doxycycline.

Supplementary Figure 2

(A) Schematic illustration of inducible TRE3G-driven pRSHIC expression vectors with Gateway-cloning cassette fused to N- (upper) or C-terminal (lower) SH-tag. (B) Flow cytometry analysis of K-562 RIEP transduced with pRSHIC_{TREtight}-GFP or pRSHIC_{TRE3G}-GFP untreated or treated for 24 h with 1 $\mu\text{g}/\text{mL}$ doxycycline. Corresponding wild-type cells are the baseline control.

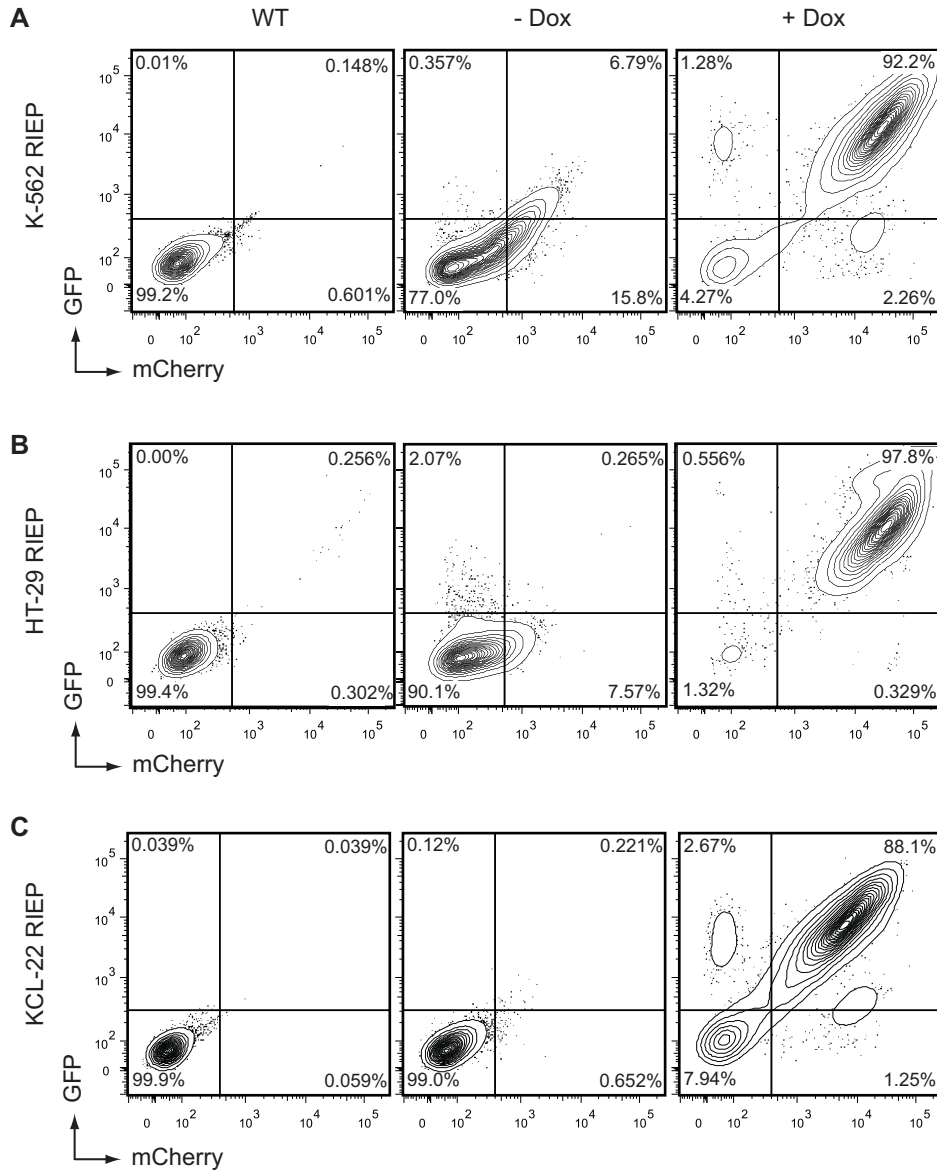
Supplementary Figure 3

(A) Ba/F3 rtTA3 cells inducibly expressing NRAS G12D or GFP were treated with 1 $\mu\text{g}/\text{mL}$ doxycycline for 24 h. Cells were lysed and immunoblotted with the indicated antibodies. (B) Flow cytometry analysis of Ba/F3 rtTA3 cells expressing NRAS G12D or GFP treated with 1 $\mu\text{g}/\text{mL}$ doxycycline for 24 h. (C) Ba/F3 rtTA3 NRAS G12D cells were induced with 1 $\mu\text{g}/\text{mL}$ doxycycline in the presence of IL-3 for 48 h. Cells were then washed once and cultured in the presence of 1 $\mu\text{g}/\text{mL}$ doxycycline and increasing concentrations of trametinib with or without IL-3 for 3 h. DMSO-treated cells were the baseline control. Subsequently cells were lysed and immunoblotted with the indicated antibodies.

Supplementary Figure 4

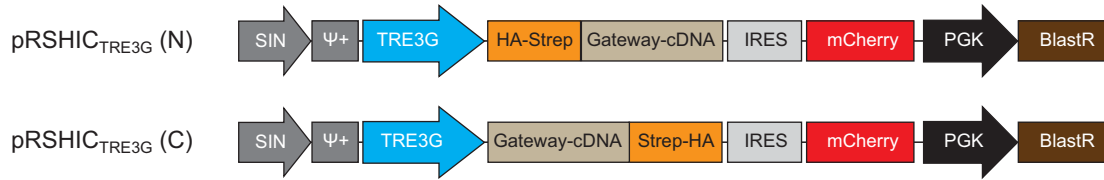
(A) Flow cytometry analysis of HT-29 RIEP MLKL S358D cells induced with 2 $\mu\text{g}/\text{mL}$ doxycycline for the indicated times. (B) Microscopy (brightfield, 10 \times) of HT-29 RIEP MLKL S358D cells uninduced or induced with 2 $\mu\text{g}/\text{mL}$ doxycycline for 24 h (scale bar: 100 μm). (C) Flow cytometry analysis of HT-29 RIEP MLKL S358D cells treated with 2 $\mu\text{g}/\text{mL}$ doxycycline and Nec-1 (10 μM), NSA (10 μM) or geldanamycin (GA, 1 μM) for 6 h.

Supplementary Figure 1

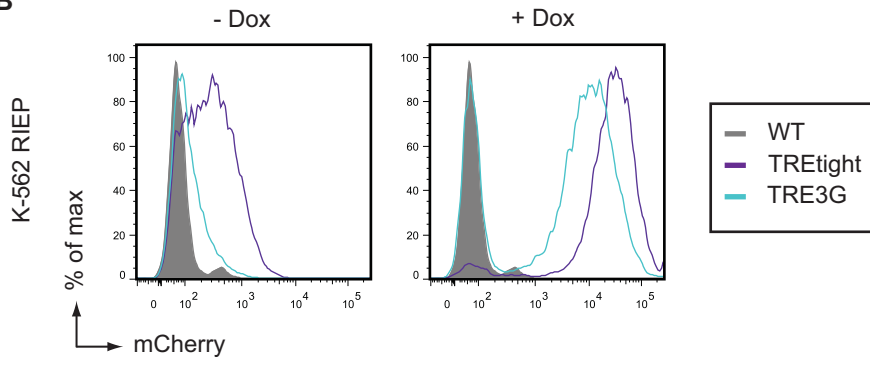


Supplementary Figure 2

A

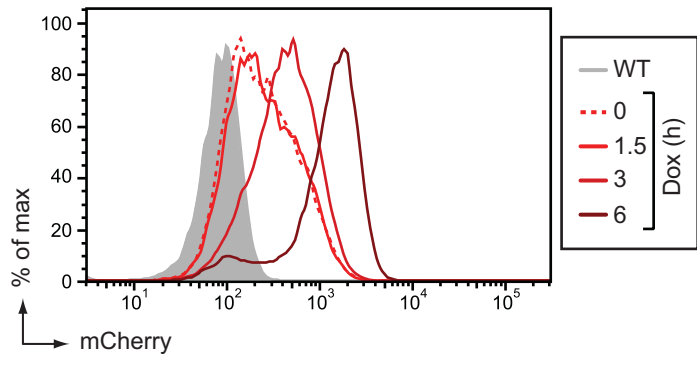


B

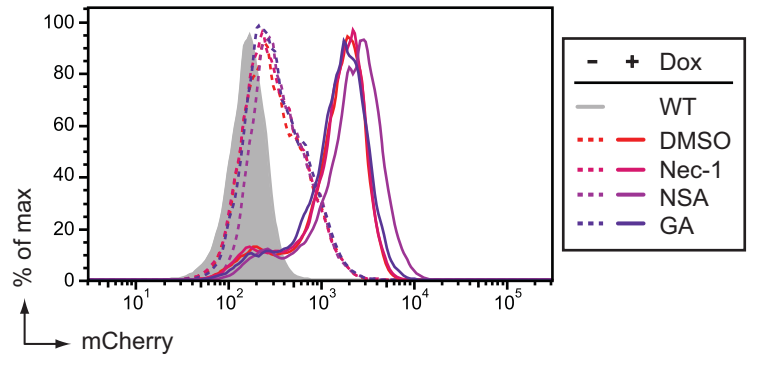


Supplementary Figure 4

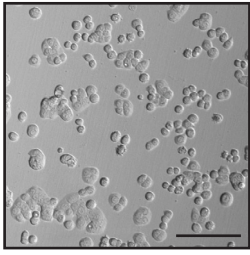
A HT-29 RIEP MLKL S358D



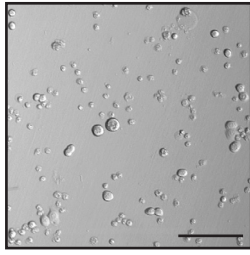
C HT-29 RIEP MLKL S358D



B -Dox



+ Dox (24h)



3. Discussion

For a long time, necrosis has been considered a passive and unregulated form of cellular demise, beyond reach of pharmacological interference. Hence, despite its wide-ranging implications in human pathology, little efforts were undertaken to study the mechanisms underlying necrotic cell death. However, the paradigm-changing discovery of necroptosis spurred significant scientific interest and the field rapidly gathered momentum. To date, several molecular pathways driving regulated necrosis have been described. The growing understanding of the molecular mechanisms underlying the different subroutines of programmed necrosis paves the way for pharmacological targeting of necrotic cell death.

3.1. Regulated Necrotic Cell Death as a Therapeutic Target

The precise functional and structural characterization of the molecular components involved in apoptosis signaling and its regulation prompted development of apoptosis-targeting therapies (Fischer & Schulze-Osthoff, 2005). Pro-apoptotic compounds, such as IAP antagonists and Bcl-2 homology 3 (BH3) mimetics, are currently undergoing clinical trials for cancer treatment (Delbridge & Strasser, 2015; Fulda, 2015). Besides first trials testing the validity of using PARP1 inhibitors to target parthanatos, none of the other so far identified regulated necrosis pathways have been targeted clinically (Conrad et al, 2016). While it remains to be seen how findings from mouse studies will translate to human disease, data obtained in preclinical models suggest that the detailed analysis of the programmed necrotic signaling pathways may translate into substantial therapeutic potential.

As a consequence of the pro-inflammatory nature of necrotic cell death, concurrent targeting of both regulated necrosis and inflammation constitutes a promising treatment option. While the release of pro-inflammatory DAMPs and alarmins associated with regulated necrosis may be favorable in anti-pathogen responses, it exacerbates tissue destruction in sterile-injury induced inflammation. Given that regulated cell death triggers inflammation and *vice versa*, the existence of a necro-inflammatory auto-amplification loop has been suggested (Linkermann et al, 2014c). This circuit may originate from an initial event of regulated necrosis accompanied by DAMP release that induces pro-inflammatory signaling, in turn causing further programmed necrotic cell death. If this amplification is not restrained, such a loop may ultimately lead to systemic inflammation and organ failure due to extensive necrosis. Therapeutic interference would optimally target and prevent the primary event of regulated necrosis. However, once clinical symptoms of injury manifest in a patient, the necro-inflammatory loop has progressed and engaged a pro-inflammatory response. Accordingly, blocking both driving forces of the necro-inflammatory circuit by combined pharmacological targeting of inflammation and regulated necrotic cell death holds most

promise of clinical benefit (Linkermann et al, 2014c). Interestingly, cyclosporine A, an immunosuppressant widely used in solid organ transplantation, has been identified to simultaneously inhibit MPT-dependent necrosis (Linkermann et al, 2014a; Nakagawa et al, 2005). The efficacy of this drug in preventing graft loss might thus be based on its ability to concomitantly block regulated cell death and mediate immunosuppression (Linkermann & Green, 2014).

The various subroutines of regulated cell death have so far commonly been studied as separate entities. Yet, there is increasing awareness of the high level of interconnectedness between the various apoptotic and necrotic pathways (Silke et al, 2015). While the understanding of how these different signaling pathways crosstalk in relevant *in vivo* pathological settings is still limited, first studies suggest that concurrent targeting of more than one regulated cell death may prove advantageous. Combinatorial therapy simultaneously targeting MPT-dependent necrosis, ferroptosis and necroptosis has been shown to provide strong beneficial effects in a model of renal IR injury, whereas inhibition of singular pathways yielded only limited cytoprotection (Linkermann et al, 2013a; Linkermann et al, 2014b). Similarly, Zhao et al. (Zhao et al, 2015) have shown the advantage of such a combinatorial treatment strategy in kidney transplant-mediated lung injury. In this *in vivo* model, the organ damage in the lung is triggered by circulating DAMPs and pro-inflammatory molecules, which are induced and released by regulated necrosis occurring due to renal IR injury following transplantation. While single treatment with Nec-1 or a PARP-1 inhibitor reduced remote lung injury to a certain extent, the combined treatment with both agents provided strong protection against organ damage, suggesting that cell death in the lung is mainly due to necroptosis and parthanatos in this setting. Importantly, cell death pathways may not be uniformly regulated across different pathophysiological conditions and cell types (Berghe et al, 2014). For instance, the phenotype resulting from RIPK1 deficiency is highly dependent on the respective tissue background. The psoriasis-like phenotype induced by RIPK1 deficiency in keratinocytes can be rescued by deletion of *Ripk3* (Dannappel et al, 2014). In contrast, deletion of *Ripk1* in intestinal endothelial cells triggers apoptotic cell death, which can be prevented by concomitant loss of CASP8, but not RIPK3 (Takahashi et al, 2014). Accordingly, establishing clear links between the forms of regulated cell death and the respective disease model is of importance for the design of combinatorial targeting strategies.

3.2. Targeting Necroptosis

Necroptosis has been shown to have detrimental effects in several common clinical disorders, including stroke, myocardial infarction and pancreatitis (Linkermann et al, 2014c). Accordingly, translating necroptosis inhibition into clinics may hold ample benefit. Yet,

several aspects remain to be addressed to establish necroptosis as a practicable therapeutic target.

First, the unambiguous determination of cell types and disease processes affected by necroptosis is of crucial importance. As discussed above, the various subroutines of regulated necrosis share common morphological features. Hence, there is a need for reliable biomarkers capable of distinguishing the various forms of regulated necrotic cell death by their distinct molecular features. The first such tool for identification of necroptotic cells and their detection in primary human tissues is a recently developed monoclonal antibody, which detects phosphorylation of T357 and S358 on the human MLKL protein (Wang et al, 2014a). This antibody has been employed to investigate the contribution of necroptosis to acute liver damage. Cells undergoing necroptosis, marked by positive staining for phospho-MLKL, were detected in necrotic areas of liver biopsy samples from patients with drug-induced liver injury. However, additional validation will be required to establish the applicability of using phosphorylated MLKL as a reliable marker for the *in situ* identification of necroptosis in human tissues. In this regard, the recent emergence of similar tools for detection of murine phospho-MLKL will prove valuable for the closer characterization of regulated necrotic cell death occurring in mouse models of human diseases.

Secondly, despite a number of tool compounds that can be used to query the necroptosis pathway, no inhibitors of necroptotic cell death are available for clinical use. Accordingly the identification of small molecule necroptosis inhibitors for potential clinical application constitutes a major goal of research at present. Increasing insight into the molecular basis of the necroptosis signaling pathway identified a number of potential targets that could be exploited pharmacologically, however, target selection for development of small molecule necroptosis inhibitors needs careful consideration. In principle, therapeutic interference with necroptosis could be aimed at the activating receptor, RIPK1, RIPK3, MLKL, necrosome assembly, as well as at potential further intermediate and downstream signaling mediators yet to be identified. The redundancy of molecular mechanisms shared by various pathways of regulated necrosis as well as the diversity in signaling outcome is assumedly higher at the trigger and initial pathway stages. Accordingly, targeting necroptosis closer to the execution level may prove more effective (Berghe et al, 2014). Importantly, efficient therapeutic targeting of the necroptosis pathway members will require detailed understanding of their respective functions in the different subroutines of cell death. In particular, dissecting the differences between the scaffold function of RIPK1 and RIPK3 and their kinase activity poses a challenge (Feoktistova & Leverkus, 2015). In order to block scaffold-associated signaling functions of RIPK1 and RIPK3, the development of specific inhibitors targeting RHIM-domain mediated interactions may be required. RIPK1 is put forward as a safe therapeutic target for blocking necroptosis by the finding that mice expressing kinase-inactive RIPK1 are viable

and healthy (Kaiser et al, 2014; Newton et al, 2014). The fact, that RIPK1 can also induce apoptosis in a CASP8-dependent manner in certain instances (Feoktistova et al, 2011; Tenev et al, 2011) may render the effects of targeting RIPK1 even more potent. However, targeting RIPK1 may not be sufficient to protect from necroptotic cell death, as, depending on the respective upstream inducer of necroptotic cell death, RIPK3 can drive necroptosis independently of RIPK1 (He et al, 2011; Kaiser et al, 2013; Thapa et al, 2013; Upton et al, 2012). Greater caution may be required in targeting RIPK3. Development of clinically usable RIPK3 inhibitors faces the challenge of avoiding the perturbation of the kinase domain proposed to release the brake on RHIM-mediated apoptosis induction (Mandal et al, 2014). Indeed, high concentrations of the recently identified RIPK3 inhibitors GSK'843 and GSK'872 have been reported to promote RIPK1-dependent activation of CASP8 and apoptosis upon TNF stimulation (Mandal et al, 2014). In contrast, the RIPK3 inhibitor GSK'840 does not display pro-apoptotic properties. Yet, GSK'840 fails to block murine RIPK3, thus precluding its use in experimental mouse models of human diseases. Concerning the targeting of RIPK3, it remains to be clarified whether additional substrates beyond MLKL exist, which would be affected by such inhibition. In this regard, MLKL seems an appealing drug target as, besides its role in necroptosis execution, no other function has so far been assigned to this protein (Czabotar & Murphy, 2015). The generation of *Mlkl*^{-/-} mice has paved the way to assess whether MLKL deficiency will result in equal beneficial outcomes as RIPK1 inhibition or lack of RIPK3 in models of necroptosis-associated disease and inflammation. The first small molecule reported to inhibit necroptosis by targeting MLKL was NSA (Sun et al, 2012). The binding of NSA to the N-terminal part of the pseudokinase does not inhibit the interaction with and phosphorylation by RIPK3, but blocks MLKL oligomerization and membrane translocation. In detail, NSA alkylates Cys86 in human MLKL, which is absent in the murine protein, rendering NSA a human-specific MLKL inhibitor. Given that residue Cys86 is exposed on the surface of the protein rather than being located in the binding pocket, NSA may exhibit substantial target promiscuity without offering much possibility for improving specificity for MLKL (Sun & Wang, 2014). In contrast, the more recently described MLKL inhibitor compound 1 targets the pseudokinase domain and interferes with the conformational switch required to release the necroptosis executioner 4HB domain (Hildebrand et al, 2014). Despite being catalytically inactive, targeting the pseudokinase domain of MLKL thus constitutes a valid strategy for blocking the function of this protein. However, compound 1 has recently been found to similarly bind and block RIPK1, calling its specificity into question (Conrad et al, 2016). In-depth analysis of the necroptosis pathway may serve to reveal additional potential targets such as, for instance, further necroptosis effectors acting downstream of MLKL. The exact mechanism by which MLKL leads to membrane destabilization has not yet been unambiguously clarified. The membrane

recruitment of MLKL has been shown to be mediated by binding to PIPs (Dondelinger et al, 2014; Wang et al, 2014a). Furthermore, the involvement of ion channels in the execution of necroptotic cell death has been suggested (Cai et al, 2013; Chen et al, 2013). Importantly, inhibition of PIP formation as well as blocking ion flux has been shown to reduce necroptotic cell death, indicating that pharmacological interference with phospholipid metabolism or ion channels may constitute additional options for the therapeutic targeting of necroptosis.

In contrast to necroptosis inhibition, induction of necroptotic cell death has been suggested as a potential treatment to overcome cancer drug resistance. Various apoptosis-avoiding mechanisms have been identified in malignant cells, making resistance to cell death one of the hallmarks of cancer (Hanahan & Weinberg, 2011). As a result, pro-apoptotic BH-3 mimetics are currently test in clinical trials as anti-cancer therapy (Delbridge & Strasser, 2015; Fulda, 2015). Given that tumor survival depends on the maintenance of a highly reduced intracellular environment, perturbing ROS homeostasis by ferroptosis-inducing agents such as erastin may constitute an alternative approach to target cancer cells (Dixon & Stockwell, 2014). Necroptotic cell death can be induced pharmacologically using the small molecule E6, showing moderate activity in cell-based systems (Mou et al, 2015). Current efforts are directed at identifying the responsible molecular target as well as more potent derivatives for potential use in drug-resistant cancer. However, in contrast to apoptosis, the role of programmed necrotic cell death in malignant cells has not yet been studied extensively. Loss of RIPK3 expression has been reported as a mechanism conferring resistance to necroptosis during development of melanoma (Geserick et al, 2015). Induction of necroptosis would thus require pathway reactivation in these cells, if the necroptosis inducer targets an element upstream of MLKL. In contrast to apoptosis, programmed necrotic cell death is associated with pro-inflammatory signals. While necroptosis may thus have the beneficial effect of counteracting hyperproliferation of malignant cells, the immune cells recruited by the inflammatory signaling mediators may actually be advantageous for the tumor by fostering cell growth, angiogenesis and invasiveness (Hanahan & Weinberg, 2011). In light of these considerations, the possibility to target cancer by necroptosis induction clearly requires further investigation and experimental evidence.

Finally, the thorough dissection of the protein network and molecular checkpoints steering necroptosis signaling will provide a detailed appreciation of how the pathway is controlled and contributes to human disease. Identifying regulators that contribute to fine-tuning of the signaling outcome may furthermore reveal additional potential targets for modulation of the necroptosis pathway.

Along these major lines of current research, we aimed at expanding the available set of pharmacological tools as well as to broaden the chemical premises for scaffold-based design of clinical necroptosis inhibitors by performing a small molecule screen. We thereby identified

two FDA-approved drugs, ponatinib and pazopanib, as efficient inhibitors of necroptosis. Moreover, to provide the basis for proteomic analysis of the necroptosis pathway, a novel inducible expression system for SH-based TAP-LC-MS approaches was established. Employing this system, we identified and validated MLKL as an HSP90 client protein, expanding the role of HSP90 in regulating necroptosis and providing further rationale for blocking necroptotic cell death using HSP90 inhibitors.

3.3. The FDA-Approved Drugs Ponatinib and Pazopanib Inhibit Necroptosis

So far, all chemical agents described to block necroptosis by inhibiting RIPK1, RIPK3, or MLKL are tool compounds with insufficiently assessed pharmacokinetic and selectivity profiles. The rapid emergence of necroptosis as an exciting therapeutic target incited us to screen a representative panel of FDA-approved drugs in order to identify necroptosis inhibitors for potential medical use. Drugs having gained FDA-approval represent a valuable basis for medicinal chemistry optimization due to their established safety and pharmacokinetic profiles. To avoid pitfalls frequently encountered upon validation of hits from target-based approaches, such as toxicity or lack of target engagement in the context of entire cells (Moffat et al, 2014), we performed a phenotypic screen in FADD-deficient Jurkat cells. In the setup chosen, compounds blocking the necroptosis pathway but concurrently exhibiting toxicity were excluded *a priori*. The library queried contained 268 drugs, selected to optimally represent the chemical and biological space of clinical compounds. In order to remain within pharmacologically relevant concentrations as well as to avoid excessive polypharmacology, the drugs were assayed at low concentrations. Out of the 268 drugs tested, the two kinase inhibitors ponatinib and pazopanib robustly protected the cells from necroptotic cell death.

The orally available tyrosine kinase inhibitor ponatinib targets the fusion protein BCR-ABL, which drives chronic myeloid leukemia (CML) and Philadelphia chromosome-positive acute lymphoblastic leukemia (Ph+ ALL) (O'Hare et al, 2009), and is thus one of the five BCR-ABL inhibitors presently in clinical use. The first developed and present front-line therapy imatinib has proven highly effective in treatment of CML, yielding remarkable response and survival rates (Deininger et al, 2005). However, resistance arising in many patients prompted development of the second-generation drugs nilotinib, dasatinib, and bosutinib. Ponatinib, finally, was the result of a structure-guided drug design effort to target the BCR-ABL gatekeeper mutant T315I. This mutation confers resistance to all other currently available BCR-ABL inhibitors, as drug access to the ATP binding site of the enzyme is blocked by the bulky isoleucine side chain (Huang et al, 2010). The key structural characteristic of ponatinib is a triple bond, which skirts this steric hindrance. As initial clinical trials reported good results (Cortes et al, 2012; Cortes et al, 2013), ponatinib was granted accelerated FDA-approval.

However, the follow-up of these studies revealed a high incidence of vascular occlusion events, leading to interim market withdrawal and premature termination of a phase III clinical trial evaluating ponatinib as first-line treatment (Jain et al, 2015). As it remains the sole effective therapy for T315I-positive CML or Ph+ ALL, the sales suspension for ponatinib was partially lifted shortly afterwards. Yet, revised clinical practice guidelines and a new black box warning were issued. While selective kinase assays have revealed that ponatinib also inhibits members of the vascular endothelial growth factor receptor (VEGFR), fibroblast growth factor receptor (FGFR) and platelet derived growth factor receptor (PDGFR) families (O'Hare et al, 2009), no global analysis of its target spectrum has been performed so far. This study thus provides the first comprehensive description of the cellular target spectrum of ponatinib. This cellular target profile may allow pinpointing targets that are responsible for the clinically observed side effects of the drug. The more detailed understanding of the polypharmacological properties exerted by ponatinib may help to minimize toxicity by compensation via dose adjustments or adjunct therapies. Moreover, these data constitute a valuable resource for identifying additional drug targets, possibly opening new therapeutic points of intervention for ponatinib and thus expanding its curative potential. Despite the broad overlap of the target spectra of the clinically available BCR-ABL inhibitors (Hantschel et al, 2008; Rensing Rix et al, 2008), the capability to target the necroptosis pathway is unique for ponatinib. Inhibition of RIPK1 and RIPK3 constitutes the main molecular mechanism for necroptosis inhibition by ponatinib. However, additional drug targets may contribute to the cell death-protective phenotype. In this regard, also TAK1, TAB1, and TAB2 are targeted solely by ponatinib as compared to the other BCR-ABL inhibitors. Indeed, competition binding assays affirmed subnanomolar affinity of ponatinib for TAK1. The best described function of TAK1 is its role in NF- κ B activation upon IL-1 or TNF stimulation (Takaesu et al, 2003). The importance of TAK1 for cell survival is further evidenced by the early embryonic lethality of *Tak1* knockout mice (Shim, 2005). Correspondingly, TAK1 inhibition was shown to induce apoptosis (Lamothe et al, 2012; Morioka et al, 2014), yet this cytotoxic phenotype is cellular context-dependent (Wang et al, 2015). Furthermore, a possible regulatory function of TAK1 in necroptosis signaling has been suggested recently (Mihaly et al, 2014; Morioka et al, 2014). More precisely, prolonged TAK1 activation was demonstrated to promote RIPK3-dependent necrotic cell death (Morioka et al, 2014). In light of the varied functions reported for this kinase, untangling the respective contribution of TAK1 targeting by ponatinib from RIPK1/RIPK3 inhibition proves challenging and will be eased by future clarification of the precise role TAK1 plays in necroptosis signaling. Nevertheless, we ascertained that sole targeting of TAK1 is insufficient to explain the protective effect of ponatinib, as the TAK1 inhibitor (5Z)-7-oxozeaenol (Wu et al, 2013b) fails to prevent TNF-induced necroptosis. Importantly, ponatinib stands out among the so far

described necroptosis inhibitors as the first compound that concurrently targets both RIP kinases which are relevant for necroptotic cell death. Identification of ponatinib as a dual RIPK1/RIPK3 inhibitor thus adds another sharp tool to the currently available armamentarium for scrutinizing the necroptosis pathway.

Concerning pazopanib, we propose that RIPK1 constitutes the main target mediating the protective effect against necroptotic cell death. Pazopanib is an oral, multi-targeted tyrosine kinase inhibitor approved for treatment of advanced renal cell carcinoma (RCC) and soft tissue sarcoma (van der Graaf et al, 2012; Ward & Stadler, 2010). The drug was reported to perform noninferior to sunitinib, the second tyrosine kinase inhibitor available as frontline treatment for RCC (Motzer et al, 2013). While showing similar efficacy, pazopanib exhibits a favorable safety and tolerability profile. Yet, the drug has been reported to impact liver function (McCormack, 2014; Sternberg et al, 2010), and a black-box warning related to severe and fatal hepatotoxicity was issued in the United States. Pazopanib had been included in a study testing the selectivity of 72 kinase inhibitors against a panel of 442 kinase assays (Davis et al, 2011). Besides the expected targets VEGFR-1, -2 and -3, PDGFR- α and - β , and the stem cell factor receptor c-Kit (Harris et al, 2008; McCormack, 2014), these competition binding assays revealed nanomolar binding affinity ($K_D = 260$ nM) for RIPK1. The inhibitory effect of pazopanib on necroptosis is unlikely to rely on its primary targets as vandetanib, which has a largely overlapping target spectrum yet does not bind RIPK1 (Davis et al, 2011), failed to protect cells from undergoing necroptosis. We verified that RIPK1, but neither RIPK3 nor MLKL are efficiently targeted by pazopanib. However, a possible contribution of other yet undescribed or formerly identified targets, as for example phosphatidylinositol-5-phosphate 4-kinase, type II, gamma (PIP4K2C) or TAO kinase 3 (TAOK3) (Davis et al, 2011), cannot be formally excluded at this point.

3.4. An Inducible Expression System for TAP-MS Approaches Enables Identification of MLKL as an HSP90 Client

Dynamic signaling networks of interacting proteins form the basis of most cellular functions (Gingras et al, 2007). The detailed study of protein-protein interactions and protein complexes is thus vital to uncover the molecular foundation on which cellular processes are being built upon. Investigating protein interaction networks may furthermore allow predicting the functionality of previously uncharacterized proteins as well as aid the discovery of novel potential drug targets for a given disease. Applying a TAP-MS approach to study necroptosis has so far been hampered by the fact that stable ectopic expression of the necroptosis key signaling proteins can trigger pathway auto-activation and result in cell death. Cell lines commonly employed for inducible expression of SH-tagged bait proteins, as for example HEK293, are resistant to necroptosis due to lack of RIPK3 expression (He et al, 2009). Yet,

in order to obtain biologically relevant interaction data, TAP-MS experiments for a specific protein need to be performed in context of its functional signaling pathway. The inducible expression system pRSHIC (retroviral expression of SH-tagged proteins for interaction proteomics and color-tracing) described in this study is compatible with SH-based TAP-MS approaches in a wide variety of cellular backgrounds and thus opens the possibility to systematically map the signaling network underlying necroptotic cell death. Such an approach is expected to lead to the identification of novel signal relays and potential additional targets for pharmacological interference.

The applicability of pRSHIC for SH-based interaction studies was illustrated by delineating the interactome of the oncogenic G12D mutant of NRAS in murine Ba/F3 cells (Palacios & Steinmetz, 1985). The proteomic characterization of such oncogenic gene variants can make a crucial contribution to the identification of their respective disease mechanisms, as for example demonstrated for CCAAT/enhancer binding protein alpha (CEBPA)-mutated acute myeloid leukemia (AML) (Grebien et al, 2015). The proteomic analysis accurately reflected previously published and anticipated interaction partners of NRAS G12D, establishing pRSHIC as a convenient tool to chart the interactome of proteins carrying cancer-associated mutations.

By utilizing pRSHIC to inducibly express the phosphomimetic S358D mutant form of MLKL in HT-29 cells, we unraveled another fine detail of necroptosis biology. For interaction proteomics experiments, the temporal length of MLKL S358D expression was tailored to optimally exploit the time window of robust bait protein expression prior to onset of cell death. In light of previous studies employing the HSP90 inhibitor geldanamycin (Whitesell et al, 1994) as an unspecific means to block necroptosis (Holler et al, 2000), the interaction between MLKL and HSP90 merited further investigation. HSP90 is a molecular chaperone that assists its client proteins to attain proper folding, and is thus of crucial importance for their stability and function (Taipale et al, 2010). Both RIPK1 and RIPK3 are clients of the HSP90-cell division cycle 37 (CDC37) complex and are subjected to proteasomal degradation upon HSP90 inhibition (Cho et al, 2009; Lewis et al, 2000; Li et al, 2015). The necroptosis protection conferred by geldanamycin has thus been attributed to destabilization of these two kinases. Our results show that, besides RIPK1 and RIPK3, HSP90 inhibition also affects MLKL. In general, two criteria need to be met by a given protein to confirm its HSP90 client status, namely physical interaction and decreased function upon HSP90 inhibition (Taipale et al, 2010). Indeed, we demonstrate that both the MLKL wildtype as well as the MLKL S358D mutant protein interact with HSP90. Inhibition of HSP90 efficiently prevented MLKL S358D-induced cell death by triggering proteasomal degradation of the mutant protein. We verified that wildtype MLKL was similarly destabilized upon geldanamycin treatment, thus validating MLKL as a novel HSP90 client protein. We cannot firmly exclude

that some of the HSP90 molecules identified in MLKL co-immunoprecipitation and pulldown experiments are piggybacking on the MLKL interactor RIPK3. However, the fact that MLKL S358D-induced cell death is efficiently blocked by HSP90 inhibition, yet proceeds independently of RIPK3, strongly supports a direct effect of HSP90 on MLKL.

In addition to proteomics studies, pRSHIC moreover opens the possibility to perform targeted chemical screens. In this regard, assaying MLKL S358D-induced cell death against a library of small molecule inhibitors may reveal additional compounds that block MLKL or yet unidentified downstream pathway members. Indeed, such an approach has been employed in a parallel study by Jacobsen et al. (Jacobsen et al, 2016). A library of 438 small molecules was screened in both *Mkl*- fibroblasts inducibly expressing the constitutively active MLKL mutant Q343A, as well as wild-type murine fibroblasts induced to undergo necroptosis. In agreement with our results, seven HSP90 inhibitors were identified to block necroptotic cell death in both cell types, corroborating the relevance of HSP90 for MLKL-mediated cell death. HSP90 activity was proposed to be essential for the formation of higher order MLKL complexes and subsequent membrane translocation (Jacobsen et al, 2016). Moreover, siRNA-mediated knockdown of *CDC37* was shown to reduce cell death induced by a phosphomimetic MLKL mutant, corroborating that this kinase-specific co-chaperone serves as an adaptor for HSP90 recruitment, as suggested by the interaction proteomics data presented here.

As many oncogenes have been shown to depend on HSP90, several HSP90 inhibitors are currently undergoing clinical trials for cancer therapy (Trepel et al, 2010). Notably, the geldanamycin-analogue 17-DMAG, which has undergone preclinical assessment for several cancers (Garcia-Carbonero et al, 2013), was shown to attenuate necroptosis *in vivo* in a rat model of TNF-induced SIRS (Li et al, 2015). Given the current efforts to develop compounds for therapeutic use in necroptosis-associated diseases, identification of another class of clinical stage agents capable of blocking necroptotic cell death is of significant interest. Conversely, these findings raise the need to address whether the inhibitory effect on necroptosis has implications for the use of HSP90 inhibitors in cancer treatment.

3.5. Towards Necroptosis Inhibitors for Clinical Use

Vital issues that need to be addressed regarding the potential clinical application of necroptosis inhibitors include identification of the disease conditions most likely to benefit from such treatment as well as the time window and required duration of therapy. Given the rapid temporal course of necroptosis, inhibitors may hold most promise for clinical conditions in which necroptotic cell death can be anticipated, such as IR injury following transplantation or vessel occlusion (Linkermann et al, 2013b). Among the conditions with therapeutic potential for necroptosis inhibition described so far, solid-organ transplantation may be the

scenario holding the most favorable benefit-to-risk ratio for first clinical trials (Linkermann et al, 2014c).

The identification of the FDA-approved drugs ponatinib and pazopanib as efficient necroptosis inhibitors puts them forward as possible candidates for clinical application. Yet, both these drugs are associated with strong side effects, which may be acceptable for anti-cancer treatment, but precludes their use in less severe conditions. Nevertheless, most adverse drug effects, such as onset of hepatotoxicity, are seen after several weeks of continuous therapy (Shah et al, 2013). In contrast, interference with necroptosis may require only short-term or even a single dose of drug treatment. As a matter of fact, a single dose of ponatinib has been reported to be generally well tolerated in healthy subjects (Narasimhan et al, 2013). However, with attention to the safety concerns as well as the low specificity of pazopanib and ponatinib for the necroptosis-relevant targets, using their scaffolds as starting point for development of highly selective necroptosis inhibitors may prove a fruitful strategy. In a study performed in parallel to the work presented here, Najjar et al. (Najjar et al, 2015) also identified ponatinib as necroptosis inhibitor, and applied such a structure-guided design strategy to the drug in order to develop derivatives with increased selectivity for RIPK1. Combination of the ATP pocket-binding moiety of ponatinib with the RIPK1 inhibitor Nec-1 led to creation of the hybrid molecule PN10, displaying enhanced potency, higher selectivity for RIPK1, and lower cytotoxicity. Both ponatinib as well as the ponatinib-based hybrid inhibitor protected against TNF-induced toxicity *in vivo* and showed higher activity than Nec-1 regarding survival and tissue injury (Najjar et al, 2015). While further evaluation of this ponatinib-Nec-1 hybrid molecule in other preclinical models of necroptosis-associated pathology will be needed to interrogate its therapeutic potential, these results highlight the value of medicinal chemistry for the development of drug-like necroptosis inhibitors. In like manner to RIPK1-specific agents, alternative modifications of the ponatinib scaffold may allow to establish more selective pan-RIPK inhibitors. In fact, ponatinib has recently been found to also inhibit the RIP kinase family member RIPK2 (Canning et al, 2015). The first crystal structure of RIPK2 has been solved in complex with ponatinib, and can thus serve as a basis for the rational design of RIPK2-selective compounds.

To date, the only other candidate proposed for clinical application as anti-necroptosis agent is the BRAF^{V600E} inhibitor dabrafenib, which was shown to have an off-target effect on RIPK3 (Li et al, 2014). Taking the sequence similarity of RIPK1 and RIPK3, as well as the conformational resemblance of RIPK1 and BRAF into account, Li and coworkers (Li et al, 2014) tested a selected panel of eight BRAF inhibitors for their effect on RIPK3. Six of those small molecules blocked RIPK3 activity in kinase assays, dabrafenib bearing the most potent impact. Dabrafenib was subsequently shown to inhibit necroptosis in cellular models as well as to reduce acetaminophen-induced RIPK3-mediated liver injury in mice (Li et al, 2014).

Clinically, dabrafenib is approved for use in BRAF^{V600E}-mutated metastatic melanoma (McGettigan, 2014). Similar to ponatinib and pazopanib, the numerous common side effects described for this drug pose a constraint on direct repurposing endeavors for necroptosis-related diseases, despite its generally acceptable human safety profile. However, as necroptosis inhibition by dabrafenib occurs independently of its effect on BRAF, structure-activity relationship (SAR) studies aimed at discerning the moieties mediating RIPK3 and BRAF inhibition may serve to develop selective RIPK3 inhibitors. The effect of this newly described off-target of dabrafenib in its approved indications is a matter of current investigation (Geserick et al, 2015).

Taken together, the discovery of FDA-approved drugs blocking necroptotic signaling, together with elucidation of the respective molecular targets involved, opens new avenues for the development of anti-necroptosis agents for clinical use.

3.6. Conclusion and Future Prospects

Major advances in understanding the molecular machinery and pathophysiological roles of necroptosis have been made since its first description ten years ago (Degterev et al, 2005). Despite its relatively recent discovery, evidence for the implication of programmed necrotic cell death in human pathology has accumulated quickly over the past years. Hence, the growing insight into the molecular mechanisms of necroptosis entails the exciting prospect of bringing therapeutic benefit to patients in the future. Yet, a number of questions remain to be addressed in order to be able to translate the therapeutic advantage gained by blocking necroptosis in preclinical models into cytoprotective therapies for clinical use. It will be of crucial importance to elucidate to which extent the different pathways of regulated necrosis are integrated, as maximum clinical benefit may require concomitant targeting of multiple cell death programs (Linkermann et al, 2014c). In-depth examination of the necroptosis cascade should optimally involve the dynamic characterization of the interaction partners and complexes associated with the individual pathway members. In this regard, establishment of an inducible expression system, which allows proteomic analysis of the necroptosis pathway in the relevant cellular setting, opened the way for mapping the protein interaction network underlying necroptotic cell death and other programmed necrosis pathways. In addition to the potential identification of further regulators, such studies will pinpoint the molecular checkpoints of the necroptosis pathway and thus provide valuable information as to which signaling step constitutes the optimal entry point for therapeutic intervention. Major efforts should further be dedicated to the development of cytoprotective pharmacological agents which are eligible for clinical application. In this respect, identification of necroptosis inhibitors among drugs which are currently in clinical development as well as already approved drugs, combined with elucidation of their precise molecular mode of action, provides a valuable chemical basis for the development of potent anti-necroptosis agents. Preclinical studies in mouse models will be of crucial importance in assessing the potential of these compounds for treatment of necroptosis-related diseases. As the first dual RIPK1/RIPK3 inhibitor, ponatinib can here be used to decipher whether dual inhibition results in improved outcome as compared to separate targeting of these kinases. Future will tell whether necroptosis inhibition in human disease will meet the expectations raised by current data and enter clinical practice.

*“The field of cell death,
like that of any fundamentally central phenomenon of life,
is a window onto the world of a cell and its existence in the organism as a whole.*

*As such,
it is necessarily linked to other processes,
and how it is linked, with the resulting complexity,
is intertwined with other fundamental fields of study.*

Yes, there is more to do.

So get out of here, we’re not done.

And don’t forget to dance now and then.”

(Green, 2016)

Douglas R. Green is a molecular biologist known for his work on the role of cell death in cancer and during immune responses. Having made major contributions to the fields of apoptosis, autophagy and regulated necrosis, he is one of the world’s most highly cited scientists.

References

- Andrabi SA, Dawson TM, Dawson VL (2008) Mitochondrial and Nuclear Cross Talk in Cell Death. *Annals of the New York Academy of Sciences* **1147**: 233-241
- Ashburn TT, Thor KB (2004) Drug repositioning: identifying and developing new uses for existing drugs. *Nature Reviews Drug Discovery* **3**: 673-683
- Baines CP, Kaiser RA, Purcell NH, Blair NS, Osinska H, Hambleton MA, Brunskill EW, Sayen MR, Gottlieb RA, Dorn GW, Robbins J, Molkentin JD (2005) Loss of cyclophilin D reveals a critical role for mitochondrial permeability transition in cell death. *Nature* **434**: 658-662
- Balamayooran T, Batra S, Balamayooran G, Cai S, Kobayashi KS, Flavell RA, Jeyaseelan S (2011) Receptor-Interacting Protein 2 Controls Pulmonary Host Defense to Escherichia coli Infection via the Regulation of Interleukin-17A. *Infection and Immunity* **79**: 4588-4599
- Berger SB, Harris P, Nagilla R, Kasparcova V, Hoffman S, Swift B, Dare L, Schaeffer M, Capriotti C, Ouellette M, King BW, Wisnoski D, Cox J, Reilly M, Marquis RW, Bertin J, Gough PJ (2015) Characterization of GSK'963: a structurally distinct, potent and selective inhibitor of RIP1 kinase. *Cell Death Discovery* **1**: 15009
- Berghe TV, Linkermann A, Jouan-Lanhouet S, Walczak H, Vandenabeele P (2014) Regulated necrosis: the expanding network of non-apoptotic cell death pathways. *Nature Reviews Molecular Cell Biology* **15**: 135-147
- Bergsbaken T, Fink SL, Cookson BT (2009) Pyroptosis: host cell death and inflammation. *Nature Reviews Microbiology* **7**: 99-109
- Bigenzahn JW, Fauster A, Rebsamen M, Kandasamy RK, Scorzoni S, Vladimer GI, Mueller AC, Gstaiger M, Zuber J, Bennett KL, Superti-Furga G (2015) An inducible retroviral expression system for tandem affinity purification mass-spectrometry-based proteomics identifies MLKL as an HSP90 client. *Molecular & Cellular Proteomics*
- Black RA, Rauch CT, Kozlosky CJ, Peschon JJ, Slack JL, Wolfson MF, Castner BJ, Stocking KL, Reddy P, Srinivasan S, Nelson N, Boiani N, Schooley KA, Gerhart M, Davis R, Fitzner JN, Johnson RS, Paxton RJ, March CJ, Cerretti DP (1997) A metalloproteinase disintegrin that releases tumour-necrosis factor- α from cells. *Nature* **385**: 729-733
- Bonnet Marion C, Preukschat D, Welz P-S, van Loo G, Ermolaeva Maria A, Bloch W, Haase I, Pasparakis M (2011) The Adaptor Protein FADD Protects Epidermal Keratinocytes from Necroptosis In Vivo and Prevents Skin Inflammation. *Immunity* **35**: 572-582
- Bouwmeester T, Bauch A, Ruffner H, Angrand P-O, Bergamini G, Croughton K, Cruciat C, Eberhard D, Gagneur J, Ghidelli S, Hopf C, Huhse B, Mangano R, Michon A-M, Schirle M, Schlegl J, Schwab M, Stein MA, Bauer A, Casari G, Drewes G, Gavin A-C, Jackson DB, Joberty G, Neubauer G, Rick J, Kuster B, Superti-Furga G (2004) A physical and functional map of the human TNF- α /NF- κ B signal transduction pathway. *Nature Cell Biology* **6**: 97-105
- Brennan MA, Cookson BT (2000) Salmonella induces macrophage death by caspase-1-dependent necrosis. *Mol Microbiol* **38**: 31-40
- Brigelius-Flohé R, Maiorino M (2013) Glutathione peroxidases. *Biochimica et Biophysica Acta (BBA) - General Subjects* **1830**: 3289-3303
- Brinkmann V, Reichard U, Goosmann C, Fauler B, Uhlemann Y, Weiss DS, Weinrauch Y, Zychlinsky A (2004) Neutrophil extracellular traps kill bacteria. *Science* **303**: 1532-1535
- Cai Z, Jitkaew S, Zhao J, Chiang H-C, Choksi S, Liu J, Ward Y, Wu L-g, Liu Z-G (2013) Plasma membrane translocation of trimerized MLKL protein is required for TNF-induced necroptosis. *Nature Cell Biology* **16**: 55-65
- Caligiuri M, Molz L, Liu Q, Kaplan F, Xu JP, Majeti JZ, Ramos-Kelsey R, Murthi K, Lievens S, Tavernier J, Kley N (2006) MASPIT: Three-Hybrid Trap for Quantitative Proteome Fingerprinting of Small Molecule-Protein Interactions in Mammalian Cells. *Chemistry & Biology* **13**: 711-722
- Canning P, Ruan Q, Schwerd T, Hrdinka M, Maki Jenny L, Saleh D, Suebsuwong C, Ray S, Brennan Paul E, Cuny Gregory D, Uhlig Holm H, Gyrd-Hansen M, Degterev A, Bullock Alex N (2015) Inflammatory Signaling by NOD-RIPK2 Is Inhibited by Clinically Relevant Type II Kinase Inhibitors. *Chemistry & Biology* **22**: 1174-1184

- Carette JE, Guimaraes CP, Varadarajan M, Park AS, Wuethrich I, Godarova A, Kotecki M, Cochran BH, Spooner E, Ploegh HL, Brummelkamp TR (2009) Haploid Genetic Screens in Human Cells Identify Host Factors Used by Pathogens. *Science* **326**: 1231-1235
- Carette JE, Raaben M, Wong AC, Herbert AS, Obernosterer G, Mulherkar N, Kuehne AI, Kranzusch PJ, Griffin AM, Ruthel G, Cin PD, Dye JM, Whelan SP, Chandran K, Brummelkamp TR (2011) Ebola virus entry requires the cholesterol transporter Niemann–Pick C1. *Nature* **477**: 340-343
- Ch'en IL, Beisner DR, Degterev A, Lynch C, Yuan J, Hoffmann A, Hedrick SM (2008) Antigen-mediated T cell expansion regulated by parallel pathways of death. *Proceedings of the National Academy of Sciences* **105**: 17463-17468
- Ch'en IL, Tsau JS, Molckentin JD, Komatsu M, Hedrick SM (2011) Mechanisms of necroptosis in T cells. *Journal of Experimental Medicine* **208**: 633-641
- Chan FK-M, Luz NF, Moriwaki K (2015) Programmed Necrosis in the Cross Talk of Cell Death and Inflammation. *Annual Review of Immunology* **33**: 79-106
- Chan FK, Chun HJ, Zheng L, Siegel RM, Bui KL, Lenardo MJ (2000) A domain in TNF receptors that mediates ligand-independent receptor assembly and signaling. *Science* **288**: 2351-2354
- Chan FKM, Shisler J, Bixby JG, Felices M, Zheng L, Appel M, Orenstein J, Moss B, Lenardo MJ (2003) A Role for Tumor Necrosis Factor Receptor-2 and Receptor-interacting Protein in Programmed Necrosis and Antiviral Responses. *Journal of Biological Chemistry* **278**: 51613-51621
- Chaudhary PM, Eby M, Jasmin A, Bookwalter A, Murray J, Hood L (1997) Death receptor 5, a new member of the TNFR family, and DR4 induce FADD-dependent apoptosis and activate the NF-kappaB pathway. *Immunity* **7**: 821-830
- Chautan M, Chazal G, Cecconi F, Gruss P, Golstein P (1999) Interdigital cell death can occur through a necrotic and caspase-independent pathway. *Curr Biol* **9**: 967-970
- Chen W, Wu J, Li L, Zhang Z, Ren J, Liang Y, Chen F, Yang C, Zhou Z, Sean Su S, Zheng X, Zhang Z, Zhong C-Q, Wan H, Xiao M, Lin X, Feng X-H, Han J (2015) Ppm1b negatively regulates necroptosis through dephosphorylating Rip3. *Nature Cell Biology* **17**: 434-444
- Chen X, Li W, Ren J, Huang D, He W-t, Song Y, Yang C, Li W, Zheng X, Chen P, Han J (2013) Translocation of mixed lineage kinase domain-like protein to plasma membrane leads to necrotic cell death. *Cell Research* **24**: 105-121
- Cho Y, Challa S, Moquin D, Genga R, Ray TD, Guildford M, Chan FK-M (2009) Phosphorylation-Driven Assembly of the RIP1-RIP3 Complex Regulates Programmed Necrosis and Virus-Induced Inflammation. *Cell* **137**: 1112-1123
- Christofferson DE, Li Y, Hitomi J, Zhou W, Upperman C, Zhu H, Gerber SA, Gygi S, Yuan J (2012) A novel role for RIP1 kinase in mediating TNF α production. *Cell Death and Disease* **3**: e320
- Christofferson DE, Li Y, Yuan J (2014) Control of Life-or-Death Decisions by RIP1 Kinase. *Annual Review of Physiology* **76**: 129-150
- Chu ZL, McKinsey TA, Liu L, Gentry JJ, Malim MH, Ballard DW (1997) Suppression of tumor necrosis factor-induced cell death by inhibitor of apoptosis c-IAP2 is under NF-kappaB control. *Proc Natl Acad Sci U S A* **94**: 10057-10062
- Clarke PG, Clarke S (1996) Nineteenth century research on naturally occurring cell death and related phenomena. *Anat Embryol (Berl)* **193**: 81-99
- Clarke SJ, McStay GP, Halestrap AP (2002) Sanglifehrin A Acts as a Potent Inhibitor of the Mitochondrial Permeability Transition and Reperfusion Injury of the Heart by Binding to Cyclophilin-D at a Different Site from Cyclosporin A. *Journal of Biological Chemistry* **277**: 34793-34799
- Conrad M, Angeli JPF, Vandenabeele P, Stockwell BR (2016) Regulated necrosis: disease relevance and therapeutic opportunities. *Nat Rev Drug Discov* **advance online publication**
- Cook WD, Moujalled DM, Ralph TJ, Lock P, Young SN, Murphy JM, Vaux DL (2014) RIPK1- and RIPK3-induced cell death mode is determined by target availability. *Cell Death and Differentiation* **21**: 1600-1612
- Cortes JE, Kantarjian H, Shah NP, Bixby D, Mauro MJ, Flinn I, O'Hare T, Hu S, Narasimhan NI, Rivera VM, Clackson T, Turner CD, Haluska FG, Druker BJ, Deininger MWN, Talpaz M (2012) Ponatinib in Refractory Philadelphia Chromosome–Positive Leukemias. *New England Journal of Medicine* **367**: 2075-2088

- Cortes JE, Kim DW, Pinilla-Ibarz J, le Coutre P, Paquette R, Chuah C, Nicolini FE, Apperley JF, Khoury HJ, Talpaz M, DiPersio J, DeAngelo DJ, Abruzzese E, Rea D, Baccarani M, Müller MC, Gambacorti-Passerini C, Wong S, Lustgarten S, Rivera VM, Clackson T, Turner CD, Haluska FG, Guilhot F, Deininger MW, Hochhaus A, Hughes T, Goldman JM, Shah NP, Kantarjian H (2013) A Phase 2 Trial of Ponatinib in Philadelphia Chromosome–Positive Leukemias. *New England Journal of Medicine* **369**: 1783-1796
- Czabotar PE, Murphy JM (2015) A tale of two domains - a structural perspective of the pseudokinase, MLKL. *FEBS Journal* **282**: 4268-4278
- Dannappel M, Vlantis K, Kumari S, Polykratis A, Kim C, Wachsmuth L, Eftychi C, Lin J, Corona T, Hermance N, Zelic M, Kirsch P, Basic M, Bleich A, Kelliher M, Pasparakis M (2014) RIPK1 maintains epithelial homeostasis by inhibiting apoptosis and necroptosis. *Nature* **513**: 90-94
- Davis MI, Hunt JP, Herrgard S, Ciceri P, Wodicka LM, Pallares G, Hocker M, Treiber DK, Zarrinkar PP (2011) Comprehensive analysis of kinase inhibitor selectivity. *Nature Biotechnology* **29**: 1046-1051
- de Almagro MC, Vucic D (2015) Necroptosis: Pathway diversity and characteristics. *Seminars in Cell & Developmental Biology* **39**: 56-62
- Degterev A, Hitomi J, Germscheid M, Ch'en IL, Korkina O, Teng X, Abbott D, Cuny GD, Yuan C, Wagner G, Hedrick SM, Gerber SA, Lugovskoy A, Yuan J (2008) Identification of RIP1 kinase as a specific cellular target of necrostatins. *Nature Chemical Biology* **4**: 313-321
- Degterev A, Huang Z, Boyce M, Li Y, Jagtap P, Mizushima N, Cuny GD, Mitchison TJ, Moskowitz MA, Yuan J (2005) Chemical inhibitor of nonapoptotic cell death with therapeutic potential for ischemic brain injury. *Nature Chemical Biology* **1**: 112-119
- Degterev A, Maki JL, Yuan J (2012) Activity and specificity of necrostatin-1, small-molecule inhibitor of RIP1 kinase. *Cell Death and Differentiation* **20**: 366-366
- Degterev A, Zhou W, Maki JL, Yuan J (2014) Assays for Necroptosis and Activity of RIP Kinases. **545**: 1-33
- Deininger M, Buchdunger E, Druker BJ (2005) The development of imatinib as a therapeutic agent for chronic myeloid leukemia. *Blood* **105**: 2640-2653
- Delbridge ARD, Strasser A (2015) The BCL-2 protein family, BH3-mimetics and cancer therapy. *Cell Death and Differentiation* **22**: 1071-1080
- Denton D, Nicolson S, Kumar S (2011) Cell death by autophagy: facts and apparent artefacts. *Cell Death and Differentiation* **19**: 87-95
- Devalaraja-Narashimha K, Diener AM, Padanilam BJ (2009) Cyclophilin D gene ablation protects mice from ischemic renal injury. *Am J Physiol Renal Physiol* **297**: F749-759
- Dillon Christopher P, Weinlich R, Rodriguez Diego A, Cripps James G, Quarato G, Gurung P, Verbist Katherine C, Brewer Taylor L, Llambi F, Gong Y-N, Janke Laura J, Kelliher Michelle A, Kanneganti T-D, Green Douglas R (2014) RIPK1 Blocks Early Postnatal Lethality Mediated by Caspase-8 and RIPK3. *Cell* **157**: 1189-1202
- Dixon Scott J, Lemberg Kathryn M, Lamprecht Michael R, Skouta R, Zaitsev Eleina M, Gleason Caroline E, Patel Darpan N, Bauer Andras J, Cantley Alexandra M, Yang Wan S, Morrison B, Stockwell Brent R (2012) Ferroptosis: An Iron-Dependent Form of Nonapoptotic Cell Death. *Cell* **149**: 1060-1072
- Dixon SJ, Stockwell BR (2014) The role of iron and reactive oxygen species in cell death. *Nat Chem Biol* **10**: 9-17
- Doitsh G, Galloway NLK, Geng X, Yang Z, Monroe KM, Zepeda O, Hunt PW, Hatano H, Sowinski S, Muñoz-Arias I, Greene WC (2013) Cell death by pyroptosis drives CD4 T-cell depletion in HIV-1 infection. *Nature* **505**: 509-514
- Dondelinger Y, Declercq W, Montessuit S, Roelandt R, Goncalves A, Bruggeman I, Hulpiau P, Weber K, Sehon Clark A, Marquis Robert W, Bertin J, Gough Peter J, Savvides S, Martinou J-C, Bertrand Mathieu JM, Vandenabeele P (2014) MLKL Compromises Plasma Membrane Integrity by Binding to Phosphatidylinositol Phosphates. *Cell Reports* **7**: 971-981
- Duprez L, Takahashi N, Van Hauwermeiren F, Vandendriessche B, Goossens V, Vanden Berghe T, Declercq W, Libert C, Cauwels A, Vandenabeele P (2011) RIP Kinase-Dependent Necrosis Drives Lethal Systemic Inflammatory Response Syndrome. *Immunity* **35**: 908-918

- Dynek JN, Goncharov T, Dueber EC, Fedorova AV, Izrael-Tomasevic A, Phu L, Helgason E, Fairbrother WJ, Deshayes K, Kirkpatrick DS, Vucic D (2010) c-IAP1 and Ubch5 promote K11-linked polyubiquitination of RIP1 in TNF signalling. *The EMBO Journal* **29**: 4198-4209
- Eder J, Sedrani R, Wiesmann C (2014) The discovery of first-in-class drugs: origins and evolution. *Nature Reviews Drug Discovery* **13**: 577-587
- Ellis HM, Horvitz HR (1986) Genetic control of programmed cell death in the nematode *C. elegans*. *Cell* **44**: 817-829
- Elrod JW, Molckentin JD (2013) Physiologic Functions of Cyclophilin D and the Mitochondrial Permeability Transition Pore. *Circulation Journal* **77**: 1111-1122
- Fauster A, Rebsamen M, Huber KV, Bigenzahn JW, Stukalov A, Lardeau CH, Scorzoni S, Bruckner M, Gridling M, Parapatics K, Colinge J, Bennett KL, Kubicek S, Krautwald S, Linkermann A, Superti-Furga G (2015) A cellular screen identifies ponatinib and pazopanib as inhibitors of necroptosis. *Cell Death Dis* **6**: e1767
- Feng S, Yang Y, Mei Y, Ma L, Zhu D-e, Hoti N, Castanares M, Wu M (2007) Cleavage of RIP3 inactivates its caspase-independent apoptosis pathway by removal of kinase domain. *Cellular Signalling* **19**: 2056-2067
- Feoktistova M, Geserick P, Kellert B, Dimitrova Diana P, Langlais C, Hupe M, Cain K, MacFarlane M, Häcker G, Leverkus M (2011) cIAPs Block Ripoptosome Formation, a RIP1/Caspase-8 Containing Intracellular Cell Death Complex Differentially Regulated by cFLIP Isoforms. *Molecular Cell* **43**: 449-463
- Feoktistova M, Leverkus M (2015) Programmed necrosis and necroptosis signalling. *FEBS Journal* **282**: 19-31
- Fink SL, Cookson BT (2006) Caspase-1-dependent pore formation during pyroptosis leads to osmotic lysis of infected host macrophages. *Cellular Microbiology* **8**: 1812-1825
- Fischer U, Schulze-Osthoff K (2005) Apoptosis-based therapies and drug targets. *Cell Death and Differentiation* **12**: 942-961
- Friedmann Angeli JP, Schneider M, Proneth B, Tyurina YY, Tyurin VA, Hammond VJ, Herbach N, Aichler M, Walch A, Eggenhofer E, Basavarajappa D, Rådmark O, Kobayashi S, Seibt T, Beck H, Neff F, Esposito I, Wanke R, Förster H, Yefremova O, Heinrichmeyer M, Bornkamm GW, Geissler EK, Thomas SB, Stockwell BR, O'Donnell VB, Kagan VE, Schick JA, Conrad M (2014) Inactivation of the ferroptosis regulator Gpx4 triggers acute renal failure in mice. *Nature Cell Biology* **16**: 1180-1191
- Fuchs Y, Steller H (2011) Programmed Cell Death in Animal Development and Disease. *Cell* **147**: 742-758
- Fulda S (2015) Smac mimetics as IAP antagonists. *Seminars in Cell & Developmental Biology* **39**: 132-138
- Galluzzi L, Bravo-San Pedro JM, Vitale I, Aaronson SA, Abrams JM, Adam D, Alnemri ES, Altucci L, Andrews D, Annicchiarico-Petruzzelli M, Baehrecke EH, Bazan NG, Bertrand MJ, Bianchi K, Blagosklonny MV, Blomgren K, Borner C, Bredesen DE, Brenner C, Campanella M, Candi E, Cecconi F, Chan FK, Chandel NS, Cheng EH, Chipuk JE, Cidlowski JA, Ciechanover A, Dawson TM, Dawson VL, De Laurenzi V, De Maria R, Debatin KM, Di Daniele N, Dixit VM, Dynlacht BD, El-Deiry WS, Fimia GM, Flavell RA, Fulda S, Garrido C, Gougeon ML, Green DR, Gronemeyer H, Hajnoczky G, Hardwick JM, Hengartner MO, Ichijo H, Joseph B, Jost PJ, Kaufmann T, Kepp O, Klionsky DJ, Knight RA, Kumar S, Lemasters JJ, Levine B, Linkermann A, Lipton SA, Lockshin RA, López-Otín C, Lugli E, Madeo F, Malorni W, Marine JC, Martin SJ, Martinou JC, Medema JP, Meier P, Melino S, Mizushima N, Moll U, Muñoz-Pinedo C, Nuñez G, Oberst A, Panaretakis T, Penninger JM, Peter ME, Piacentini M, Pinton P, Prehn JH, Puthalakath H, Rabinovich GA, Ravichandran KS, Rizzuto R, Rodrigues CM, Rubinsztein DC, Rudel T, Shi Y, Simon HU, Stockwell BR, Szabadkai G, Tait SW, Tang HL, Tavernarakis N, Tsujimoto Y, Vanden Berghe T, Vandenabeele P, Villunger A, Wagner EF, Walczak H, White E, Wood WG, Yuan J, Zakeri Z, Zhivotovsky B, Melino G, Kroemer G (2014a) Essential versus accessory aspects of cell death: recommendations of the NCCD 2015. *Cell Death and Differentiation* **22**: 58-73
- Galluzzi L, Kepp O, Krautwald S, Kroemer G, Linkermann A (2014b) Molecular mechanisms of regulated necrosis. *Seminars in Cell & Developmental Biology* **35**: 24-32
- Galluzzi L, Vitale I, Abrams JM, Alnemri ES, Baehrecke EH, Blagosklonny MV, Dawson TM, Dawson VL, El-Deiry WS, Fulda S, Gottlieb E, Green DR, Hengartner MO, Kepp O, Knight RA, Kumar S,

- Lipton SA, Lu X, Madeo F, Malorni W, Mehlen P, Nuñez G, Peter ME, Piacentini M, Rubinsztein DC, Shi Y, Simon HU, Vandenabeele P, White E, Yuan J, Zhivotovsky B, Melino G, Kroemer G (2011) Molecular definitions of cell death subroutines: recommendations of the Nomenclature Committee on Cell Death 2012. *Cell Death and Differentiation* **19**: 107-120
- Garcia-Carbonero R, Carnero A, Paz-Ares L (2013) Inhibition of HSP90 molecular chaperones: moving into the clinic. *The Lancet Oncology* **14**: e358-e369
- Gautheron J, Vucur M, Reisinger F, Cardenas DV, Roderburg C, Koppe C, Kreggenwinkel K, Schneider AT, Bartneck M, Neumann UP, Canbay A, Reeves HL, Luedde M, Tacke F, Trautwein C, Heikenwalder M, Luedde T (2014) A positive feedback loop between RIP3 and JNK controls non-alcoholic steatohepatitis. *EMBO Molecular Medicine* **6**: 1062-1074
- Gavin A-C, Hopf C (2006) Protein co-membership and biochemical affinity purifications. *Drug Discovery Today: Technologies* **3**: 325-330
- Geserick P, Wang J, Schilling R, Horn S, Harris PA, Bertin J, Gough PJ, Feoktistova M, Leverkus M (2015) Absence of RIPK3 predicts necroptosis resistance in malignant melanoma. *Cell Death and Disease* **6**: e1884
- Gibson BA, Kraus WL (2012) New insights into the molecular and cellular functions of poly(ADP-ribose) and PARPs. *Nature Reviews Molecular Cell Biology* **13**: 411-424
- Gingras A-C, Gstaiger M, Raught B, Aebersold R (2007) Analysis of protein complexes using mass spectrometry. *Nature Reviews Molecular Cell Biology* **8**: 645-654
- Graves PR, Haystead TAJ (2002) Molecular Biologist's Guide to Proteomics. *Microbiology and Molecular Biology Reviews* **66**: 39-63
- Grebien F, Vedadi M, Getlik M, Giamb Bruno R, Grover A, Avellino R, Skucha A, Vittori S, Kuznetsova E, Smil D, Barsyte-Lovejoy D, Li F, Poda G, Schapira M, Wu H, Dong A, Senisterra G, Stukalov A, Huber KV, Schonegger A, Marcellus R, Bilban M, Bock C, Brown PJ, Zuber J, Bennett KL, Al-Awar R, Delwel R, Nerlov C, Arrowsmith CH, Superti-Furga G (2015) Pharmacological targeting of the Wdr5-MLL interaction in C/EBPalpha N-terminal leukemia. *Nat Chem Biol* **11**: 571-578
- Green DR (2016) The Cell's Dilemma, or the Story of Cell Death. An Entertainment in Three Acts. *FEBS Journal*: n/a-n/a
- Günther C, Martini E, Wittkopf N, Amann K, Weigmann B, Neumann H, Waldner MJ, Hedrick SM, Tenzer S, Neurath MF, Becker C (2011) Caspase-8 regulates TNF- α -induced epithelial necroptosis and terminal ileitis. *Nature* **477**: 335-339
- Guo H, Omoto S, Harris Philip A, Finger Joshua N, Bertin J, Gough Peter J, Kaiser William J, Mocarski Edward S (2015) Herpes Simplex Virus Suppresses Necroptosis in Human Cells. *Cell Host & Microbe* **17**: 243-251
- Haas TL, Emmerich CH, Gerlach B, Schmukle AC, Cordier SM, Rieser E, Feltham R, Vince J, Warnken U, Wenger T, Koschny R, Komander D, Silke J, Walczak H (2009) Recruitment of the Linear Ubiquitin Chain Assembly Complex Stabilizes the TNF-R1 Signaling Complex and Is Required for TNF-Mediated Gene Induction. *Molecular Cell* **36**: 831-844
- Halestrap AP, Davidson AM (1990) Inhibition of Ca²⁺(+)-induced large-amplitude swelling of liver and heart mitochondria by cyclosporin is probably caused by the inhibitor binding to mitochondrial-matrix peptidyl-prolyl cis-trans isomerase and preventing it interacting with the adenine nucleotide translocase. *Biochem J* **268**: 153-160
- Hanahan D, Weinberg Robert A (2011) Hallmarks of Cancer: The Next Generation. *Cell* **144**: 646-674
- Hantschel O, Rix U, Superti-Furga G (2008) Target spectrum of the BCR-ABL inhibitors imatinib, nilotinib and dasatinib. *Leuk Lymphoma* **49**: 615-619
- Hardy S, Legagneux V, Audic Y, Paillard L (2010) Reverse genetics in eukaryotes. *Biology of the Cell* **102**: 561-580
- Harris PA, Bandyopadhyay D, Berger SB, Campobasso N, Capriotti CA, Cox JA, Dare L, Finger JN, Hoffman SJ, Kahler KM, Lehr R, Lich JD, Nagilla R, Nolte RT, Ouellette MT, Pao CS, Schaeffer MC, Smallwood A, Sun HH, Swift BA, Totoritis RD, Ward P, Marquis RW, Bertin J, Gough PJ (2013) Discovery of Small Molecule RIP1 Kinase Inhibitors for the Treatment of Pathologies Associated with Necroptosis. *ACS Medicinal Chemistry Letters* **4**: 1238-1243
- Harris PA, Bloor A, Cheung M, Kumar R, Crosby RM, Davis-Ward RG, Epperly AH, Hinkle KW, Hunter RN, 3rd, Johnson JH, Knick VB, Laudeman CP, Luttrell DK, Mook RA, Nolte RT, Rudolph SK,

- Szewczyk JR, Truesdale AT, Veal JM, Wang L, Stafford JA (2008) Discovery of 5-[[4-[(2,3-dimethyl-2H-indazol-6-yl)methylamino]-2-pyrimidinyl]amino]-2-methyl-benzenesulfonamide (Pazopanib), a novel and potent vascular endothelial growth factor receptor inhibitor. *J Med Chem* **51**: 4632-4640
- Hay M, Thomas DW, Craighead JL, Economides C, Rosenthal J (2014) Clinical development success rates for investigational drugs. *Nat Biotechnol* **32**: 40-51
- He S, Liang Y, Shao F, Wang X (2011) Toll-like receptors activate programmed necrosis in macrophages through a receptor-interacting kinase-3-mediated pathway. *Proc Natl Acad Sci U S A* **108**: 20054-20059
- He S, Wang L, Miao L, Wang T, Du F, Zhao L, Wang X (2009) Receptor Interacting Protein Kinase-3 Determines Cellular Necrotic Response to TNF- α . *Cell* **137**: 1100-1111
- Henry T, Monack DM (2007) Activation of the inflammasome upon *Francisella tularensis* infection: interplay of innate immune pathways and virulence factors. *Cellular Microbiology* **9**: 2543-2551
- Hildebrand JM, Tanzer MC, Lucet IS, Young SN, Spall SK, Sharma P, Pierotti C, Garnier J-M, Dobson RCJ, Webb AI, Tripaydonis A, Babon JJ, Mulcair MD, Scanlon MJ, Alexander WS, Wilks AF, Czabotar PE, Lessene G, Murphy JM, Silke J (2014) Activation of the pseudokinase MLKL unleashes the four-helix bundle domain to induce membrane localization and necroptotic cell death. *Proceedings of the National Academy of Sciences* **111**: 15072-15077
- Hitomi J, Christofferson DE, Ng A, Yao J, Degterev A, Xavier RJ, Yuan J (2008) Identification of a Molecular Signaling Network that Regulates a Cellular Necrotic Cell Death Pathway. *Cell* **135**: 1311-1323
- Holler N, Zaru R, Micheau O, Thome M, Attinger A, Valitutti S, Bodmer JL, Schneider P, Seed B, Tschopp J (2000) Fas triggers an alternative, caspase-8-independent cell death pathway using the kinase RIP as effector molecule. *Nat Immunol* **1**: 489-495
- Hopf C, Bantscheff M, Drewes G (2007) Pathway Proteomics and Chemical Proteomics Team Up in Drug Discovery. *Neurodegenerative Diseases* **4**: 270-280
- Hsu H, Huang J, Shu HB, Baichwal V, Goeddel DV (1996a) TNF-dependent recruitment of the protein kinase RIP to the TNF receptor-1 signaling complex. *Immunity* **4**: 387-396
- Hsu H, Shu HB, Pan MG, Goeddel DV (1996b) TRADD-TRAF2 and TRADD-FADD interactions define two distinct TNF receptor 1 signal transduction pathways. *Cell* **84**: 299-308
- Hsu H, Xiong J, Goeddel DV (1995) The TNF receptor 1-associated protein TRADD signals cell death and NF-kappa B activation. *Cell* **81**: 495-504
- Huang W-S, Metcalf CA, Sundaramoorthi R, Wang Y, Zou D, Thomas RM, Zhu X, Cai L, Wen D, Liu S, Romero J, Qi J, Chen I, Banda G, Lentini SP, Das S, Xu Q, Keats J, Wang F, Wardwell S, Ning Y, Snodgrass JT, Broudy MI, Russian K, Zhou T, Commodore L, Narasimhan NI, Mohemmad QK, Iulucci J, Rivera VM, Dalgarno DC, Sawyer TK, Clackson T, Shakespeare WC (2010) Discovery of 3-[2-(Imidazo[1,2-b]pyridazin-3-yl)ethynyl]-4-methyl-N-{4-[(4-methylpiperazin-1-yl)methyl]-3-(trifluoromethyl)phenyl}benzamide (AP24534), a Potent, Orally Active Pan-Inhibitor of Breakpoint Cluster Region-Abelson (BCR-ABL) Kinase Including the T315I Gatekeeper Mutant. *Journal of Medicinal Chemistry* **53**: 4701-4719
- Huang Z, Wu S-Q, Liang Y, Zhou X, Chen W, Li L, Wu J, Zhuang Q, Chen Ca, Li J, Zhong C-Q, Xia W, Zhou R, Zheng C, Han J (2015) RIP1/RIP3 Binding to HSV-1 ICP6 Initiates Necroptosis to Restrict Virus Propagation in Mice. *Cell Host & Microbe* **17**: 229-242
- Huber KVM, Olek KM, Müller AC, Tan CSH, Bennett KL, Colinge J, Superti-Furga G (2015) Proteome-wide drug and metabolite interaction mapping by thermal-stability profiling. *Nature Methods* **12**: 1055-1057
- Humphries F, Yang S, Wang B, Moynagh PN (2014) RIP kinases: key decision makers in cell death and innate immunity. *Cell Death and Differentiation* **22**: 225-236
- Inglese J, Auld DS, Jadhav A, Johnson RL, Simeonov A, Yasgar A, Zheng W, Austin CP (2006) Quantitative high-throughput screening: A titration-based approach that efficiently identifies biological activities in large chemical libraries. *Proceedings of the National Academy of Sciences* **103**: 11473-11478
- Jacobsen AV, Lowes KN, Tanzer MC, Lucet IS, Hildebrand JM, Petrie EJ, van Delft MF, Liu Z, Conos SA, Zhang JG, Huang DCS, Silke J, Lessene G, Murphy JM (2016) HSP90 activity is required for

- MLKL oligomerisation and membrane translocation and the induction of necroptotic cell death. *Cell Death and Disease* **7**: e2051
- Jacobson MD, Weil M, Raff MC (1997) Programmed cell death in animal development. *Cell* **88**: 347-354
- Jain P, Kantarjian H, Jabbour E, Gonzalez GN, Borthakur G, Pemmaraju N, Daver N, Gachimova E, Ferrajoli A, Kornblau S, Ravandi F, O'Brien S, Cortes J (2015) Ponatinib as first-line treatment for patients with chronic myeloid leukaemia in chronic phase: a phase 2 study. *Lancet Haematol* **2**: e376-e383
- Javadov S, Kuznetsov A (2013) Mitochondrial permeability transition and cell death: the role of cyclophilin d. *Front Physiol* **4**: 76
- Juo P, Woo MS, Kuo CJ, Signorelli P, Biemann HP, Hannun YA, Blenis J (1999) FADD is required for multiple signaling events downstream of the receptor Fas. *Cell Growth Differ* **10**: 797-804
- Kaczmarek A, Vandenabeele P, Krysko Dmitri V (2013) Necroptosis: The Release of Damage-Associated Molecular Patterns and Its Physiological Relevance. *Immunity* **38**: 209-223
- Kaiser WJ, Daley-Bauer LP, Thapa RJ, Mandal P, Berger SB, Huang C, Sundararajan A, Guo H, Roback L, Speck SH, Bertin J, Gough PJ, Balachandran S, Mocarski ES (2014) RIP1 suppresses innate immune necrotic as well as apoptotic cell death during mammalian parturition. *Proceedings of the National Academy of Sciences* **111**: 7753-7758
- Kaiser WJ, Offermann MK (2005) Apoptosis Induced by the Toll-Like Receptor Adaptor TRIF Is Dependent on Its Receptor Interacting Protein Homotypic Interaction Motif. *The Journal of Immunology* **174**: 4942-4952
- Kaiser WJ, Sridharan H, Huang C, Mandal P, Upton JW, Gough PJ, Schon CA, Marquis RW, Bertin J, Mocarski ES (2013) Toll-like Receptor 3-mediated Necrosis via TRIF, RIP3, and MLKL. *Journal of Biological Chemistry* **288**: 31268-31279
- Kaiser WJ, Upton JW, Long AB, Livingston-Rosanoff D, Daley-Bauer LP, Hakem R, Caspary T, Mocarski ES (2011) RIP3 mediates the embryonic lethality of caspase-8-deficient mice. *Nature* **471**: 368-372
- Kaiser WJ, Upton JW, Mocarski ES (2008) Receptor-interacting protein homotypic interaction motif-dependent control of NF-kappa B activation via the DNA-dependent activator of IFN regulatory factors. *J Immunol* **181**: 6427-6434
- Kang T-B, Yang S-H, Toth B, Kovalenko A, Wallach D (2013) Caspase-8 Blocks Kinase RIPK3-Mediated Activation of the NLRP3 Inflammasome. *Immunity* **38**: 27-40
- Kataoka K, Matsumoto H, Kaneko H, Notomi S, Takeuchi K, Sweigard JH, Atik A, Murakami Y, Connor KM, Terasaki H, Miller JW, Vavvas DG (2015) Macrophage- and RIP3-dependent inflammasome activation exacerbates retinal detachment-induced photoreceptor cell death. *Cell Death and Disease* **6**: e1731
- Kawahara A, Ohsawa Y, Matsumura H, Uchiyama Y, Nagata S (1998) Caspase-independent cell killing by Fas-associated protein with death domain. *J Cell Biol* **143**: 1353-1360
- Kayagaki N, Stowe IB, Lee BL, O'Rourke K, Anderson K, Warming S, Cuellar T, Haley B, Roose-Girma M, Phung QT, Liu PS, Lill JR, Li H, Wu J, Kummerfeld S, Zhang J, Lee WP, Snipas SJ, Salvesen GS, Morris LX, Fitzgerald L, Zhang Y, Bertram EM, Goodnow CC, Dixit VM (2015) Caspase-11 cleaves gasdermin D for non-canonical inflammasome signalling. *Nature* **526**: 666-671
- Kelliher MA, Grimm S, Ishida Y, Kuo F, Stanger BZ, Leder P (1998) The death domain kinase RIP mediates the TNF-induced NF-kappaB signal. *Immunity* **8**: 297-303
- Kerr JF, Wyllie AH, Currie AR (1972) Apoptosis: a basic biological phenomenon with wide-ranging implications in tissue kinetics. *Br J Cancer* **26**: 239-257
- Khan N, Lawlor KE, Murphy JM, Vince JE (2014) More to life than death: molecular determinants of necroptotic and non-necroptotic RIP3 kinase signaling. *Current Opinion in Immunology* **26**: 76-89
- Kitur K, Parker D, Nieto P, Ahn DS, Cohen TS, Chung S, Wachtel S, Bueno S, Prince A (2015) Toxin-induced necroptosis is a major mechanism of Staphylococcus aureus lung damage. *PLoS Pathog* **11**: e1004820
- Köcher T, Superti-Furga G (2007) Mass spectrometry-based functional proteomics: from molecular machines to protein networks. *Nature Methods* **4**: 807-815

- Krepler C, Chunduru SK, Halloran MB, He X, Xiao M, Vultur A, Villanueva J, Mitsuuchi Y, Neiman EM, Benetatos C, Nathanson KL, Amaravadi RK, Pehamberger H, McKinlay M, Herlyn M (2013) The Novel SMAC Mimetic Birinapant Exhibits Potent Activity against Human Melanoma Cells. *Clinical Cancer Research* **19**: 1784-1794
- Kreuz S, Siegmund D, Scheurich P, Wajant H (2001) NF- κ B Inducers Upregulate cFLIP, a Cycloheximide-Sensitive Inhibitor of Death Receptor Signaling. *Molecular and Cellular Biology* **21**: 3964-3973
- Kriegler M, Perez C, DeFay K, Albert I, Lu SD (1988) A novel form of TNF/cachectin is a cell surface cytotoxic transmembrane protein: ramifications for the complex physiology of TNF. *Cell* **53**: 45-53
- Kroemer G, Galluzzi L, Vandenabeele P, Abrams J, Alnemri ES, Baehrecke EH, Blagosklonny MV, El-Deiry WS, Golstein P, Green DR, Hengartner M, Knight RA, Kumar S, Lipton SA, Malorni W, Nuñez G, Peter ME, Tschopp J, Yuan J, Piacentini M, Zhivotovsky B, Melino G (2008) Classification of cell death: recommendations of the Nomenclature Committee on Cell Death 2009. *Cell Death and Differentiation* **16**: 3-11
- Kroemer G, Levine B (2008) Autophagic cell death: the story of a misnomer. *Nature Reviews Molecular Cell Biology* **9**: 1004-1010
- Krysko DV, Vanden Berghe T, D'Herde K, Vandenabeele P (2008) Apoptosis and necrosis: Detection, discrimination and phagocytosis. *Methods* **44**: 205-221
- Lamothe B, Lai Y, Xie M, Schneider MD, Darnay BG (2012) TAK1 Is Essential for Osteoclast Differentiation and Is an Important Modulator of Cell Death by Apoptosis and Necroptosis. *Molecular and Cellular Biology* **33**: 582-595
- Laster SM, Wood JG, Gooding LR (1988) Tumor necrosis factor can induce both apoptic and necrotic forms of cell lysis. *J Immunol* **141**: 2629-2634
- Lau A, Wang S, Jiang J, Haig A, Pavlosky A, Linkermann A, Zhang ZX, Jevnikar AM (2013) RIPK3-Mediated Necroptosis Promotes Donor Kidney Inflammatory Injury and Reduces Allograft Survival. *American Journal of Transplantation* **13**: 2805-2818
- Lawrence CP, Chow SC (2005) FADD deficiency sensitises Jurkat T cells to TNF- α -dependent necrosis during activation-induced cell death. *FEBS Letters* **579**: 6465-6472
- Lee J, Bogoy M (2013) Target deconvolution techniques in modern phenotypic profiling. *Current Opinion in Chemical Biology* **17**: 118-126
- Lee Y, Karuppagounder SS, Shin J-H, Lee Y-I, Ko HS, Swing D, Jiang H, Kang S-U, Lee BD, Kang HC, Kim D, Tessarollo L, Dawson VL, Dawson TM (2013) Parthanatos mediates AIMP2-activated age-dependent dopaminergic neuronal loss. *Nature Neuroscience* **16**: 1392-1400
- Lewis J, Devin A, Miller A, Lin Y, Rodriguez Y, Neckers L, Liu ZG (2000) Disruption of hsp90 function results in degradation of the death domain kinase, receptor-interacting protein (RIP), and blockage of tumor necrosis factor-induced nuclear factor-kappaB activation. *J Biol Chem* **275**: 10519-10526
- Li D, Xu T, Cao Y, Wang H, Li L, Chen S, Wang X, Shen Z (2015) A cytosolic heat shock protein 90 and cochaperone CDC37 complex is required for RIP3 activation during necroptosis. *Proceedings of the National Academy of Sciences* **112**: 5017-5022
- Li J, McQuade T, Siemer Ansgar B, Napetschnig J, Moriwaki K, Hsiao Y-S, Damko E, Moquin D, Walz T, McDermott A, Chan Francis K-M, Wu H (2012) The RIP1/RIP3 Necrosome Forms a Functional Amyloid Signaling Complex Required for Programmed Necrosis. *Cell* **150**: 339-350
- Li JX, Feng JM, Wang Y, Li XH, Chen XX, Su Y, Shen YY, Chen Y, Xiong B, Yang CH, Ding J, Miao ZH (2014) The B-RafV600E inhibitor dabrafenib selectively inhibits RIP3 and alleviates acetaminophen-induced liver injury. *Cell Death and Disease* **5**: e1278
- Li Y (2011) The tandem affinity purification technology: an overview. *Biotechnology Letters* **33**: 1487-1499
- Licitra EJ, Liu JO (1996) A three-hybrid system for detecting small ligand-protein receptor interactions. *Proc Natl Acad Sci U S A* **93**: 12817-12821
- Lin J, Li H, Yang M, Ren J, Huang Z, Han F, Huang J, Ma J, Zhang D, Zhang Z, Wu J, Huang D, Qiao M, Jin G, Wu Q, Huang Y, Du J, Han J (2013) A Role of RIP3-Mediated Macrophage Necrosis in Atherosclerosis Development. *Cell Reports* **3**: 200-210

- Lin Y, Devin A, Rodriguez Y, Liu ZG (1999) Cleavage of the death domain kinase RIP by caspase-8 prompts TNF-induced apoptosis. *Genes Dev* **13**: 2514-2526
- Lindsay MA (2003) Target discovery. *Nat Rev Drug Discov* **2**: 831-838
- Linkermann A, Brasen JH, Darding M, Jin MK, Sanz AB, Heller JO, De Zen F, Weinlich R, Ortiz A, Walczak H, Weinberg JM, Green DR, Kunzendorf U, Krautwald S (2013a) Two independent pathways of regulated necrosis mediate ischemia-reperfusion injury. *Proceedings of the National Academy of Sciences* **110**: 12024-12029
- Linkermann A, Brasen JH, De Zen F, Weinlich R, Schwendener RA, Green DR, Kunzendorf U, Krautwald S (2012) Dichotomy between RIP1- and RIP3-mediated necroptosis in tumor necrosis factor- α -induced shock. *Mol Med* **18**: 577-586
- Linkermann A, Chen G, Dong G, Kunzendorf U, Krautwald S, Dong Z (2014a) Regulated Cell Death in AKI. *Journal of the American Society of Nephrology* **25**: 2689-2701
- Linkermann A, Green DR (2014) Necroptosis. *New England Journal of Medicine* **370**: 455-465
- Linkermann A, Hackl MJ, Kunzendorf U, Walczak H, Krautwald S, Jevnikar AM (2013b) Necroptosis in Immunity and Ischemia-Reperfusion Injury. *American Journal of Transplantation* **13**: 2797-2804
- Linkermann A, Skouta R, Himmerkus N, Mulay SR, Dewitz C, De Zen F, Prokai A, Zuchtriegel G, Krombach F, Welz P-S, Weinlich R, Vanden Berghe T, Vandenabeele P, Pasparakis M, Bleich M, Weinberg JM, Reichel CA, Bräsen JH, Kunzendorf U, Anders H-J, Stockwell BR, Green DR, Krautwald S (2014b) Synchronized renal tubular cell death involves ferroptosis. *Proceedings of the National Academy of Sciences* **111**: 16836-16841
- Linkermann A, Stockwell BR, Krautwald S, Anders H-J (2014c) Regulated cell death and inflammation: an auto-amplification loop causes organ failure. *Nature Reviews Immunology* **14**: 759-767
- Lockshin RA (2015) Programmed cell death 50 (and beyond). *Cell Death and Differentiation* **23**: 10-17
- Lockshin RA, Williams CM (1964) Programmed cell death—II. Endocrine potentiation of the breakdown of the intersegmental muscles of silkworms. *Journal of Insect Physiology* **10**: 643-649
- Lockshin RA, Zakeri Z (2001) Programmed cell death and apoptosis: origins of the theory. *Nat Rev Mol Cell Biol* **2**: 545-550
- Long JS, Ryan KM (2012) New frontiers in promoting tumour cell death: targeting apoptosis, necroptosis and autophagy. *Oncogene* **31**: 5045-5060
- Lowe SW, Schmitt EM, Smith SW, Osborne BA, Jacks T (1993) p53 is required for radiation-induced apoptosis in mouse thymocytes. *Nature* **362**: 847-849
- Lu JV, Chen HC, Walsh CM (2014) Necroptotic signaling in adaptive and innate immunity. *Seminars in Cell & Developmental Biology* **35**: 33-39
- Lu JV, Weist BM, van Raam BJ, Marro BS, Nguyen LV, Srinivas P, Bell BD, Luhrs KA, Lane TE, Salvesen GS, Walsh CM (2011) Complementary roles of Fas-associated death domain (FADD) and receptor interacting protein kinase-3 (RIPK3) in T-cell homeostasis and antiviral immunity. *Proc Natl Acad Sci U S A* **108**: 15312-15317
- MacBeath G, Schreiber SL (2000) Printing proteins as microarrays for high-throughput function determination. *Science* **289**: 1760-1763
- Majno G, Joris I (1995) Apoptosis, oncosis, and necrosis. An overview of cell death. *Am J Pathol* **146**: 3-15
- Mandal P, Berger Scott B, Pillay S, Moriwaki K, Huang C, Guo H, Lich John D, Finger J, Kasparcova V, Votta B, Ouellette M, King Bryan W, Wisnoski D, Lakdawala Ami S, DeMartino Michael P, Casillas Linda N, Haile Pamela A, Sehon Clark A, Marquis Robert W, Upton J, Daley-Bauer Lisa P, Roback L, Ramia N, Dovey Cole M, Carette Jan E, Chan Francis K-M, Bertin J, Gough Peter J, Mocarski Edward S, Kaiser William J (2014) RIP3 Induces Apoptosis Independent of Pronecrotic Kinase Activity. *Molecular Cell* **56**: 481-495
- Manning G, Whyte DB, Martinez R, Hunter T, Sudarsanam S (2002) The protein kinase complement of the human genome. *Science* **298**: 1912-1934
- Manolio TA (2010) Genomewide association studies and assessment of the risk of disease. *N Engl J Med* **363**: 166-176

- McCormack PL (2014) Pazopanib: A Review of Its Use in the Management of Advanced Renal Cell Carcinoma. *Drugs* **74**: 1111-1125
- McGettigan S (2014) Dabrafenib: A New Therapy for Use in BRAF-Mutated Metastatic Melanoma. *J Adv Pract Oncol* **5**: 211-215
- McNamara CR, Ahuja R, Osafo-Addo AD, Barrows D, Kettenbach A, Skidan I, Teng X, Cuny GD, Gerber S, Degterev A (2013) Akt Regulates TNF α synthesis downstream of RIP1 kinase activation during necroptosis. *PLoS ONE* **8**: e56576
- McPherson M, Yang Y, Hammond PW, Kreider BL (2002) Drug receptor identification from multiple tissues using cellular-derived mRNA display libraries. *Chem Biol* **9**: 691-698
- McQuade T, Cho Y, Chan Francis K-M (2013) Positive and negative phosphorylation regulates RIP1- and RIP3-induced programmed necrosis. *Biochemical Journal* **456**: 409-415
- Micheau O, Tschopp J (2003) Induction of TNF Receptor I-Mediated Apoptosis via Two Sequential Signaling Complexes. *Cell* **114**: 181-190
- Mihaly SR, Ninomiya-Tsuji J, Morioka S (2014) TAK1 control of cell death. *Cell Death and Differentiation* **21**: 1667-1676
- Mocarski ES, Guo H, Kaiser WJ (2015) Necroptosis: The Trojan horse in cell autonomous antiviral host defense. *Virology* **479-480**: 160-166
- Mocarski ES, Upton JW, Kaiser WJ (2012) Viral infection and the evolution of caspase 8-regulated apoptotic and necrotic death pathways. *Nat Rev Immunol* **12**: 79-88
- Moffat JG, Rudolph J, Bailey D (2014) Phenotypic screening in cancer drug discovery — past, present and future. *Nature Reviews Drug Discovery* **13**: 588-602
- Molina DM, Jafari R, Ignatushchenko M, Seki T, Larsson EA, Dan C, Sreekumar L, Cao Y, Nordlund P (2013) Monitoring Drug Target Engagement in Cells and Tissues Using the Cellular Thermal Shift Assay. *Science* **341**: 84-87
- Moquin DM, McQuade T, Chan FK (2013) CYLD deubiquitinates RIP1 in the TNF α -induced necrosome to facilitate kinase activation and programmed necrosis. *PLoS ONE* **8**: e76841
- Morgan MJ, Kim Y-S (2015) The serine threonine kinase RIP3: lost and found. *BMB Reports* **48**: 303-312
- Morioka S, Broglie P, Omori E, Ikeda Y, Takaesu G, Matsumoto K, Ninomiya-Tsuji J (2014) TAK1 kinase switches cell fate from apoptosis to necrosis following TNF stimulation. *The Journal of Cell Biology* **204**: 607-623
- Moriwaki K, Chan FKM (2013) RIP3: a molecular switch for necrosis and inflammation. *Genes & Development* **27**: 1640-1649
- Motzer RJ, Hutson TE, Cella D, Reeves J, Hawkins R, Guo J, Nathan P, Staehler M, de Souza P, Merchan JR, Boleti E, Fife K, Jin J, Jones R, Uemura H, De Giorgi U, Harmenberg U, Wang J, Sternberg CN, Deen K, McCann L, Hackshaw MD, Crescenzo R, Pandite LN, Choueiri TK (2013) Pazopanib versus Sunitinib in Metastatic Renal-Cell Carcinoma. *New England Journal of Medicine* **369**: 722-731
- Mou J, Park A, Cai Y, Yuan J, Yuan C (2015) Structure–activity relationship study of E6 as a novel necroptosis inducer. *Bioorganic & Medicinal Chemistry Letters* **25**: 3057-3061
- Munos B (2009) Lessons from 60 years of pharmaceutical innovation. *Nature Reviews Drug Discovery* **8**: 959-968
- Murakami Y, Matsumoto H, Roh M, Giani A, Kataoka K, Morizane Y, Kayama M, Thanos A, Nakatake S, Notomi S, Hisatomi T, Ikeda Y, Ishibashi T, Connor KM, Miller JW, Vavvas DG (2013) Programmed necrosis, not apoptosis, is a key mediator of cell loss and DAMP-mediated inflammation in dsRNA-induced retinal degeneration. *Cell Death and Differentiation* **21**: 270-277
- Murakami Y, Matsumoto H, Roh M, Suzuki J, Hisatomi T, Ikeda Y, Miller JW, Vavvas DG (2012) Receptor interacting protein kinase mediates necrotic cone but not rod cell death in a mouse model of inherited degeneration. *Proc Natl Acad Sci U S A* **109**: 14598-14603
- Murphy James M, Czabotar Peter E, Hildebrand Joanne M, Lucet Isabelle S, Zhang J-G, Alvarez-Diaz S, Lewis R, Lalaoui N, Metcalf D, Webb Andrew I, Young Samuel N, Varghese Leila N, Tannahill Gillian M, Hatchell Esme C, Majewski Ian J, Okamoto T, Dobson Renwick CJ, Hilton Douglas J, Babon

- Jeffrey J, Nicola Nicos A, Strasser A, Silke J, Alexander Warren S (2013) The Pseudokinase MLKL Mediates Necroptosis via a Molecular Switch Mechanism. *Immunity* **39**: 443-453
- Murphy James M, Lucet Isabelle S, Hildebrand Joanne M, Tanzer Maria C, Young Samuel N, Sharma P, Lessene G, Alexander Warren S, Babon Jeffrey J, Silke J, Czabotar Peter E (2014) Insights into the evolution of divergent nucleotide-binding mechanisms among pseudokinases revealed by crystal structures of human and mouse MLKL. *Biochemical Journal* **457**: 369-377
- Murphy JM, Silke J (2014) Ars Moriendi; the art of dying well - new insights into the molecular pathways of necroptotic cell death. *EMBO reports* **15**: 155-164
- Najjar M, Suebsuwong C, Ray Soumya S, Thapa Roshan J, Maki Jenny L, Nogusa S, Shah S, Saleh D, Gough Peter J, Bertin J, Yuan J, Balachandran S, Cuny Gregory D, Degterev A (2015) Structure Guided Design of Potent and Selective Ponatinib-Based Hybrid Inhibitors for RIPK1. *Cell Reports* **10**: 1850-1860
- Nakagawa T, Shimizu S, Watanabe T, Yamaguchi O, Otsu K, Yamagata H, Inohara H, Kubo T, Tsujimoto Y (2005) Cyclophilin D-dependent mitochondrial permeability transition regulates some necrotic but not apoptotic cell death. *Nature* **434**: 652-658
- Narasimhan NI, Dorer DJ, Niland K, Haluska F, Sonnichsen D (2013) Effects of food on the pharmacokinetics of ponatinib in healthy subjects. *Journal of Clinical Pharmacy and Therapeutics* **38**: 440-444
- Nembrini C, Kisielow J, Shamshiev AT, Tortola L, Coyle AJ, Kopf M, Marsland BJ (2009) The Kinase Activity of Rip2 Determines Its Stability and Consequently Nod1- and Nod2-mediated Immune Responses. *Journal of Biological Chemistry* **284**: 19183-19188
- Newton K (2015) RIPK1 and RIPK3: critical regulators of inflammation and cell death. *Trends in Cell Biology* **25**: 347-353
- Newton K, Dugger DL, Wickliffe KE, Kapoor N, de Almagro MC, Vucic D, Komuves L, Ferrando RE, French DM, Webster J, Roose-Girma M, Warming S, Dixit VM (2014) Activity of protein kinase RIPK3 determines whether cells die by necroptosis or apoptosis. *Science* **343**: 1357-1360
- Newton K, Sun X, Dixit VM (2004) Kinase RIP3 Is Dispensable for Normal NF- κ Bs, Signaling by the B-Cell and T-Cell Receptors, Tumor Necrosis Factor Receptor 1, and Toll-Like Receptors 2 and 4. *Molecular and Cellular Biology* **24**: 1464-1469
- Northington FJ, Chavez-Valdez R, Graham EM, Razdan S, Gauda EB, Martin LJ (2010) Necrostatin decreases oxidative damage, inflammation, and injury after neonatal HI. *Journal of Cerebral Blood Flow & Metabolism* **31**: 178-189
- O'Hare T, Shakespeare WC, Zhu X, Eide CA, Rivera VM, Wang F, Adrian LT, Zhou T, Huang W-S, Xu Q, Metcalf CA, Tyner JW, Loriaux MM, Corbin AS, Wardwell S, Ning Y, Keats JA, Wang Y, Sundaramoorthi R, Thomas M, Zhou D, Snodgrass J, Commodore L, Sawyer TK, Dalgarno DC, Deininger MWN, Druker BJ, Clackson T (2009) AP24534, a Pan-BCR-ABL Inhibitor for Chronic Myeloid Leukemia, Potently Inhibits the T315I Mutant and Overcomes Mutation-Based Resistance. *Cancer Cell* **16**: 401-412
- O'Donnell MA, Perez-Jimenez E, Oberst A, Ng A, Massoumi R, Xavier R, Green DR, Ting AT (2011) Caspase 8 inhibits programmed necrosis by processing CYLD. *Nature Cell Biology* **13**: 1437-1442
- O'Donnell MA, Ting AT (2012) NF κ B and ubiquitination: partners in disarming RIPK1-mediated cell death. *Immunologic Research* **54**: 214-226
- Oberst A (2015) Death in the fast lane: what's next for necroptosis? *FEBS Journal*: n/a-n/a
- Oberst A, Dillon CP, Weinlich R, McCormick LL, Fitzgerald P, Pop C, Hakem R, Salvesen GS, Green DR (2011) Catalytic activity of the caspase-8-FLIPL complex inhibits RIPK3-dependent necrosis. *Nature* **471**: 363-367
- Oerlemans MI, Liu J, Arslan F, den Ouden K, van Middelaar BJ, Doevendans PA, Sluijter JP (2012) Inhibition of RIP1-dependent necrosis prevents adverse cardiac remodeling after myocardial ischemia-reperfusion in vivo. *Basic Res Cardiol* **107**: 270
- Ofengeim D, Ito Y, Najafov A, Zhang Y, Shan B, DeWitt Judy P, Ye J, Zhang X, Chang A, Vakifahmetoglu-Norberg H, Geng J, Py B, Zhou W, Amin P, Lima Jonilson B, Qi C, Yu Q, Trapp B, Yuan J (2015) Activation of Necroptosis in Multiple Sclerosis. *Cell Reports* **10**: 1836-1849
- Ofengeim D, Yuan J (2013) Regulation of RIP1 kinase signalling at the crossroads of inflammation and cell death. *Nature Reviews Molecular Cell Biology* **14**: 727-736

- Onizawa M, Oshima S, Schulze-Topphoff U, Oses-Prieto JA, Lu T, Tavares R, Prodhomme T, Duong B, Whang MI, Advincula R, Agelidis A, Barrera J, Wu H, Burlingame A, Malynn BA, Zamvil SS, Ma A (2015) The ubiquitin-modifying enzyme A20 restricts ubiquitination of the kinase RIPK3 and protects cells from necroptosis. *Nature Immunology* **16**: 618-627
- Orozco S, Yatim N, Werner MR, Tran H, Gunja SY, Tait SW, Albert ML, Green DR, Oberst A (2014) RIPK1 both positively and negatively regulates RIPK3 oligomerization and necroptosis. *Cell Death and Differentiation* **21**: 1511-1521
- Palacios R, Steinmetz M (1985) II-3-dependent mouse clones that express B-220 surface antigen, contain Ig genes in germ-line configuration, and generate B lymphocytes in vivo. *Cell* **41**: 727-734
- Pan T, Wu S, He X, Luo H, Zhang Y, Fan M, Geng G, Ruiz VC, Zhang J, Mills L, Bai C, Zhang H (2014) Necroptosis takes place in human immunodeficiency virus type-1 (HIV-1)-infected CD4+ T lymphocytes. *PLoS ONE* **9**: e93944
- Park JH, Kim YG, McDonald C, Kanneganti TD, Hasegawa M, Body-Malapel M, Inohara N, Nunez G (2007) RICK/RIP2 Mediates Innate Immune Responses Induced through Nod1 and Nod2 but Not TLRs. *The Journal of Immunology* **178**: 2380-2386
- Pasparakis M, Vandenabeele P (2015) Necroptosis and its role in inflammation. *Nature* **517**: 311-320
- Pavlosky A, Lau A, Su Y, Lian D, Huang X, Yin Z, Haig A, Jevnikar AM, Zhang ZX (2014) RIPK3-Mediated Necroptosis Regulates Cardiac Allograft Rejection. *American Journal of Transplantation* **14**: 1778-1790
- Pazdernik NJ, Donner DB, Goebel MG, Harrington MA (1999) Mouse receptor interacting protein 3 does not contain a caspase-recruiting or a death domain but induces apoptosis and activates NF-kappaB. *Mol Cell Biol* **19**: 6500-6508
- Petrone PM, Wassermann AM, Lounkine E, Kutchukian P, Simms B, Jenkins J, Selzer P, Glick M (2013) Biodiversity of small molecules – a new perspective in screening set selection. *Drug Discovery Today* **18**: 674-680
- Polykratis A, Hermance N, Zelic M, Roderick J, Kim C, Van TM, Lee TH, Chan FKM, Pasparakis M, Kelliher MA (2014) Cutting Edge: RIPK1 Kinase Inactive Mice Are Viable and Protected from TNF-Induced Necroptosis In Vivo. *The Journal of Immunology* **193**: 1539-1543
- Pop C, Oberst A, Drag M, Van Raam Bram J, Riedl Stefan J, Green Douglas R, Salvesen Guy S (2011) FLIPL induces caspase 8 activity in the absence of interdomain caspase 8 cleavage and alters substrate specificity. *Biochemical Journal* **433**: 447-457
- Ratjen F, Döring G (2003) Cystic fibrosis. *The Lancet* **361**: 681-689
- Rebsamen M, Heinz LX, Meylan E, Michallet M-C, Schroder K, Hofmann K, Vazquez J, Benedict CA, Tschopp J (2009) DAI/ZBP1 recruits RIP1 and RIP3 through RIP homotypic interaction motifs to activate NF-kB. *EMBO reports* **10**: 916-922
- Remijnsen Q, Berghe TV, Wirawan E, Asselbergh B, Parthoens E, De Rycke R, Noppen S, Delforge M, Willems J, Vandenabeele P (2010) Neutrophil extracellular trap cell death requires both autophagy and superoxide generation. *Cell Research* **21**: 290-304
- Remijnsen Q, Goossens V, Grootjans S, Van den Haute C, Vanlangenakker N, Dondelinger Y, Roelandt R, Bruggeman I, Goncalves A, Bertrand MJM, Baekelandt V, Takahashi N, Berghe TV, Vandenabeele P (2014) Depletion of RIPK3 or MLKL blocks TNF-driven necroptosis and switches towards a delayed RIPK1 kinase-dependent apoptosis. *Cell Death and Disease* **5**: e1004
- Remijnsen Q, Kuijpers TW, Wirawan E, Lippens S, Vandenabeele P, Vanden Berghe T (2011) Dying for a cause: NETosis, mechanisms behind an antimicrobial cell death modality. *Cell Death and Differentiation* **18**: 581-588
- Rensing Rix LL, Rix U, Colinge J, Hantschel O, Bennett KL, Stranzl T, Müller A, Baumgartner C, Valent P, Augustin M, Till JH, Superti-Furga G (2008) Global target profile of the kinase inhibitor bosutinib in primary chronic myeloid leukemia cells. *Leukemia* **23**: 477-485
- Rickard James A, O'Donnell Joanne A, Evans Joseph M, Lalaoui N, Poh Ashleigh R, Rogers T, Vince James E, Lawlor Kate E, Ninnis Robert L, Anderton H, Hall C, Spall Sukhdeep K, Pheese Toby J, Abud Helen E, Cengia Louise H, Corbin J, Mifsud S, Di Rago L, Metcalf D, Ernst M, Dewson G, Roberts Andrew W, Alexander Warren S, Murphy James M, Ekert Paul G, Masters Seth L, Vaux David L, Croker Ben A, Gerlic M, Silke J (2014) RIPK1 Regulates RIPK3-MLKL-Driven Systemic Inflammation and Emergency Hematopoiesis. *Cell* **157**: 1175-1188

- Rieser E, Cordier SM, Walczak H (2013) Linear ubiquitination: a newly discovered regulator of cell signalling. *Trends in Biochemical Sciences* **38**: 94-102
- Rix U, Superti-Furga G (2009) Target profiling of small molecules by chemical proteomics. *Nature Chemical Biology* **5**: 616-624
- Robinson N, McComb S, Mulligan R, Dudani R, Krishnan L, Sad S (2012) Type I interferon induces necroptosis in macrophages during infection with *Salmonella enterica* serovar Typhimurium. *Nature Immunology* **13**: 954-962
- Rothe M, Pan MG, Henzel WJ, Ayres TM, Goeddel DV (1995) The TNFR2-TRAF signaling complex contains two novel proteins related to baculoviral inhibitor of apoptosis proteins. *Cell* **83**: 1243-1252
- Roychowdhury S, McMullen MR, Pisano SG, Liu X, Nagy LE (2013) Absence of receptor interacting protein kinase 3 prevents ethanol-induced liver injury. *Hepatology* **57**: 1773-1783
- Sansonetti PJ, Phalipon A, Arondel J, Thirumalai K, Banerjee S, Akira S, Takeda K, Zychlinsky A (2000) Caspase-1 activation of IL-1 β and IL-18 are essential for *Shigella flexneri*-induced inflammation. *Immunity* **12**: 581-590
- Sato K, Li S, Gordon WC, He J, Liou GI, Hill JM, Travis GH, Bazan NG, Jin M (2013) Receptor Interacting Protein Kinase-Mediated Necrosis Contributes to Cone and Rod Photoreceptor Degeneration in the Retina Lacking Interphotoreceptor Retinoid-Binding Protein. *Journal of Neuroscience* **33**: 17458-17468
- Savitski MM, Reinhard FBM, Franken H, Werner T, Savitski MF, Eberhard D, Molina DM, Jafari R, Dovega RB, Klaeger S, Kuster B, Nordlund P, Bantscheff M, Drewes G (2014) Tracking cancer drugs in living cells by thermal profiling of the proteome. *Science* **346**: 1255784-1255784
- Sawai H, Domae N (2011) Discrimination between primary necrosis and apoptosis by necrostatin-1 in Annexin V-positive/propidium iodide-negative cells. *Biochemical and Biophysical Research Communications* **411**: 569-573
- Sche PP, McKenzie KM, White JD, Austin DJ (1999) Display cloning: functional identification of natural product receptors using cDNA-phage display. *Chem Biol* **6**: 707-716
- Schinzel AC, Takeuchi O, Huang Z, Fisher JK, Zhou Z, Rubens J, Hetz C, Danial NN, Moskowitz MA, Korsmeyer SJ (2005) Cyclophilin D is a component of mitochondrial permeability transition and mediates neuronal cell death after focal cerebral ischemia. *Proceedings of the National Academy of Sciences* **102**: 12005-12010
- Schweichel JU, Merker HJ (1973) The morphology of various types of cell death in prenatal tissues. *Teratology* **7**: 253-266
- Seiler A, Schneider M, Förster H, Roth S, Wirth EK, Culmsee C, Plesnila N, Kremmer E, Rådmark O, Wurst W, Bornkamm GW, Schweizer U, Conrad M (2008) Glutathione Peroxidase 4 Senses and Translates Oxidative Stress into 12/15-Lipoxygenase Dependent- and AIF-Mediated Cell Death. *Cell Metabolism* **8**: 237-248
- Shah RR, Morganroth J, Shah DR (2013) Hepatotoxicity of Tyrosine Kinase Inhibitors: Clinical and Regulatory Perspectives. *Drug Safety* **36**: 491-503
- Shalem O, Sanjana NE, Zhang F (2015) High-throughput functional genomics using CRISPR-Cas9. *Nature Reviews Genetics* **16**: 299-311
- Shalini S, Dorstyn L, Dawar S, Kumar S (2014) Old, new and emerging functions of caspases. *Cell Death and Differentiation* **22**: 526-539
- Shi J, Zhao Y, Wang K, Shi X, Wang Y, Huang H, Zhuang Y, Cai T, Wang F, Shao F (2015) Cleavage of GSDMD by inflammatory caspases determines pyroptotic cell death. *Nature* **526**: 660-665
- Shim JH (2005) TAK1, but not TAB1 or TAB2, plays an essential role in multiple signaling pathways in vivo. *Genes & Development* **19**: 2668-2681
- Shimada K, Chen S, Dempsey PW, Sorrentino R, Alsabeh R, Slepentin AV, Peterson E, Doherty TM, Underhill D, Crother TR, Arditi M (2009) The NOD/RIP2 pathway is essential for host defenses against *Chlamydia pneumoniae* lung infection. *PLoS Pathog* **5**: e1000379
- Shu HB, Takeuchi M, Goeddel DV (1996) The tumor necrosis factor receptor 2 signal transducers TRAF2 and c-IAP1 are components of the tumor necrosis factor receptor 1 signaling complex. *Proc Natl Acad Sci U S A* **93**: 13973-13978

- Silke J, Rickard JA, Gerlic M (2015) The diverse role of RIP kinases in necroptosis and inflammation. *Nature Immunology* **16**: 689-697
- Stanger BZ, Leder P, Lee TH, Kim E, Seed B (1995) RIP: a novel protein containing a death domain that interacts with Fas/APO-1 (CD95) in yeast and causes cell death. *Cell* **81**: 513-523
- Sternberg CN, Davis ID, Mardiak J, Szczylik C, Lee E, Wagstaff J, Barrios CH, Salman P, Gladkov OA, Kavina A, Zarba JJ, Chen M, McCann L, Pandite L, Roychowdhury DF, Hawkins RE (2010) Pazopanib in Locally Advanced or Metastatic Renal Cell Carcinoma: Results of a Randomized Phase III Trial. *Journal of Clinical Oncology* **28**: 1061-1068
- Strittmatter SM (2014) Overcoming Drug Development Bottlenecks With Repurposing: Old drugs learn new tricks. *Nature Medicine* **20**: 590-591
- Sun L, Wang H, Wang Z, He S, Chen S, Liao D, Wang L, Yan J, Liu W, Lei X, Wang X (2012) Mixed Lineage Kinase Domain-like Protein Mediates Necrosis Signaling Downstream of RIP3 Kinase. *Cell* **148**: 213-227
- Sun L, Wang X (2014) A new kind of cell suicide: mechanisms and functions of programmed necrosis. *Trends in Biochemical Sciences* **39**: 587-593
- Sun X, Lee J, Navas T, Baldwin DT, Stewart TA, Dixit VM (1999) RIP3, a novel apoptosis-inducing kinase. *J Biol Chem* **274**: 16871-16875
- Tabor HK, Risch NJ, Myers RM (2002) Candidate-gene approaches for studying complex genetic traits: practical considerations. *Nat Rev Genet* **3**: 391-397
- Taipale M, Jarosz DF, Lindquist S (2010) HSP90 at the hub of protein homeostasis: emerging mechanistic insights. *Nature Reviews Molecular Cell Biology* **11**: 515-528
- Tait SWG, Ichim G, Green DR (2014) Die another way - non-apoptotic mechanisms of cell death. *Journal of Cell Science* **127**: 2135-2144
- Tait Stephen WG, Oberst A, Quarato G, Milasta S, Haller M, Wang R, Karvela M, Ichim G, Yatim N, Albert Matthew L, Kidd G, Wakefield R, Frase S, Krautwald S, Linkermann A, Green Douglas R (2013) Widespread Mitochondrial Depletion via Mitophagy Does Not Compromise Necroptosis. *Cell Reports* **5**: 878-885
- Takaesu G, Surabhi RM, Park K-J, Ninomiya-Tsuji J, Matsumoto K, Gaynor RB (2003) TAK1 is Critical for I κ B Kinase-mediated Activation of the NF- κ B Pathway. *Journal of Molecular Biology* **326**: 105-115
- Takahashi N, Duprez L, Grootjans S, Cauwels A, Nerinckx W, DuHadaway JB, Goossens V, Roelandt R, Van Hauwermeiren F, Libert C, Declercq W, Callewaert N, Prendergast GC, Degterev A, Yuan J, Vandenabeele P (2012) Necrostatin-1 analogues: critical issues on the specificity, activity and in vivo use in experimental disease models. *Cell Death and Disease* **3**: e437
- Takahashi N, Vereecke L, Bertrand MJM, Duprez L, Berger SB, Divert T, Gonçalves A, Sze M, Gilbert B, Kourula S, Goossens V, Lefebvre S, Günther C, Becker C, Bertin J, Gough PJ, Declercq W, van Loo G, Vandenabeele P (2014) RIPK1 ensures intestinal homeostasis by protecting the epithelium against apoptosis. *Nature* **513**: 95-99
- Tang P, Hung MC, Klostergaard J (1996) Human pro-tumor necrosis factor is a homotrimer. *Biochemistry* **35**: 8216-8225
- Tanzer MC, Tripaydonis A, Webb AI, Young SN, Varghese LN, Hall C, Alexander WS, Hildebrand JM, Silke J, Murphy JM (2015) Necroptosis signalling is tuned by phosphorylation of MLKL residues outside the pseudokinase domain activation loop. *Biochemical Journal* **471**: 255-265
- Tenev T, Bianchi K, Darding M, Broemer M, Langlais C, Wallberg F, Zachariou A, Lopez J, MacFarlane M, Cain K, Meier P (2011) The Ripoptosome, a Signaling Platform that Assembles in Response to Genotoxic Stress and Loss of IAPs. *Molecular Cell* **43**: 432-448
- Teng X, Degterev A, Jagtap P, Xing X, Choi S, Denu R, Yuan J, Cuny GD (2005) Structure-activity relationship study of novel necroptosis inhibitors. *Bioorganic & Medicinal Chemistry Letters* **15**: 5039-5044
- Terstappen GC, Schlüpen C, Raggiaschi R, Gaviraghi G (2007) Target deconvolution strategies in drug discovery. *Nature Reviews Drug Discovery* **6**: 891-903
- Thapa RJ, Nogusa S, Chen P, Maki JL, Lerro A, Andrade M, Rall GF, Degterev A, Balachandran S (2013) Interferon-induced RIP1/RIP3-mediated necrosis requires PKR and is licensed by FADD and caspases. *Proceedings of the National Academy of Sciences* **110**: E3109-E3118

- Trauth BC, Klas C, Peters AM, Matzku S, Moller P, Falk W, Debatin KM, Krammer PH (1989) Monoclonal antibody-mediated tumor regression by induction of apoptosis. *Science* **245**: 301-305
- Trepel J, Mollapour M, Giaccone G, Neckers L (2010) Targeting the dynamic HSP90 complex in cancer. *Nature Reviews Cancer* **10**: 537-549
- Upton JW, Kaiser WJ, Mocarski ES (2010) Virus Inhibition of RIP3-Dependent Necrosis. *Cell Host & Microbe* **7**: 302-313
- Upton Jason W, Kaiser William J, Mocarski Edward S (2012) DAI/ZBP1/DLM-1 Complexes with RIP3 to Mediate Virus-Induced Programmed Necrosis that Is Targeted by Murine Cytomegalovirus vIRA. *Cell Host & Microbe* **11**: 290-297
- van der Graaf WT, Blay JY, Chawla SP, Kim DW, Bui-Nguyen B, Casali PG, Schoffski P, Aglietta M, Staddon AP, Beppu Y, Le Cesne A, Gelderblom H, Judson IR, Araki N, Ouali M, Marreaud S, Hodge R, Dewji MR, Coens C, Demetri GD, Fletcher CD, Dei Tos AP, Hohenberger P (2012) Pazopanib for metastatic soft-tissue sarcoma (PALETTE): a randomised, double-blind, placebo-controlled phase 3 trial. *Lancet* **379**: 1879-1886
- Vandenabeele P, Galluzzi L, Vanden Berghe T, Kroemer G (2010) Molecular mechanisms of necroptosis: an ordered cellular explosion. *Nature Reviews Molecular Cell Biology* **11**: 700-714
- Varfolomeev E, Blankenship JW, Wayson SM, Fedorova AV, Kayagaki N, Garg P, Zobel K, Dynek JN, Elliott LO, Wallweber HJA, Flygare JA, Fairbrother WJ, Deshayes K, Dixit VM, Vucic D (2007) IAP Antagonists Induce Autoubiquitination of c-IAPs, NF- κ B Activation, and TNF α -Dependent Apoptosis. *Cell* **131**: 669-681
- Varfolomeev E, Goncharov T, Fedorova AV, Dynek JN, Zobel K, Deshayes K, Fairbrother WJ, Vucic D (2008) c-IAP1 and c-IAP2 Are Critical Mediators of Tumor Necrosis Factor (TNF)-induced NF- κ B Activation. *Journal of Biological Chemistry* **283**: 24295-24299
- Varfolomeev EE, Boldin MP, Goncharov TM, Wallach D (1996) A potential mechanism of "cross-talk" between the p55 tumor necrosis factor receptor and Fas/APO1: proteins binding to the death domains of the two receptors also bind to each other. *J Exp Med* **183**: 1271-1275
- Varfolomeev EE, Schuchmann M, Luria V, Chiannikulchai N, Beckmann JS, Mett IL, Rebrikov D, Brodianski VM, Kemper OC, Kollet O, Lapidot T, Soffer D, Sobe T, Avraham KB, Goncharov T, Holtmann H, Lonai P, Wallach D (1998) Targeted disruption of the mouse Caspase 8 gene ablates cell death induction by the TNF receptors, Fas/Apo1, and DR3 and is lethal prenatally. *Immunity* **9**: 267-276
- Vaux DL, Cory S, Adams JM (1988) Bcl-2 gene promotes haemopoietic cell survival and cooperates with c-myc to immortalize pre-B cells. *Nature* **335**: 440-442
- Vercammen D, Beyaert R, Denecker G, Goossens V, Van Loo G, Declercq W, Grooten J, Fiers W, Vandenabeele P (1998) Inhibition of caspases increases the sensitivity of L929 cells to necrosis mediated by tumor necrosis factor. *J Exp Med* **187**: 1477-1485
- Vercammen D, Vandenabeele P, Beyaert R, Declercq W, Fiers W (1997) Tumour necrosis factor-induced necrosis versus anti-Fas-induced apoptosis in L929 cells. *Cytokine* **9**: 801-808
- Vince James E, Wong WW-L, Gentle I, Lawlor Kate E, Allam R, O'Reilly L, Mason K, Gross O, Ma S, Guarda G, Anderton H, Castillo R, Häcker G, Silke J, Tschopp J (2012) Inhibitor of Apoptosis Proteins Limit RIP3 Kinase-Dependent Interleukin-1 Activation. *Immunity* **36**: 215-227
- Vitner EB, Salomon R, Farfel-Becker T, Meshcheriakova A, Ali M, Klein AD, Platt FM, Cox TM, Futerman AH (2014) RIPK3 as a potential therapeutic target for Gaucher's disease. *Nature Medicine* **20**: 204-208
- Vogt CI (1842) *Untersuchungen über die Entwicklungsgeschichte der Geburtshelferkröte (Alytes obstetricans)*, Solothurn: Jent & Gassmann.
- Wajant H, Pfizenmaier K, Scheurich P (2003) Tumor necrosis factor signaling. *Cell Death Differ* **10**: 45-65
- Wang CY, Mayo MW, Korneluk RG, Goeddel DV, Baldwin AS, Jr. (1998) NF- κ B antiapoptosis: induction of TRAF1 and TRAF2 and c-IAP1 and c-IAP2 to suppress caspase-8 activation. *Science* **281**: 1680-1683
- Wang H, Sun L, Su L, Rizo J, Liu L, Wang L-F, Wang F-S, Wang X (2014a) Mixed Lineage Kinase Domain-like Protein MLKL Causes Necrotic Membrane Disruption upon Phosphorylation by RIP3. *Molecular Cell* **54**: 133-146

- Wang JS, Wu D, Huang DY, Lin WW (2015) TAK1 inhibition-induced RIP1-dependent apoptosis in murine macrophages relies on constitutive TNF- α signaling and ROS production. *J Biomed Sci* **22**: 76
- Wang L, Du F, Wang X (2008) TNF- α Induces Two Distinct Caspase-8 Activation Pathways. *Cell* **133**: 693-703
- Wang X, Jiang W, Yan Y, Gong T, Han J, Tian Z, Zhou R (2014b) RNA viruses promote activation of the NLRP3 inflammasome through a RIP1-RIP3-DRP1 signaling pathway. *Nature Immunology* **15**: 1126-1133
- Wang Y, Kim NS, Haince J-F, Kang HC, David KK, Andrabi SA, Poirier GG, Dawson VL, Dawson TM (2011) Poly(ADP-Ribose) (PAR) Binding to Apoptosis-Inducing Factor Is Critical for PAR Polymerase-1-Dependent Cell Death (Parthanatos). *Science Signaling* **4**: ra20-ra20
- Wang Z, Jiang H, Chen S, Du F, Wang X (2012) The Mitochondrial Phosphatase PGAM5 Functions at the Convergence Point of Multiple Necrotic Death Pathways. *Cell* **148**: 228-243
- Ward JE, Stadler WM (2010) Pazopanib in Renal Cell Carcinoma. *Clinical Cancer Research* **16**: 5923-5927
- Wartha F, Henriques-Normark B (2008) ETosis: A Novel Cell Death Pathway. *Science Signaling* **1**: pe25-pe25
- Wassermann AM, Camargo LM, Auld DS (2014) Composition and applications of focus libraries to phenotypic assays. *Front Pharmacol* **5**: 164
- Weinlich R, Oberst A, Dillon Christopher P, Janke Laura J, Milasta S, Lukens John R, Rodriguez Diego A, Gurung P, Savage C, Kanneganti Thirumala D, Green Douglas R (2013) Protective Roles for Caspase-8 and cFLIP in Adult Homeostasis. *Cell Reports* **5**: 340-348
- Welz P-S, Wullaert A, Vlantis K, Kondylis V, Fernández-Majada V, Ermolaeva M, Kirsch P, Sterner-Kock A, van Loo G, Pasparakis M (2011) FADD prevents RIP3-mediated epithelial cell necrosis and chronic intestinal inflammation. *Nature* **477**: 330-334
- Wertz IE, O'Rourke KM, Zhou H, Eby M, Aravind L, Seshagiri S, Wu P, Wiesmann C, Baker R, Boone DL, Ma A, Koonin EV, Dixit VM (2004) De-ubiquitination and ubiquitin ligase domains of A20 downregulate NF- κ B signalling. *Nature* **430**: 694-699
- Whitesell L, Mimnaugh EG, De Costa B, Myers CE, Neckers LM (1994) Inhibition of heat shock protein HSP90-pp60v-src heteroprotein complex formation by benzoquinone ansamycins: essential role for stress proteins in oncogenic transformation. *Proc Natl Acad Sci U S A* **91**: 8324-8328
- Wu J, Huang Z, Ren J, Zhang Z, He P, Li Y, Ma J, Chen W, Zhang Y, Zhou X, Yang Z, Wu S-Q, Chen L, Han J (2013a) Mkl1 knockout mice demonstrate the indispensable role of Mkl1 in necroptosis. *Cell Research* **23**: 994-1006
- Wu J, Powell F, Larsen NA, Lai Z, Byth KF, Read J, Gu R-F, Roth M, Toader D, Saeh JC, Chen H (2013b) Mechanism and In Vitro Pharmacology of TAK1 Inhibition by (5Z)-7-Oxozeaenol. *ACS Chemical Biology* **8**: 643-650
- Wu XN, Yang ZH, Wang XK, Zhang Y, Wan H, Song Y, Chen X, Shao J, Han J (2014) Distinct roles of RIP1-RIP3 hetero- and RIP3-RIP3 homo-interaction in mediating necroptosis. *Cell Death and Differentiation* **21**: 1709-1720
- Wu YT, Tan HL, Huang Q, Sun XJ, Zhu X, Shen HM (2010) zVAD-induced necroptosis in L929 cells depends on autocrine production of TNF α mediated by the PKC-MAPKs-AP-1 pathway. *Cell Death and Differentiation* **18**: 26-37
- Yamamoto K, Yamazaki A, Takeuchi M, Tanaka A (2006) A versatile method of identifying specific binding proteins on affinity resins. *Analytical Biochemistry* **352**: 15-23
- Yang Wan S, SriRamaratnam R, Welsch Matthew E, Shimada K, Skouta R, Viswanathan Vasanthi S, Cheah Jaime H, Clemons Paul A, Shamji Alykhan F, Clish Clary B, Brown Lewis M, Girotti Albert W, Cornish Virginia W, Schreiber Stuart L, Stockwell Brent R (2014) Regulation of Ferroptotic Cancer Cell Death by GPX4. *Cell* **156**: 317-331
- Yatim N, Jusforgues-Saklani H, Orozco S, Schulz O, Barreira da Silva R, Reis e Sousa C, Green DR, Oberst A, Albert ML (2015) RIPK1 and NF- κ B signaling in dying cells determines cross-priming of CD8(+) T cells. *Science* **350**: 328-334

- Yeh WC, de la Pompa JL, McCurrach ME, Shu HB, Elia AJ, Shahinian A, Ng M, Wakeham A, Khoo W, Mitchell K, El-Deiry WS, Lowe SW, Goeddel DV, Mak TW (1998) FADD: essential for embryo development and signaling from some, but not all, inducers of apoptosis. *Science* **279**: 1954-1958
- Yonehara S, Ishii A, Yonehara M (1989) A cell-killing monoclonal antibody (anti-Fas) to a cell surface antigen co-downregulated with the receptor of tumor necrosis factor. *J Exp Med* **169**: 1747-1756
- Yonish-Rouach E, Resnitzky D, Lotem J, Sachs L, Kimchi A, Oren M (1991) Wild-type p53 induces apoptosis of myeloid leukaemic cells that is inhibited by interleukin-6. *Nature* **352**: 345-347
- Young AB (2003) Huntingtin in health and disease. *J Clin Invest* **111**: 299-302
- Yu PW, Huang BC, Shen M, Quast J, Chan E, Xu X, Nolan GP, Payan DG, Luo Y (1999) Identification of RIP3, a RIP-like kinase that activates apoptosis and NFkappaB. *Curr Biol* **9**: 539-542
- Yu SW, Wang H, Poitras MF, Coombs C, Bowers WJ, Federoff HJ, Poirier GG, Dawson TM, Dawson VL (2002) Mediation of poly(ADP-ribose) polymerase-1-dependent cell death by apoptosis-inducing factor. *Science* **297**: 259-263
- Zhang D, Lin J, Han J (2010) Receptor-interacting protein (RIP) kinase family. *Cellular and Molecular Immunology* **7**: 243-249
- Zhang DW, Shao J, Lin J, Zhang N, Lu BJ, Lin SC, Dong MQ, Han J (2009) RIP3, an Energy Metabolism Regulator That Switches TNF-Induced Cell Death from Apoptosis to Necrosis. *Science* **325**: 332-336
- Zhang H, Zhou X, McQuade T, Li J, Chan FK-M, Zhang J (2011) Functional complementation between FADD and RIP1 in embryos and lymphocytes. *Nature* **471**: 373-376
- Zhang J, Cado D, Chen A, Kabra NH, Winoto A (1998) Fas-mediated apoptosis and activation-induced T-cell proliferation are defective in mice lacking FADD/Mort1. *Nature* **392**: 296-300
- Zhang JH, Kang ZB, Ardayfio O, Ho Pi, Smith T, Wallace I, Bowes S, Hill WA, Auld DS (2013) Application of Titration-Based Screening for the Rapid Pilot Testing of High-Throughput Assays. *Journal of Biomolecular Screening* **19**: 651-660
- Zhao H, Ning J, Lemaire A, Koumpa F-S, Sun JJ, Fung A, Gu J, Yi B, Lu K, Ma D (2015) Necroptosis and parthanatos are involved in remote lung injury after receiving ischemic renal allografts in rats. *Kidney International* **87**: 738-748
- Zhao J, Jitkaew S, Cai Z, Choksi S, Li Q, Luo J, Liu ZG (2012) Mixed lineage kinase domain-like is a key receptor interacting protein 3 downstream component of TNF-induced necrosis. *Proc Natl Acad Sci U S A* **109**: 5322-5327
- Zheng W, Degterev A, Hsu E, Yuan J, Yuan C (2008) Structure-activity relationship study of a novel necroptosis inhibitor, necrostatin-7. *Bioorganic & Medicinal Chemistry Letters* **18**: 4932-4935
- Zhong CQ, Li Y, Yang D, Zhang N, Xu X, Wu Y, Chen J, Han J (2014) Quantitative phosphoproteomic analysis of RIP3-dependent protein phosphorylation in the course of TNF-induced necroptosis. *Proteomics* **14**: 713-724
- Zhou W, Yuan J (2014) Necroptosis in health and diseases. *Seminars in Cell & Developmental Biology* **35**: 14-23
- Zong WX (2004) Alkylating DNA damage stimulates a regulated form of necrotic cell death. *Genes & Development* **18**: 1272-1282

CURRICULUM VITAE

Full name Astrid Veronika Fauster
Date of birth 10th of November, 1985
Citizenship Austrian
Address Breitenfeldergasse 5/16, 1080 Vienna
Phone +43 1 40160 70045 | +43 650 3007391
E-mail afauster@cemm.oeaw.ac.at | a_fauster@hotmail.com

EDUCATION AND TRAINING

2010 - present PhD Student at CeMM Research Center for Molecular Medicine of the Austrian Academy of Sciences, Molecular Signal Transduction Program, Medical University of Vienna, Austria

2008 - 2010 MSc in Molecular Microbiology, University of Graz, Austria passed with distinction

2004 - 2008 BSc in Molecular Biology, University of Graz, Austria passed with distinction

RESEARCH EXPERIENCE

2010 - present PhD Thesis: "Identification and Molecular Characterization of Inhibitors of Necroptosis"
Supervisor: Prof. Giulio Superti-Furga

2009 - 2010 Master Thesis: "*Campylobacter fetus venerealis*: FIC1 and FIC2 – Characterization of two putative effector proteins"
Supervisor: Prof. Ellen L. Zechner

2009 Project Laboratory: "Bacterial conjugation enhances biofilm formation: Investigating extent and impact of transfer activity in the first generation of transconjugants"
Supervisor: DI Dr. Andreas Reisner

2006 Internship at the University of Natural Resources and Applied Life Sciences Vienna
Laboratory of Prof. Alois Jungbauer

SCHOLARSHIPS

2007/2008	Mobility Scholarship (ERASMUS), Aarhus University, Denmark
2004/2005	Merit Scholarship

TEACHING

2009	Teaching assistant for laboratory course: “Bacteriology and Bacterial Genetics”, University of Graz, Austria
2014/2015	Supervision of internship students

CONFERENCES AND POSTER PRESENTATIONS

2011	TOLL2011 Meeting: Decoding Innate Immunity, Riva del Garda, Italy (Poster)
2011	7th YSA Symposium, Medical University of Vienna, Austria (Poster)
2011	EMBO Meeting 2011, Vienna, Austria
2012	European Congress of Immunology (ECI), Glasgow, UK (Poster)
2014	Gordon Research Conference: Cell Death Mechanisms at the Interface of Health and Disease, West Dover, VT, USA (Poster)
2015	23 rd Euroconference on Apoptosis – Death Pathways and Beyond, Geneva, Switzerland (Poster)

PUBLICATIONS:

1. Bigenzahn, J.W.*, **Fauster, A.***, Rebsamen, M., Kandasamy, R.K., Scorzoni, S., Vladimer, G.I., Mueller, A.C., Gstaiger, M., Zuber, J., Bennett, K.L., and Superti-Furga, G. (2015). An inducible retroviral expression system for tandem affinity purification mass-spectrometry-based proteomics identifies MLKL as an HSP90 client. *Mol Cell Proteomics*.
2. **Fauster, A.***, Rebsamen, M.*, Huber, K.V., Bigenzahn, J.W., Stukalov, A., Lardeau, C.H., Scorzoni, S., Bruckner, M., Gridling, M., Parapatics, K., Colinge, J., Bennett, K.L., Kubicek, S., Krautwald, S., Linkermann, A., and Superti-Furga, G. (2015). A cellular screen identifies ponatinib and pazopanib as inhibitors of necroptosis. *Cell Death Dis* 6, e1767.
3. Heinz, L.X.*, Baumann, C.L.*, Koberlin, M.S., Snijder, B., Gawish, R., Shui, G., Sharif, O., Aspalter, I.M., Muller, A.C., Kandasamy, R.K., Breitwieser, F.P., Pichlmair, A., Bruckner, M., Rebsamen, M., Bluml, S., Karonitsch, T., **Fauster, A.**, Colinge, J., Bennett, K.L., Knapp, S., Wenk, M.R., and Superti-Furga, G. (2015). The Lipid-Modifying Enzyme SMPDL3B Negatively Regulates Innate Immunity. *Cell Rep* 11, 1919-1928.
4. Koberlin, M.S.*, Snijder, B.*, Heinz, L.X., Baumann, C.L., **Fauster, A.**, Vladimer, G.I., Gavin, A.C., and Superti-Furga, G. (2015). A Conserved Circular Network of Coregulated Lipids Modulates Innate Immune Responses. *Cell* 162, 170-183.
5. Rebsamen, M., Pochini, L., Stasyk, T., de Araujo, M.E., Galluccio, M., Kandasamy, R.K., Snijder, B., **Fauster, A.**, Rudashevskaya, E.L., Bruckner, M., Scorzoni, S., Filipek, P.A., Huber, K.V., Bigenzahn, J.W., Heinz, L.X., Kraft, C., Bennett, K.L., Indiveri, C., Huber, L.A., and Superti-Furga, G. (2015). SLC38A9 is a component of the lysosomal amino acid sensing machinery that controls mTORC1. *Nature* 519, 477-481.
6. Pichlmair, A., Kandasamy, K., Alvisi, G., Mulhern, O., Sacco, R., Habjan, M., Binder, M., Stefanovic, A., Eberle, C.A., Goncalves, A., Burckstummer, T., Muller, A.C., **Fauster, A.**, Holze, C., Lindsten, K., Goodbourn, S., Kochs, G., Weber, F., Bartenschlager, R., Bowie, A.G., Bennett, K.L., Colinge, J., and Superti-Furga, G. (2012). Viral immune modulators perturb the human molecular network by common and unique strategies. *Nature* 487, 486-490.
7. Kienesberger, S., Schober Trummler, C., **Fauster, A.**, Lang, S., Sprenger, H., Gorkiewicz, G., and Zechner, E.L. (2011). Interbacterial macromolecular transfer by the *Campylobacter fetus* subsp. *venerealis* type IV secretion system. *J Bacteriol* 193, 744-758.